ARTIFICIAL JOINTS: THEIR TRIBOLOGY AND WEAR PARTICLE ANALYSIS

Amy Kinbrum

Artificial Joints: Their Tribology and Wear Particle Analysis

By Amy Kinbrum, MEng

Submitted for the degree of Doctor of Philosophy.

University of Durham

Centre for Biomedical Engineering

School of Engineering

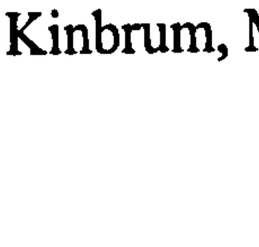

July 2008

Abstract
The wear,friction, lubrication and particle distribution of differently heat treated CoCrMo cast prostheses provided by the same supplier were analysed. Wear tests were conducted on both pin-on-plate and simulation rigs. Friction tests were also performed at intervals throughout testing. The surfaces of all bearing couples were analysed and the roughness was recorded in order to help analyse the lubrication and wear mechanism. The particles from each test were saved and frozen at -20°C, later analysis allowed further insight into the mechanism of wear of each material tested. The particles underwent protein digestion by enzymatic protocol this was the least harmful way of separating the particles from the protein. The particles were then analysed using a NanoSight LM10, this instrument can identify particles from a 0.5 ml solution by highlighting the particles with a laser and recording the movement of the particles. Using the Stokes-Einstein equation the size of the particles can be calculated by the motion recorded.
Recently metal-on-plastic prostheses have not been sufficient for the younger osteoarthritic patient, therefore the market has demanded alternative, low wearing bearing couples, both metal-on-metal and ceramic-on-ceramic have come to the market as alternatives for the younger more active patient. The Birmingham Hip Resurfacing (BHR) came to the market in the early 1990's and was produced by casting methods. Theory suggested that heat treatment may improve the tribological properties of the CoCrMo alloy. This thesis set out to assess the physical mechanism of failure of these joints. This study aims to look at the problem from as many angles as possible therefore the wear rates, friction, surfaces and particle debris were analysed.
The pin-on-plate tests were very useful as they allow the analysis of the surface interaction without the complication of lubrication. This showed that the hard carbides in the as-cast material play ed an important part in the wear mechanism and caused mainly abrasive wear to occur. As annealing was performed a single time and then repeatedly, fewer carbides were seen in the material and the wear pattern changed from mainly scratching in the direction of sliding to what appeared to be pitting, which pointed towards adhesive wear. The particle analysis from the pin-on-plate tests corroborated the wear hypothesis, showing as-cast debris to be all of similar size range at around 200 nm and the shape was round to needle shaped.Repeated annealing showed two different size distributions of 100nm and 2 microns. these larger particles were flake like. Testing from the wear simulators showed little difference between any as-cast joints. Thirty eight mm joints, 50 mm joints and modular designs all showed a similar wear pattern. The particles were round to oval in the size range of 200 nm as with the pin-on-plate debris. The friction results indicated that all joints ran in from a boundary/mixed regime towards a fluid film lubrication regime. The double heat treated components showed very low wear but there were micro cracks on the reverse of the prostheses which may have had an effect on the gravimetric results. The debris showed far fewer particles than the pin-on-plate results but the same bimodal distribution of large flakes and smaller granular particles was seen. The friction indicated mixed lubrication and the friction factor reduced over time but no real improvement in the lubrication was seen. Other particles analysed from previous tests on novel polymers showed that polycarbonate urethane particles appeared as flat disks and were uniform. Carbon fibre reinforced PEEK debris was also analysed and showed a bimodal distribution of small granular particles of less than 100 nm and larger particles of around 2 to 3 microns.

Table of contents

Nomenclature

α	Constant, amplitude, semi-angle subtended by aperture
η	Viscosity
λ	Separation ratio, Wavelength
μ	Constant of proportionality
ρ	Density
A	Swing angle
E	Youngs modulus
F	Frictional force
I	Inverse
K	Wear coefficient
L	Load
N	Normal
R	Radius
T	Torque
V	Volume
X	Sliding distance
f	Friction factor, frequency
h	Film thickness
i	Index
k	Constant of proportionality,
p	Hardness
r	Radius, smallest separation between two features
u	Entraining velocity
v	Velocity
z	Sommerfeld number

List of abbreviations

Ac	As Cast
AFM	Atomic force microscope
ANOVA	Analysis of Variance

ATP	Adenosine triphosphate
BHR	Birmingham hip resurfacing
C-O-C	Ceramic-on-ceramic
CFR-PEEK	Carbon fibre reinforced Polyetheretherketone
CMC	Carboxymethylecellulose
EDTA	Ethylenediaminetetraacetic acid
EDX	Energy Dispersive X-ray
EDXA	Energy Dispersive X-ray analysis
ESEM	Environmental Scanning electron microscope
FCC	Face centred cubic
HCP	Hexagonal close Packed
IL-1	Interleukin 1
IL-6	Interleukin 6
ISO	International standard
Lc	Low Carbide
M-O-M	Metal-on-metal
PBS	Phosphate buffered saline
PEEK	Polyetheretherketone
PGE 2	Prostaglandin E2
P-O-P	Pin-on-plate
PMMA	Polymethylmethacrylate
PTFE	Polytetrafluroethene
PU	Poly urethane
SDS	Sodium Dodecyl Sulphate
SEM	Scanning electron microscope
SPSS	Statistical Package
TEM	Transmission electron microscope
TNF-α	Tumour necrosis factor
UHMWPE	Ultra high molecular weight polyethylene

Acknowledgements

My thanks go to many people, without whom this journey would have been a lot harder.

To Smith and Nephew Orthopaedics for funding this research and supplying the test specimens.

To Professor Unsworth for his guidance and encouragement.

To Dr Susan Scholes and Dr Katelia Vassiliou who taught me many things including how to work the equipment in our labs.

To Dr Katelia Vasiliou and Dr SiuMan Lee with whom some of this work was carried out jointly

To Dr Tony Fawcet in the Department of Biological Sciences and to Judith Chambers for showing me the ropes.

To the Electronic and Mechanical workshops for fixing all the things I could not.

Especially to Arthur Newman for his brute force when things got stuck and for making the holders for all the test specimens amongst other creations.

To all my friends in the Engineering Department, for making life more enjoyable.

To Mum and Dad for having the patience to teach me to read and write.

To Mark for everything else and just being there.

Declaration

The work contained in this thesis has not been submitted elsewhere for any other degree or qualification and unless referenced otherwise is the authors own work.

1. Introduction

Orthopaedic research has endeavoured to eliminate the pain and suffering of arthritis for many years. Joint arthroplasty has evolved from a simple cup placed over the arthritic head of the femur, to the huge range of materials and designs that are available today, including ceramic-on-ceramic, metal-on-metal and metal or ceramic on plastic combinations. The designs range from traditional total arthroplasties where the damaged head of the femur is replaced with a prosthetic head, secured with a stem which is inserted into the femoral cavity, to resurfacing, a concept made popular in the 1990's. During the common metal-on-metal resurfacing arthroplasty, the femoral head is machined into a cylindrical shape and the metal head is cemented onto the top. This preserves femoral bone. In both cases the head articulates against a cup which is placed in the reamed out acetabulum.

As the design and materials of prostheses have improved over the last several decades, the patient age at initial arthroplasty has decreased. The younger patient demands more from the arthroplasty as often they will be more physically active and will need a longer survivorship. The traditional metal on ultra high molecular weight polyrthylene (UHMWPE) struggles to provide these higher demands and therefore a trend has developed to place metal-on-metal hip joints into the younger patient. The new resurfacing design so far has good short to mid-term results [1-3].

Many prosthetic joints have been shown to operate under mixed lubrication, which leads to wear. The debris that is produced is in the form of particles. As metal-on-metal joints have become more popular it is important to know the effects of metal particles on the body. As metal particles are not inert like UHMWPE they may cause, as yet, unknown problems when the metal ions from the particles disperse through out the body. Long term results from the original metal-on-metal McKee-Farrar and the Muller give some idea of what will happen with the modern implants [4-6] and to date there seems little cause for concern but the evidence is still being evaluated.

Heat treatment of CoCrMo cast alloy prostheses is a controversial technique used by some manufacturers to improve the mechanical and wear properties of the alloy. Current views have drawn no firm conclusions as to whether heat treatment improves or worsens the wear properties of cobalt chrome alloy to date, and this thesis offers further input to this debate.

Novel materials may also provide a solution to the problem of longevity in the younger patient with knee or hip arthroplasties. Polyurethane (PU) was developed as a very low friction material for both hip and knee arthroplasty [7]. The simulator wear tests for both were successful and biological toxicity and stability tests have confirmed that in the polycarbonate urethane formation the material is suitable for implantation. Polyetheretherketone (PEEK) is another novel polymer that has been used as an arthroplasty material. This material is also used in both hips and knees and has also proved to be extremely low wear [8]. The particulate debris caused by wear from both these materials has not been studied to date, so this thesis adds to the debate that has been conducted so far to determine if these materials are suitable for orthopaedic devices.

An in-depth material and hip simulator study of the tribology and particle analysis of three different heat treatments of a CoCrMo alloy was undertaken to asses the effects of annealing. Particle analysis of plasma carburised CoCrMo and as-cast CoCrMo as well as new modular designs were investigated. Other particle analyses of novel plastic materials for arthroplasty such as PEEK and PU were also conducted to assess the size of particles produced during wear simulator studies of the normal walking cycle. It is hoped that this study will provide insight into the longer term effects of materials used in total hip arthroplasty.

2. Literature Review

2.1. Introduction

Many metal-on-metal prosthetic hip joints were implanted in the 1960's [4]. These early metal joints often loosened causing pain and required revision of the procedure. Loosening was thought to be caused by large frictional torques between the acetabular cup and the femoral head due to equatorial contact leading to high frictional torque [9]. The introduction of new low friction materials such as polytetrafluroethylene (PTFE) [10] later superceded by ultra high molecular weight polyethylene was thought to solve these problems. The new materials were low friction, thought to be low wear and inert, therefore they were well tolerated within the body. However the PTFE on metal prostheses wore out relatively quickly and the UHMWPE on metal joints eventually came loose after several years of wear [11, 12].

Prosthetic hip joints have been found to fail for a variety of reasons but one of the most common being that the hip joint became loose at the bone-prosthesis or bone cement interface. If looseness develops after several years then the process is known as late aseptic loosening. Late aseptic loosening results in pain for the patient and the need for revision. Loosening at both the acetabulum and the femoral component can occur [13].

It was assumed that the loosening was a result of bone lysis by poly methyl methacrylate (PMMA) bone cement that was used to attach the prosthesis to the bone. This became known as cement disease [14]. Harris [15] conducted a review of particle disease in the hip and concluded that it was not the cement that caused late aseptic loosening but particulate debris from polyethylene cups. This was based on a review of both cemented and uncemented prostheses both of which suffered osteolysis. Lysis is thought to be due to the wear particles from the UHMWPE which cause macrophage activation and lead to bone resorption around the prosthesis.

Harris' studies [15, 16] started a trend towards the reintroduction of metal-on-metal total hip arthroplasties (THR). Modern designs of metal-on-metal joints and finishing techniques now allow the manufacture of prostheses that are rarely affected by high frictional torques under normal conditions [17].

Since a large number of metal-on-polyethylene hips have been implanted, much research has been conducted on the polyethylene particles produced by cup wear. Particles have been assessed for size, shape [11, 16, 18, 19] and particle induced biological activity [20-22]. However, metal-on-metal implants have become more common these days and analysis of the wear induced particles from these joints has become an essential part of the research to improve their design [23-27].

2.2. The synovial joint

Joints affected by osteoarthritis in particular include diarthrodial joints (e.g. finger, hip, knee and toe joints). The hip joint is commonly replaced largely due to rheumatoid arthritis or more commonly osteoarthritis. The hip joint is described in Gray's anatomy as being "formed by two contiguous bony surfaces, covered with cartilage, connected by ligaments and lined by synovial membrane" [28]. The hip is a ball and socket joint and is encapsulated within a synovial sack which contains synovial fluid. Synovial fluid lubricates and provides nutrition for the natural joint. It consists mainly of blood plasma and a substance known as hyaluronic acid which is secreted by the synovial cells surrounding the joint into the plasma causing it to become more viscous [29]. The synovial fluid also provides the only nutrition to the articular cartilage during adult life, since the blood supply to the cartilage is cut off at maturity due to the formation of a sub-chondral plate which is a thickening of the bone supporting the cartilaginous layer.

2.3. Forces and loading cycles

In the 1960's Paul investigated the loading and motion of the human hip involved in the standard walking cycle [30]. This paved the way for most of the *in vitro* hip simulators currently used. The Paul loading cycle consists of a double peak, one at heel strike and one at toe off (see Figure 1 below). The highest peak can be up to 4

times body weight. The cycle shows a large force on the hip as the heel strike occurs then a decrease in the force over the stance phase and a larger force at toe off. Paul's walking cycle was obtained using force plates but *in vivo* measurements using strain gauged prostheses (English and Kilvington model, [31]) tended to show much closer to a square wave loading pattern.

The difficulty with relying on muscle electro detection to define which muscles are acting to produce the force, is skin and subcutaneous fat deposit interference to the signal detected. Also there are many different muscles acting on the hip joint in the gait cycle some of which may work at the same instant. It is therefore difficult to differentiate between the signals or use simple static analysis. Deeper muscles are even more difficult to record without percutaneous receivers. Individual gait pattern and footwear have an influence on muscle activation and performance therefore making comparison between subjects difficult.

Paul in his analysis of loading the hip joint in 2002 notes that there are many daily activities which cause greater loading than walking *inter alia* getting into and out of a car can load the hip 150% that of walking, however, these overload activities occur less frequently than walking and are on average unlikely to exceed 0.3% of normal walking loading cycles [32].

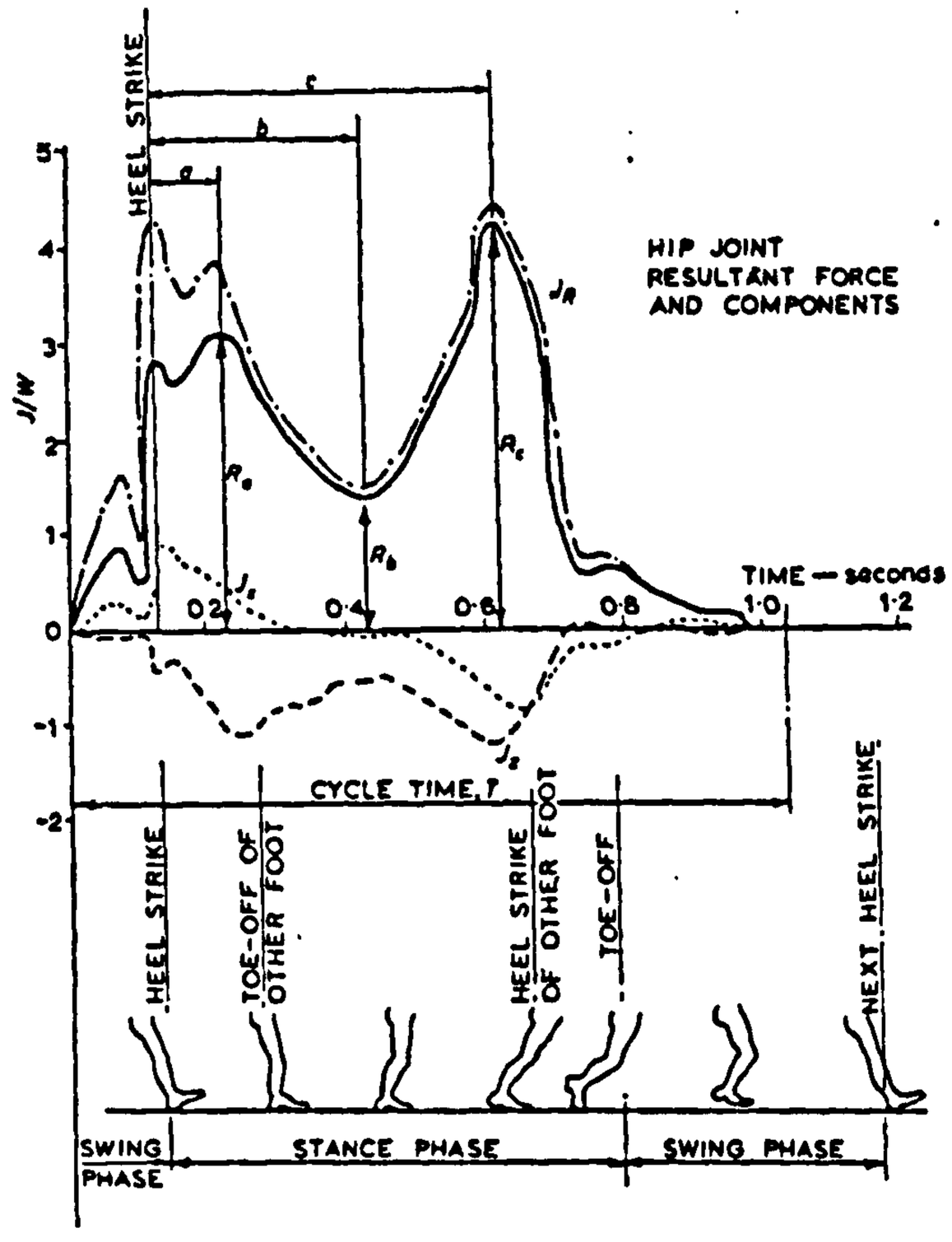

Figure 1 The Paul Loading Cycle [30]

2.4. Disease of the hip

There are two main diseases that may cause the hip joint to need replacement, osteoarthritis is the major cause but also rheumatoid arthritis can affect these large joints.

Osteoarthritis is caused by the wearing out of the articular cartilage within the joint. This results in pain and inflammation within the joint. The major weight bearing joints, e.g. hips and knees, are the first to be affected with this disease.

Rheumatoid arthritis is an autoimmune disease whereby the soft tissues of the entire body may be inflamed. This causes the synovial fluid within the joints to be less viscous as the synovial cells are compromised in their ability to work properly. As the quality of the synovial fluid deteriorates its ability to keep the cartilaginous surfaces apart decreases resulting in articular damage. The smaller joints e.g.

metacarpophalangeal joints are likely to be affected first. Other organs may also be affected by this disease[33].

Another reason for a total hip replacement is injury. A severe injury to the cartilage pelvis or femur can necessitate a total hip replacement. Pelvic or femoral trauma may lead to a total hip replacement due to the severe nature of the break. The Textbook of rheumatology [34] pp1685 States that "primary mechanical joint deterioration can itself cause secondary processes, particularly in the synovium, as the result of cartilage fragmentation" this suggests that if the cartilage is damaged through injury inflammation of the joint may cause secondary arthritis.

2.5. Theory

2.5.1. History

At the beginning of the 20th Century two pieces of research seemingly unconnected were reported in Germany [35, 36]. These two concepts came together to jump start what was going to be a giant leap for the orthopaedic medical industry. These were Hertzian contact theory [35], studying how two components behave when in intimate contact and a theory of ball bearing lubrication by Stribeck [36]. Together these two pieces of research formed the mechanical basis of the study of hip joint replacements.

There have been many attempts to relieve the pain of arthritis in the hip joint. One of the most successful designs was originated by Charnley. The design in 1959 of a small femoral head of metal articulating against a plastic liner which was cemented into the acetabulum [10] proved to be successful and a modified version is used even to this day.

Charnley [37] realised that the prosthesis must be properly fixed in order for it to withstand the loading necessary to walk and any tiny movement of bone against prosthesis would cause pain to the patient. The polymer PMMA was used as a bone cement to secure the prosthesis and has been successfully used since, in its different forms. Charnley was the first to use bone cement to secure the polymer cup, along

with a small head which in theory gave the patient more plastic liner to wear away before a new prosthesis would be needed. Also the reason for the redesign by Charnley was to reduce the "moment of the frictional force". However, the main cause of revision or further surgery has been pain caused by aseptic loosening.

Alternatives to the Charnley included large diameter metal-on-metal designs e.g. The McKee-Farrar was a first generation total hip arthroplasty consisting of both head and cup in 1956 and the Muller followed soon after in 1965 [38], however, these tended to fail in most cases due to frictional torque of the head against the cup. Many of the early designs only replaced the damaged femoral head with either metal or plastic and this would articulate against bone in the acetabular socket. Metal-on-metal designs came back into favour when the cause of aseptic loosening had been discovered [16] as they produced much less wear and offered the possibility of greater stability by using large diameters.

The large majority of the prostheses on offer between the beginning (1950) to the mid 1990's were total hip arthroplasties, which in cases of osteoarthritis in younger patients, resects a lot more bone than is now considered necessary. A new design of hip replacement was evidently needed to help this growing number of patients who would need a long lasting replacement hip as they were still young but offered the promise of easier revision to THA if required later. The Birmingham Hip Resurfacing, went back to its roots with a simple head firmly fixed over the top of the damaged femoral head and a metal cup in the acetabular socket. A similar Smith-Peterson design had not worked in the 1930's and 40's due to fixation problems [38] but with the invention of bone cement and hydroxyapatite coatings, the two components could be properly fixed resulting in much less bone resection.

2.5.2. Friction

Stribeck's work in the 1900's [36](Jacobson *et al* stribeck memorial lecture, Stribeck R, 1902, Die Wesenlichen eigenchaften der Gleit- und Rollen-lager Z. Deutsch. Ing. 46 1341) defined 3 different types of lubrication, boundary, mixed and fluid film (section 2.5.9-2.5.11). These different types of lubrication were defined using the Stribeck curve of Sommerfeld number against friction factor. In analysing

the friction it is possible more fully to understand the lubrication regime. Unsworth [39] designed and built a machine which can measure the friction of both hips and knees *in vitro*.

Amonton [40] observed two basic properties of frictional force culminating in the fact that friction is proportional to normal load

$$F=\mu L \qquad [1]$$

Equation 1 Friction is proportional to normal load

Where F is frictional force, L is load and μ is a constant of proportionality known as the coefficient of friction. It was found that friction was not related to the apparent area of contact, that is the area over which is it possible that asperities from the two bearing surfaces could touch. But it was the actual contact area that mattered [35] and this was related to the hardness of the material and the normal load on the two sliding surfaces.

μ is no longer constant if the primary form of friction is created from adhesive behaviour, in which case μ varies as load to the φ, where φ for a purely elastic material is -1/3. However, in practice almost all materials display some portion of plastic behaviour and therefore, the figure is generally greater.

The coefficient of friction can be estimated, if the surfaces are fluid film lubricated and the lubricant is Newtonian.

$$\mu=\alpha\eta u/Lh_{cen} \qquad [2]$$

Equation 2 The coefficient of friction

$$\frac{h_{\min}}{R_s} = 2.798\left(\frac{\eta u}{E^1 R_x}\right)^{0.65}\left(\frac{L}{E^1 R_x^{\,2}}\right)^{-0.21} \qquad [3]$$

Equation 3 Film thickness equation

$$\lambda = \frac{h_{min}}{Rq} \quad [4]$$

Equation 4 Separation ratio

Where α gives a number proportional to the contact regime of the two surfaces, η is the viscosity of the Newtonian lubricant and h_{cen} is the thickness of lubricant at the centre of the articulating surfaces. Hertzian analysis gives the contact regime in the cases of polymer and metal bearing surfaces.

For full fluid film lubrication to occur the surface separation ratio λ should be greater than 3. The equation is shown below

The three forms of lubrication can be identified from the Stribeck curve. These are full fluid film as mentioned above where $\lambda>3$ and boundary lubrication where $\lambda<1$, mixed lubrication occurs between the two. The different lubrication regimes are identified on Stribeck's plot of Friction factor (f) against Sommerfeld number (z) where these are defined by Unsworth [41] as:

$$z=\eta uR/L \quad [5]$$

Equation 5 Sommerfeld number

$$f=T/RL \quad [6]$$

Equation 6 Friction factor

where u is entraining velocity defined as

$$u= (u_1+u_2)/2 \quad [7]$$

Equation 7 Entraining velocity

u_1 is the velocity of one of the articulating surfaces and u_2 is the other. R is the radius of the bearing and as mentioned above, L is load and η the viscosity of the lubricating fluid.

In Equation 6, T is the torque generated between the articulating surfaces L is again the load and R is the radius of the femoral head or in the case of the knee the radius of the section of the condyle under consideration.

The Stribeck plot Figure 2 identifies the type of lubrication from these frictional results by comparing the shape of the points plotted to the standard graph.

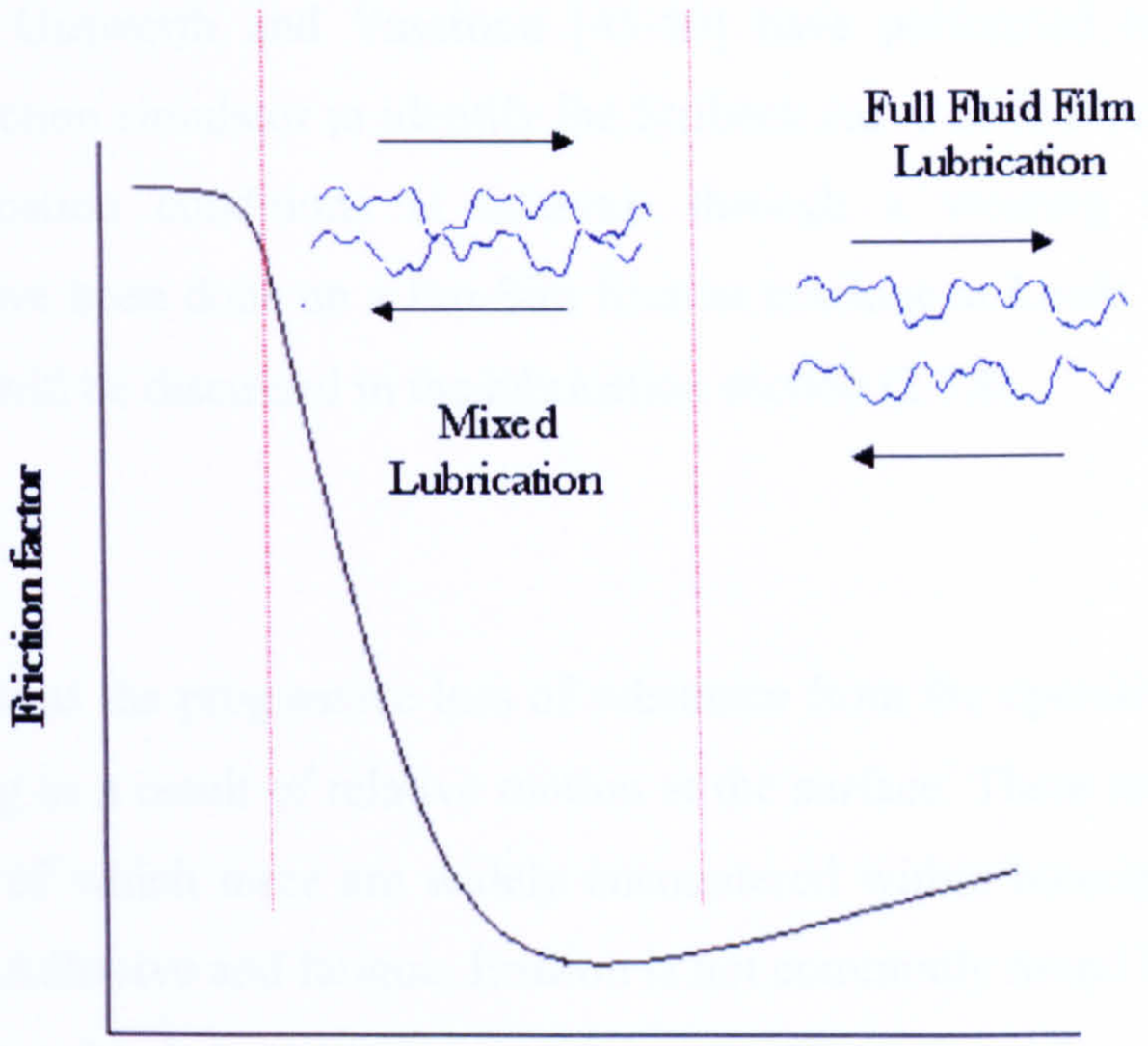

Figure 2 Stribeck plot

Unsworth *et al* in 1975 [42] designed a series of pendulum experiments to investigate the friction and therefore lubrication of synovial and artificial joints. See lubrication section (2.5.8).

A comparison of the friction of Charnley, Muller and compliant layer bearings was conducted by Unsworth *et al* [39]. The results showed that compliant layer bearings in hip joints produce a much lower coefficient of friction which is dependent on the compliance of the layer. Both Muller and Charnley joints were found to have mixed lubrication as found in an earlier study by Unsworth [43], However the compliant layer bearing appeared to be supporting fluid film lubrication and friction was consequently reduced.

Unsworth *et al* [44] investigated the frictional properties of both new and explanted Charnley prostheses. All joints tested showed mixed lubrication. The apposing metal to the UHMWPE seemed to have very little effect suggesting that it was the shearing of the UHMWPE that caused the frictional torque measured. Thirty percent of explanted joints had high friction but these did not coincide with loosening of the prostheses.

Scholes, Hall, Unsworth and Vassiliou [45-50] have performed tests using the Durham hip friction simulator to identify the Stribeck curve of different joints under different lubrication conditions at intervals through a wearing regime. Other experiments have been done on a Pro-Sim friction machine at Leeds university [51, 52], and these will be discussed in the lubrication section (2.5.8).

2.5.3. Wear

Wear is defined as the progressive loss of substance from the operating surface of a body, occurring as a result of relative motion at the surface. There are five different types of wear of which three are widely encountered within bioengineering, these are; Abrasive, Adhesive and fatigue. Erosion is not commonly found in the body and it has been thought that corrosion is only seen after years of an implant being attacked by the body. However, recent evidence is leading to some doubt about this Yan *et al* studied tribo-corrosion influences on CoCrMo amongst other materials. Yan *et al* [53] concluded that bovine serum lubricant accelerated the breakdown of the passivating surface layer of CoCrMo and aided ion release

Within a natural hip joint fluid film lubrication takes place, [43] though it has been found that the THR is not commonly lubricated as effectively as a natural hip joint. This means that a prosthetic joint undergoes mixed lubrication which is a combination of fluid film and boundary lubrication [54] (pp 257).

2.5.4. Abrasive Wear

Abrasive wear is by far the most common and the least preventable form of wear. This form of wear occurs when a hard, rough surface ploughs grooves into a softer

surface e.g. a rough metal surface ploughing grooves through a softer UHMWPE bearing partner. Two-body abrasive wear occurs when only the two articulating surfaces are causing wear. Asperities from the hard surface plough grooves into the softer surface [55]. Within the hip joint three-body abrasive wear also occurs. Hard particles, asperities that have broken off, are trapped between two surfaces sliding against each other. Grooves are ploughed into the softer surface and the material from those grooves is displaced in the form of wear particles, in this case three body loose wear particles. In many cases metal third body particles are pressed into the softer UHMWPE bearing causing abrasive wear of the metal surface by the work hardened particle.

2.5.5. Adhesive wear

Adhesive wear is caused by two smooth bodies sliding over each other and fragments are pulled off one surface and adhere to the other. This arises from the strong adhesive forces set up when atoms come into intimate contact. During sliding, a small patch on one surface comes into contact with a similar patch on the other surface. There is a small, but finite probability that when this contact is broken, the break will not occur at the original interface but within one of the materials. There is a higher likelihood that adhesive wear will occur when the two surfaces are homogenous and of the same material and when the surfaces are smooth so intimate contact is more likely. This type of wear can also occur when there is no sliding. This type of wear can not be eliminated only reduced [54] (pp278).

2.5.6. Fatigue wear

Surface fatigue wear is observed during repeated sliding or rolling over a track. The repetitive loading and unloading of the material may induce the formation of surface or subsurface cracks. These will eventually result in the break up of the surface with the formation of large particles, which leave pits in the surface. This form of wear tends not to occur in systems where other forms of wear are occurring as surface fatigue wear only occurs in systems where the same volume of matter at the sliding surface is stressed and unstressed a large number of times e.g. a prosthetic knee.

2.5.7. Mechanical wearing

The wear volume depends on: the normal load L (N), the sliding distance X (m) and the hardness of the softer sliding component p.

$$V = \frac{kLX}{3p} \qquad [8]$$

Equation 8 Archard wear equation [40]

Where V is volume lost by wear and k is a constant representing the probability of producing a wear particle with the material used.

In this paper [40] Archard proposed that Holm was right in his suggestion that there are two areas involved in mechanical wearing, an apparent contact area which is dependent on the size of the two rubbing surfaces and a real contact area which is dependent on the number of asperities and the contact force. The real area of contact is increased by the plastic deformation of the asperities which are touching the other surface when under a g load. This leads to the theory that increasing the load increases the number of contact areas. It is therefore concluded that the wear rate is not dependent on the apparent contact area and is proportional to the load as shown in the above equation.

Archard assumes that there are two different types of particle removal, that of layer removal where the depth of the material removed is consistent and independent of the load or the radius of the contact area. The other is lump removal where the depth of material torn away is assumed to be proportional to the radius of the asperity in contact. Archard also uses a probability factor in his equation, not all the asperities in contact on the surfaces will form a wear particle and it is a property of the material what proportion of the asperities touching will wear over the sliding distance. Archard also concluded that wear rate is independent of sliding speed as long as the hardness of the softer material and the average wear per sliding distance stays constant, i.e. that the material properties do not change as a consequence of the higher sliding speed e.g. due to frictional heat. As can be seen by the wear equation above wear rate is independent of the model used to represent the surfaces i.e. a pin

rubbing against a plate should both wear equally as long as their material properties are the same. Archard's wear equation is used by many researchers to identify the wear rate (k) of the materials being tested [56, 57].

2.5.8. Lubrication

A human joint within the body undergoes fluid film lubrication [58]. This type of lubrication results in low wear as the surfaces are separated (λ>3) except on starting and stopping the motion. Fluid film lubrication relies upon a film of fluid that lies between the two surfaces. This film is thicker than the combined height of the asperities on the two adjacent surfaces. Mixed lubrication takes place in most prosthetic joints, and occasionally in synovial joints This is a combination of fluid film and boundary lubrication. Boundary lubrication occurs when a physically adsorbed film is formed on the contacting surfaces and the repulsive forces between those two films carry much of the load. This occurs from time to time in prosthetic joints.

Scholes and Unsworth [48] investigated metal-on-metal, metal-on-plastic and ceramic-on-ceramic joint lubrication using the Durham friction simulator, the lubricants used were CMC fluids, silicone fluids and synovial fluid. Both metal-on-metal and metal on plastic demonstrated mixed lubrication with CMC and silicone fluid, however, ceramic-on-ceramic demonstrated fluid film lubrication. When tested with synovial fluid the friction of the ceramic joint was increased ten fold and the metal-on-metal joint friction was reduced by 40% . Jalali-Vahid *et al* discussed the possible lubrication regimes of a metal on UHMWPE hip joint concluding that all current forms of metal on UHMWPE hip replacements operate in the mixed lubrication regime [59]. Femoral head radii of 11, 14 and 16 mm were investigated.

2.5.9. Fluid Film Lubrication

Fluid film lubrication can be achieved by various methods. These include squeeze film, hydrodynamic and elastohydrodynamic lubrication. Squeeze film lubrication occurs when a load is applied to surfaces which have no tangential motion. But between which exists a thickness of viscous fluid. The force causes the fluid to be squeezed out of the gap but the viscosity acts against that action. This generates a

pressure in the fluid which apposes the load and allows fluid film lubrication to take place for a limited amount of time [60] until the asperities touch. The time taken depends on the viscosity of the fluid, the size of the contact, the surface roughness ad the original film thickness.

Hydrodynamic lubrication occurs when a thick film of fluid between the two surfaces is created which prevents their touching. This arises from the entraining action between the two bearing surfaces. The normal load is supported by the pressure within this film. The entraining velocity between the two surfaces and the fluid viscosity can create a pressure big enough to support the normal load on the surfaces [54] if the velocity is sufficient.

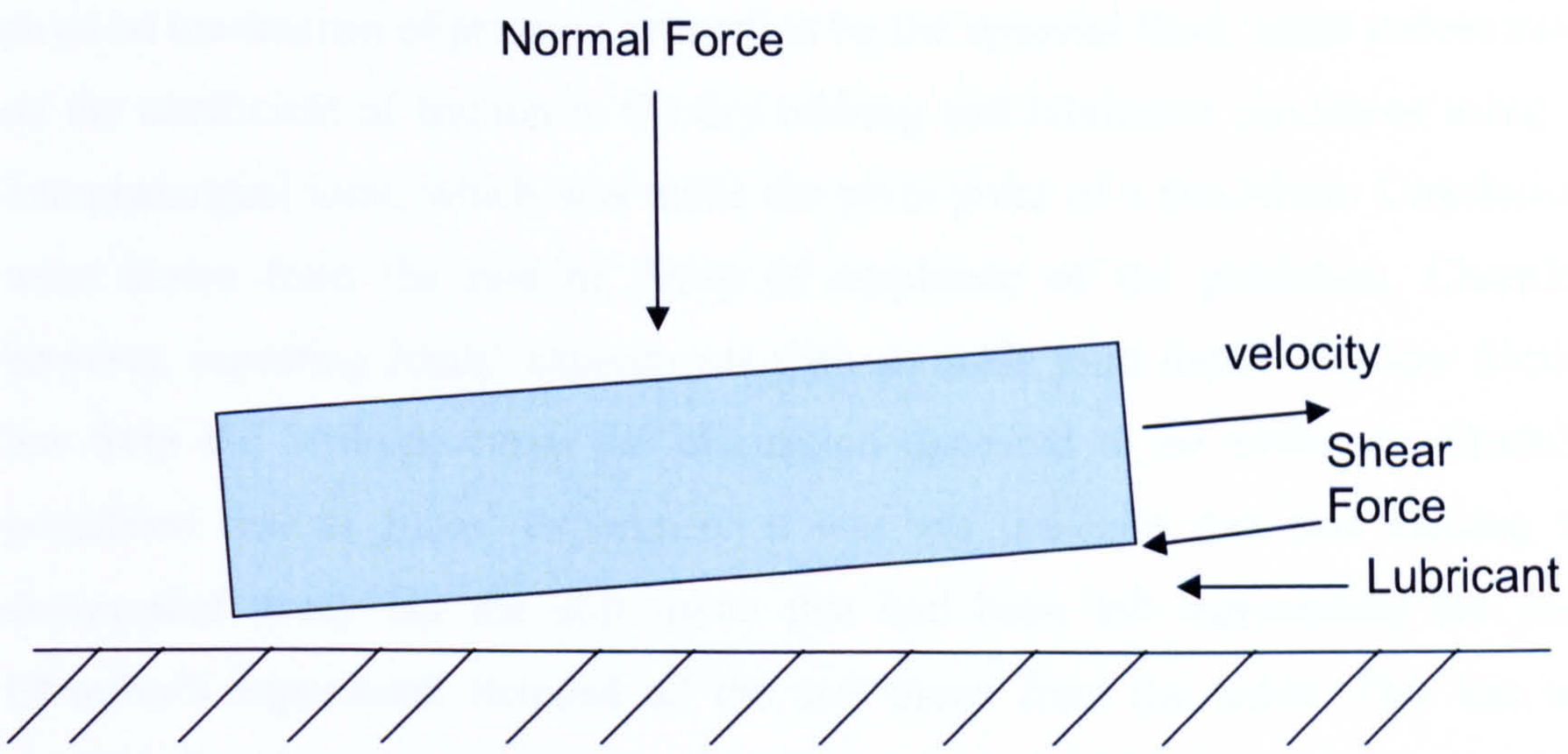

Figure 3 Hydrodynamic lubrication process

Elastohydrodynamic lubrication is like hydrodynamic lubrication but the pressure in the fluid film is sufficiently great to deform the bearing surfaces [54], leading to a larger thicknesses of film. This results in separation being achieved at lower viscosities of lubricant and lower entraining velocities than rigid surfaces. Hamrock and Dowson [61] solved the full equations for the isothermal elastohydrodynamic elliptical contacts for low elastic modulus materials operating under fully flooded conditions.

Microelastohydrodynamic lubrication occurs when the pressure in the fluid film deforms the asperities of the bearing surfaces, hence the surfaces become smoother and the lubrication regime can work more towards fluid film [7].

Friction may be used to help identify the mode of lubrication of a joint. In simulator tests, friction is analysed at intervals and this enables the assessment of the progression of wear and thus gives an idea of how long it will take *in vivo* before the lubrication regime reaches equilibrium.

Unsworth wrote of Reynolds statement in 1886 [58] as the first recognition that the human joint underwent hydrodynamic lubrication. MacConaill, Jones and Charnley investigated the lubrication of human joints [62-66]. MacConaill focused on the physical mechanism of pressure generation by the synovial fluid. Jones concentrated on the coefficient of friction in the dry rubbing and lubricated conditions using an interphalangeal joint, which was made the pivot point of a pendulum. Conclusions were drawn from the rate of decay of amplitude of the pendulum. Charnley, however, repeating Jones' experiments with an ankle joint found very low friction but from the Stribeck curve the lubrication appeared to be boundary. Charnley postulated that in Jones' experiment it was not the joint that was causing the exponential decay but the soft tissue that had been left surrounding the joint, Charnley's experiment stripped all the soft tissue from the ankle. This test was conducted with various viscosities of oil as a lubricating fluid. The effects of the natural lubricant, synovial fluid, which contains proteins and hyaluronic acid was not taken into account. This paper did not mention the exact load applied to the ankle joint but it was a constant load unlike a simulation of walking.

McCutchen [67] proposed a form of lubrication called weeping lubrication, the experimentation was conducted using the proximal end of the humorous of a pig. This cartilaginous surface was pressed against a glass plate and the friction measured. The cartilage when placed under pressure appeared to expel lubricant. It was proposed that the cartilage was like a sponge and that once squeezed, it took time for the small pores in the cartilage to reabsorb water in to the cartilage to allow the friction to fall again. This experiment took place with synovial fluid which would

have allowed a good representation of the action of the cartilage within the body. Walker *et al* [68], using cartilage on glass and synovial fluid as a lubricant observed what was named boosted lubrication which only differed from weeping lubrication in the direction of fluid flow (Longfield *et al* [69]). Walker *et al* suggested that water was squeezed into the cartilage when under pressure concentrating the lubricant and increasing the viscosity. Ling [70] used a model of two cartilaginous disks to prove that the direction of flow could differ in different areas of contact across the cartilage surface.

Dintenfas [71] in 1963 published an article which brought much of the work on the lubrication of natural synovial joints together. This review paper suggested the lubrication regime in synovial joints was elastohydrodynamic lubrication accompanied by squeeze film after unloaded periods. Dintenfas demonstrated that this form of lubrication would possibly cause a film thickness of 10^{-7}m but argued that elastohydrodynamic lubrication alone could not explain the lubrication of synovial joints. The thixotropic properties of synovial fluid and its affinity to cartilage surfaces would also have an effect on the bearing. Later Tanner, Dowson, Higginson and Unsworth calculated film thickness and corroborated that 10^{-7}m would be possible [72-74]. However, full fluid film lubrication could not explain this alone. Tanner suggested that squeeze film lubrication in such a joint would increase the film thickness to above the 10^{-7}m. Unsworth [41] used a simple pendulum machine and added load suddenly or steadily. A rising frictional characteristic was found with the suddenly applied load and a steady frictional value for the steadily applied load. This research corroborated the squeeze film hypothesis suggested by Tanner. These researchers showed that the predominant lubrication under dynamic loading is fluid film. Mixed and boundary lubrication become more dominant when heavy static loading is tested in a natural joint.

Linn and Radin [75] after conducting tests on canine ankle joints using bovine synovial fluid that had had the protein digested, hypothesised that the proteins caused the boundary lubrication within the synovial joint. Triptic digestion of the synovial mucin did not alter the viscosity but caused the frictional coefficient to rise and attain levels close to that found using only buffer solution. The friction was

measured under 40 lb load, at 23 °C and at 40 cycles per minute. It was concluded that the lubricating advantage was not related to the viscosity. Paul [30] and English and Kilvington [31] show that dynamic loading was very important in the lubrication regime of the synovial joint. Dynamic loading enables a pressure wedge to be built up within the joint and hydrodynamic lubrication is attained. When hyaluronic acid is used the lubricant viscosity is altered and therefore friction is increased.

Unsworth *et al* [43] found mixed lubrication from comparison with the Stribeck curve when the friction was analysed for new metal-on-metal (McKee Farrar) and metal on polymer (Charnley and Muller) joints because of the roughness and the small amount of hydrodynamic lubrication the surface asperities touched and caused wear. Higginson [76] also worked on the theoretical lubrication of compliant layer bearings, these bearings demonstrated trapped pools of lubricant in the central region of the bearing lengthening the squeeze film time, Higginson calculated that squeeze film lasted around one second. This was found to be due to the elasticity of the bearing (Bennet and Higginson [77], Higginson and Norman [78] and Unsworth *et al* [7]). Unsworth *et al* designed a compliant layer bearing for the hip joint [79]. Normal elastohydrodynamic lubrication equations do not explain the compliant layer phenomenon but it was found that the roughness of the compliant layer was smoothed by the microelastohydrodynamic lubrication causing the film thickness to be greater than the combined surface roughness and therefore $\lambda>3$ [80] .

Khan [81, 82] and Scholes [83] have recently tested compliant layer hips and knees *in vitro* and a trial of hips in ovine specimens has been carried out . Kahn tested the biostability of four types of polycarbonate urethane (PU) over a three year period as although PU are biocompatible and therefore suitable for many different medical implantable devices (for example heart valves and urethral catheters) the biostability of PU had been cast into doubt (Dow Chemical Company note regarding long term medical implantation 1998). Kahn's results showed Corethane 80A showed the best biostability. Tests in ovine specimens revealed Corethane 80A performed well. The bearing surface showed no significant wear or overall biodegradation after 3 years *in vivo*. Scholes *et al* [83] used a simulator to test a Corethane 80A unicondylar knee replacements. Friction tests were also performed. The results showed very low wear

rates in lubricated conditions up to 5 million cycles. The lubrication regime was very close to full fluid film lubrication. Further clinical studies of compliant layer bearings are being undertaken at this time.

In 1978 Unsworth *et al* [84] showed the frictional torque of a metal-on-plastic prosthesis *in vitro* was less than that of a metal-on-metal joint. More recently with the revival of metal-on-metal implants Vassisilou *et al* [50] showed that over the first 3 million cycles of wearing a metal-on-metal bearing changed lubrication regime, from an initial mixed lubrication regime identified by a high frictional torque to a fluid film lubrication regime dominating. This implied that a "running-in" period was experienced by large diameter metal-on-metal bearings, when the metal surface was self polished. This has been corroborated by the wear rates *in vivo* [2, 85] and means that after this initial "running-in", very little wear will occur as the surfaces will not often touch.

2.5.10. Boundary Lubrication

Boundary lubricants act by forming adsorbed molecular films on the interacting surfaces. Repulsive forces between the films on each surface then carry much of the load and intimate contact between unprotected asperities is limited. Only small areas of naked asperities make contact and friction is lower than that of dry sliding. However some wear does occur.

Rabinowicz [54] pp198 states that boundary lubrication is a form of lubrication where a thin film, of the order of one monolayer of lubricant is interposed between the contacting surfaces. This prevents wear of the surfaces as they are no longer touching.

2.5.11. Mixed lubrication

Mixed lubrication occurs in most prosthetic hip joints [48]. It is a combination of boundary lubrication and fluid film lubrication. Therefore asperity contact occurs and wear is likely. Metal on plastic prosthetic joints have a life time of around 25 years, however, many go beyond this. The joint is supported by fluid film lubrication

at the points where asperities do not protrude and by boundary lubrication where asperities protrude and are more likely to contact.

2.6. Materials

Materials for hip prostheses have several criteria to meet. The material itself and any wear debris must be biologically compatible and corrosion resistant. The material must be able to withstand very high stress levels and must have low friction against its bearing without creating excessive wear. This joint will be used for years without requiring any intervention, so high fatigue strength and toughness are also required. They must also be able to be sterilised without alteration of the material properties. Materials used within the body must be stable for the time they are within the body as breakdown of the components due to the body's own immune system may cause toxicity, inflammation and other severe problems.

Materials which satisfy these criteria are Cobalt Chromium Molybdenum alloy (CoCrMo), Stainless steel (316L), Ultra high molecular weight polyethylene (UHMWPE), Zirconia, Aluminia (Aluminium oxide ceramic), Polyetheretherketone (PEEK) and Polycarbonateurethane (PU).

Of these materials CoCrMo alloy can be modified in different ways to optimise the qualities desired. The alloy can be cast or forged then heat treatments including annealing and Hiping can be applied. These treatments change the morphology of the material's microstructure and although the material itself is chemically identical the wear properties of the material can be very different.

2.7. Non metallic joint simulation

Since 1960 metal on plastic has been a popular alternative to metal-on-metal. McKellop in 1981 [86] conducted an *in vitro* comparison of the available polymers on the market for hip replacement at that time and found that the laboratory wear model provided a valuable, clinically relevant, first stage evaluation of candidate materials. UHMWPE was found to be the lowest wearing of the materials tested and is still available today. Smith *et al* [87] investigated UHMWPE cups articulating

against CoCrMo and zirconia ceramic heads using a Durham hip joint simulator over 5 million cycles. A gravimetric wear rate of 48.2 $mm^3/10^6$cycles for CoCrMo and 38.62 $mm^3/10^6$cycles for zirconia were found and were comparable to *in vivo* results by Kabo *et al* [88] who found a wear rate of 23.4-41.6 $mm^3/10^6$cycles.

Firkins *et al* investigated a ceramic-on-metal articulation. The hip joints were tested along with commonly used metal-on-metal prostheses for comparison and a statistically significantly lower wear rate was observed [89].

Clinical results have been analysed over the long term and show good results. These data provide a good base with which to compare *in vitro* results. Berry *et al* [90] analysed the survivorship over 25 years of two thousand primary Charnley total hip replacements. Survivorship was 77.5% a trend was also noted; that the younger the patient at operation, the lower the survivorship. Women had a better 25 year survivorship than men [90]. Derbyshire and Porter [91] studied 25 patients undergoing primary total hip replacements with the Elite plus from De Puy. Mean age was 60.4 years the survivorship was 96%.Callaghan *et al* [92] reported a study of 69 under fifty's who had undergone a Charnley total hip replacement between 1970 and 1976. Twenty to twenty five years later a survivorship of 71% was reported. A correlation between activity level or gender and wear was not detected and no correlation between increased linear wear of the acetabuluar component and decreasing age at operation was found unlike Berry *et al* however all patients in the study were under 50 at operation and so only a small range of total hip replacement patients had been considered in this study.

Many other material combinations have been investigated including nanocrystaline diamond, who's results were sufficiently promising that further tests are being conducted [93]. Crosslinked polyethylene was introduced in several forms (65-89% crosslinking from irradiation in different designs) [94]. Ceramic-on-ceramic joints have become ever more popular as the manufacture of ceramics produced tougher components which were less prone to catastrophic fracture [95]. Direct contact of UHMWPE to bone was used *in vivo* for 5 to 10 years and found to be unsuccessful

due to a high rate of loosening. It was concluded that direct contact between bone and polyethylene should be avoided by a metal coating or some other material [19].

2.8. Material testing

Pin-on-plate testing is a simple material test to find out how two materials interact with one another under loading and sliding. The pin-on-plate test has been used for many combinations of materials and there are many variations on the design.

Scholes *et al* and Joyce *et al* [56, 96] have conducted tests on pin-on-plate machines proving that it is important to have rotation as well as reciprocation during a materials test.

Jin *et al* and Besong *et al* [97] [98] used mathematical models to calculate the best pin geometry. The hemispherical head appeared to be the best option as even a small misalignment with a flat ended pin can cause excessive wear rates not comparable with those found *in vivo*.

Tipper *et al* and Scholes and Unsworth [27, 96] tested both low and high carbon content cobalt chrome molybdenum alloy samples in a basic materials testing machine over a distance of between 20 km and 250 km sliding distance. Both papers agree that the high carbon content cobalt chrome performed better over the test and that reciprocation and rotation lowered the wear rate of the low carbon content cobalt chrome significantly. Tipper *et al* looked at the surface profile of the specimens and found that those that underwent rotation and reciprocation had a smoother bearing surface after the testing was completed. This was due to the "self-polishing" of the surface. Once an asperity had formed a groove from abrasive wear, the rotational aspect of the motion folded the built up edge over and smoothed out the surface. As this happened over the wear area, the surface became polished. Tipper *et al* also looked at the particulate debris where it was found that the low carbon cobalt chrome produced larger wear particles but not as large as those of a metal on UHMWPE specimen.

Cawley *et al* [99] used a micro-abrasion wear test machine to investigate CoCrMo as-cast, heat treated, Hiped, and sintered or a combination of any of the treatments. It was found that the lower the fraction of carbide in the alloy, the higher the wear. Kinbrum and Unsworth [100] agreed with this using a pin-on-plate machine having tested as-cast, heat treated and double heat treated CoCrMo.

2.9. Metal-on-metal joint simulation

Metal-on-metal hip prostheses have been used widely since the 1960's with the introduction of the McKee-Farrar THR. Many failed due to high frictional torque, however, some remain in use today. The first generation of metal-on-metal prostheses was phased out with the introduction of Charnley's metal-on-plastic alternative prosthesis. This gave much lower friction and fewer initial problems, however, by the early 1980's it was evident that late aseptic loosening was a problem caused by large amounts of inert particulate debris. A second generation of metal-on-metal joints was introduced and by this time improved manufacturing techniques led to higher tolerances. The reason for the high friction in fixation had been widely researched. Improvements in design led to polar contact bearings. Now the second generation of metal-on-metal prostheses has been accepted within Europe, the research has turned to the biological reaction to the metal ions and particles over the longer term. Concerns have been raised over hypersensitivity, carcinogenesis, necrosis and ion overload causing renal failure [101]. Currently even with these concerns metal-on-metal is a good alternative for the younger osteoarthritic patient.

First generation metal-on-metal prostheses were widely reported with the McKee-Farrar and the Ring prostheses seeming to be the most popular. In 1986 August *et al* [102] reported a long term nine year study of 808 hips of which 230 survived. Djerf and Wahlstrom in 1986 [103] studied 154 McKee-Farrar joints which survived from 177 original hips over these 5 years only 5 of these metal-on-metal hips were revised for aseptic loosening whereas 80% of the Charnley prostheses were revised due to aseptic loosening. Jacobson *et al* [4] conducted a similar study over 20 years reported in 1999 only 31 of the 107 McKee-Farrar joints survived the period. Jacobsson concluded that neither the Charnley nor the McKee-Farrar were superior. In-fact the results over the 20 year period were comparable. Brown *et al*, [104]

Higuchi *et al* [105] and Zahiri *et al* [106] all reported on similar McKee Farrar studies and Higuchi *et al* commented that metalosis was found only in unstable prostheses.

Andrew *et al* [107] and Bryant *et al* [108] reported on the survivorship of the Ring prosthesis over 8.5 and 20 years respectively. Andrew *et al* reported 154 of 179 surviving 8.5 years and Bryant *et al* reported a 60.4% survivorship of 253 original prostheses.

These first generation metal-on-metal prostheses showed low wear rates [109-111], however, loosening was often detected in those patients above 65 years of age [112, 113].

In the 1990's a second generation metal-on-metal prostheses were brought out to replace the Charnley metal on plastic prostheses for the younger osteoarthritic patient (this was the Birmingham hip resurfacing BHR). These joints had the advantage of a better surface finish and better clearances both of which improved the lubrication of the joint. Better fixation methods and a further understanding of stress concentration also aided the success of these joints. The second generation brought with it different heat treatments and CoCrMo compositions e.g. Wrought, cast, forged, annealed, hiped, sintered etc. Simulator studies have been used to verify wear rates of these novel heat treatments. Bowsher *et al* [114, 115] tested 2 groups of high carbon 40 mm diameter Hiped, solution annealed or as-cast joints. The research showed no statistical difference between the treatments. This research was conducted on an orbital simulator. The angle that the cup was held relative to the head was 35° compared with the Durham simulator which uses 33° and the Pro-Sim which uses 45°. This may have affected the wear results produced. Dowson *et al* [116] used a 10 station Pro-Sim simulator to test high and low carbon joints both as-cast and wrought materials. The low carbon material exhibited relatively high wear but there was reported to be very little discernable difference between the high carbon, as-cast and wrought materials. Vassiliou *et al* [50] investigated as-cast metal-on-metal large diameter bearings on a Durham hip simulator. An initial running in period was evident and a steady state period was seen after around 1 million cycles. The

frictional results showed an initial lubrication regime of mixed lubrication and as the test progressed the lubrication shifted towards the fluid film lubrication [50]. Scholes *et al* [57] performed an *in vitro* study of low carbon metal-on-metal joints with 2 clearances (22 μm and 40 μm) on a Durham simulator. The smaller clearance appeared to be lower wearing, however, this was not significant. Both the small and large clearances wore less than 100th of the metal-on-plastic joint which had been tested as a control. There was a distinct running-in phase present followed by a steady state for all metal-on-metal joints. Smith *et al* [52] conducted a test on the Pro-Sim hip joint simulator of a range of diameters and clearances of CoCrMo metal-on-metal joints. It was concluded that a larger diameter bearing and a smaller clearance aids lubrication towards the fluid film region therefore reducing wear. All these tests noted a distinct "running-in" phase. They were all performed in 25% bovine serum lubricant. The low carbon joints tended to wear a larger amount when tested by Dowson *et al* [117] and Scholes *et al* [57].

Some researchers have looked at the material individually [118]. A composition modified with the addition of nickel and trace elements of aluminium, titanium and boron was found not to change the casting structure but to improve the transient mechanical properties including tensile ductility of the alloy. Waltz and Karnthaler in 1997 [119] looked at the face centred cubic (FCC) to hexagonal close packed (HCP) phase change in a CoCrMo alloy by identifying twinning using TEM and AFM methods. Shear strain on the surfaces causes this transformation and a pin-on-plate study looking into the phase change [120] concluded that a heat treated CoCrMo alloy resisted this phase change therefore resulting in less wear. However, it was still found that as-cast CoCrMo alloy had the lowest wear overall. Saldivar-Garcia and Lopez [121] investigated the effect of phase transformation from FCC to HCP in CoCrMoC alloys. All hardnesses (ΔHRC) were similar with no statistical differences. Dry sliding on a pin on disk machine at 300 mm/s and contact stress of 3.0 MPa was investigated. It was concluded that the lowest wear rates were with an hcp pin against an HCP plate and the highest wear rate was with a FCC pin against FCC plate. It was also found that differential hardness due to the microstructural features plays an important role in the tribological response of the surfaces.

Since so many different heat treatments have been used on the CoCrMo alloy many different studies of *in vivo* wear rates have been reported . Itayem *et al* [3] reported on a two year follow up using migration measured radiographically as an indicator of possible future failure. It was concluded that the as-cast CoCrMo Birmingham Hip Resurfacing (BHR) introduced in 1997 and produced by Midland Medical Technology (now Smith and Nephew Orthopaedics) show extremely small migration when compared with other uncemented acetabular cups and cemented femoral components. This indicated a good survivorship, however, there are other modes of failure which cannot be analysed in this way. Itayem *et al* [85] also reported on a 5 year follow up which indicated that stability of the BHR was good in the medium term and very small migration was observed. This does not take into account other forms of failure. Sieber *et al* [122] reported the results of 118 retrieved second generation metal-on-metal implants which showed a reduced wear of metal-on-metal prostheses when compared with metal on plasticjoints as well as reporting less osteolysis. McMinn and Daniel [123] reported that double heat treated metal-on-metal resurfacing implanted before 1997 had a failure rate of more than 10% in less than 10 years. In 1997 McMinn changed to using an as-cast component and has had fewer failures since. Treacy *et al* [124] reported a 5 year follow up of 144 patients who had the BHR implanted between August 1997 and May 1998. The study confirmed that a resurfacing is a viable option for the younger patient in the short to medium term. A survival rate of 98% at 5 years was shown. Daniel *et al* [2] in a paper on metal-on-metal resurfacing shows a 99.8% survivorship at 8 years and comments that a resurfacing will allow bone density to remain high where a total hip arthroplasty could lead to a loss of bone mineral density and therefore a possibility of fracture. It is also noted that caution needs to be taken until longer term results are available. Amstutz *et al* [125] reported on a series of metal-on-metal resurfacing with a follow up of 4 years at which the survivorship was 94.4%. The study was from 400 original hips over a 4 year period. It was noted that patients implanted with smaller femoral heads had more loosening or radiolucencies than those patients with the larger diameter femoral components. Back *et al* [1] reported of the first 230 Birmingham hip resurfaces undertaken the survivorship was 99.14% at 3 years.

Visuri and Pukkala [126] demonstrated that first generation McKee-Farrar prostheses did not increase the overall incidence of cancer compared with the general population, either in site specific cancer or overall cancer rate. McMinn and Daniel [123] studied the metal ion levels in whole blood in order to compare the first generation metal ion levels with those of the Birmingham Hip Resurfacing group. There was no significant difference in the groups and McMinn thus concluded that there was no reason to suppose that the long term safety would be any different from that of the first generation of metal-on-metal prostheses. Daniel and McMinn [101] investigated the metal ions and wear rates from BHR's and concluded that the metal ion levels did rise in the blood however by 5 years follow up, metal ions were in a low steady state phase and did not continue to rise.

It is common for metal ions to be released from the metal wear particles created within a prosthetic hip as the saline concentration in the body will catalyse any oxidation reaction that takes place. The reaction is not yet known, Catelas *et al* [24] investigated the quantities of ions released into solution during particle characterisation. Urine and blood tests can show high ion levels in patients with metal-on-metal hip prostheses [127-129]. Cobalt and chromium in different forms can be toxic to the body, when the toxic metal ions get into the blood stream and are distributed about the body.

There is substantial evidence *in vivo* that large diameter metal-on-metal joints have very good short to medium term results. There are reservations about metallic debris causing hypersensitivity, carcinogenic effects and renal failure. Concerns have also been raised about cup angle, an angle greater than 45° has been seen to cause increased volumes of wear debris [130].

2.10. Wear particle debris

Particles are produced during wear due to the contact of asperities. Wear particles vary in size due to material properties and the wear conditions. UHMWPE produces wear particles that lie in the region of 0.3 microns to 10 microns and this particular size range is thought to produce a large amount of macrophage activation which will eventually lead to osteolysis [22]. Macrophages attempt to engulf and eliminate

foreign bodies as part of the normal immune response. When foreign bodies are made of UHMWPE which is indigestible the macrophages cause bone resorbtion. The exact mechanism of osteolysis is an ongoing subject of research, however it is thought that cytokines such as IL-1, IL-6 and tnf-alpha are produced by peri-prosthetic tissue and lead to osteoclastic bone resorbtion [131-134]. A study was reported in 1993 where different sized polymethylemethacrylate particles which were exposed to macrophages in an *in vitro* tissue culture model concluded that particles of between 1 and 12 microns activated macrophages. However, no difference was found between different cement manufacturers [135]. Since 1993 the cause of osteolysis in periprosthetic bone has been linked more to the UHMWPE debris [16, 136, 137] than PMMA.

While UHMWPE particles are biologically inert within the body's environment, CoCrMo particles are not and may cause problems when metal-on-metal bearings shed material in the course of wearing. Early studies concentrated on bulk CoCrMo which gave a variable amount of soft tissue reaction around the implant but was generally well tolerated [138-140]. However, it has been found that particulate debris from the CoCrMo articulations causes a different response so further investigations with particulate debris were undertaken [141, 142].

Size, number, method of production and type of material all alter the response of the body to the particles and so comparison between studies becomes difficult [143-146]. A standard protocol has been developed for the production and characterisation of metal particles of known size shape and concentration. The particles were intended closely to resemble those found *in vivo* and were in the size range 0.5-3microns. A Coulter multisizer was used to determine this size distribution [147].

In order to create an accurate *in vitro* response to particulate debris, the particles must be introduced to a part of the body that simulates the bone and tissue structure of the orthopaedic replacement area. Many studies used intramuscular and subcutaneous sites [140-142, 148]. Some, however used a method where particles were introduced into bone chambers and the effects on the tissue and the bone remodelling were recorded [149, 150]. These investigations found that different

materials of the same size cause different responses by the body. Goodman found that cobalt chromium particles caused a large range of foreign body reaction and chronic inflammatory responses but the high concentration injected may not represent realistic levels in the metal-on-metal articulation.

A limitation of any particle study is that the particles are administered in large quantity to a specific site. This does not accurately represent the gradual release of particles from a prosthesis over time and into a synovial sac or bursar. Further studies have injected clinically relevant particles into the synovial sack or intra-articular cavity to represent more closely the process of prosthetic joint wear [151, 152]. Howie's study of a rat knee showed lymphocyte response to the particles at 7 days. Macrophages and necrosis were seen by 3 months. In later research, Howie discovered that one year after injection few of the particles had escaped from the synovial sack and concluded that over prolonged wearing of a prosthetic joint, particle debris would build up within the intra-articular area. The introduction of cobalt chromium through intra-articular injection caused macrophage death and phagocytosis causing degeneration and necrosis of synovial and sub-synovial cells. At 4 weeks increased numbers of cytolysomes were evident suggesting increased synthetic activity of cells.

Different materials appeared to produce different responses from the macrophages, Al_2O_3 caused what appeared to be a much less severe response to the wear particles within a rat knee joint [146].

Howie *et al* in 1993 [153] showed by electron microscopy that small cobalt chromium alloy particles are engulfed by single macrophages and larger or aggregated particles are either surrounded by densely packed macrophages or by multinucleated giant cells. Even in early studies by Haynes *et al* [154, 155] an increase in TNF alpha was observed released from macrophages after exposure to cobalt chromium alloy particles and this was corroborated by the work of Chiba *et al* [155].

Howie *et. al.* [156] showed that stability of the component and therefore the cement mantle is important to prevent connective tissue formation and small amounts of cobalt chromium alloy may have a less important role in bone resorption than implant stability. There is concern over the toxicity of the individual metals of cobalt and chromium [157]. Intracellular corrosion is an important early release mechanism of cobalt ions. Cobalt chromium alloy has been found to be toxic in large doses [158, 159] but smaller doses of particles are seen to increase collagen synthesis [160]. Cobalt chromium alloy particles may initially be toxic but are well tolerated in long term animal studies [161].

Hypersensitivity is a cause for concern for metal-on-metal cobalt chrome prostheses Hallab *et al* [162] studied 4 groups of patients where hypersensitivity was tested. The groups showed the metal-on-metal total hip arthroplasty group had a statistically significant increase in cobalt and nickel sensitivity compared with the osteoarthritic and metal on polymer total hip arthroplasty groups used as controls. This was a small study and other evidence will be needed to corroborate it. An over aggressive metal immune response is not yet a predictor for poor joint performance. [163]

Catelas *et al* noted that of all the particles that were found in peri-prosthetic tissue 50% were round, 37% oval and 13% needle shaped [23]. This suggests that the particles may have been created by abrasive wear and worn down into the needle shapes due to third body wear.

2.11. Particle isolation

In order to isolate particles from bovine serum lubricant, the protein must be dissolved or digested so that the particles which are entwined can be imaged.

Isolation protocols involving digestion reagents can chemically attack metal wear particles [24], reducing their size and changing their shape. The exposure of wear particles in water to alkaline solutions caused an increasing release of chromium ions. (e.g. particles exposed to 12M KOH for 48hrs during alkali digestion to separate the particles from the serum Besong *et al* [20] display no Cr peak on X-ray

analysis as the Chromium is leached out due to the alkali.) Alkali treatments showed that particles increasingly disappear with time and concentration of alkali.

Many different methods of particle isolation have been used depending on size, particle material, the solvent and the wear mechanism. There are three main types of digestion techniques, acidic, alkaline and enzymatic. Many researchers have reported trying the three different methods and comparing the results obtained to try and discern the best method [23-25, 164]. There is no standard technique, therefore the alkali method used by one laboratory may be completely different from that used within another institution. Below is a comparison of the different methods within the 3 identified groups.

2.11.1. Acid Protocols

Acid digestion is used commonly when analysing particles of polyethylene [164] and other such inert particles and so it is a natural progression to use them on metal particles. However, if the acid is not carefully regulated it can harm the surface of the metal particles and potentially reduce their size.

Niedzwiecki *et al* [164] used 3 techniques in their paper on digestion of UHMWPE particles one of which was an acid protocol. It was found that acid protocols did not damage the UHMWPE particles that were being used. However, Catelas *et al* [23] concluded that acid digestion damaged metal particles by dissolution and this form of digestion was therefore discounted on that evidence.

Niedzwiecki *et al* [164] used 5ml of bovine serum lubricant in each of two concentration gradients using sucrose and isopropanol respectively. Both gradients were spun at 40,000 rpm in an ultracentrifuge. The particles were isolated by filtering a layer containing the particles in the density range of 0.9 to 0.96 g/ml. Acid digestion used 37% volume hydrochloric acid (HCl) added to the simulator serum in a ratio of 5 parts serum to 1 part acid. This was heated to 60°C for 45 minutes and stirred then methanol was added and the solution was filtered using a vacuum filter and a 0.2 micron pore filter paper and followed by 0.1 micron pore filter paper.

Doorn *et al* [25] used both enzyme and acid in the digestion, however as acid had the larger effect on the particles, it is considered in this section. Doorn *et al* looked at periprosthetic tissue samples and it must be borne in mind that this was very different from digesting a bovine serum based lubricant.

Doorn *et al* [25] took samples from 13 metal-on-metal periprosthetic tissues at the time of revision surgery and examined them using a TEM and x-ray diffraction analysis. The isolation protocol for the particles from the tissue involved several washing fractions and the use of MOPS (morpholino propansulphonic acid) in order to denature the proteins present in the samples. The enzyme Papin was used at 55°C.

Revel *et al* [165] also used a combination of acid and Papain enzyme using a density gradient centrifugation or filtration and propylalchol column separation.

2.11.2. Base Protocols

Alkali digestion has been the most popular with polyethylene as no ultra filtration is needed and the alkali does not digest the polyethylene particles. However, alkalis can damage metal particles by dissolution.

Firkins *et al* [26] and Tipper *et al* [18] followed a method used by Besong *et al* [20], where serum was digested using 12M potassium hydroxide for 48 hrs at 60 °C. Contaminants were removed using chloroform and methanol in a 2:1 ratio. Centrifugation then took place at 2000 g for 10 minutes at room temperature. Remaining contaminants were removed by precipitation with ice cold absolute ethanol followed by centrifugation at 2000 g for 2 hrs at 4 °C.

Catelas *et al* [23] used a very low concentration of KOH or NaOH for differing amounts of time to try and digest the protein while doing least harm to the metal particles in the solution.

2.11.3. Enzymatic Protocols

Enzymatic protocols are popular in metal-on-metal particle analyses as they cause the least surface damage to the metal particles and do not produce hazardous waste [23].

Niedzwiecki *et al* [164] used 30 mg Protinease K added to bovine serum in a 1:1 ratio. The activity range of Protinease K is pH 2-11, although a pH of 7.4 is optimal and the pH of the serum is 7.0, very close to the optimum. In this process the mixture was heated to 37°C the physiological temperature for 45 minutes. After completion of the process, 1ml of serum was diluted with 10 ml of distilled water and vacuum filtered.

Catelas *et al* [23, 24] reported the use of Protinease K, because this enzyme can cleave many of the bonds within the proteins found in bovine serum.

The enzymes used by Catelas *et al* [23] to digest the proteins within the serum were Papain, Pronase and Protinease K. Different enzymes work optimally at different temperatures and pHs therefore a tris-HCl buffer was used to obtain the ideal pH for the enzyme. The temperature and length of time of enzyme activity are key features of this type of analysis These differences in pH and temperature do have an effect on the metal particles themselves.

Catelas *et al* [23] noted that enzymatic digestion must result in complete digestion to enable analysis of the particles under the SEM, otherwise this would obscure the particles from view with undigested protein residue. Catelas *et al* also used EDXA to differentiate metal particles from serum residue.

Catelas *et al* [24] suggested that enzymatic protocols caused release of cobalt ions in solution and a corresponding decrease in Co in particle analysis. This situation is exacerbated by the use of sodium phosphate as a buffer as the decrease in the pH will increase the likelihood of a corrosion reaction with the saline in the bovine serum. There appeared to be an initial protective effect of serum proteins, as they bind to the

Cr or Co ions. Particles within a 95% bovine serum lubricant were better protected from the effects of the protocol than those within a water lubricant.

After enzymatic digestion Catelas *et al* [23] used several wash fractions to isolate the metal particles but as a result lost smaller particles in this protocol. Niedzwiecki *et al* [164] used a very simple technique using a vacuum pump, but again, this resulted in the loss of smaller particles which were able to pass through the filter paper used in the vacuum filter.

2.11.4. Assessment of the different protocols

Niedzwiecki *et al* [164] found that all three techniques were regarded as viable options for isolation of UHMWPE particles to determine size distribution and analysis.

Each method successfully removed serum proteins from particles and the particles were separable through standard filtration methods.

Acid and enzyme digestion did not require ultracentrifugation or gradient filtration techniques and the enzyme method generated the least amount of hazardous waste.

Catelas *et al* [23] found that all alkaline treatments reduced the size of all CoCrMo particles. The effects increased with concentration and incubation time. Enzymatic treatment using phosphate buffered saline affected large round and oval particles as well as smaller particles. The Tris-HCl protocol appeared to be the least damaging treatment on the larger particles and on the smaller particles, however, there was still a small difference in size after this protocol.

Methods that use simple centrifugation, inevitably lead to a loss of particles, which are found in discarded wash fractions. While ultracentrifugation of UHMWPE particles can cause altered morphology, this will not happen with metal particles.

Catelas *et al* [24] also concluded that enzymatic digestion protocol was the least damaging to the particles and appeared to be the best compromise for isolation and characterisation of metal particles, especially in 95% serum. The x-ray analysis showed that the main problem with enzymatic treatments to particles in distilled water was a release of cobalt ions after the first incubation, especially when sodium phosphate was used as a buffer. However when considering particles in 95% serum Co^{4+} ion release completely disappeared after both enzymatic treatments. It was hypothesised that this was due to an initial protective effect of the serum proteins and / or lipids. With a lower concentration of serum than that used by Catelas special care should be taken when choosing the buffers, as there will be less protective effect from the protein in the lower protein rich serum.

Revel *et al* [165] used a combination of acid and enzymatic digestion to identify sub micron particles of both titanium and cobalt chrome. These particles ranged from 0.36 to 0.87 microns in diameter. Six tissue samples were analysed and a range of 5 million to 310 million particles per gram of tissue were found. It was undisclosed in the paper what volume of tissue was analysed per sample. Catelas *et al* [23] found much smaller metal particles in *ex vivo* samples using a TEM technique which does not include acid.

The small particles with a large surface area to volume ratio may have been dissolved by Revell's acid protocol or these particles may not have been visible on the unspecified SEM used.

2.12. Particle characterisation

In order to allocate a single number to any shape particle it must be denoted by an equivalent sphere diameter. That is by using its mass and converting the shape into a perfect sphere using $4/3\pi r^3\rho$. The diameter of the sphere will then allocate a single number to the size of the particle. This enabled one unique number to define a particle instead of three or more dimensions, making analysis of a large number of particles much easier.

Using the equivalent sphere diameter, different techniques can give very different values e.g. the Mastersizer uses a low angle laser light diffraction technique. If a cylinder shaped particle were end on to the laser, the equivalent sphere would underestimate the size of the particle but if it were side on, the particles size would be overestimated. Using a large sample would resolve this issue. In an instrument such as a NanoSight the mass of the particle is measured due to the speed at which it moves under Brownian motion and this is a more accurate way of measuring the volume of a particle. An equivalent sphere diameter can then be obtained from this technique. However, these techniques can not be compared not only because the particle size range only overlaps by a very small amount but also because of the averaging technique which has been used to analyse the data. Care must also be taken when comparing these data with microscopic images. A microscope will only image a two dimensional view of the three dimensional particle or in the case of a transmission electron microscope only a section through the particle will be viewed. This makes comparison between the techniques difficult as an equivalent sphere diameter can not be compared to an actual diameter.

Metallic and ceramic wear particles were characterised by Tipper *et al* [27] using transmission electron microscopy. The method for the TEM analysis is long and complex:

Tipper *et al* fixed the pellet produced by the extraction protocol in 2.5% gluterhalderide and 0.1 M phosphate buffered saline at pH 7.4 (slightly alkaline) for 2 hours at 4°C. Samples were washed 3 times in 0.1 M phosphate buffered saline (pbs) and then set in 1% osmium tetraoxide for 1 to 2 hrs at 4°C. Samples were then washed in 0.1 M PBS for 15 minutes and dehydrated through graded ethanol. Samples were polymerised in araldite resin for 20 to 24 hrs at 70°C and 100nm samples were cut using an LKB ultra microtome fitted with a diamond knife. These sections were fitted to copper grids for staining with leas nitrate and sodium citrate for 1 to 2 minutes. The samples were double stained with 15% uranyl acetate, then observed using a TEM.

Niedzwiecki *et al* [164] used a simple technique, the debris was air dried, mounted on stubs, gold plated and examined in an SEM.

Catelas *et al* [23] found it hard to visualise the true length of the smallest particles using the TEM due to the way in which a TEM works. The random orientation of particles within the thin slices of resin meant that the projected lengths tended to be an underestimation of the true length of the particle and in some cases may cause incorrect classification of the shape. The method of preparing a specimen for the TEM can also affect the size and shape of the particles. There are several different methods used to prepare specimens. The discarding of supernatant fluid and the use of pbs and other chemicals will decrease the size of all the particles, which in turn decreases the chances of seeing very small particles as there is a limit to every instrument's resolution.

Doorn *et al* [25] found that the better method for studying metal wear particles was within tissue sections using a TEM. Isolating particles tends to cause agglomeration which makes individual particles difficult to discern under a TEM. In Doorn's study differing percentages of cobalt were found from 57% (almost that of CoCrMo) to zero. The explanation offered is that corrosion within the body reduces the cobalt content.

2.12.1. Biological response to particulate debris

Size and morphology of wear particles affect the body's response. Larger particles as seen from UHMWPE prostheses can cause aseptic loosening and metal debris can cause necrosis of the periprosthetic tissue [18]. Recent studies have shown that the size the wear particles generated in metal-on-metal prostheses are in the nanometre size range [23]. Despite lower wear rates in metal-on-metal prostheses the small particle size makes it possible for more particles to be created than metal-on-polyethylene, despite wear volumes.

Gonzales *et al* [166] studied the biological reaction to bone cement or polymethylmethacrylate (PMMA) wear debris. PMMA particles were found to enhance the release of bone resorbing mediators from macrophages *in vitro*

depending on particle size, number, surface area and volume. PMMA was shown to be non-toxic to macrophages even at high concentrations. This contrasts with Horowitz [132] who found intracellular leakage due to macrophage damage by PMMA. However Horowitz had used a different form of PMMA for the tests. Also different cell lines may have made a difference to the results. Yoneda [167] also found PMMA to be non toxic. The particles of PMMA from fretting wear at the back or stem of the prostheses may build up unnoticed due to the non toxicity of the material. Once the particles reach a certain volume, cytokines will be released and bone resorption will take place [168].

Metal particles have not been shown to give an *in vivo* inflammatory effect. However, areas of tissue necrosis have been associated with small amounts of visible metal particles [18].

Doorn *et al* [25] tested 13 samples only 8 of which appeared to contain metal particles. Particles were found in black or grey peri-prosthetic tissue from revision surgery but not in tissue of a normal colour. Doorn *et al* [25] found both crystalline and amorphous regions within CoCrMo particles the crystalline material had a composition of the original alloy, while the amorphous areas were high in chromium and oxygen but low in cobalt. The majority of the particles were rounded with an average diameter of 42nm.

It has been found in a study into UHMWPE that wear particles below 10 micrometers cause the largest biological response [169]. Green *et al* [22] used ELISA to detect secretions of IL6 IL1beta and TNF alpha amongst others. These macrophage secretions are thought to cause osteoclastic bone resorption and osteolysis, which leads to implant loosening causing pain and therefore revision surgery. Previous studies have investigated UHMWPE wear debris reaction [170]. However, the size and volume of clinically relevant UHMWPE particles were critical factors in the activation of macrophages. The most biologically active were submicrometer in size 0.24 and 0.45 microns. Particles of 1.7 micron diameter only elicit a response at the highest concentration, 100 microns cubed per cell. The major

osteolytic mediators were found to be TNF alpha, IL1, IL6 and PGE2, this was confirmed by previous studies [169, 171].

Cobalt chrome and alumina ceramic particles of relevant size (29.5nm) were generated using a pin-on-plate machine and tested *in vitro* with U937 hystiocytes and L929 fibroblasts. Adenosine triphosphate (ATP) levels were measured for necrosis and apoptosis or proliferation. Cobalt chromium alloy particles produced significant reduction in the ATP levels over 5 days indicating the particles or ions produced were cytotoxic at 5 and 50 microns cubed per cell. Particles of 10 microns cubed per cell did not produce the same reaction and it was hypothesised that a smaller surface area to volume ratio reduced the ion release [172].

Ceramic particles showed no effect on the fibroblasts and the hystiocytes were only affected at 50 microns cubed per cell from day two. Other studies [156] have shown toxic effects of cobalt chrome particles but these were not a clinically relevant size. The concentration required to produce a reaction is unlikely to occur *in vivo*. Howie *et al* (1993) [153] pointed out that the disadvantage of *in vitro* testing is that it precludes complex tissue interactions because the cell culture is separated from the blood supply and possible neural, hormonal and metabolic control mechanisms. *In vitro* data must therefore be treated cautiously.

Goodman *et al* [134] looked at the relation of IL1 and IL6 to the loosening of joints and found that there was a statistically significant difference between well fixed and loose prostheses in the amount of IL1 and IL6 this is corroborated by other research [173-175] both *in vivo* and *in vitro* studies.

Carbon composites are becoming more popular as an alternative bearing material, preliminary tests were undertaken to asses the bio toxicity of clinically relevant particle debris *in vitro*. The results showed no cytotoxic effects on cells used as an *in vitro* model for monocyte and macrophage activation [81].

2.12.2. Range Of particle size

The range of metal particle sizes found by Tipper *et al* was 9-66 nm and the majority of metal particles were round to oval in shape [18].

Current evidence indicates that the sizes of wear particles created by metal-on-metal articulations are very small. Catelas *et al* [23] using a TEM method found particles that ranged from 6 to 744 nm which suggests that Revell *et al* [165] who found particles between 360 and 870 nm may have been unable to detect some particles that Catelas *et al* saw. This may have been due to the acid protocol used by Revell which may have caused dissolution. Alternatively, the magnification of the SEM used may have been insufficient to view particles of that size. Revell *et al* do not state what type of SEM was used to image the samples.

Doorn *et al* [25] found particles from McKee-Farrar peri-prosthetic tissue using a TEM technique. The particles ranged in size from 20 to 834 nm and there was little variation in size and shape amongst these particles. The particles found in this experiment were larger than taken from Catelas *et al* [23], however the overlap was large and the error due to the orientation of the particles in the TEM section may explain this result.

Leeds University researchers [18, 26, 27, 176] found particles from 9 to 66 nm and in early papers [27, 177] it was stated that these particles were found using a filtration method where the particles were caught on 0.1 micron bore filter paper and imaged using an SEM. Later work used a TEM and these papers show images of agglomerated particles with no clearly discernable edges [18, 26].

2.13. Lubricant Composition and behaviour

Synovial fluid is a complex lubricant which cannot be replicated exactly for laboratory purposes. Bovine serum with CMC (carboxymethylecellulose) and sodium azide added is used in varying concentrations to replicate the effects of synovial fluids during laboratory experiments. Scholes *et al* [96] used 30% bovine serum to replicate the effect of synovial fluid in pin-on-plate tests. Bowsher *et al*

[178] used 25% bovine serum as a lubricant in an orbital hip joint simulator. Catelas *et al* [24] used 95% serum to replicate the effects of synovial fluid. The use of 25% bovine serum resulted in 14 g/l protein which was consistent with previous studies undertaken previous to this work and resembles the protein content of synovial fluid.

Bovine serum contains albumins and globulins, however, it lacks hyaluronic acid which is the constituent in synovial fluid that causes it to be viscous. The proteins in bovine serum are sheared during wear testing and so the lubricant is replaced periodically through out the test. In the body the synovial fluid is continually refreshed from the blood plasma that passes through the semi-permeable membrane called the synovial membrane. The cells of this membrane also excrete hyaluronic acid which increases the viscosity of the fluid. The less viscous the synovial fluid in the joint capsule is the more likely it is that the two cartilaginous surfaces will come into contact at some point and start to wear.

In a test to determine the effects of differing concentrations of bovine serum and therefore protein for *in vitro* simulation, Scholes and Unsworth [48] found that metal-on-metal joints show a significant decrease in friction factor between 0% bovine serum and all other concentrations. This was thought to be due to the adsorption of the proteins onto the metal surface and the rubbing of protein on protein causes less friction than that of metal-on-metal, though the reduction in surface tension of the biological lubricants may play a part (Sarah Curran 4th year project mechanical engineering 2008, Lubrication of metal-on-metal hip resurfacing joints).

In summary the aim of this work was to:

- Assess the effect of heat treatments of CoCrMo on wear using a pin-on-plate test.

- Assess the effect of heat treatments of CoCrMo on the friction, lubrication and wear of hip joints over the duration of simulator wear testing.

- Assess the effect of pre-worn and smaller diameter joints on the friction lubrication and wear of CoCrMo hip joints.

- Develop a method of separating CoCrMo wear debris from the lubricant without damage to allow nanoscale characterisation of large numbers of particles.

- Compare the size of debris produced by pin-on-plate tests and simulator tests using matching material and heat treatment.

- Investigate the size of debris produced during simulator tests as a function of material type, joint design and progression through test.

3. Apparatus

The apparatus described in this chapter is used for the analysis of wear of hip joints of different material combinations. The section on pin-on-plate machines describes a material testing device. This machine is used to compare the wear properties of new materials. The Durham hip wear simulator mimics the gait undertaken by *in vivo* joints to provide a wear performance comparable with clinical data over a sustained period. The friction simulator is a tool that is used to determine the different lubrication regimes present on the bearing surfaces to give an idea of whether the lubrication is boundary, mixed or full fluid film (section 2.5.8).

Once the wear rates had been assessed, the particles that were created by these machines were analysed. The surface of the specimens were topographically analysed by a non contacting white light profilometer, the atomic force microscope and the scanning electron microscope. A transmission electron microscope was also used to identify the size and shape of the wear particles that were created by the wear mechanisms of the bearing surfaces and a NanoSight provided particle size data for large, statistically relevant, numbers of particles.

All of these, help to further the understanding of how prosthetic hip bearings wear and will enable future materials and designs to last longer and survive the environment of the body.

3.1. Pin-on-plate rig

A pin-on-plate machine is a material testing device which tests the wear performance of one material when rubbing against another. The machine is versatile and the stroke length, rotation speed, load and reciprocation speed can all be altered to suit the criteria desired.

Pin-on-plate machines have been used for many years to compare the wear properties of material combinations [86, 96, 179]. Some devices provide reciprocation only but these do not represent *in vivo* motion as well as devices with a

rotating frictional vector so rotational and reciprocation designs were introduced to give more realistic wear mechanisms and consequently wear rates [96]. Whilst the stroke length, frequency and stress levels should be similar to the real situation, the geometry of the pins and plates remains simple (flat on flat or sphere on flat) so the contact geometry of real bearings or artificial joints is not reproduced in these pin-on-plate machines. As relatively small samples of a simple configuration are used, the expense of preparing actual prototypes is spared. Also this geometry can be such as to eliminate any possible fluid film lubrication thereby ensuring that the material properties alone are measured. If it is required to investigate boundary lubricants then again these can be examined without the complication of fluid film lubrication. Of course for full tribological assessment full simulators are required (these are described later in detail).

The pin-on-plate apparatus used in this work is described in Joyce *et al* [56]. Figure 4 and Figure 5 below show a schematic diagram of the machine used for the test. All tests were conducted using a reciprocation and rotation motion on all four stations. The machine consisted of a sledge (Figure 4, 6) driven by a 150W DC shunt motor (Figure 1, 8) producing reciprocation along two parallel bars. The CoCrMo plates (Figure 4, 7) were secured in a heated bath which was filled with a lubricant after securing it to the sledge. A plastic frame held the plates in place with grub screws and the frame was itself held in place with a screw and washer in the centre of the bath. The motor was set to 1 Hz to simulate normal walking speed. This ensured that the frictional heating was consistent with hip function as well as the rates of shearing the surfaces of the specimens. A stroke length of 18 mm was used which represents a flexion-extension of 45° on a 50 mm diameter component. A lever arm (Figure 4, 2) provided the 40 N load to the pins. Four 12 V motors (Figure 5, 10) generated the rotation, also at 1 Hz. The level of lubricant in the reservoir was maintained by a level sensor (Figure 4, 9). A feedback loop connected to a k-type thermocouple was used to maintain the temperature at 37°C whilst a counter provided an accurate measurement of the number of cycles allowing the calculation of the total distance slid. The whole apparatus was protected by a plastic cover to help prevent contamination from the atmosphere.

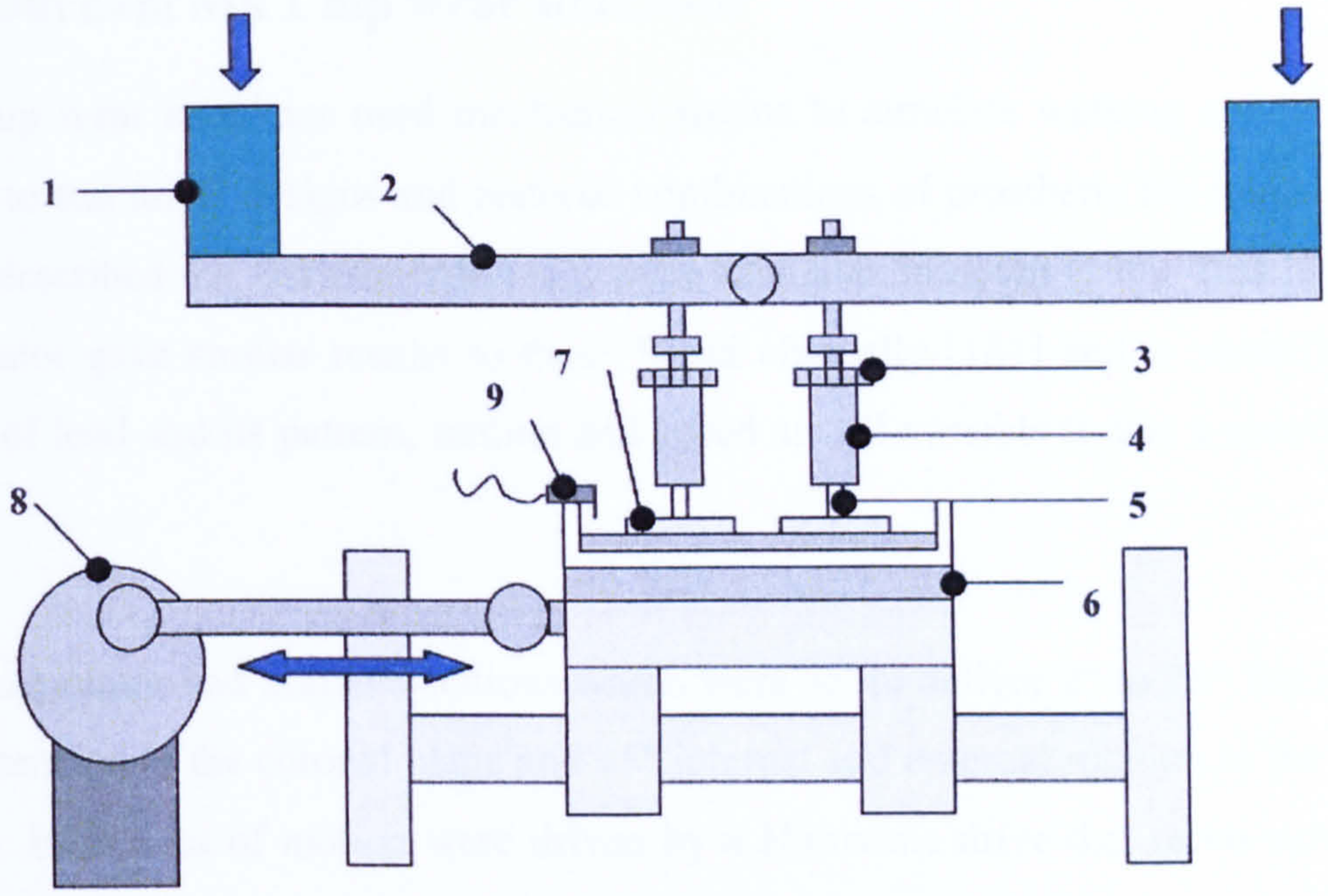

Figure 4 Drawing of Pin-on-plate rig Front view

(1, Mass, 2, lever arm, 3,rotational motor 4, pin holder, 5, pin, 6, sledge, 7, plate, 8, reciprocation motor, 9, level sensor)

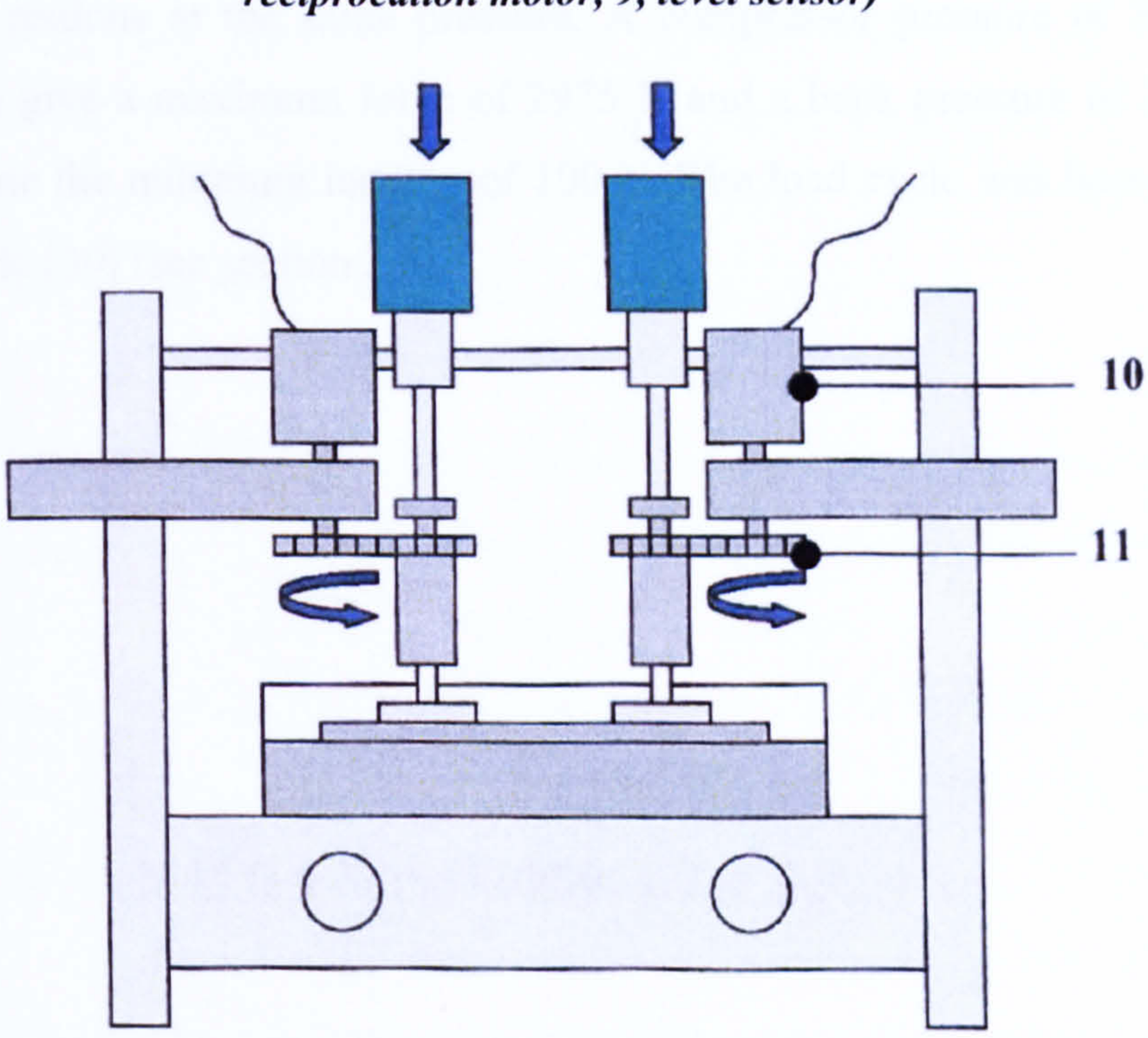

Figure 5: Drawing of pin-on-plate Rig Side View (10, rotation motor, 11, gearing)

3.2. Durham Mk 1 hip wear simulator

The hip wear simulator used mechanical means to simulate walking conditions in order to test novel designs and material combinations of prosthetic hip joints. Smith *et al* described the Durham MK 1 hip wear simulator in detail [180]. This hip wear simulator gave similar results to those found clinically [181] and is versatile. The level of load and its pattern, motion and speed are all variable to test a specific gait cycle.

This simulator had 5 active stations which were set to deliver 2° to 25° flexion and 0° extension in the coronal plane and ±5° internal and external rotation in the sagital plane. Both axes of motion were driven by a Harmonic drive d.c. servo-motor, the speed was also controlled and kept at 1Hz. The sixth station was a loaded control with no motion. The 6 stations were loaded using identical pneumatic actuators via a proportional valve which was used to control pressure to the actuators. A booster valve was also used to amplify the pneumatic pressure and a manifold then fed the air to all 6 stations at the same pressure. A compressor pressure of 8.2 bar was necessary to give a maximum force of 2975 N and a back pressure of 2.5 bar was used to define the minimum loading of 100 N. The load cycle was based on Paul's walking cycle [30] (see section 2.3).

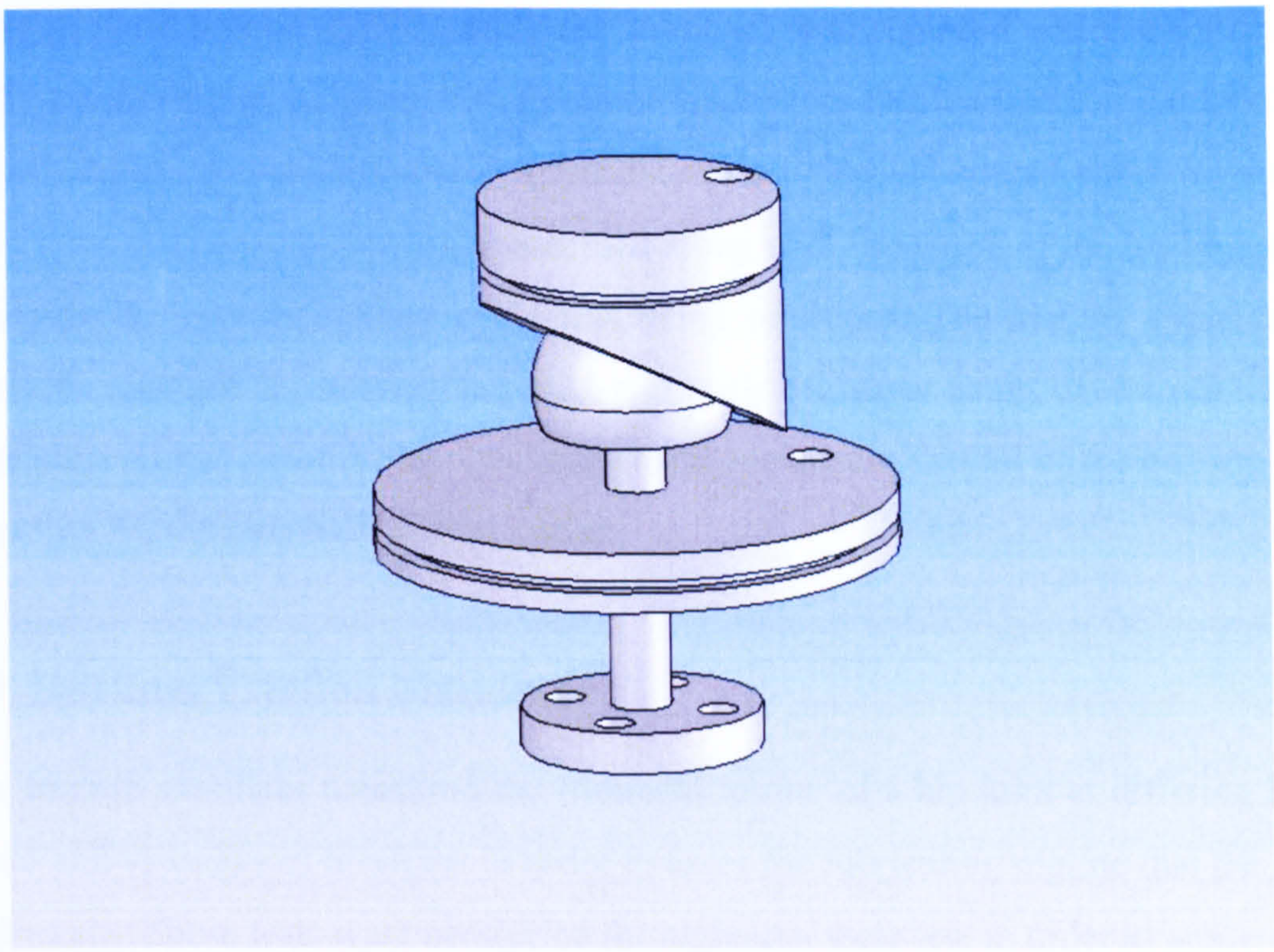

Figure 6 A schematic diagram of the orientation of a complete joint within its holder.

The joints were tested in the anatomical position and, Figure 6 above shows the joint orientation. Each joint was placed within a cell filled with lubricant and the cups were orientated at 33° to the horizontal to ensure that the loading forces were applied at the same angle to the acetabulum *in vitro* as *in vivo* (i.e. circa 12° medially). This assumed the ideal angle of the acetabular component of 45°.

Within each cell the head was fixed to a base plate, using a grub screw to prevent rotation. The baseplate was screwed into the station and the cups were press fitted into ultra high molecular weight polyethylene holders and clamped down with stainless steel rings. A dual pin design at the back of the specimen cup prevented rotation of the cup within the holder. The cup holders were then secured into the simulator with three metal dowels to prevent rotation or rocking motion. The joints were encased within a gaiter and approximately 500 ml of lubricant was added to each joint capsule. The entire cell was inverted to expel air from any pockets which may have been trapped. This ensured continuous lubrication of the joint during testing. Cleaning of the entire cell was easily accomplished as all the parts could be disassembled and washed separately, this helped prevent contamination.

At every half million cycles, while the lubricant was replaced and the joints and holders washed and weighed, the simulator loads were recalibrated using a load cell placed in the control station which fed data to an "Excel" spread sheet where the maximum and minimum could be assessed along with the shape of the loading cycle to ensure the correct loading cycle was being produced. The loading cycle could easily be changed by altering the inlet and back pressures using the valves on the simulator. At this point the rig was also greased to ensure that all of the bearings ran smoothly for the next half million cycles.

3.3. Durham Friction Simulator

The friction simulator measured the frictional torque of a hip joint at differing load, speed and viscosity of lubricant in order to asses the lubrication regime that the joint underwent. These tests were conducted throughout a wear test in order to analyse the lubrication of the bearing surfaces as they "run in". The friction simulator was flexible in its use. The load and the angle of flexion / extension were adjustable between 0-5000 N and 0-40°.

The initial friction tests in the early 1970's were undertaken by Unsworth *et al* [84] at Leeds University using a pendulum machine where the fulcrum of the rig was either a natural hip joint or a conventional metal on plastic or metal-on-metal joint. A special hydrostatic load carriage measured the frictional resistance directly with either a static or dynamic load applied.

The friction hip simulator was born out of the pendulum machine idea [39] but this new device was run by a pc connected to a microprocessor controller, which allowed the angle, load, position and friction to be controlled and recorded. The load was controlled using a servo-controller and servo actuator to provide a square wave loading pattern with minimum and maximum loads adjustable between 100 N and 2000 N. The tests undertaken in this work were divided between the Durham hip function simulator number 1 and the Durham friction simulator number 2. The Durham hip function simulator 1 was originally commissioned by Roberts nd Unsworth in 1982 [182]. The Durham friction simulator number 2 was commissioned later in 1993 by Jon Blamey [183]. Both of these machines have been

described in detail elsewhere [39]. Simulator II is similar to Simulator I, however, there are differences. The loading is applied from above in simulator I and below in simulator II. Simulator II has a larger load range (0-5000 N compared with 0-2000 N) and can be adapted for knees. A brief description of the basic principles of both machines is given below.

These machines are controlled hydraulically and linked to a computer using a microprocessor. The outputs from the rig are analogue and are converted to digital inputs for the computer. The recorded data are friction, angle, angular velocity, encoder position and load. The load is controlled with a feedback loop that regulates the high and low load over the swing and stationary phases of the cycle. There are 4 load cells beneath the carriage supports, one at each corner and the outputs from these load cells are summed and the resultant force measurement is sent to the computer where if necessary an adjustment to the input is made and corrective values are sent to the hydraulic pump to apply more or less force to the joint in a feedback loop.

A dynamic loading cycle based on a smoothed version of the Paul loading cycle and similar to the load recorded by English and Killvington [31] was implemented using a servo-hydraulic cylinder, this cycle had a low load of 100N and a high load of 2000N. The swing was ±24° in the flexion extension plane with a sinusoidal motion and period was 1.2 s.

The joint was tested in the inverted position with the relative angle of the head to the cup kept at 33° as discussed in section 3.2 above. The acetabular cup was placed in a carriage which was lifted on externally pressurised bearings to attain very low friction. The friction generated in these bearings was negligible in comparison with the joints themselves. Two additional bearings sat on top of one another to allow small amounts of lateral medial and anterior posterior movement in order for the cup to centre underneath the fixed head. This method provided a self centring bearing.

A Kistler piezoelectric force transducer was calibrated directly to measure the torque generated by the friction once the load and flexion–extension motion had been

applied. As the piezoelectric crystal in the force transducer was loaded due to the friction within the joint, the crystal produced a charge proportional to the frictional force which was amplified and converted to a digital signal to be recorded by the computer. This force was multiplied by the moment arm of the transducer from the centre of rotation of the joint to give the torque.

Using a jig that accurately matched the dimensions of the friction simulator, the centre of rotation of the joint was located close to the centre of rotation of the measurement carriage (±20 μm).

The Friction factor was used Equation 6 to help define the lubrication regime. The friction factor differs slightly from the coefficient of friction due to the contact area of the ball and cup. The friction factor would equal the coefficient of friction if point contact was occurring between the ball and the socket.

Frictional torque was measured 128 times throughout each of 41 cycles. Cycle 1, 21 and 41 were recorded. Over the high load section 25 points were selected (these points differed for the normal and inverse cycles) each subsequent 5 points were averaged to give 5 average points within the highly loaded region of the cycle. These 5 points were then plotted. Each joint underwent 3 runs at each of 5 viscosities in both the normal and inverse direction.

In order to reduce the error on the frictional torque output, the rig was run in both the normal and inverse directions. This compensated for any eccentricity of the head due to mal alignment of the parts in the flexion extension direction or due to deflections caused by hydrodynamic pressure of the lubrication.

The 5 different viscosities were made up using 25% bovine serum lubricant plus carboxymethylcellulose.

A Ferranti Shirley cone on plate viscometer was used to measure the viscosity of the lubricant. The fluid sample was sheared in a gap between the cone and plate which increased linearly with radius. The apex of the cone just touched the centre of the

plate. A variable speed motor drove the cone and a dynamometer was used to measure the viscous traction of the cone. The dynamometer consisted of a torque spring and a potentiometer. The viscous traction of the cone was calibrated to give the viscosity of the fluid.

The P.C. on which the data were collected was also used for analysis. The values fed to the computer from the microprocessor were encoder position *i*, applied load *Li*, Frictional torque *Ti*, and swing angle *Ai*. With these variables the mean load, frictional torque and angle were calculated. In order to combine the normal (L_{Ni}, T_{Ni} and A_{Ni}) and inverse($L_{I(i=64)}$, $T_{I(i+64)}$, $A_{I(i+64)}$)cycles and take into account the phase difference, the loading cycle for the inverse direction was i+64.

Friction factor was determined at each point using Equation 6 above.

Velocity could be calculated at any point of the cycle using the equation shown below (3.5)

$$u_i = \left\{ \frac{\pi^2 \alpha}{180} f \cos\left(\frac{2\pi i}{128} \right) \right\} R_h \qquad [9]$$

Equation 9 Calculation of velocity during the swing

Where u is entraining velocity, f was the frequency of flexion extension motion, α was the amplitude of motion (24°) and R_h was the radius of the joint.

Finally the Sommerfeld number could be calculated using Equation 5.

A Stribeck curve was then be plotted of friction factor against Sommerfeld number to asses the lubrication regime of the joint (see theory section 2.5.8)

3.4. Non-contacting interferometer

A non contacting interferometer (Zygo Newview 100) uses white light to asses the topography of a surface within a 0.2 by 0.3 mm area (depending on the

magnification). The machine gave a numerical assessment of the roughness of the surface allowing quantitive analysis.

This interferometric profilometer relied on the interference produced by the recombination, with a beam splitter, of two optical beams of white light, one reflected on the sample surface and one from a reference mirror. An optical lens of X2 and a zoom of X10 was used to give an image size of 0.3 by 0.2 mm. Vertical resolution was up to 0.1 nm which was comparable with an atomic force microscope, however, the XY resolution was not as good as an atomic force microscope at 1.1 microns. The software also calculated the average roughness (Sa) the root mean square roughness (Sq) the peak to valley height (PV) and the skewness (Ssk) value over the image area.(where these roughness's etc. are derived from in theory section of in appendix I)

3.5. Scanning Electron Microscope

The scanning electron microscope (Hitachi S2400) bombards a specimen with high energy electrons and records the scattered and re-emitted electrons and energy to build up a picture of the specimen on a microscopic scale. It was used to identify small surface features and to analyse the materials present in the specimen.

The scanning electron microscope operated within a vacuum where electrons were fired at a target. The energy given to the specimen by the primary electron beam could produce several secondary electrons which were magnetically drawn towards the collector. The electron source was rastered across the area causing secondary electron signals to be given off. These signals originated from the inelastic collisions between the high energy primary electrons and the electrons within the specimen. Primary electrons had energies up to 50 kiloelectron volts (keV), the secondary electrons produced from the collision had only a few eV.

3.6. Transmission Electron Microscope

The transmission electron microscope was used to identify nanometer sized features of a specimen. The materials present could also be identified using energy dispersive x-ray spectrometery.

A transmission electron microscope behaves more like a traditional transmission light microscope than the scanning electron microscope. The electron gun fires accelerated electrons (typically 200-400keV) through a vacuum towards the specimen. The beam is controlled and condensed using a magnetic field, this allows the beam to be focused. The beam then passes through the thinly sliced specimen (no thicker than 200 nm). Secondary and backscattered electrons were created as were light photons and x-rays however they were not collected. The electrons that were transmitted through the specimen were projected via lenses onto a cathodoluminescent screen in order to get a visual image. Local brightness on the screen is proportional to local electron beam density.

Theoretical resolution of the TEM is

$$r_1 = 0.61\frac{\lambda}{\alpha} \qquad [10]$$

Equation 10 Theoretical resolution of TEM

Where r_1 is the smallest separation between two point features which allows them to be distinguished.

λ is the wavelength of the radiation (typically 0.0037 nm)

α is the semi-angle subtended by an aperture (typically 0.1)

Therefore the smallest resolution is 0.02 nm or 0.2 Å.

Backscattered electrons gave a little more than topographical information. The electrons given off as backscatter had comparable energy with the primary electrons

and were sensitive to the atomic number of the specimen. For more precise elemental analysis, energy dispersive x-ray analysis was used. This technique used the energy and number of characteristic x-rays emitted from the specimen to determine elemental makeup. The x-ray detector was a thin slice of silicon or germanium with a surface area in the region of 300 mm^2. As x-rays could not be channelled, the detector had a large surface area. A Berillium window protected the x-ray detector from contamination from the vacuum pump oil. The thin slice of silicon was doped with lithium to form a semiconducting x-ray detector when maintained under high vacuum at liquid nitrogen temperatures. This wafer was located between thin metal electrodes to maintain a bias voltage, this electrode was usually gold. This cooling, doping and biasing ensured a low background electrical current from which it was easier to detect a pulse. A pulse was produced from the incident x-rays on the detector. Each x-ray has a specific energy depending on which element caused it. This energy will give rise to electron hole-pairs being formed in the detector. The charge caused by these electron hole-pairs was swept from the detector by the bias voltage. This was integrated to give a pulse which had an amplitude proportional to both the energy of the incident photon and number of x-ray photons. Thus providing the specific element and concentration of the element. The energy detected was separated into a number of energy bands and recorded. A spectrum showing all the detectable elements from the specimen could be displayed and recorded.

3.7. Atomic Force Microscope

The atomic force microscope (AFM) is a type of scanned proximity probe microscope. It uses the attractive or repulsive forces between a tip and the specimen surface. In contact mode (repulsive force mode) the AFM lightly touches the tip at the end of a flexible cantilever on to the sample. A raster scan drags the tip over the sample and a laser which is focused on the end of the cantilever detects the vertical deflection of the tip. The laser beam is reflected off the cantilever and strikes the position sensitive photo detector consisting of two side by side photodiodes. The difference between the two photodiode signals indicates the position of the laser spot on the detector and thus the angular deflection of the cantilever. The tips are generally made using microlithography, the radius of the end of the tip is most important as it determines the resolution of the AFM. In this way a 3 dimensional

image of the specimen can be built up. AFM's contain a feedback loop which regulates the pressure of the tip on the sample. This allows acquisition of images at very low forces. The feedback loop aims to keep the deflection of the cantilever constant by adjusting the voltage applied. The feedback loop is a PID therefore, the faster the deviation of the cantilever can be corrected, the faster an image can be recorded.

3.8. Mastersizer

The Malvern Mastersizer was a low angle light diffraction measurement device used for analysing the size of particles dispersed within a liquid.

The Malvern Mastersizer used a small sample dispersion unit to feed wet samples into the chamber where low angle laser light was fired through the sample and the deflection of the sample was used to calculate the size of the particles present. The diffraction angle of the laser light is directly proportional to the inverse of the size of the particle. There are two main ways of calculating the particle size. By solving Maxwells equations exactly using Mie theory which takes a long time but gives an extremely accurate answer or by using Fraunhoffer theory which approximates the answer. For larger particles (>10μm) the Fraunhoffer method accurately simulates the Mie theory. However this is not so for particles less than 10 μm. With the improvement in computational power it is now possible for the Mie theory to be used for all particle sizing allowing more accuracy in the size distribution which will be focused on in this thesis.

The mastersizer, like all laser diffraction instruments uses a laser which was fired through a beam processing unit at a particle ensemble. The light is scattered, some of the scattered light is collected by the fourier lens and directed to the multi element detector. In the case of this machine the sample is dispersed in water and driven through a glass cell. The cell must be clean and scratch free for an accurate particle distribution to be gathered. A background reading was conducted every test to avoid any small imperfections affecting the results.

This instrument allowed the analysis of millions of particles every test giving statistical reliability to the results and minimising the impact of any outliers. The mastersizer also assumed that all particles were spherical. From previous work [24] it is known that the particles range from round to needle shaped thus the mastersizer accentuated the range of sizes as it may measure the narrowest or widest part of the same particle.

3.9. NanoSight

The NanoSight is an instrument designed for the purpose of identifying the size of nanometer sized particles in a liquid environment. The theory of Brownian motion is used in conjunction with the Stokes- Einstein equation to calculate the volume of the particle from the speed at which it moves within a liquid of known viscosity.

The NanoSight LM10 consists of a microscope with a CCD camera attachment, the camera is connected to a computer. The microscope does not use a light, a small box is placed where normally a microscope slide would be placed. The box encases a class 4 laser and incorporates a cell into which the liquid containing particles could be placed. The red laser light passes through the liquid in the cell and is diffracted around the particles. By focusing the microscope onto the laser light the evidence of particle can be recorded by the camera.

The camera feeds the video to the computer where it is stored and analysed later. The video is run using the NanoSight software, which records each laser light dot visible at each frame and tracks each dot as the video continues frame by frame. Each dot representing a particle, is individually analysed and the speed of its movement is used to calculate its volume using the Stokes-Einstein equation. The data are then recorded and a histogram is plotted showing how many particles of each size were recorded in the duration of the video clip. Any particles bigger than 2 microns will not be seen as they will usually sink out of the focal plane of the microscope, depending on the density of the liquid and of the particle. Any Particle that is not visible for longer than 7 frames will automatically be discarded. The particles move in the z plane in and out of the focal plane so some may disappear during the video clip and some may appear.

Although this instrument can analyse the volume of a particle it can not predict shape so every particle is assumed to be a sphere. From the literature and images taken by SEM, TEM and AFM this is not true, the particle's shapes range from spheres to needle shape.

4. Materials and Methods

4.1. Materials

Permanent implants for orthopaedic functions have been available for almost a decade. Over this time, the materials and manufacturing procedure of these components has vastly changed. Charnley in the 1960's favoured polymer bearing components as they are bio-inert, however when it came to light that the large amounts of wear debris were causing osteolysis, metal components became more popular and cobalt chrome molybdenum has proved to be a lower wearing bearing material. There are still concerns over the metal ion release from the wear debris, however, metal-on-metal bearings produce much less debris than UHMWPE, and few cases of hypersensitivity and necrosis have been reported so long as the components are positioned correctly.

4.1.1. High carbon as-cast cobalt chromium molybdenum alloy

Cobalt chrome molybdenum alloy is a well used metal for both metal-on-metal and metal-on-polymer hip resurfacing devices. It is corrosion resistant which makes it ideal for use within the harsh environment of the body. The cast form of cobalt chrome (F75) has hard carbides embedded into a softer matrix of material. This makes the material hard to polish. The polishing process can pull the carbides out of the matrix leaving holes in the polished surface giving an initial negative skewness on the surface. Cobalt chrome is a ductile, corrosion resistant, biocompatible material. It is made up of two types of crystal lattice structures, face cantered cubic and hexagonal close packed.

Figure 7 micrograph of etched as-cast surface

4.1.2. Medium carbide heat treated cobalt chromium molybdenum

Medium carbide cobalt chrome molybdenum alloy is a single annealed (1300ºC for 4 hours) form of the cast material. It is solution annealed at 1300°C for 4 hours and then quenched to room temperature. This allows some of the carbides to dissolve into the CoCrMo matrix making a more homogeneous material.

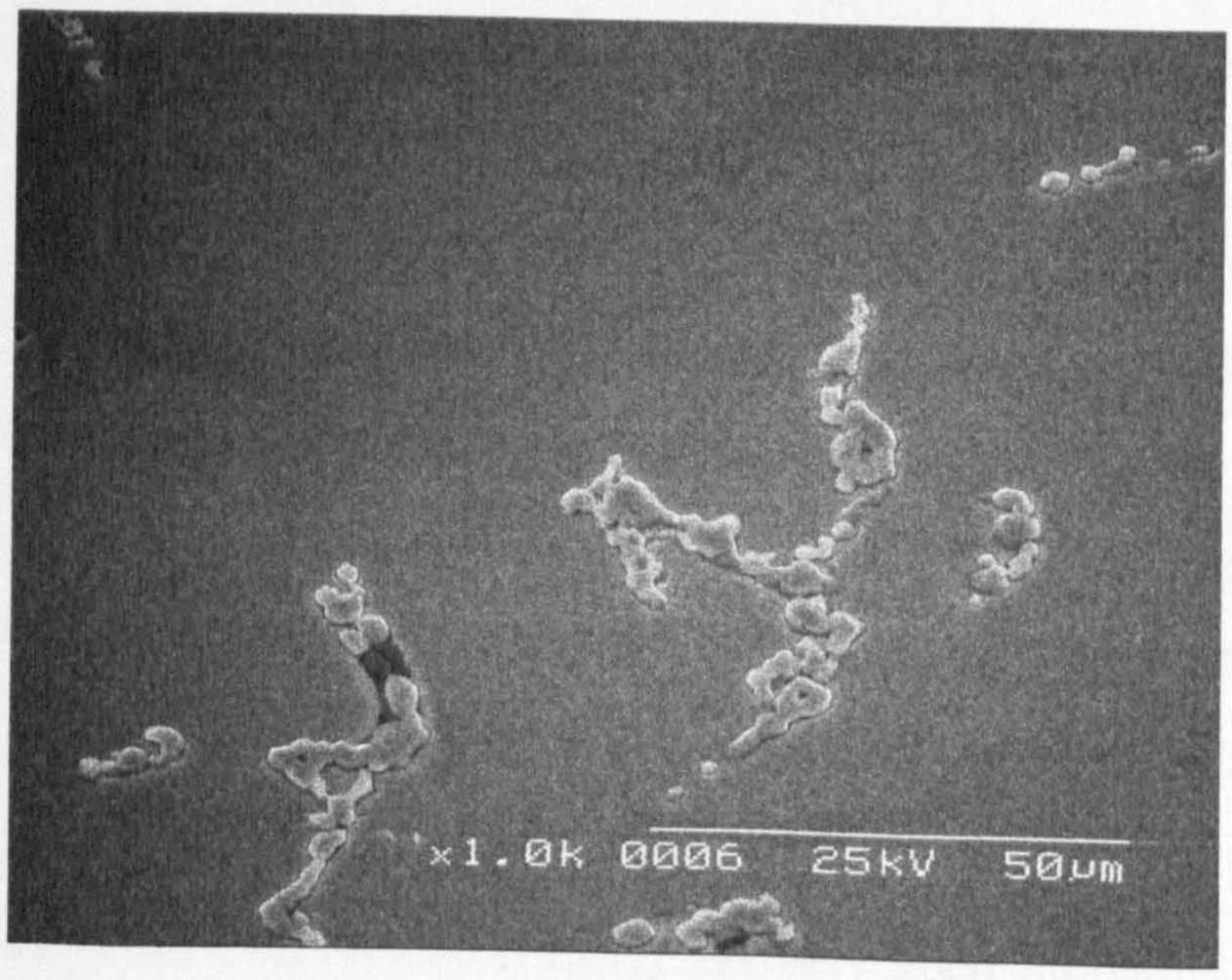

Figure 8 micrograph of etched single annealed surface

4.1.3. Low carbide double heat treated cobalt chromium molybdenum alloy

Low carbide cobalt chrome molybdenum alloy is a repeated annealed (1300ºC for 4 hours twice) form of the as-cast version. The as-cast material undergoes two heat treatments each of 4 hours at 1300°C and then quenching to room temperature. This treatment dissolves practically all of the block carbides found in the as-cast composition into the matrix material making the material homogenous.

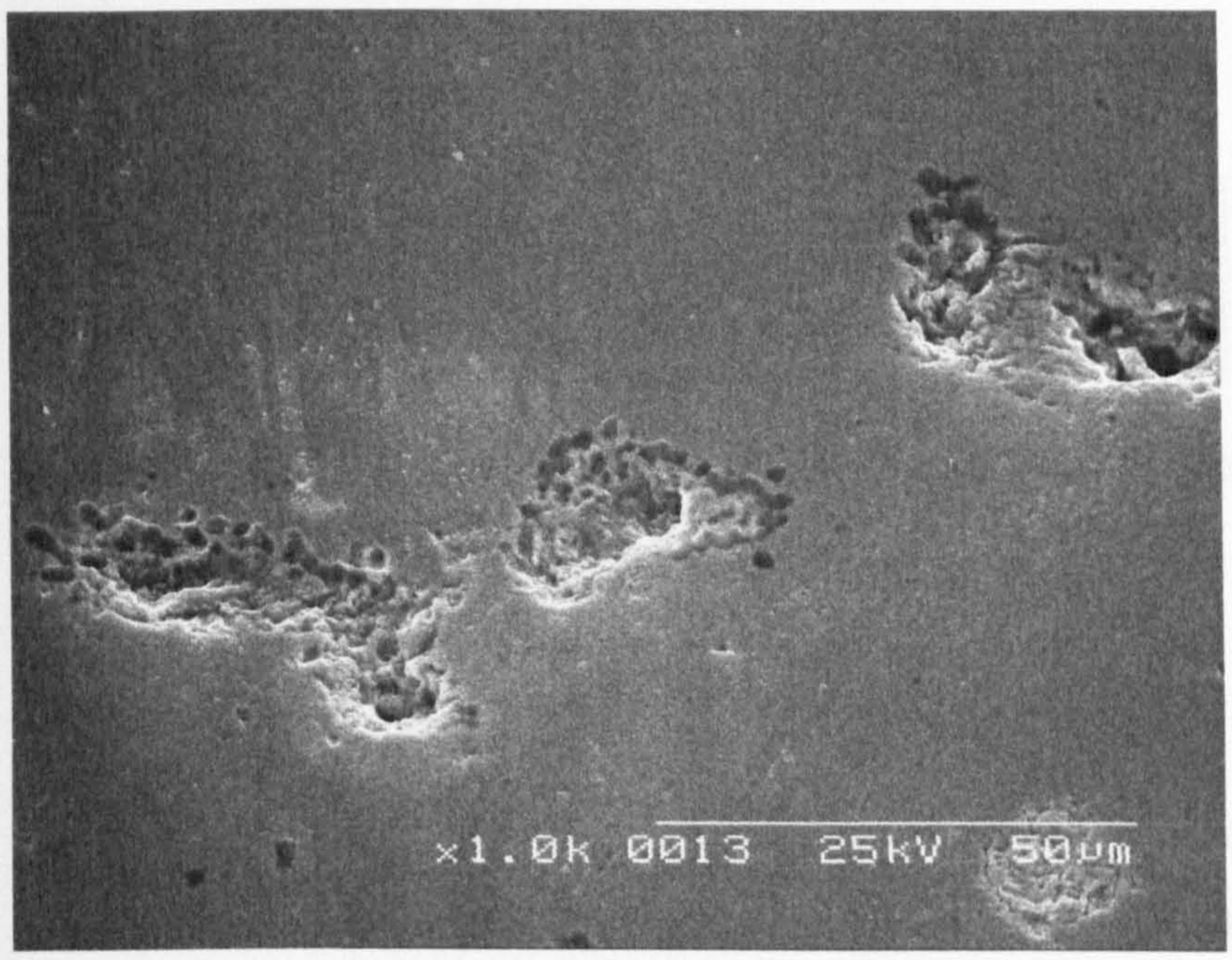

Figure 9 micrograph of etched repeated annealed surface

4.1.4. Plasma carburised cobalt chromium molybdenum alloy

Cobalt chrome molybdenum alloy which is as-cast form is then coated with a layer of carbon by deposition of a fine carbon powder using an oxygen plasma. This coating is less than a micron thick and is a much harder, more brittle material.

4.1.5. PolyEtherEtherKetone

Polyetheretherkeytone (PEEK) has very good properties especially heat resistance melting at around 350°C. This durable material is used for many medical as well as engineering applications. PEEK is partially crystalline with two glass transition temperatures at around 140°C and 275°C depending on precise formation. PEEK is

often reinforced with around 30% carbon fibre, this improves some of its properties for example flexural stiffness and thermal conductivity.

The chemical resistance of PEEK is high to alkalis, alcohols and aromatic hydrocarbons. Its resistance to some types of acid is poor e.g. concentrated sulphuric, nitric, hydrochloric and other mineral acids. PEEK shows very poor resistance to hydrofluoric acid and oleum.

PEEK's structure can be seen below

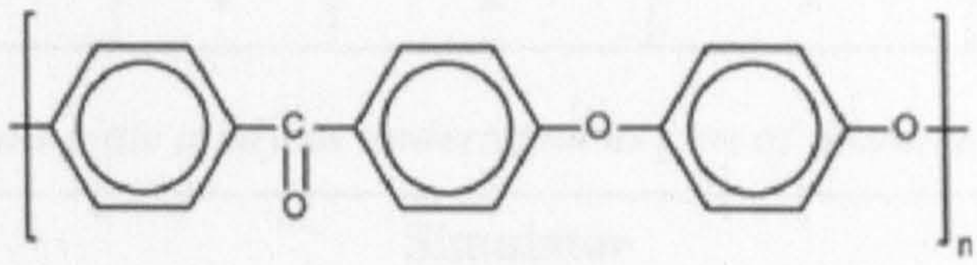

PEEK can be described as [-oxy-1,4-phenylene-oxy-1,4-phenylene-carbonyl-1,4-phenylene-].

4.1.6. Polycarbonate urethane

Polycarbonateurethane is a common polymer consisting of liquid diisocyanates and liquid polyester diols linked by a urethane group. The polyurethane group has a wide variety of uses varying from spandex or lycra to upholstery foam and sail boards. Polyurethane is a very versatile material and can be altered to be biocompatible and non toxic as well as malleable. For artificial joints polyurethane is used as a compliant layer bearing [7].

4.2. Methods

There are now several different laboratory test which combined enable a greater understanding of the tribological performance of novel materials and designs for artificial joints. Tables 1 and 2 summarise the work that has been performed in this thesis or by others (referenced).

Pin-on-plate				
	As-cast	Single heat treated	Double heat treated	PEEK (Pan) against ceramic
Wear test	✓	✓	✓	Scholes
Zygo	✓	✓	✓	Scholes
SEM	✓	✓	✓	×
Particle analysis	✓	✓	✓	✓
NanoSight	✓	✓	✓	✓
TEM	✓	✓	✓	×
AFM	×	×	×	✓
Mastersizer	×	×	×	×

Table 1 Pin-on-plate analyses undertaken as part of this and other studies

Simulator							
	As-cast 38 mm	As-cast 50 mm	As-cast Modular head vs worn cup	Double heat treated	Plasma carburised	PEEK acetabular cups	P.U. Knees
Wear test	✓	✓	✓	✓	Vassiliou [50]	Scholes [8]	Scholes [83]
Zygo	✓	✓	✓	✓	Vassiliou [50]	Scholes [8]	Scholes [83]
Friction	✓	✓	✓	✓	Vassiliou [50]	Scholes [8]	Scholes [83]
ESEM	×	×	✓	×	×	×	×
Particle analysis	✓	✓	✓	✓	✓	✓	✓
Nanosight	✓	✓	✓	✓	✓	✓	✓
TEM	✓	✓	✓	✓	✓	×	×
AFM	×	×	×	×	×	✓	✓
Mastersizer	×	×	×	✓	×	✓	×

Table 2 Simulator studies undertaken as part of this and other studies

4.2.1. Pin-on-plate

Three materials have been tested on a pin-on-plate test rig; as-cast high carbon (0.266wt%) high carbide material, heat treated high carbon (0.266wt%) medium carbide and double heat treated high carbon (0.266wt%) low carbide.

For each material five pin and plate pairs supplied by (Smith and Nephew) were tested on the Durham pin-on-plate machine to 3 million cycles. Four of the pins and plates underwent rotation and reciprocation at a frequency of 1 Hz and the final pair was used as a control. The Stroke length was 18mm. The load on the pins was 40N. Surface topography was measured at the start and end of the test using a Zygo NewView 100 non-contacting profilometer. Ten roughness measurements of each of Sa, Srms, PV, Ssk were taken from each of the plates and one from the pins. Only one reading of the pins was taken initially as the hemispherical head could only be analysed at the pole. The method described and equipment used is identical for each of the 3 tests performed.

The pins were 6mm diameter and cylindrical in shape. The bearing end was hemispherical and a flat was added to the side to secure them with a grub screw in the pin holder. The plates were 25mm diameter with a segment ground off on one edge to hold them with a grub screw in the lubricant bath. These were made from the same materials as the pins. All three materials were chemically identical to each other, the material has undergone various heat treatments to alter the internal morphology. Therefore the material behaviour was expected to be different even though the material was chemically indistinguishable.

Specimens were cleaned and weighed initially and after each period of approximately 250 000 cycles of wear, following the ISO standards 14242-2 [184] (appendix II shows the full cleaning protocol). A Mettler AE200 balance was used to weigh the samples. This balance measured up to 205 g with a sensitivity of 0.1mg. The changes in weight were recorded and the volume loss was calculated using the density of the material (0.0082 g/mm^3).

The test was carried out in bovine serum lubricant (batch number 5030401, Harlan Sera-lab, total protein content 56 g/l) diluted to 25% with distilled water. Added to this was 0.2% sodium azide and 20 mM EDTA (ethylenediaminetetraacetic acid) to help resist biodegradation of the lubricant and calcium deposit formation respectively. The test was carried out at 37 °C and the lubricant temperature was monitored using a K-type thermocouple which was attached over the edge of the bath. The unused serum was kept frozen at -20 °C and made up as needed, after which it was kept refrigerated at 4 °C.

Each of the 5 plates were washed cleaned and weighed following the ISO standard, the surfaces were examined using the Zygo New View 100 non-contacting interferometer. The Durham pin-on-plate machine was taken apart and cleaned in order to avoid any contamination. The 4 test samples were secured in to a specially designed holder made from perspex with the use of a grub screw which located against the flat on the test plate. This secured the plate and prevented rotation, therefore ensuring the wear area was consistent. The pin was held in a pin holder attached to a 12 V, 6.25 W motor. The fifth, control pin and plate, were placed in a sealed jar of lubricant within a water bath set at 37 °C. The machine was re-assembled with all four pins and plates in place. The pin-on-plate machine was filled with 50 ml lubricant and reciprocation and rotation was initiated for 250,000 cycles. During the 250,000 any water that evaporated from the covered lubricant bath was automatically replaced with distilled water from a reservoir. The pin-on-plate machine was stopped as close to 250,000 cycles as was feasible, the machine was dismantled and the pins and plates were removed carefully. The lubricant was saved and the lubricant bath was rinsed with distilled water which was added to the lubricant so that as few particles as possible were lost. The pins and plates were again cleaned and weighed and the protocol was repeated until 3 million cycles were reached. At 3 million cycles, after cleaning and weighing, the surfaces were again examined using the Zygo New View 100 non contacting interferometer and roughness measurements were taken. The plates were then examined using an Hitachi S-2400 scanning electron microscope.

4.2.2. Cleaning and Weighing

The cleaning and weighing of all the specimens took place before each test was started in the case of the pin-on-plate specimens the test the cleaning and weighting protocol was carried out at each 250,000 cycles and at the end of the test. These gravimetric data were used to calculate the mass loss over the testing period. The density of the material was used to calculate the volume loss over number of cycles and the stroke length was then incorporated to give volume loss per km slid. The gradient of this data, when plotted, then gave the wear rate for each specimen.

For the test joints the cleaning and weighing protocol took place before testing, then again after friction testing and thereafter every 500,000 cycles in the wear simulator until 3 million cycles.

4.2.3. Non contacting interferometer

The non contacting interferometer used a non invasive technique to identify and quantify surface characteristics of the materials tested. The surfaces were analysed before the start of each test and at the 3 million cycle point. If the test went on to 5 million cycles the surfaces were analysed at the termination of the test. This allowed the quantification of the surface roughness at intervals during the test. The roughness along with the minimum film thickness (hmin) allowed the calculation of lambda (λ) see chapter (2.5.8). The lambda value gave an indication of the theoretical lubrication regime.

The skewness was also measured. This gave an indication of whether the surface underwent boundary, mixed or fluid film lubrication (see section 2.5.8).

The specimen was placed on the microscope platform in a holder to maintain the correct orientation, e.g. in the case of the head the wear patch was imaged. The light was adjusted to allow the best possible image to be taken. The image was taken and the clean joint was moved with a gloved hand so another wear area could be imaged. This was repeated until 10 readings had been recorded for each specimen. The images were saved and roughness values tabulated for later analysis.

4.2.4. Wear Simulation

Sets of 38 mm and 50 mm joints were tested up to 5 million cycles in Durham wear simulator I (described in section 3.2). The joints were paired to obtain clearances of similar size for each set of 5 heads and 5 cups. The paired components were cleaned, dried and weighed using the protocol described (Appendix II). The components were assembled into individual units with the head sitting below the cup within a lubricant of 25% bovine serum (14g/l protein). The cup was press fitted into an UHMWPE cup holder and the head was push fit onto a tapered stem which was height adjustable via a base plate. A rubber gaiter was placed over the entire cell and the lubricant was poured into the sealed cell via a tube. Finally the tube was attached to the cell at both ends. The load cycle was checked using an independent load cell and confirmed to be the Paul loading cycle of maximum 2975N and minimum 100N. Once everything had been checked for leaks, the simulator was started for half a million cycles. At the 500,000th cycle the simulator automatically turned itself off and as soon as possible each of the 5 cells were dismantled carefully and the serum was siphoned off into bottles. The dismantled parts were cleaned and the heads and cups were washed, cleaned, dried and weighed according to the protocol (Appendix II). The gravimetric change was recorded and another half million cycles were conducted. This continued until 5 million cycles had been achieved. Non contacting white light interferometer measurements of the bearing surfaces were taken at 0, 3 and 5 million cycles along with friction tests.

4.2.5. Friction simulation

In order to asses the lubrication regime of the joints friction tests were carried out at 0, 3 and 5 million cycles. Lubricants were made up of 25% bovine serum (14g/l protein) with added EDTA and sodium azide and the viscosity was altered with the addition of corboxymethyle cellulose. Five different viscosities were made at $1x10^{-3}$ Pa s, $3x10^{-3}$ Pa s, $10x10^{-3}$ Pa s, $30x10^{-3}$ Pa s and $100x10^{-3}$ Pa s and kept refrigerated at 4 °C until needed. The Ferranti Shirley cone on plate viscometer was used to measure the viscosity of the lubricants at 3000 s^{-1}. Altering the viscosity changed the Sommerfeld number (Equation 5) and when plotted against the Friction factor obtained from the frictional torque during testing a Stribeck plot was given.

The shape and position of this graph would indicate the lubrication regime of the joint.

Once the components had been washed, dried and weighed the head height was set. The head was placed onto a taper and secured with a grub screw, the taper fit into a larger holder and was secured with a long screw from the bottom of the holder. Once the head was secured the height of the highest part of the head was measured with a vertical height dial gauge. The femoral head was set so that the height of the centre of the head coincided with the centre of rotation of the friction machine. If necessary the head height was boosted with metal washers. Once the head height had been set, the head, secured within the holder, was placed in a specially made jig. The acetabular component was press fitted into an ultra high molecular weight polyethelene holder at a fixed angle of 33 ° to the horizontal and a known rotational orientation. The rotational orientation was identical every time the test was done and coincided with the orientation of the cup in the wear simulator. The fixation method employed, ensured that this was possible. The cup holder was then placed in a metal holder which fitted into the friction rig. The metal holder had a screw thread to enable the cup to be raised and lowered in the holder. The cup was raised to give a 1 mm gap between the head and the cup. The heights for the head and cup were then set and the components were transferred to the friction rig.

The frictional torque, angle and load were calibrated and testing was carried out. The joint was placed into the friction rig. The head was secured to the reciprocating part of the rig, but the cup was allowed to sit loosely within the bearings underneath. The highest viscosity lubricant was used first to avoid scratching the highly polished joint. A 5 ml volume of lubricant was placed in the acetabular component before it was placed into the friction rig.

The control computer was switched on and the dimensions of the joint, the load, the viscosity, joint identification number and user name were entered. The normal cycle was selected, the bearings were turned on, then the load and finally, after and initial period, the motion was initiated. A 90 second friction analysis was performed. The joint was removed and the lubricant was cleaned off and sterilised using gigascept

first, then with distilled water and finally with acetone. The joint was replaced into the head height jig and the height was once again checked. If any change was seen the height was corrected. The joint was then lubricated with the highest viscosity lubricant and replaced in the friction machine. The head was again secured into the friction machine. All data after this point for this joint were valid and a series of 3 tests, for each of the 5 viscosities, both in the normal and inverse directions, were recorded. Between each different viscosity the head was cleaned with gigascept and acetone and finally rinsed with water. Each joint undergoing friction analysis was tested using the above methodology.

4.2.6. Serum Mixture

The lubricant for wear, friction and pin-on-plate tests was made from bovine calf serum. The serum was diluted to 25% with distilled water (14g/l protein). EDTA and sodium azide were added to deter calcium phosphate deposition and retard bacterial growth respectively. NaOH was added to the mixture to increase the pH and allow the EDTA to dissolve. The mixture was mixed at room temperature within a fume cupboard and then the necessary amount was immediately refrigerated at 4 °C and the rest was frozen at -20 °C.

4.2.7. Enzyme digestion

The samples of serum were fully thawed and were shaken to distribute the particles. A 10 ml sample was taken from each bottle of used serum. Due to the protein's adhering to the particles a series of steps were taken to cleave the particles from the bovine serum constituents. The sample was placed in a 20 ml pyrex centrifuge tube and spun at 16000 g for 10 minutes. Once spun the supernatant was disposed of and the pellet was re-suspended in 1 ml of 2.5% sodium dodecyl sulphate (SDS) in distilled deionised water. The samples were decanted from the larger tubes into 1.5 ml Eppendorf tubes. These tubes had lids, which were pierced with a needle to avoid the tubes boiling over. The Eppendorf tubes were then placed into a heater block and the samples were boiled for 10 minutes to aid the activation of the SDS before allowing to cool for ten minutes. Once the samples were cool enough to handle they were placed in a centrifuge and spun at 16000 g for 10 minutes. The samples were extracted from the centrifuge and the supernatant removed carefully. This left a

pellet at the bottom of the Eppendorf tube. The pellet was re-suspended in 80% acetone and spun once more at 16000 g (this step was only for metal samples). The particles were washed another 3 times with 1 mL of 250 mM sodium phosphate buffer (pH 7.4) to clean the particles. The particles were suspended in a sonic bath and sonicated for 10 minutes. The particles were then incubated in sodium phosphate buffer and 1.5 U Papain (Acros Organics Fisher Scientific 41676-0100) in a water bath at 65°C for 24 hours.

After 24 hours of incubation the particles were centrifuged at 16000g for 10 minutes and re-suspended in 2.5% sodium dodecyl sulphate. The particles were then boiled and cooled as before and recentrifuged at 16000 g for 10 minutes. The specimens were washed twice with 50 mM tris-HCl buffer at 7.6 pH. The particles were suspended in Eppendorf tubes in an ultrasonic bath and sonicated for 10 minutes and finally 400 µg of Proteinase K (Fisher BioReagents BPE 1700-100 Fisher Scientific) was added to 1 ml of tris-HCl buffer for 24 hours at 55 °C. The Proteinase K broke down the peptide bonds between the amino acids i.e. the primary structure of the albumin and globulin proteins.

Once the second incubation had been completed the particles were centrifuged at 16000 g for 10 minutes and the pellet was re-suspended in 2.5% sodium dodecyl sulphate. The specimens were boiled in a heater block for 10 minutes and left to cool for a further 10 minutes. The particles were washed once with 1 ml tris-HCl buffer and once with 500 µl 80% Acetone plus 3% SDS (this step was only for metal particles) finally the particles were washed with 1 ml distilled deionised water and re-suspended in 1 ml distilled deionised water for particle sizing using the electron microscopes, atomic force microscope and the NanoSight and on rare occasions the Mastersizer.

4.2.8. SEM, TEM and AFM

The preparation for the SEM, TEM and AFM specimens were the same. The sample that was enzyme digested, see section (4.2.7), was placed on a carbon coated nickel grid or glass plate. The specimens were dried using a lamp or a hotplate. Once dry the specimens were placed into the vacuum chamber of the electron microscope or

onto the vacuum stage of the atomic force microscope. The electron microscope sample chamber was sealed and a vacuum of $1.5x10^{-3}$ Pa was created. The image of the particles was then obtained; several images of each sample were taken. The AFM did not operate under vacuum. The glass plate was scanned using a raster mechanism with the tip of the AFM which gave an image of the topography of the particles. The AFM was used for particles that charge e.g. polyurethane and PEEK so that gold coating was not required and therefore did not cause artefacts on the specimens.

4.2.9. Malvern Mastersizer

The mastersizer was used for any particles larger than 2 μm diameter. A large sample was needed for the mastersizer. The mastersizer took a background reading then the sample was dispersed into the small sample dispersion unit where the sample was agitated using a stirrer. The sample was fed through the sample chamber and the laser light was passed through the sample. Several readings were taken as the sample was recycled through the dispersion unit and sample chamber. The results showed the equivalent sphere diameter of the particles.

4.2.10. NanoSight

Once enzyme digestion had taken place the samples were suspended in 1 ml of distilled deionised water in a 1.5 ml Epindorf tube. The particles were agitated manually by shaking then by using an ultrasonic bath for two minutes or until the visible pellet dispersed.

Trial and error was used to dilute the particles to the correct concentration for the NanoSight. Each concentration was noted so that an accurate particle volume could be calculated after testing.

The sample chamber was disassembled and thoroughly cleaned, using a lint free wipe and isopropanol, and then dried thoroughly using an air duster before reassembling. Initially a blank was used to obtain a background reading, this was distilled deionised water. Three readings were taken and the chamber was once again cleaned dried and reassembled. Using a 1 ml syringe, a sample of particle debris in

solution was diluted in distilled deionised water until the evidence of the particles could clearly be seen individually under the microscope. The dilution was noted and the testing commenced. Using a syringe the sample was pushed into the sample chamber through the lure and the chamber was tilted vertically to ensure all air was released to prevent bubble formation. Once the chamber was full, the sample chamber was placed back on the microscope stage with the syringe still attached. The laser was switched on and a line of red light was visible through the sample. The particles were focused using the microscope controls and once in focus a particular part of the sample chamber was moved to the centre of the visual field.

Once the microscope was setup the shutter was moved to allow the camera to image the particles. The image was then refocused to appear on the computer. If at this stage the dilution of the sample was not correct, the sample was taken out, the instrument cleaned and a different dilution was tried. Once the correct dilution had been obtained the test could be completed. The duration of video recording was set to 60 seconds, the shutter was adjusted to allow the most particles to be seen as were the gain and brightness (in some circumstances). The particles were recorded for 60 seconds. If there were any vibrations that affected the particles (if the particles had all visibly moved on the screen) the video was discarded and another was taken.

Analysis then took place. All the settings were adjusted in order for the computer to recognise the maximum number of real particles possible. Analysis software created histograms and raw data files. These raw data files were processed in Matlab and compiled in excel and finally origin was used to produce the data in a graphical format. The results could also be seen on the screen as the video was being processed.

This protocol was followed 3 times for each sample and between each the machine was disassembled cleaned, dried and reassembled. Once one particle sample had been used the serum was drawn back into the syringe and disposed of in the correct manner. Each sample used a sterile sealed syringe to avoid contamination.

5. Results

5.1. Pin-on-plate

Figure 10 shows the average and standard deviation of each gravimetric measurement at each quarter of a million cycles for each material. The overall result, Figure 10, shows the as-cast, high carbide material is the lowest wearing, the double heat treated material is the highest wearing and the single heat treated material lies in between them.

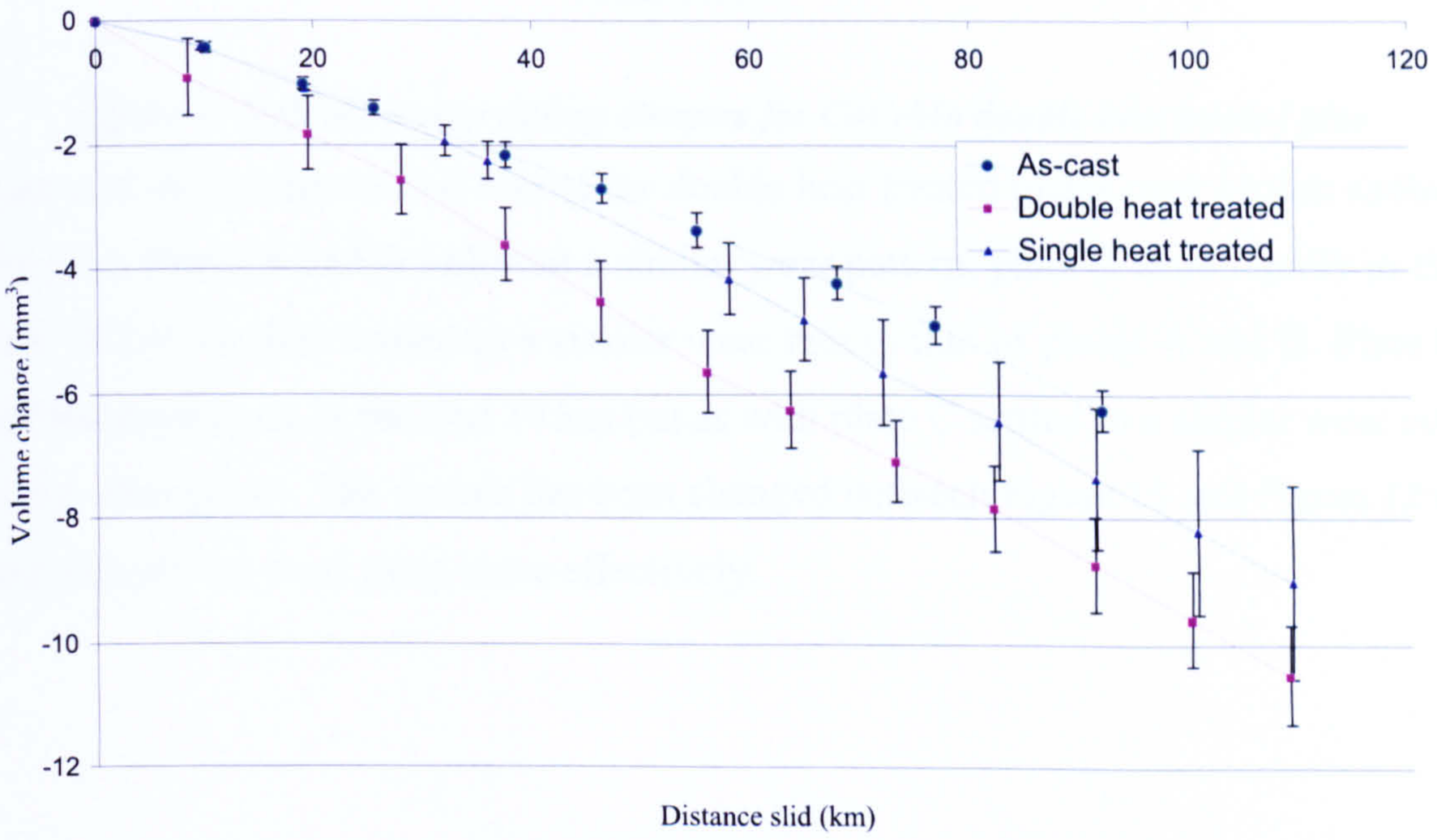

Figure 10 Volume change versus sliding distance for each of the three materials

Figure 11 shows the volume loss over 115 km sliding distance for the double heat treated pins. The graph shows linear wear. The four pins show similar wear.

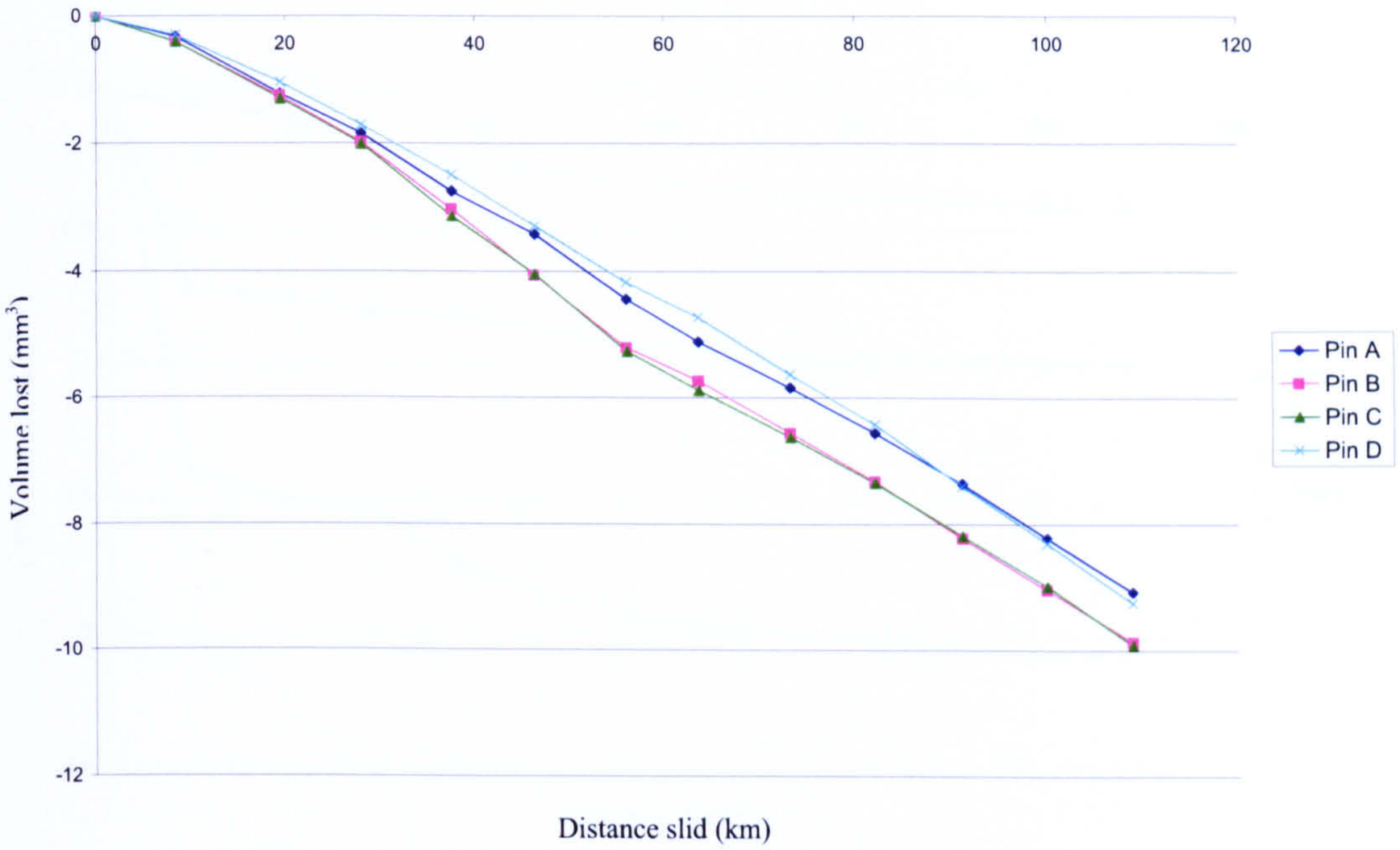

Figure 11 Volume versus sliding distance for CoCrMo double heat treated pins

Figure ***12*** shows the volume loss of the double heat treated plates over 115km sliding distance. Plates A and B followed a similar wear pattern; plate C wore rapidly in the first 10 km but then settled to a similar wear rate to that of plates A and B. Plate D lost the most mass in the first 10 km but as with plate C settled to a similar wear rate to the other plates. The y-scale has been changed between Figure 11 and Figure ***12*** to demonstrate the wear trend more effectively.

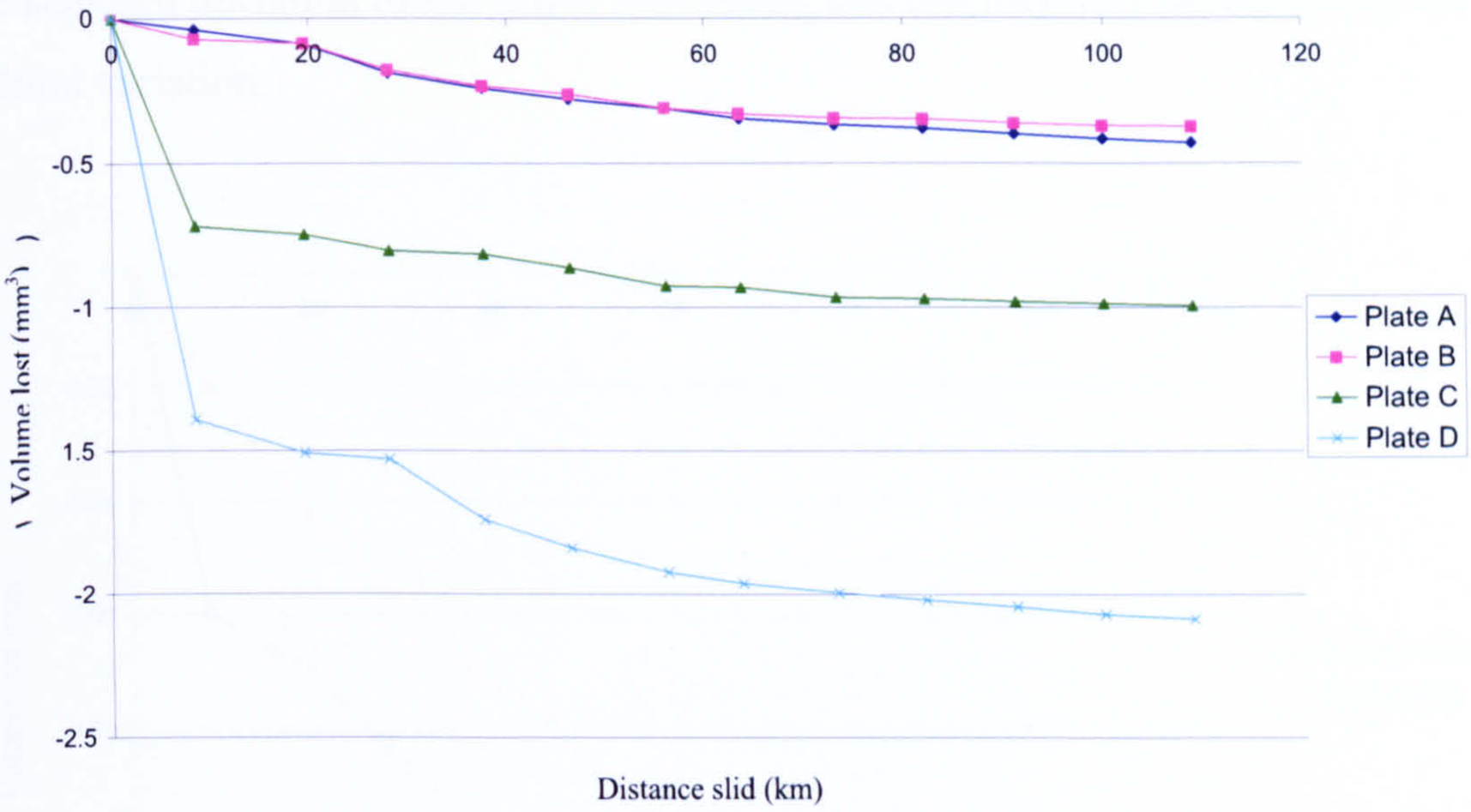

Figure 12 Volumetric wear versus sliding distance for the CoCrMo double heat treated plates.

Figure 13 shows the wear rates for the double heat treated pin and plate pairs. The graph shows a linear trend. All four pairs of specimens wore at similar rates and with similar trends.

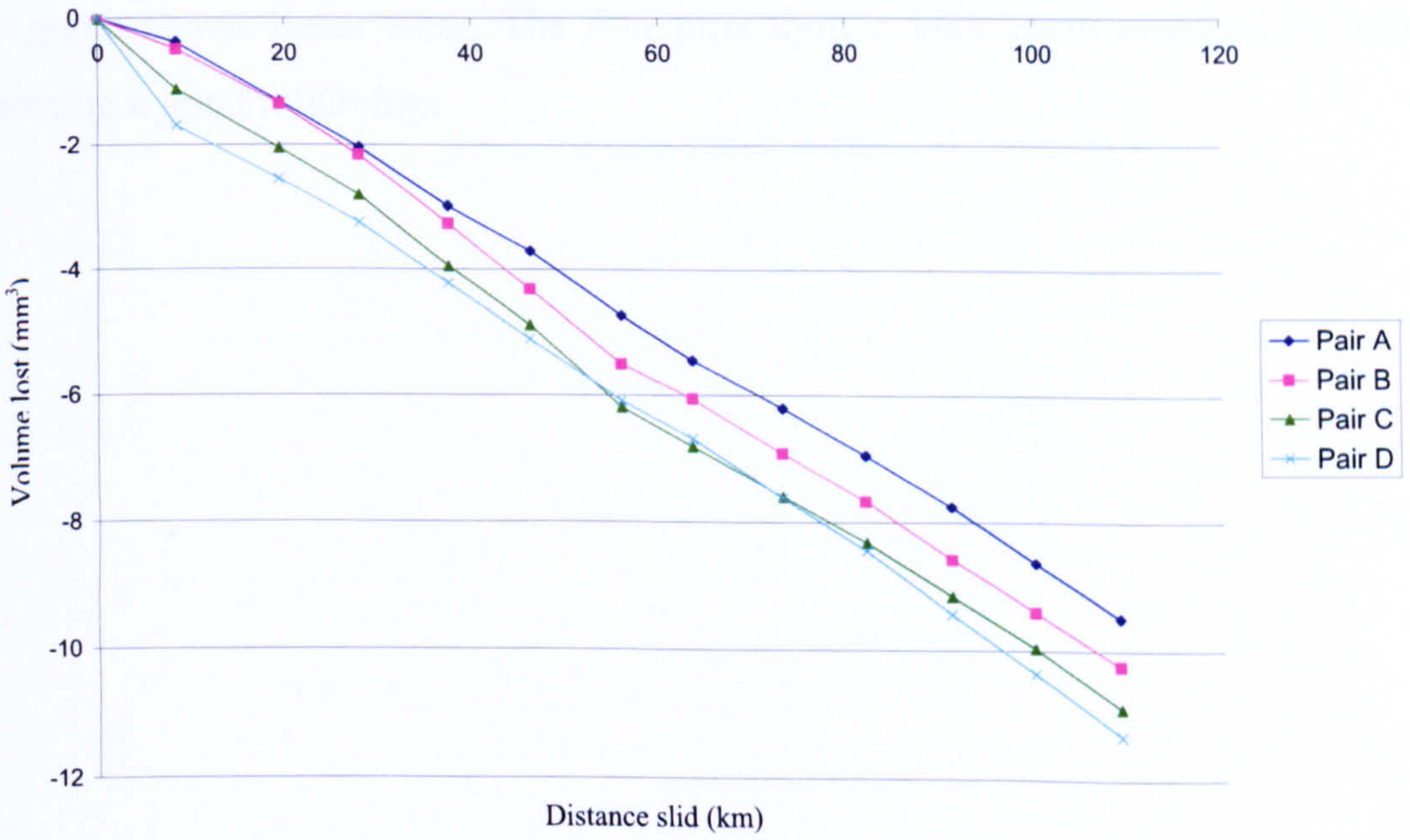

Figure 13 volume lost versus distance slid for the double heat treated pin and plate pairs

The control specimens show a very small change over the same period as when the active pins and plates were wearing. Although the trend is negative the volume

change is minimal. The change in volume of the control specimens is smaller than the standard deviation of the active specimens, and can therefore be accounted for as natural variation.

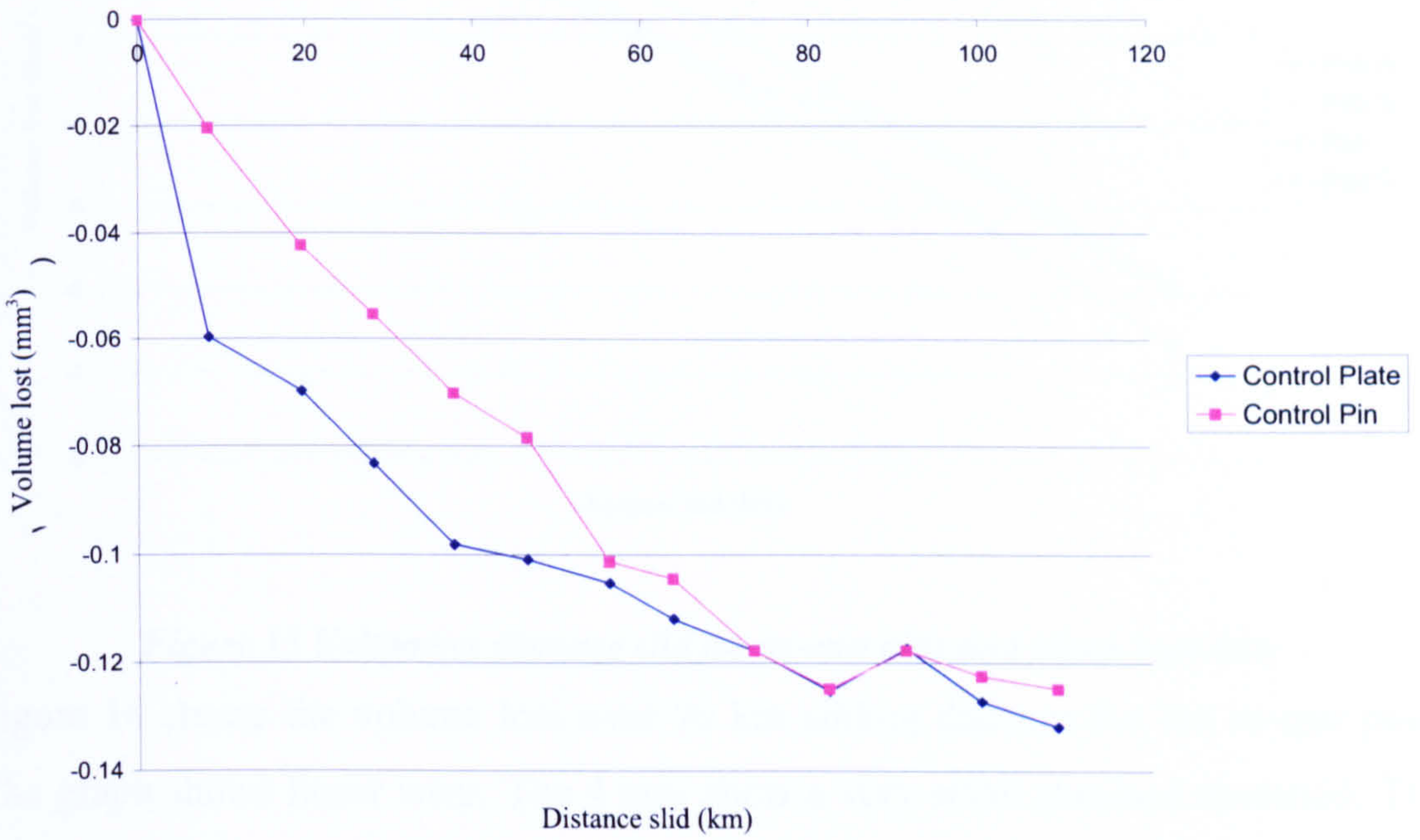

Figure 14 Control Graph for double heat treated specimens

Figure 15 shows the volume loss over 90 km sliding distance for the as-cast pairs. The graph shows linear wear. The four pins show a very small standard deviation indicating a good reliability.

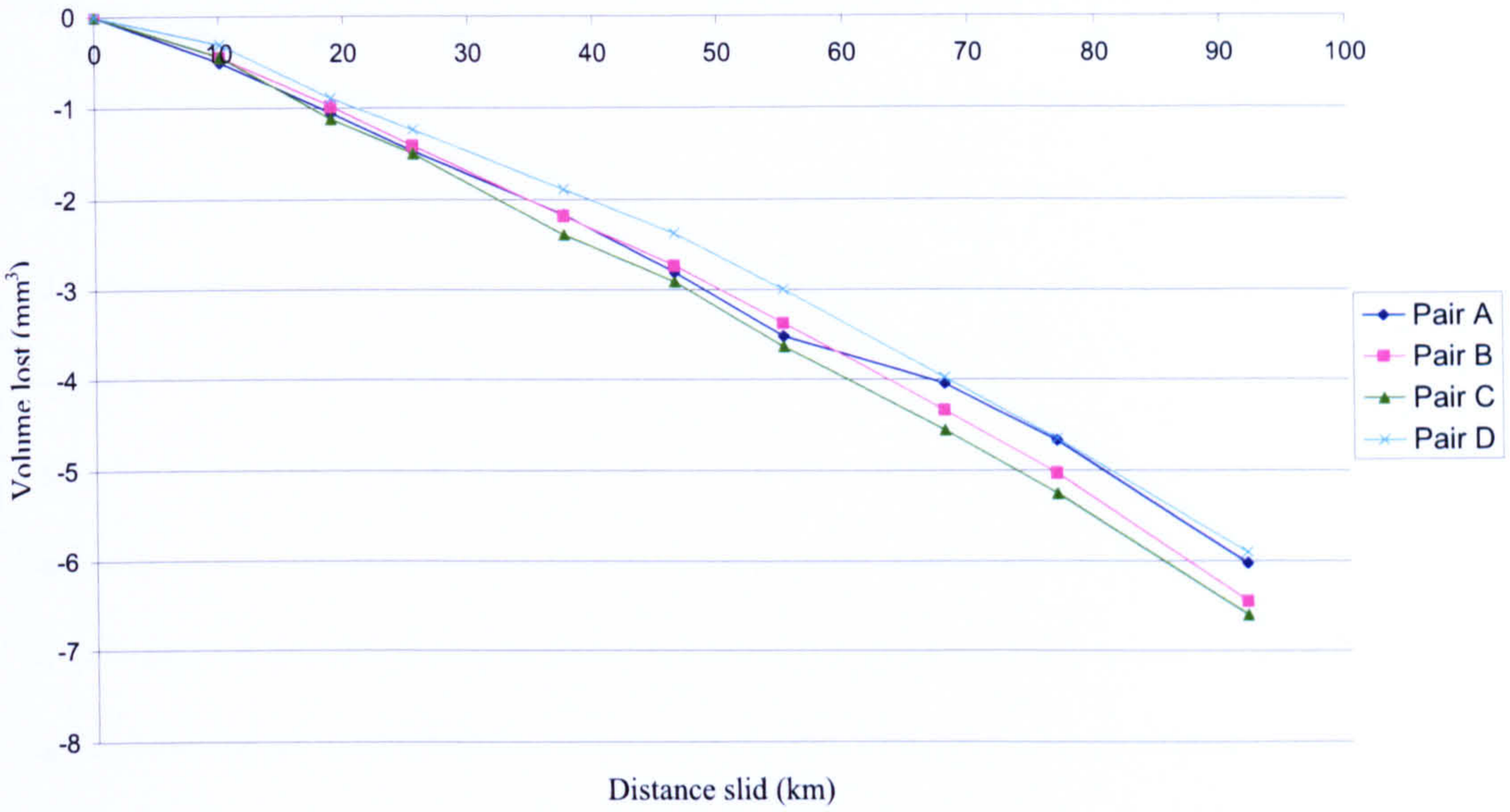

Figure 15 Volume vs distance slid for as-cast pins and plates together.

Figure 16 shows the volume loss over 90 km sliding distance for the as-cast pins. The graph shows linear wear. The 4 pins show a very small standard deviation. The majority of the wear has taken place by the pins and Figure 15 and Figure 16 look similar as pin wear dominates the overall wear.

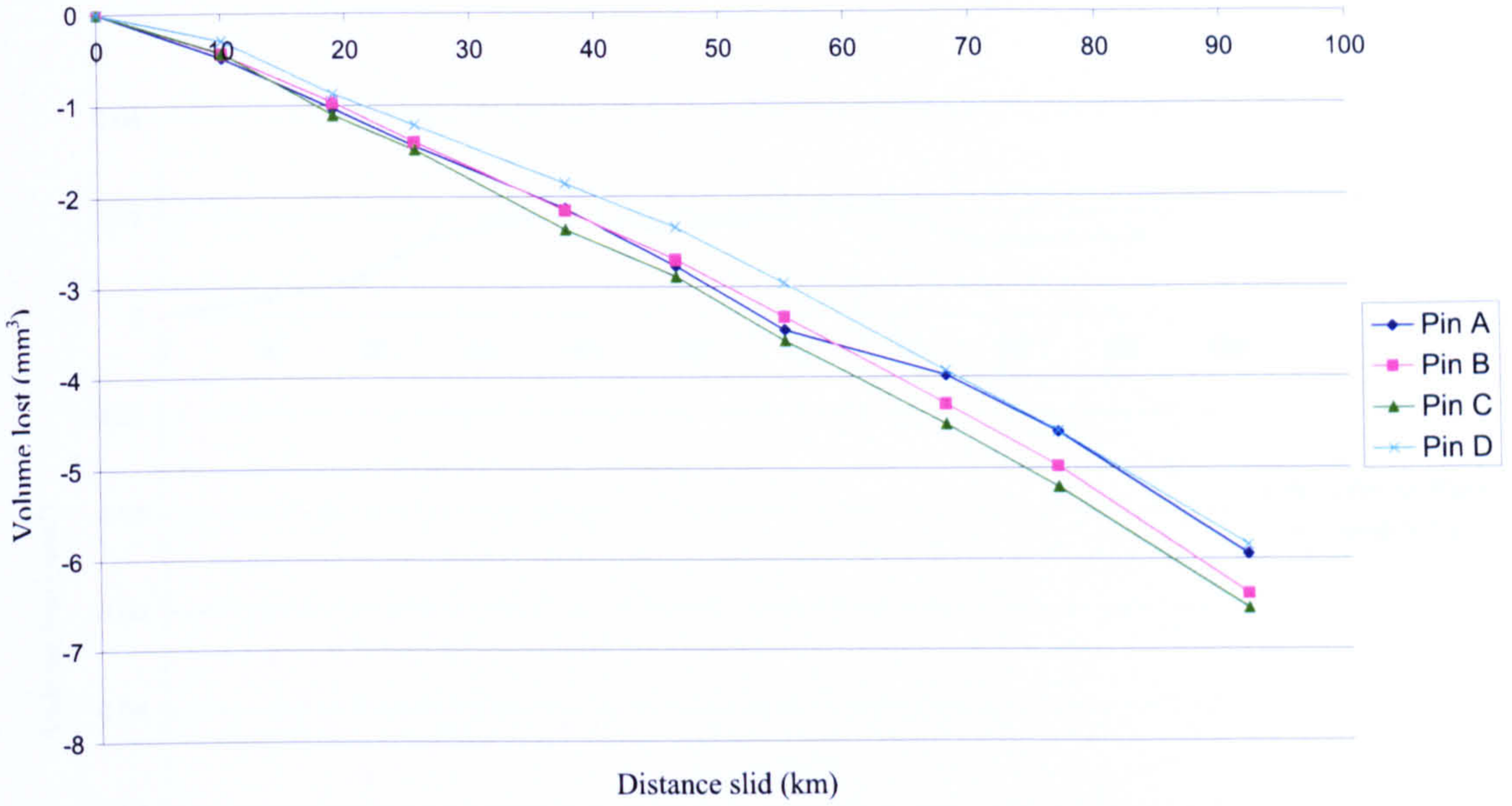

Figure 16 Volumetric wear versus distance slid for the as-cast high carbide CoCrMo pins

Figure 17 shows volume loss of the plates over 90 km sliding distance. The general trend is linear and the standard deviation is large in comparison to the volume lost but the overall volume lost is small. As can be seen in Figure 17 the wear of the plates was much lower than the wear of the pins (Figure 16). The total wear is therefore dominated by the wear of the pins.

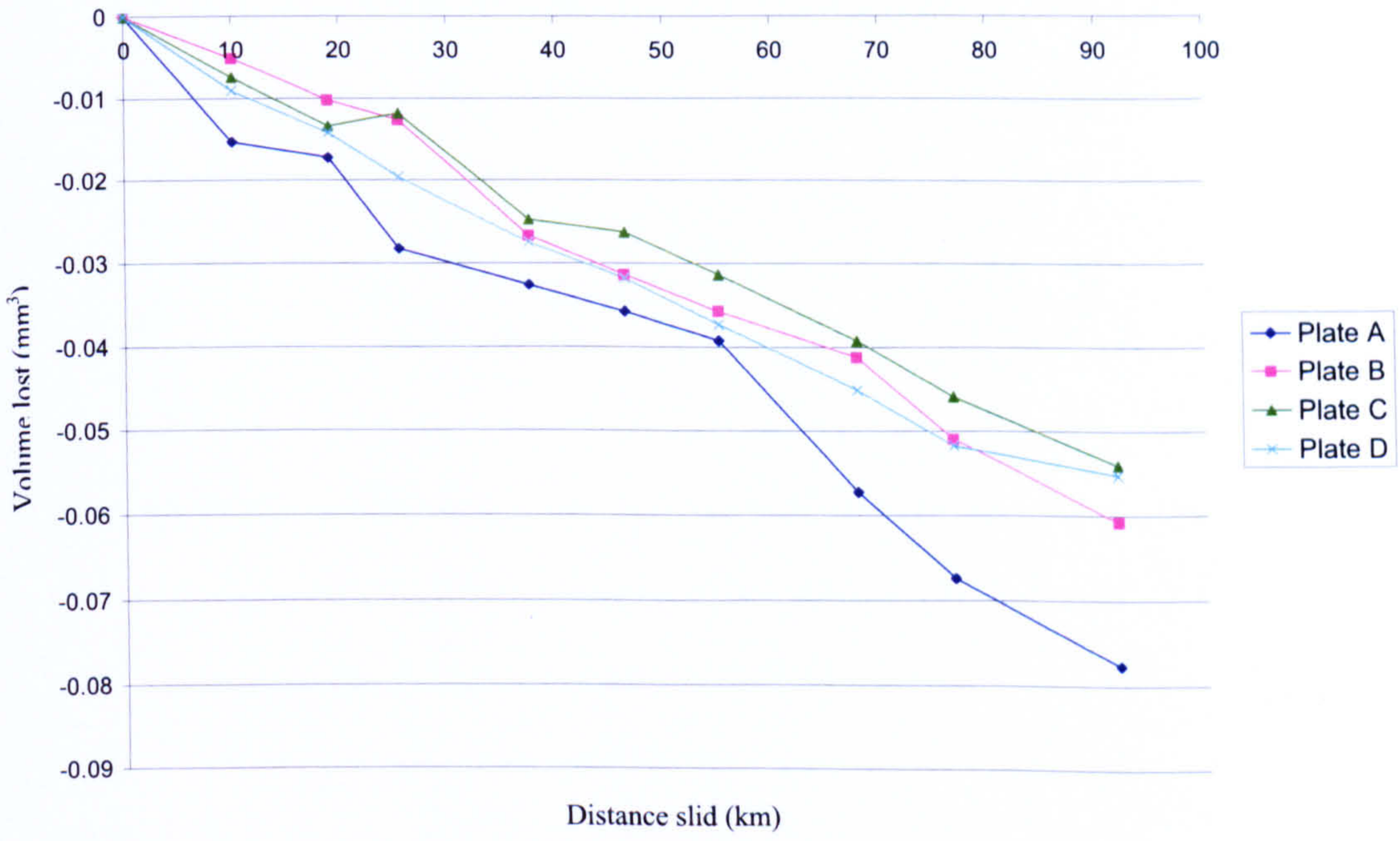

Figure 17 Volume loss versus distance slid for the as-cast high carbide CoCrMo plates.

The control shows very little change over the course of the test.

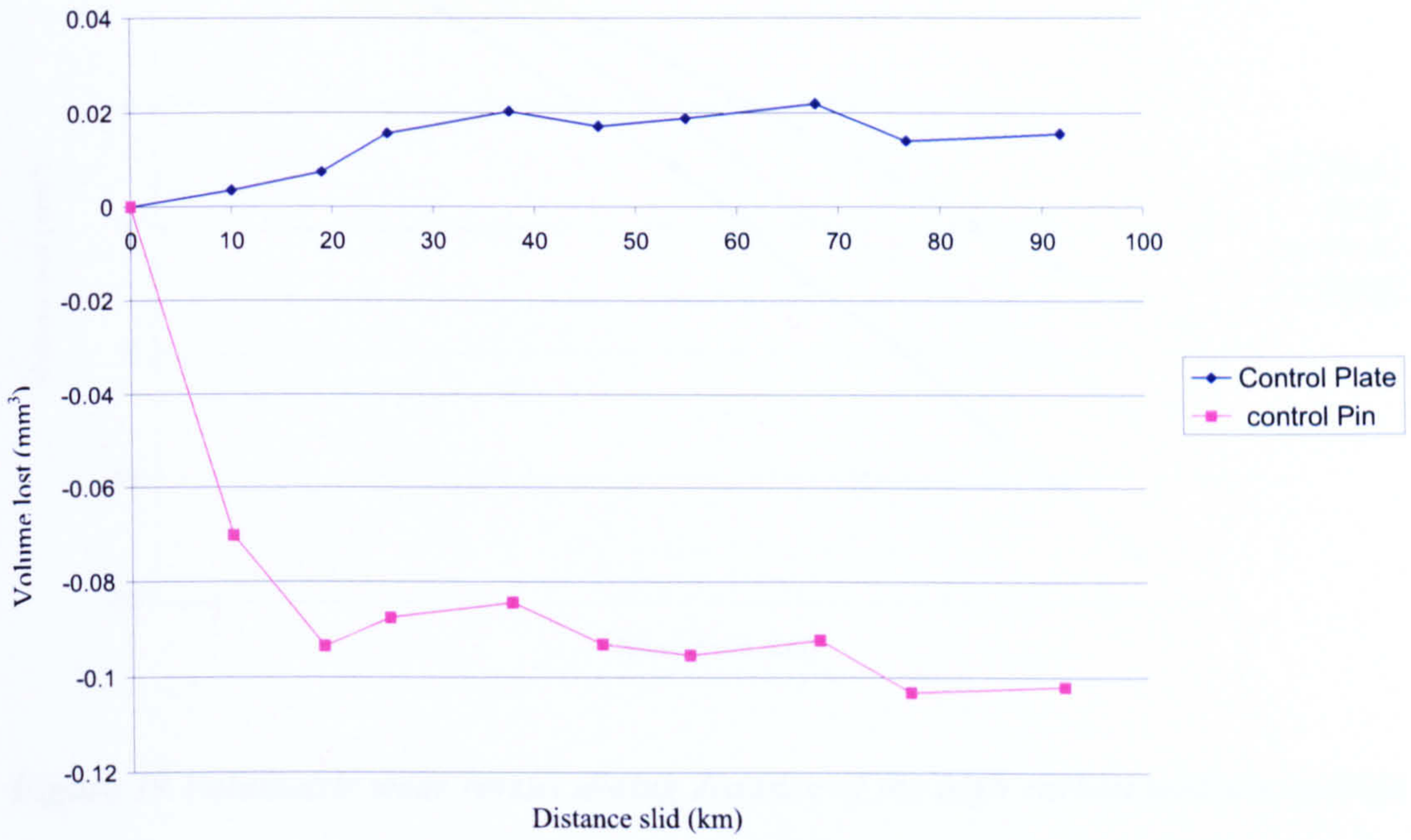

Figure 18 Control graph for as-cast specimens

Figure 19 shows the volume loss over 115 km sliding distance of the high carbon single heat treated pins. The graph shows a linear trend but also the largest standard deviation of the 3 materials.

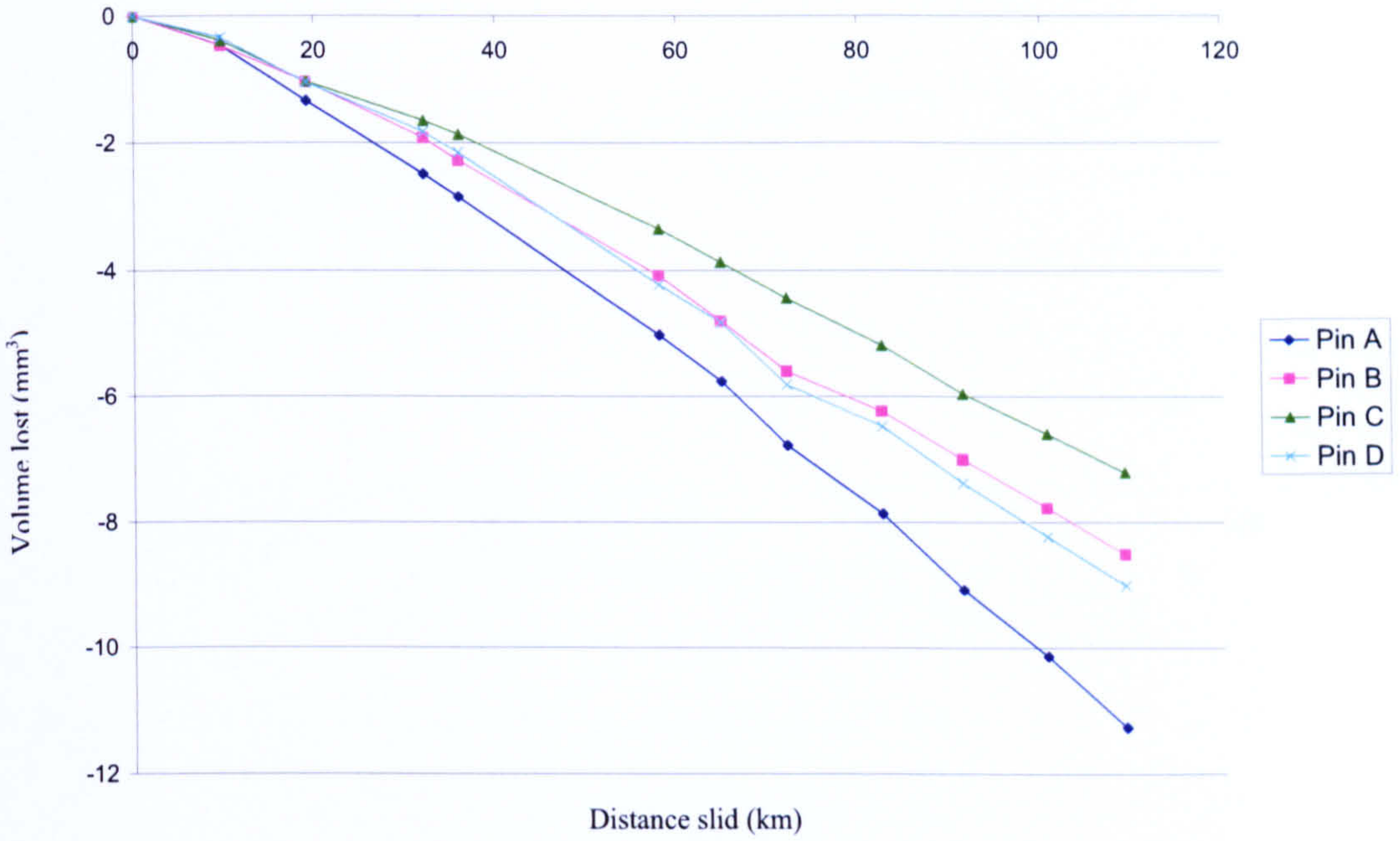

Figure 19 Volumetric wear versus sliding distance of the high carbon medium carbide heat treated pins.

Figure 20 shows the volume loss over 115 km sliding distance of the single heat treated plates. Plates B, C, and D show a very small amount of volume loss. Plate A gained weight rapidly up to 40 km then the rate of increase lessened. Further tests are needed to explain this anomaly. As can be seen the plates wore much less than the pins over the 115 km sliding distance.

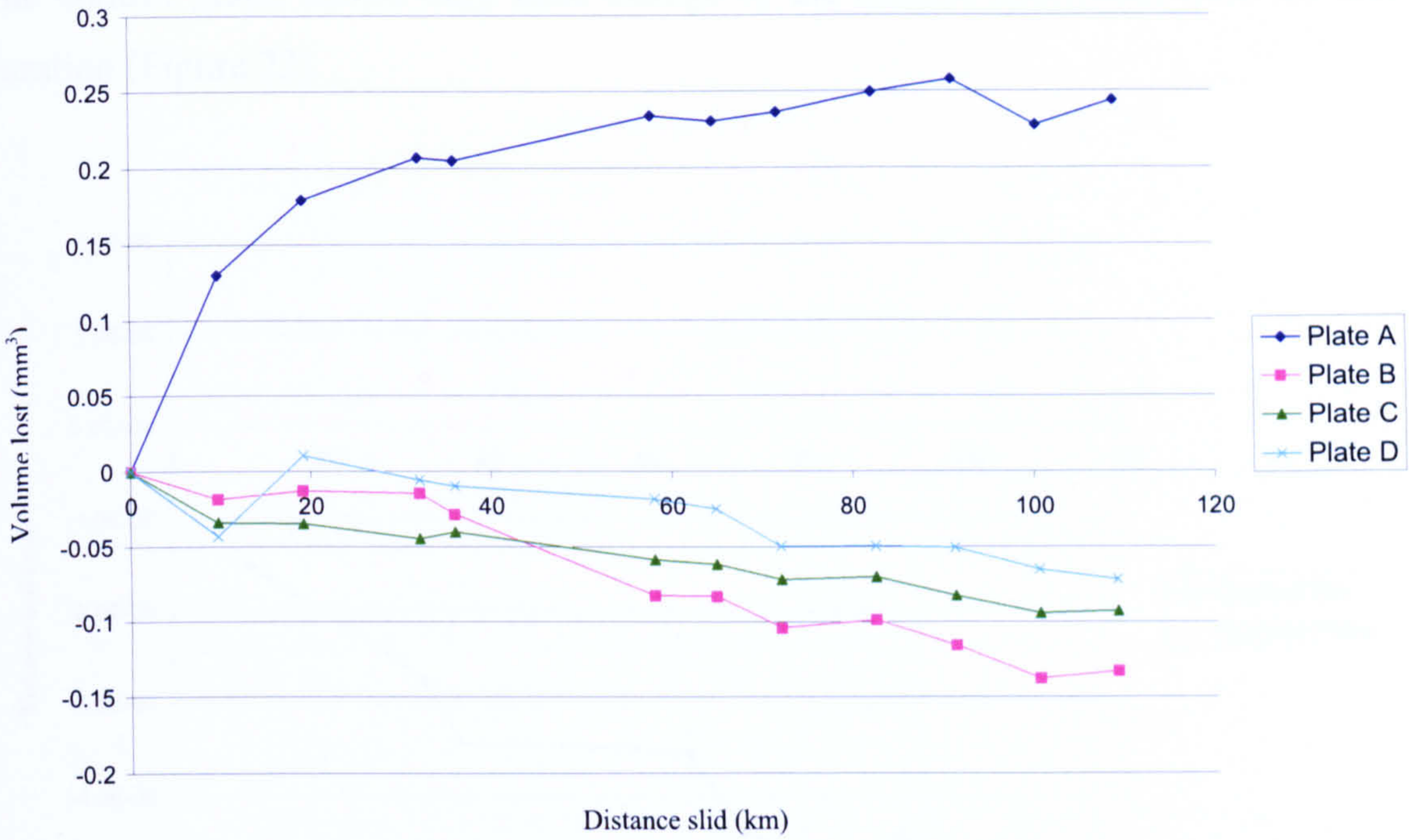

Figure 20 Volumetric wear versus distance slid of the high carbon single heat treated plates.

Figure 21 shows the wear for all 4 plates and pins combined over the 115 km sliding distance, as can be seen the pins dominate the wear and the plates have a very small effect on this graph.

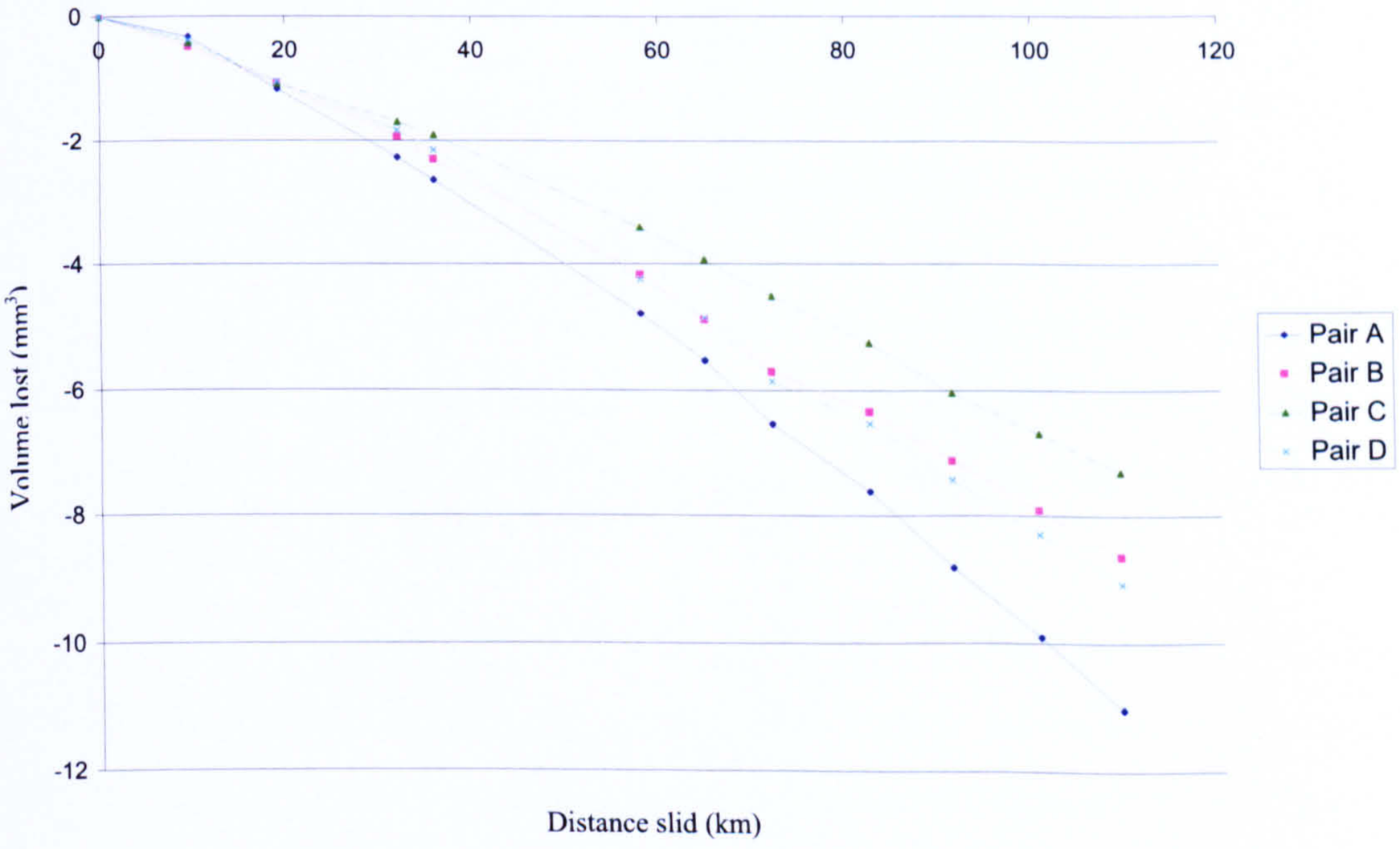

Figure 21 volumetric wear vs distance slid of the single heat treated pairs.

The control graph shows very little change to the control specimens over the test duration (Figure 22).

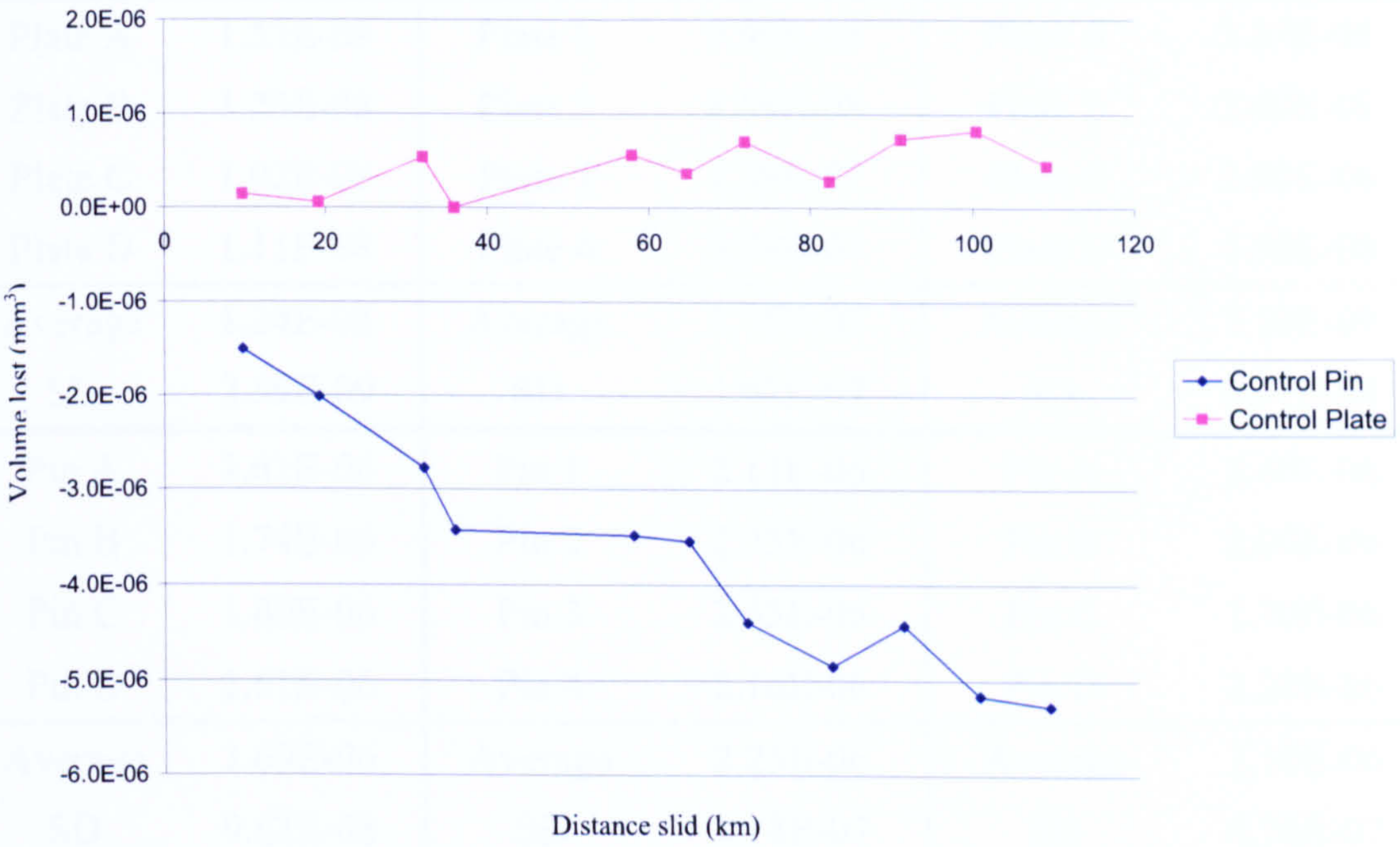

Figure 22 control graph for single heat treated specimens

As-cast		Double heat treated		Single heat treated	
Pin/ Plate	K (mm^3/Nm)	Pin/ Plate	K (mm^3/Nm)	Pin/ Plate	K (mm^3/Nm)
Plate A	1.57E-08	Plate 1	9.99E-08	Plate A	3.87E-08
Plate B	1.25E-08	Plate 2	8.58E-08	Plate B	3.40E-08
Plate C	1.02E-08	Plate 3	1.39E-07	Plate C	1.80E-08
Plate D	1.11E-08	Plate 4	3.08E-07	Plate D	1.50E-08
Average	1.24E-08	Average	1.58E-07	Average	7.10E-09
SD	2.39E-09	SD	1.02E-07	SD	3.17E-08
Pin A	1.61E-06	Pin 1	2.13E-06	Pin A	2.60E-06
Pin B	1.74E-06	Pin 2	2.35E-06	Pin B	2.00E-06
Pin C	1.80E-06	Pin 3	2.35E-06	Pin C	1.70E-06
Pin D	1.61E-06	Pin 4	2.16E-06	Pin D	2.20E-06
Average	1.69E-06	Average	2.25E-06	Average	2.10E-06
SD	9.63E-08	SD	1.18E-07	SD	4.76E-07
Pair A	1.61E-06	Pair 1	2.23E-06	Pair A	2.60E-06
Pair B	1.74E-06	Pair 2	2.44E-06	Pair B	2.10E-06
Pair C	1.80E-06	Pair 3	2.49E-06	Pair C	1.70E-06
Pair D	1.61E-06	Pair 4	2.47E-06	Pair D	2.20E-06
Average	1.69E-06	Average	2.41E-06	Average	2.10E-06
SD	9.49E-08	SD	1.19E-07	SD	3.63E-07

Table 3 Wear coefficients (K) for individual pins, plates and the pairs for the varying carbide test.

Table 3 provides the numerical values of what can be seen in the graphs that the plate wear is much lower than the pin wear and therefore has less effect on the total wear of the pairs. The as-cast specimens wear less than the single or double heat treated specimens.

Figure 23 shows that as-cast and double heat treated materials are statistically significantly different and the single heat treated material lies in between the two.

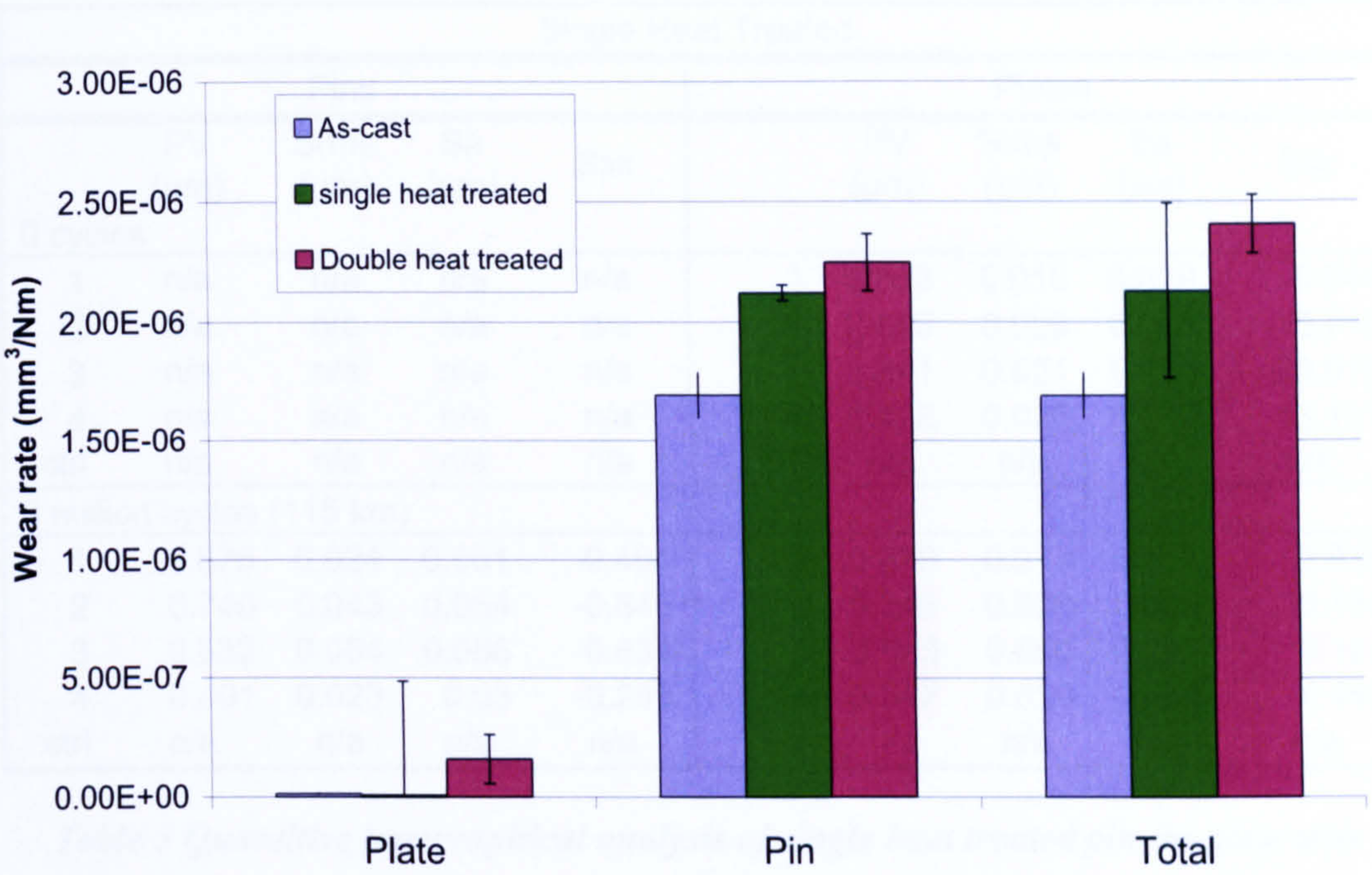

Figure 23 A bar chart showing the differing wear rates of the 3 different materials.

Table 4 to Table 6 show the average surface analysis data taken at the beginning and end of the tests. The error bars show the standard deviation of all data taken. The data were analysed using ANOVA in SPSS. The p value represents the significance between the initial and final values. A p value of less than 0.05 shows a significant difference and is highlighted in the tables. Due to the rounded end of the pins only one reading could be taken initially and therefore statistical analysis could not be done.

Double Heat Treated									
Pins					Plates				
0 cycles	PV (µm)	Srms (µm)	Sa (µm)	Ssk		PV (µm)	Srms (µm)	Sa (µm)	Ssk
1	1.119	0.153	0.114	-1.008	1	1.179	0.025	0.014	-3.141
2	1.904	0.177	0.139	0.095	2	1.009	0.016	0.008	-7.769
3	1.260	0.250	0.209	-0.135	3	1.509	0.027	0.015	-13.568
4	1.875	0.301	0.247	0.152	4	1.125	0.027	0.012	-9.354
ctrl	0.700	0.081	0.066	-0.627	ctrl	0.826	0.015	0.009	-0.630
3 million cycles (115 km)									
1	1.042	0.049	0.036	2.087	1	1.378	0.086	0.065	-0.818
2	0.837	0.017	0.012	-1.843	2	1.344	0.128	0.094	-1.457
3	0.896	0.114	0.091	-0.958	3	1.016	0.112	0.094	0.024
4	0.861	0.073	0.057	-0.438	4	0.945	0.052	0.036	-1.498
ctrl	0.834	0.092	0.074	-0.435	ctrl	1.115	0.024	0.011	-7.361

Table 4 Quantitive topographical analysis of double heat treated pin-on-plate tests

Single Heat Treated									
Pins					Plates				
0 cycles	PV (µm)	Srms (µm)	Sa (µm)	Ssk		PV (µm)	Srms (µm)	Sa (µm)	Ssk
1	n/a	n/a	n/a	n/a	1	0.858	0.016	0.029	-6.044
2	n/a	n/a	n/a	n/a	2	2.695	0.029	0.045	-10.716
3	n/a	n/a	n/a	n/a	3	2.841	0.021	0.034	-20.016
4	n/a	n/a	n/a	n/a	4	2.428	0.026	0.042	-13.117
ctrl	n/a	n/a	n/a	n/a	ctrl	n/a	n/a	n/a	n/a
3 million cycles (115 km)									
1	0.675	0.024	0.031	-0.494	1	0.379	0.013	0.017	0.938
2	0.740	0.043	0.054	-0.846	2	0.240	0.026	0.032	0.134
3	0.532	0.054	0.066	-0.634	3	0.543	0.050	0.062	0.182
4	0.401	0.023	0.03	-0.286	4	0.347	0.023	0.030	-0.443
ctrl	n/a	n/a	n/a	n/a	ctrl	n/a	n/a	n/a	n/a

Table 5 Quantitive topographical analysis of single heat treated pin-on-plate tests

As-cast									
Pins					Plates				
0 cycles	PV (µm)	Srms (µm)	Sa (µm)	Ssk		PV (µm)	Srms (µm)	Sa (µm)	Ssk
1	6.576	0.462	0.356	-0.453	1	0.899	0.031	0.021	-2.557
2	3.225	0.265	0.220	-0.316	2	0.861	0.029	0.020	-2.349
3	7.497	0.429	0.316	-0.983	3	0.827	0.026	0.018	-2.354
4	7.847	1.212	0.987	0.735	4	0.717	0.023	0.016	-2.194
ctrl					ctrl	1.037	0.035	0.024	-2.461
2.5 million cycles (90 km)									
1	2.014	0.172	0.134	-1.081	1	1.270	0.051	0.032	-0.429
2	1.823	0.094	0.07	-0.171	2	3.556	0.253	0.145	2.486
3	1.978	0.133	0.106	-0.290	3	2.269	0.208	0.159	-0.030
4	1.628	0.106	0.083	0.011	4	3.221	0.216	0.137	1.441
ctrl	3.039	0.565	0.468	0.151	ctrl	1.097	0.034	0.025	-2.149

Table 6 Quantitive topographical analysis of as-cast pin-on-plate tests

The tables show that the plates show statistical differences in roughness over the 3 million cycles (115 km). The statistics were unable to be applies to the pins as only one reading was taken at 0 km as the head was hemispherical. Highlighted values show an increase in roughness or peak to valley height over the test.

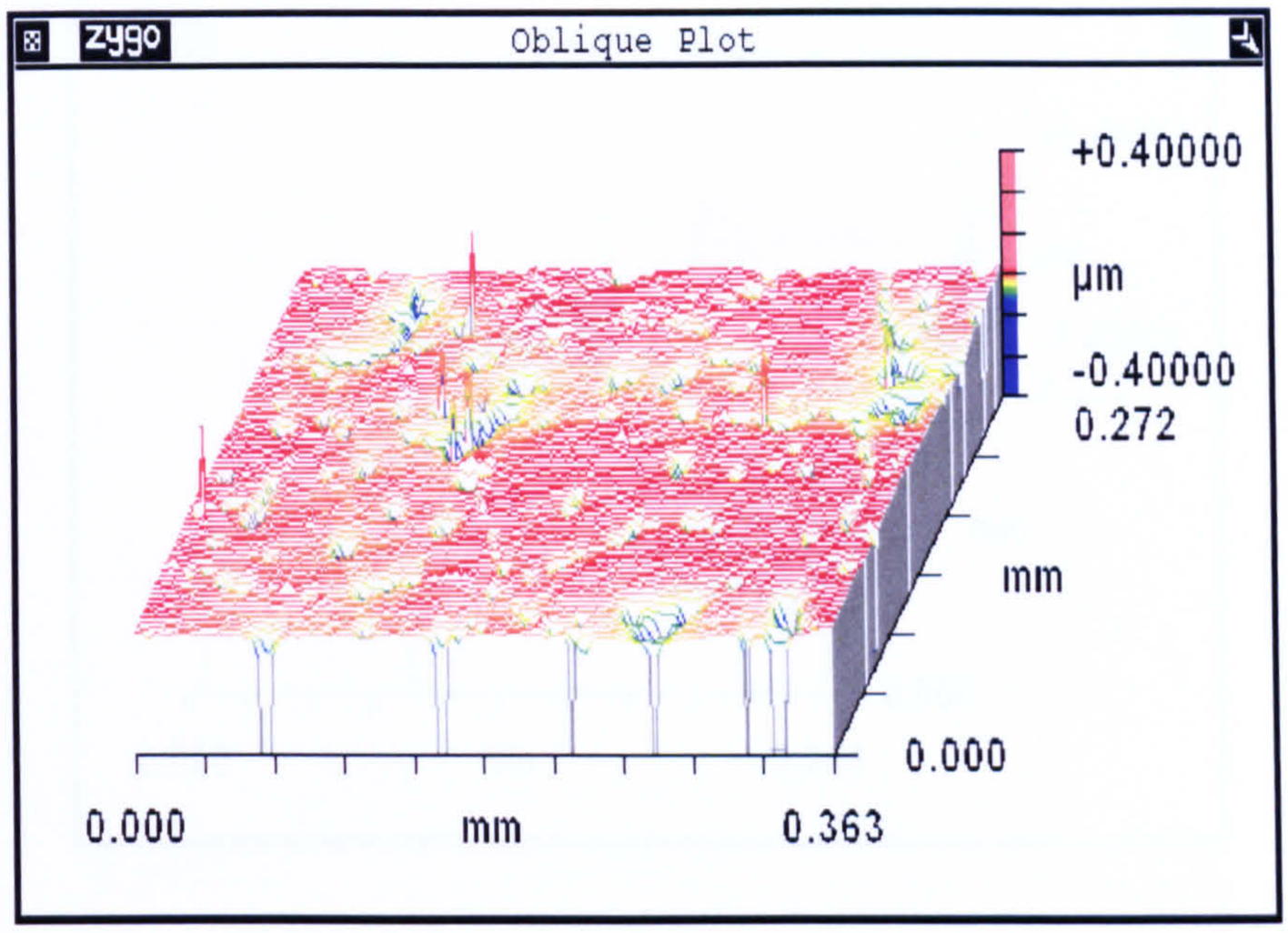

Figure 24 Double heat treated specimen at zero km sliding distance

Figure 24 shows the plate at the start of the test, the surface looks similar to the as-cast plate surface with smaller hollows. No carbides can be seen and there are many small hollows visible. The material was designed to have fewer carbides than the as-cast material. These images have been selected to fit to the same scale so that comparison can be made more easily they are typical of what was seen over the 10 repeated images.

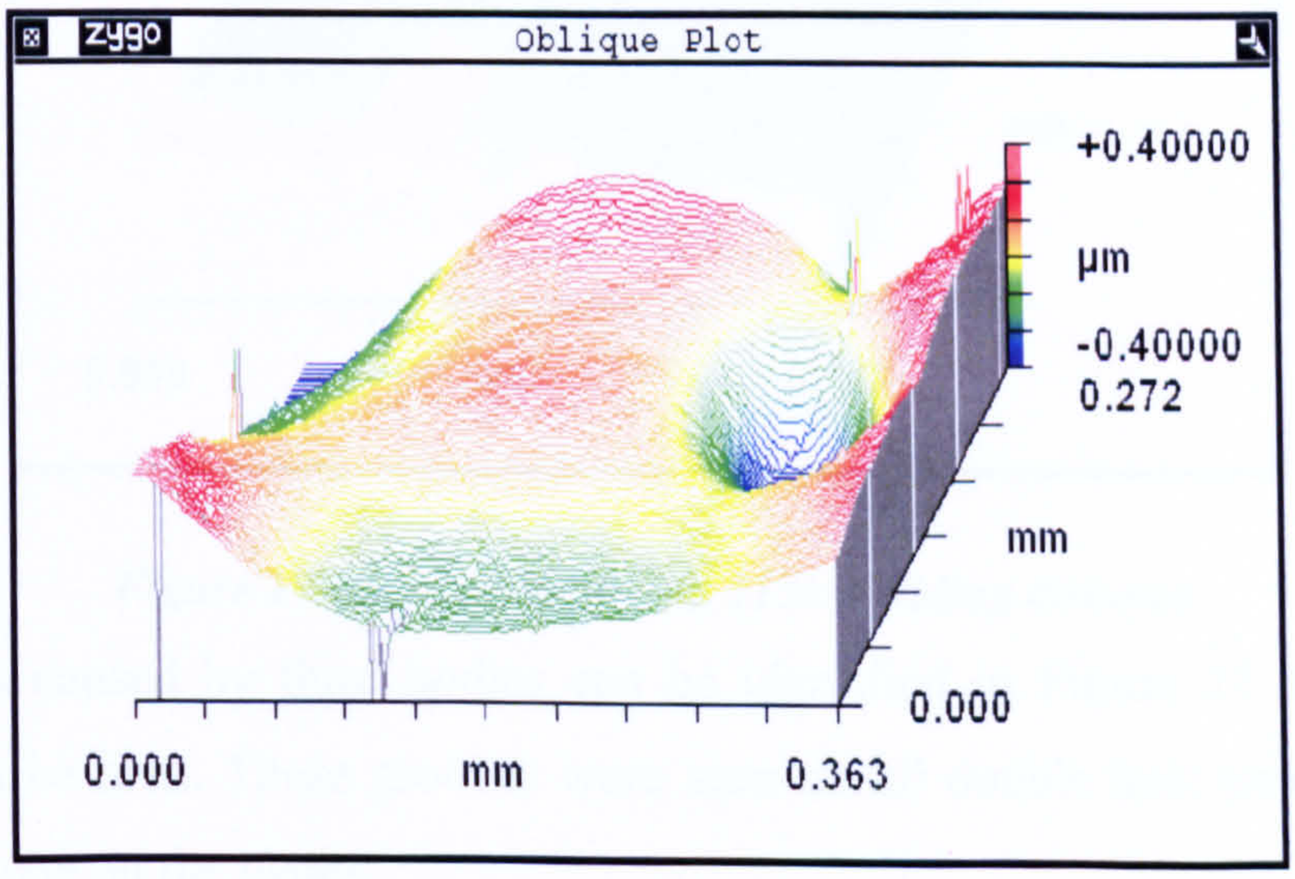

Figure 25 Double heat treated pin at zero km sliding distance

Figure 25 shows the double heat treated pin at the beginning of the test it looks smooth and hemi-spherical; no small dips or hollows can be seen, the surface undulates slightly.

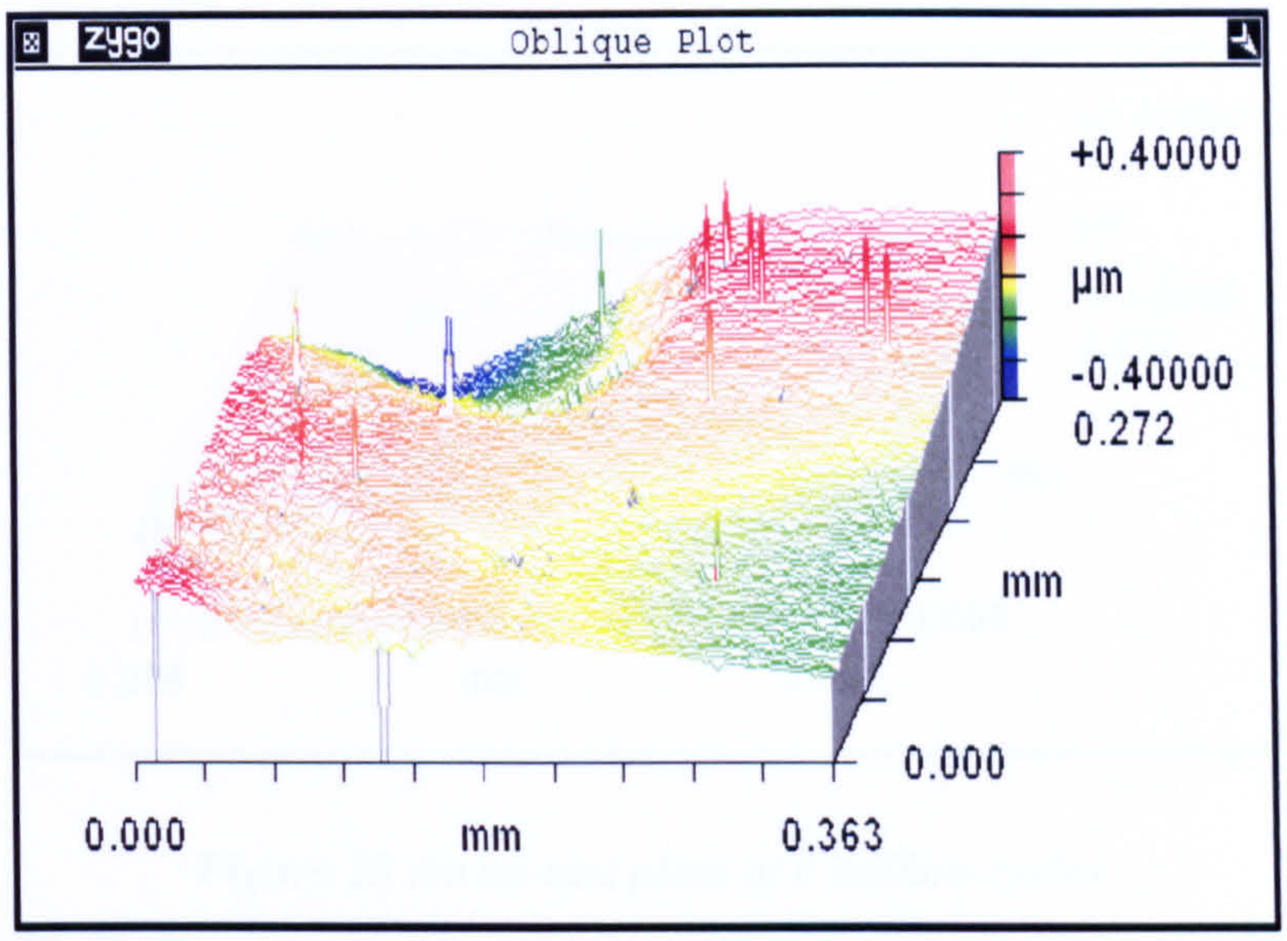

Figure 26 Double heat treated plate at 115km sliding distance

Figure 26 shows a rougher surface than the initial surface analysis showing no protruding carbides.

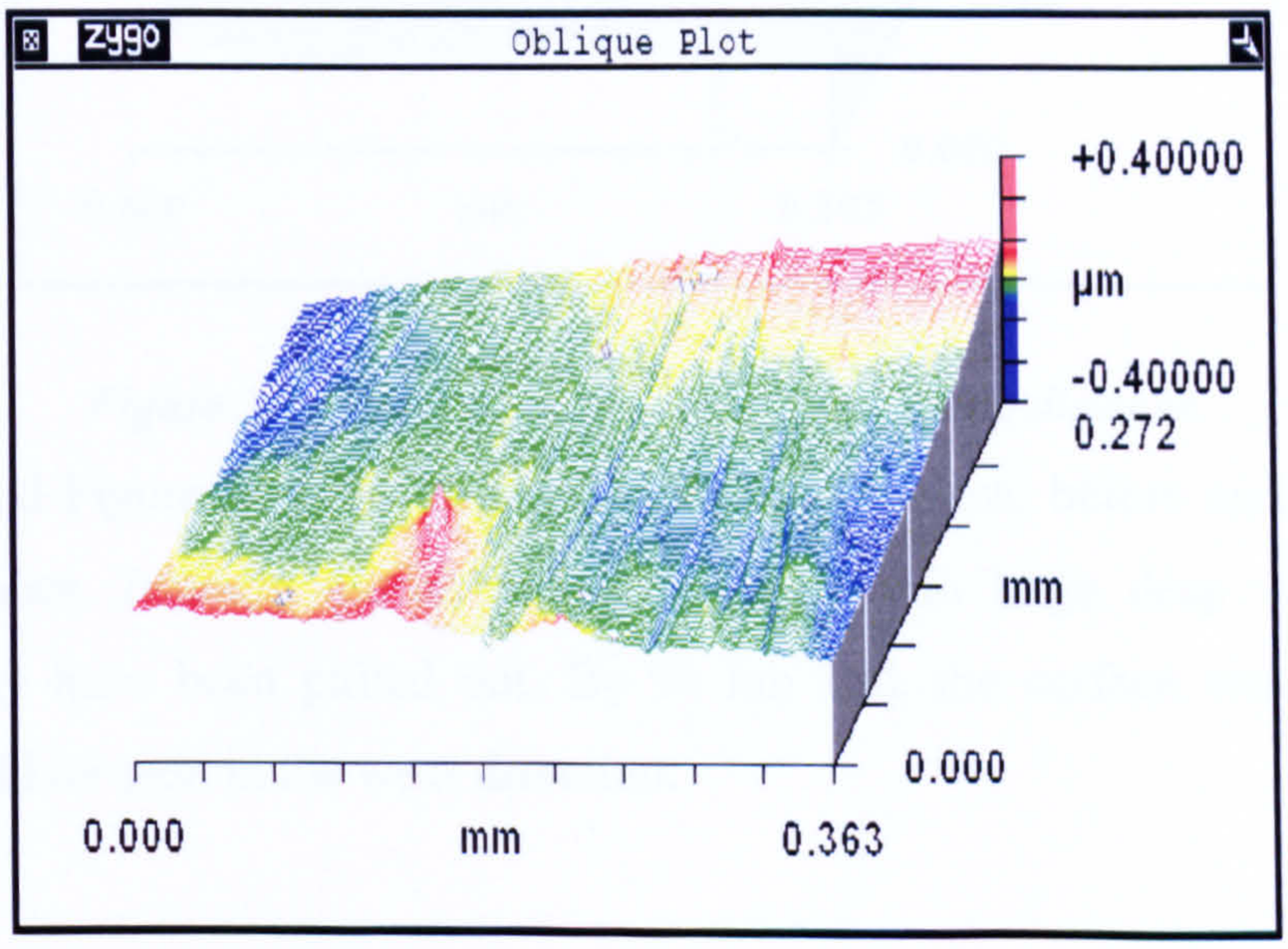

Figure 27 Low carbide Pin at 115km sliding distance

The grooves caused by third bodies can be identified in Figure 27 and again no carbides can be seen. These grooves were seen on all double heat treated pins, but there were none on the plates.

The as-cast material showed striations on the plates emanating from the large blocks of carbides (Figure 29).

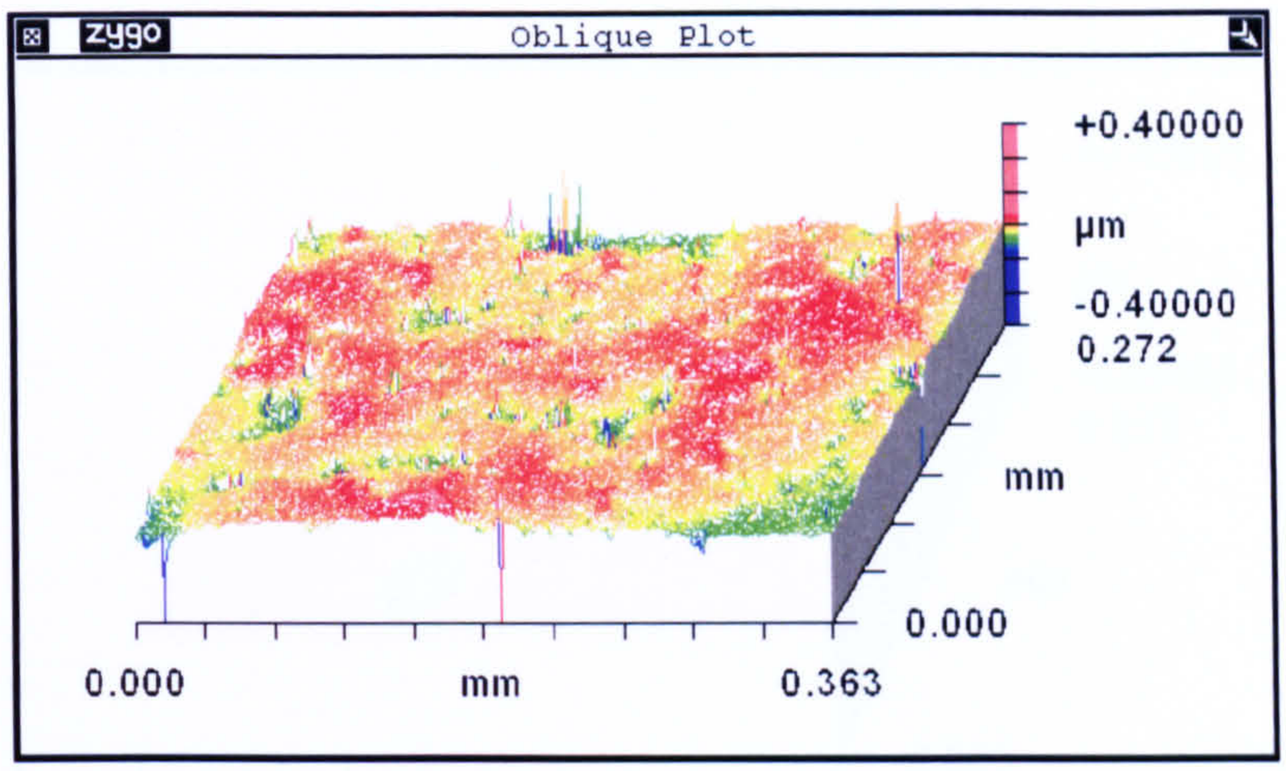

Figure 28 An as-cast plate at 0 million cycles

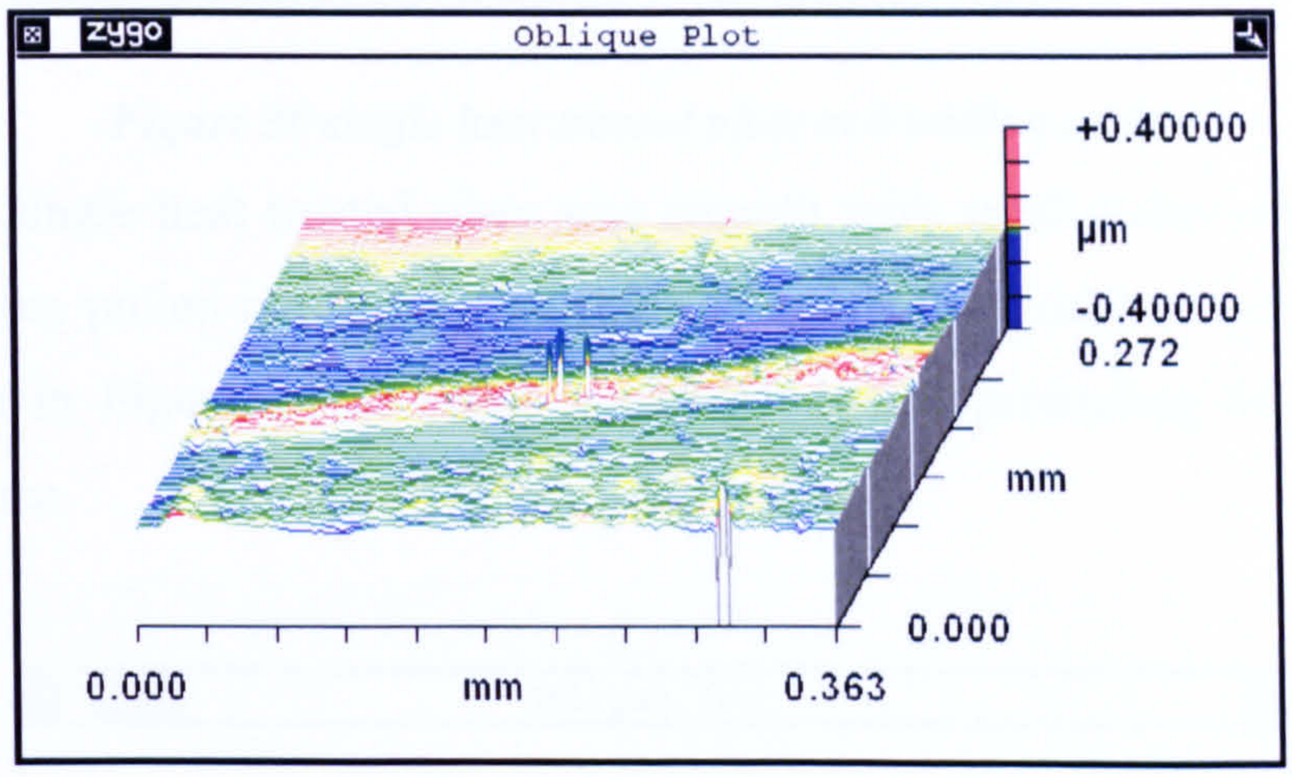

Figure 29 the as-cast plate after 97 km sliding distance.

Figure 28 and Figure 29 show the as-cast bearing surface, before and after 90 km sliding distance. Initially the surface is polished with large deep valleys where carbides may have been pulled out. By 90 km slid, the surface was smooth and grooves could be seen in the wear direction.

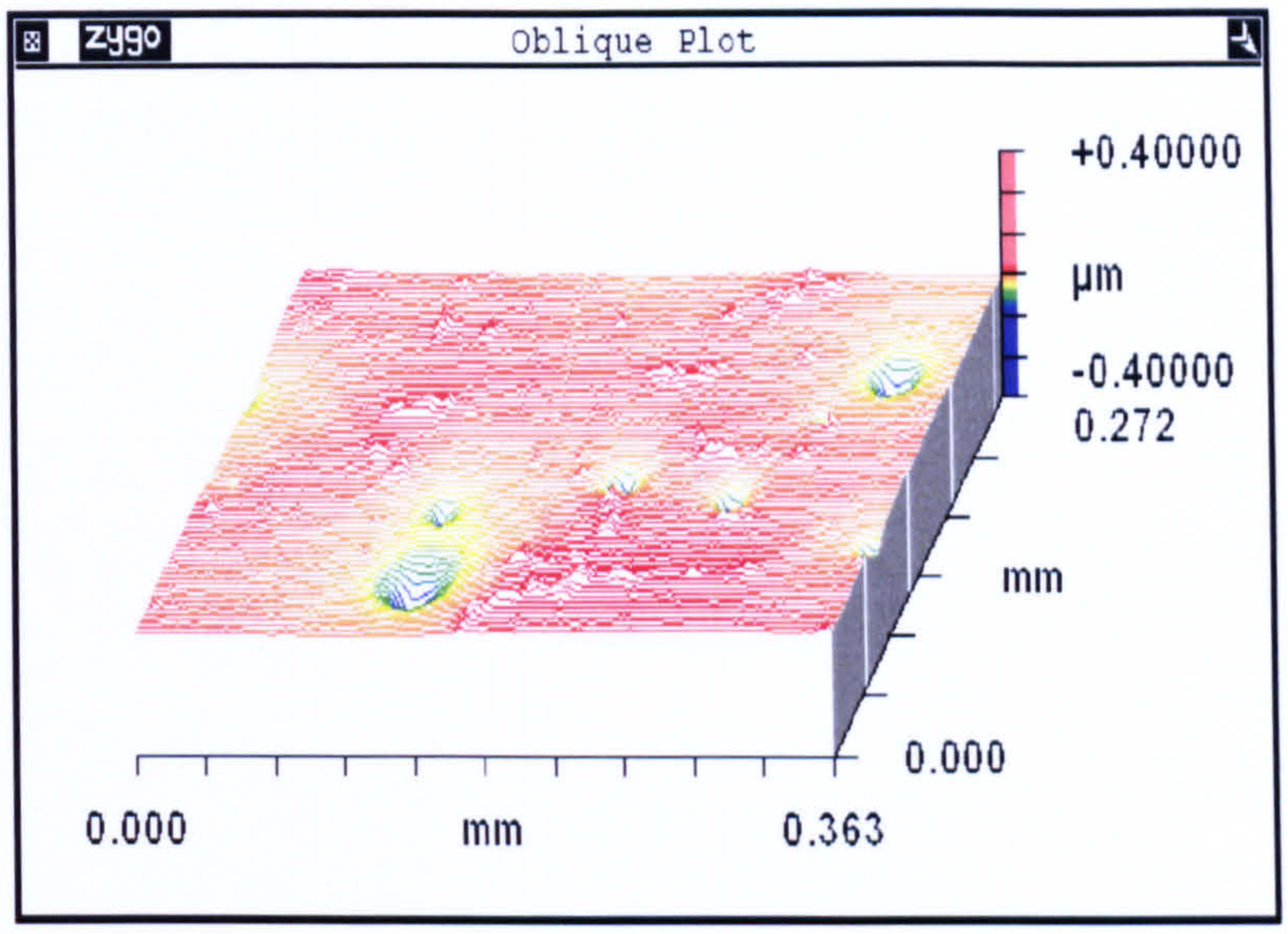

Figure 30 single heat treated plate at 0 million cycles

Initially the single heat treated plate was smooth with small holes where carbides may have been pulled out during polishing. The small partially dissolved carbides can be seen in Figure 30 as small roughened lumps protruding from otherwise smooth surface.

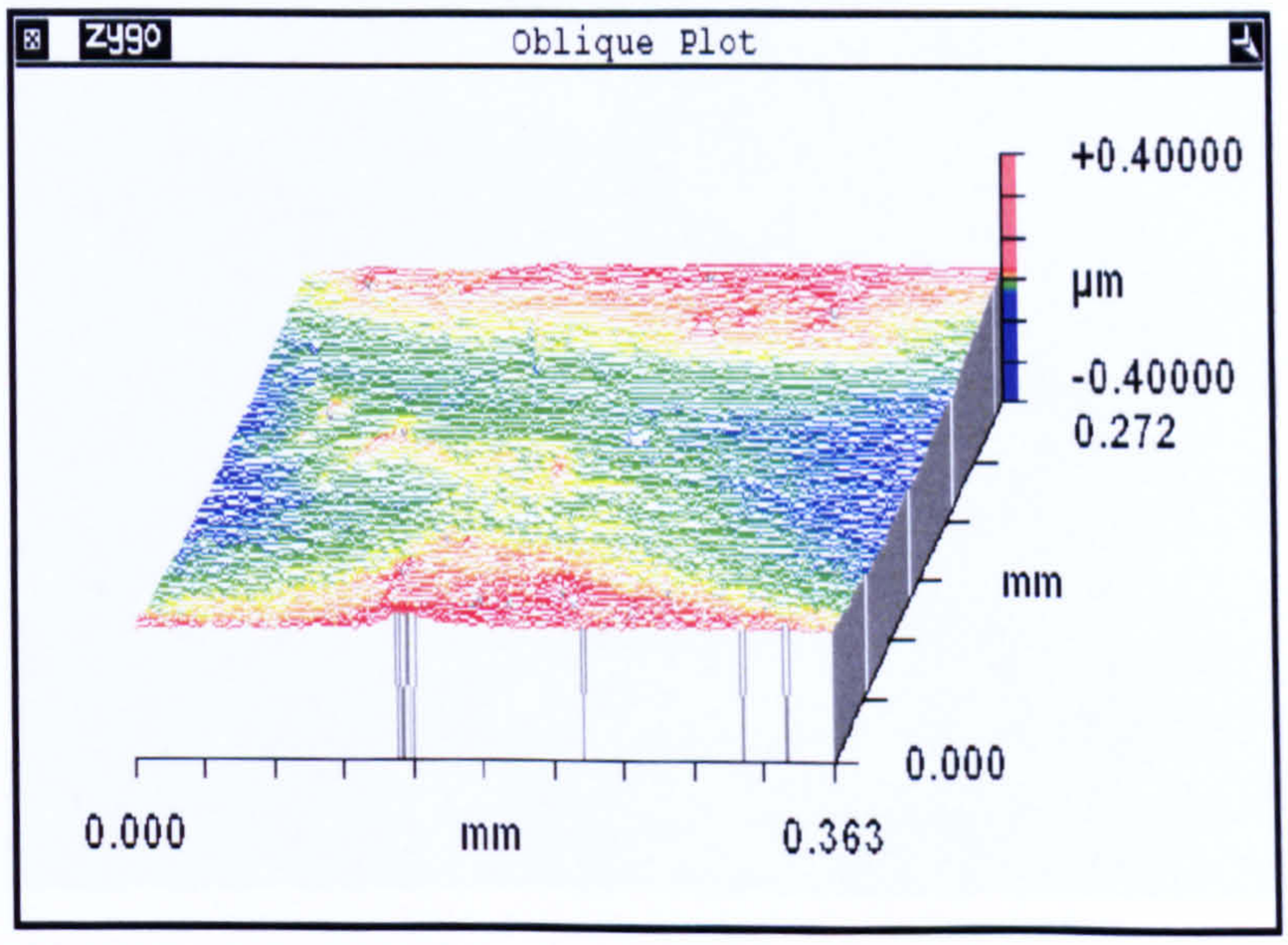

Figure 31 Single heat treated plate after 3 million cycles

After 115 km sliding distance Figure 31 shows the plate surface was rougher and a few small carbides could be seen protruding from the surface

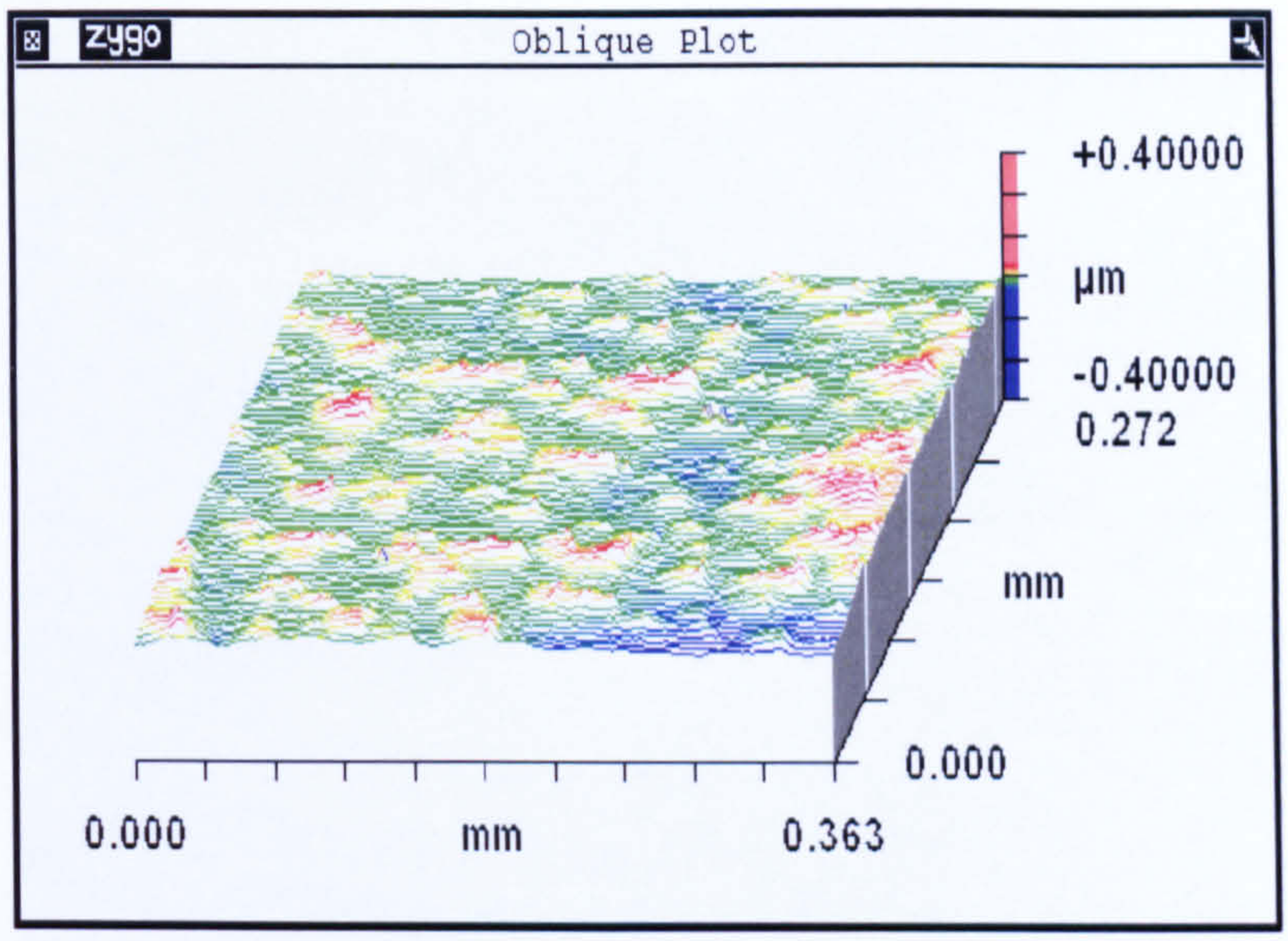

Figure 32 Pin after 3 million cycles single heat treated

At 115 km slid Figure 32 shows the pin surface had many more protruding carbides than the plate. The material debris could be seen lying behind the carbide in the direction of rotation.

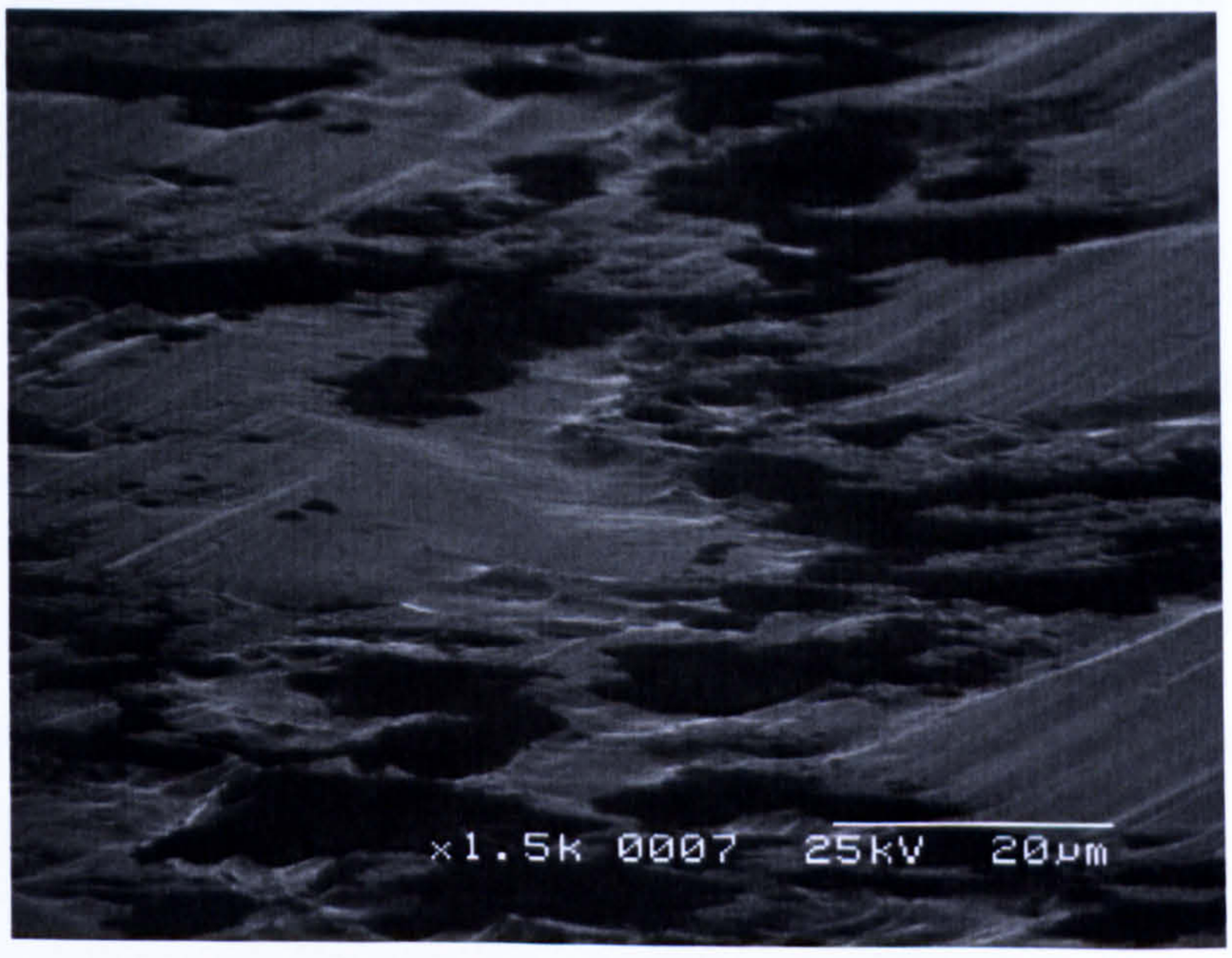

Figure 33 A low magnification image of the as-cast specimen after the wear test was completed

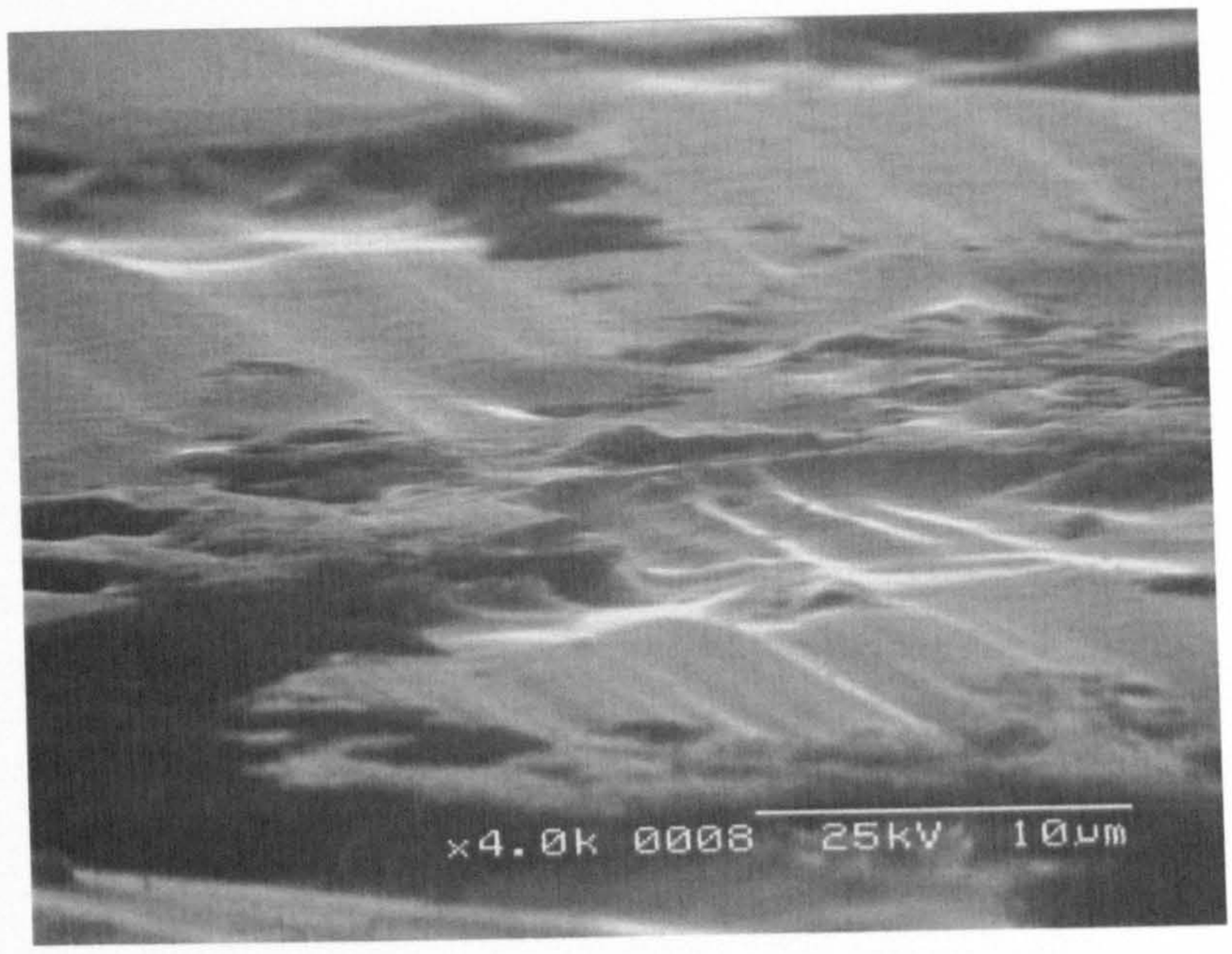

Figure 34 SEM high magnification image of as-cast specimen at 3 million cycles.

Figure 35 SEM image of Medium carbide specimen at 3 million cycles.

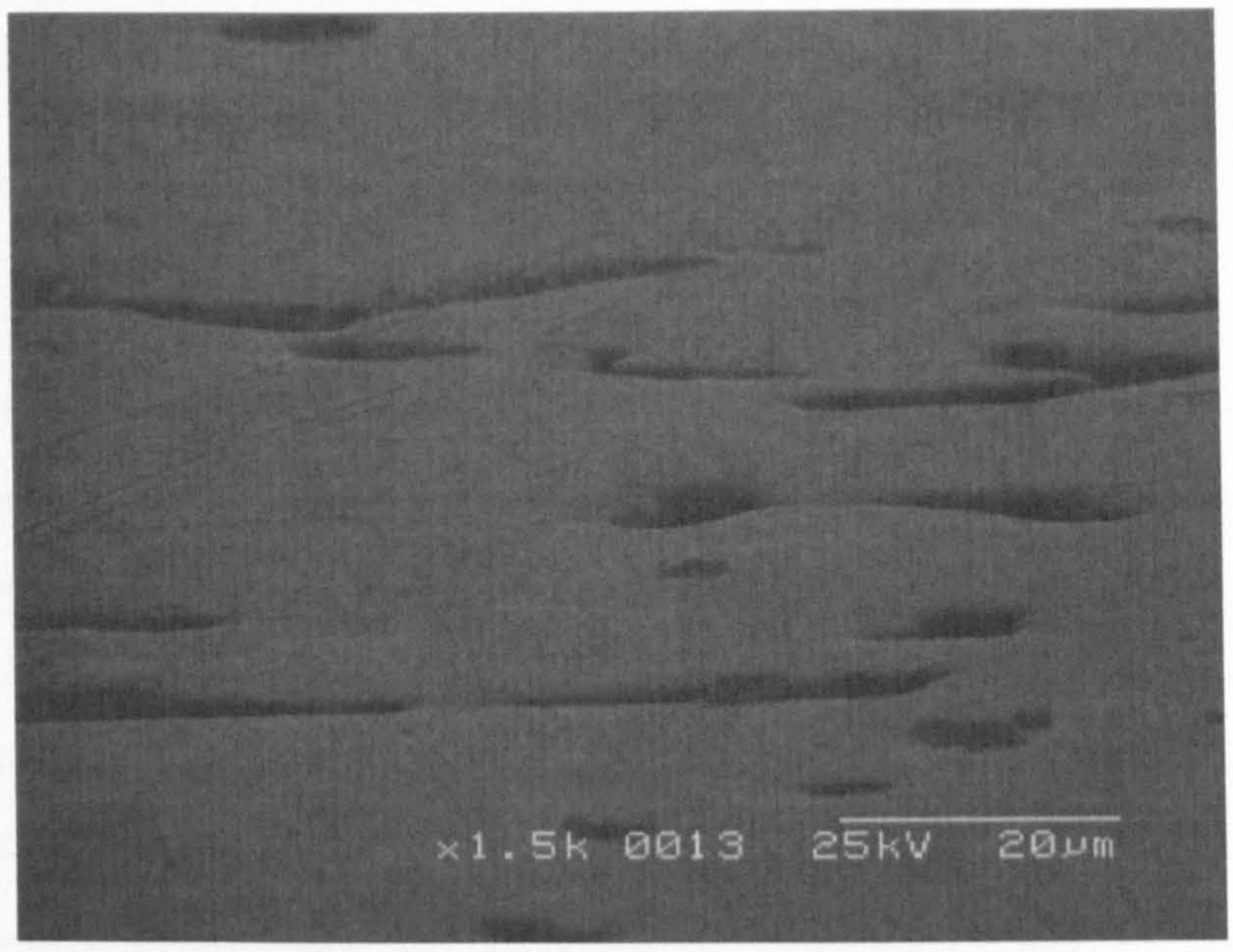

Figure 36 SEM image of a double heat treated specimen at 3 million cycles

Figure 37 high magnification image of a hole created in the double heat treated specimen during wearing

Figure 33, Figure 34, Figure 35, Figure 36 and Figure 37 show scanning electron micrographs of the 3 different CoCrMo specimens after wearing. Grooves identifying abrasive wear could be seen in Figure 33 and a build up of material could be seen at the edges of the harder block carbides. The Medium Carbide specimen in Figure 35 shows small pits and some grooves.

Figure 37 shows the worn surface of the double heat treated specimen, large holes where material has been ripped out can be seen.

5.2. Simulator tests

5.2.1. Double heat treated heads and cups

Cup	Head	Joint Number	Clearance
4	Lc 2	Control	0.4107
5	Lc 1	Test Pair 5	0.252
2	Lc 3	Test Pair 4	0.2444
6	Lc 5	Test Pair 3	0.2431
1	Ac1	Test Pair 2	0.2421
3	Ac2	Test Pair 1	0.2399

Table 7 Table showing pairings of joints

Lc – low carbide double heat treated head, Ac – as-cast head, all cups were double heat treated.

Table 7 shows the head and cup diameters for each component. The head diameter is taken away from the cup diameter to give a clearance. Ideally these clearances should be identical in order to eliminate the effect of clearances on the test. The clearances that have been chosen, highlighted above, are as close to each other as the samples would allow. The head and cup pairs that were decided upon are listed in Table 7.

5.2.1.1. Wear

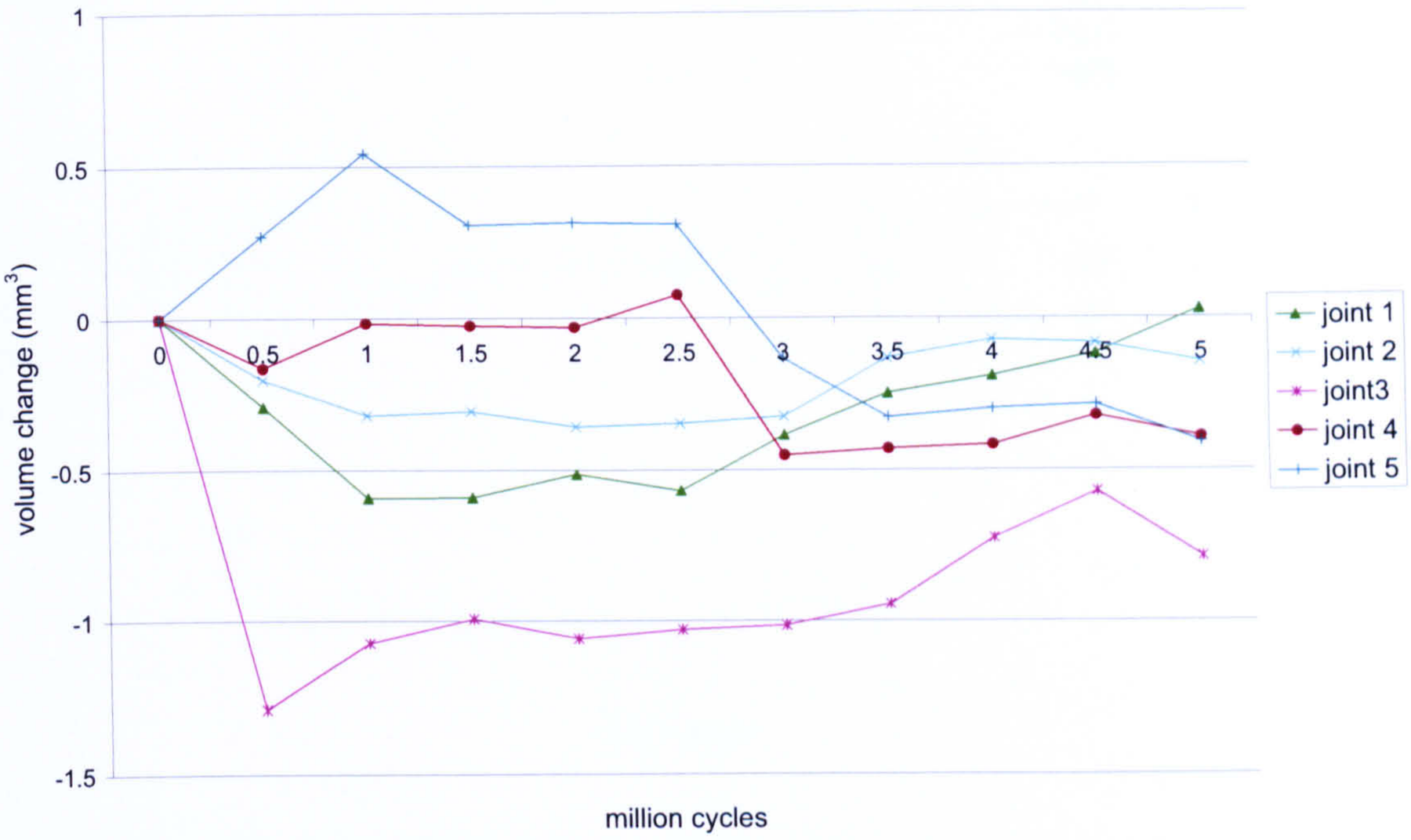

Figure 38: Wear rates for the 5 million cycle test of double heat treated cups on double heat treated or as-cast heads taking the control into account.

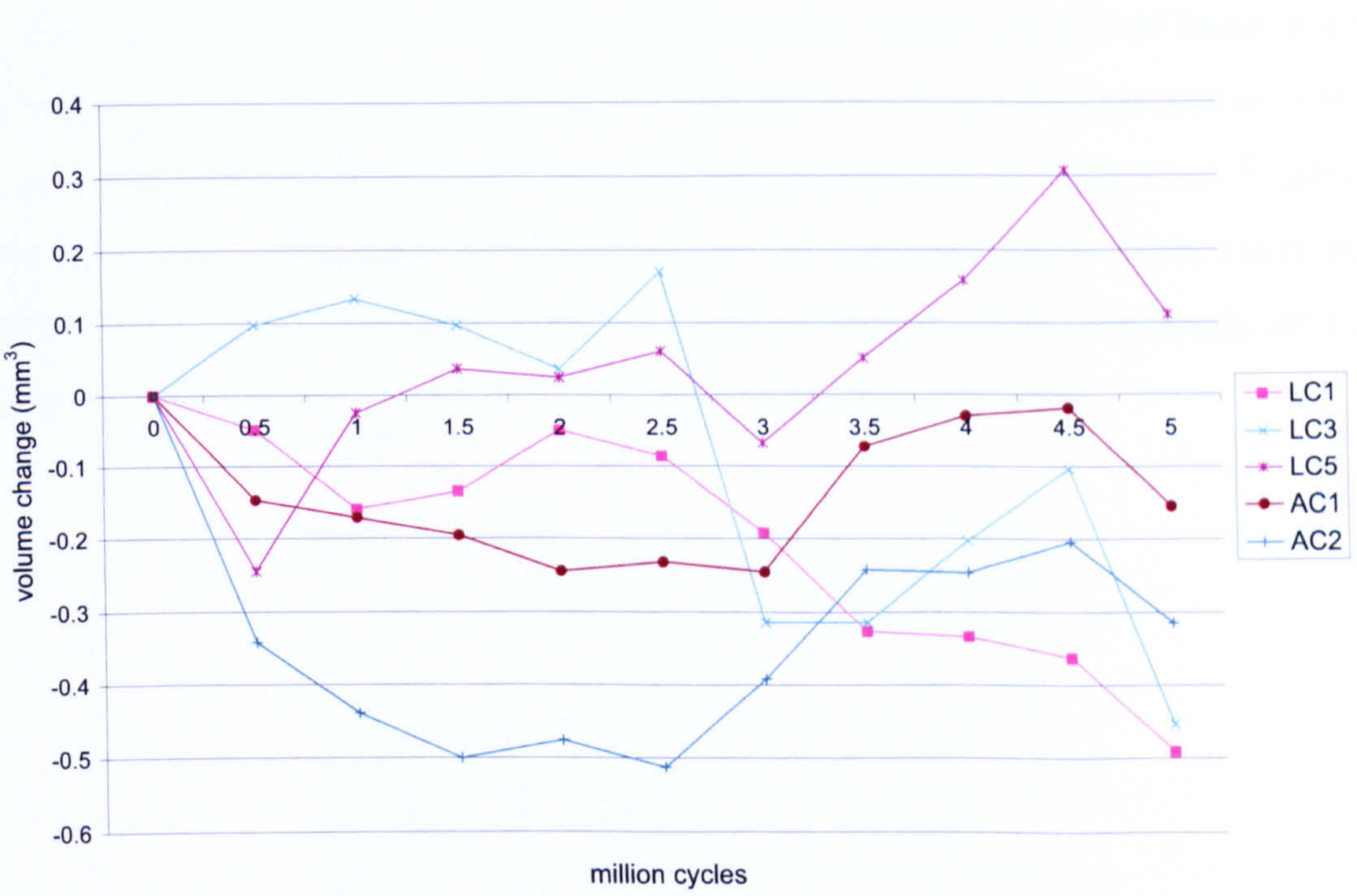

Figure 39 Volume change for as-cast and low carbide heads over 5 million cycles taking the control into account.

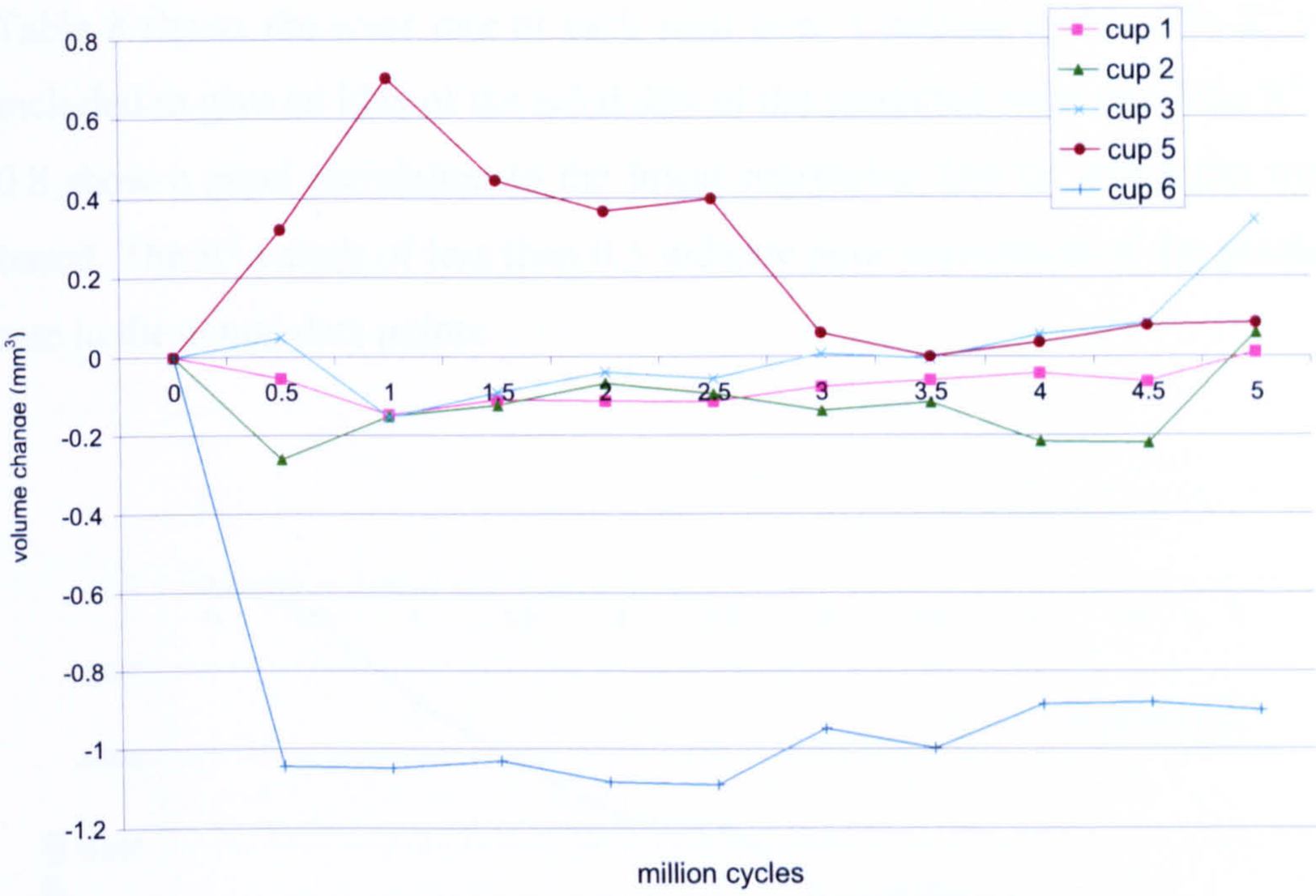

Figure 40 Volume change of the low carbide CoCrMo cups over a 5 million cycle test taking the control into account.

Figure 38 shows the wear of double heat treated cups against as-cast and double heat treated heads. The graph shows very little wear over the 5 million cycles, on average the wear is less than 0.5 mm^3. Figure 39 shows the volume change of three double heat treated heads and two as-cast heads. Very little wear can be seen and no trends can be identified. Figure 40 shows the volume change for the cups over 5 million cycles and show very little wear. However, the measurements taken every half million cycles were consistent. Joints 1, 2 and 3 were heat treated heads on heat treated cups, Joints 4 and 5 were as-cast heads on heat treated cups.

Joint	Wear rate for 5 million cycles (mm^3/Mc)	Regression coefficient R^2
1	0.0005	0.537
2	0.0011	0.6887
3	-0.0005	0.7635
4	0.0004	0.4921
5	0.0009	0.8173

Table 8 wear rates without the control included over the 5 million cycle test

Table 8 shows the wear rate of each joint over 5 million cycles. The R^2 value was included to give an idea of the reliability of the predicted wear rate. The R^2 values of 0.8 show a good correlation to the linear regression line on which the wear rate is based. The R^2 values of less than 0.5 indicate poor correlation of the predicted wear rate to the actual data points.

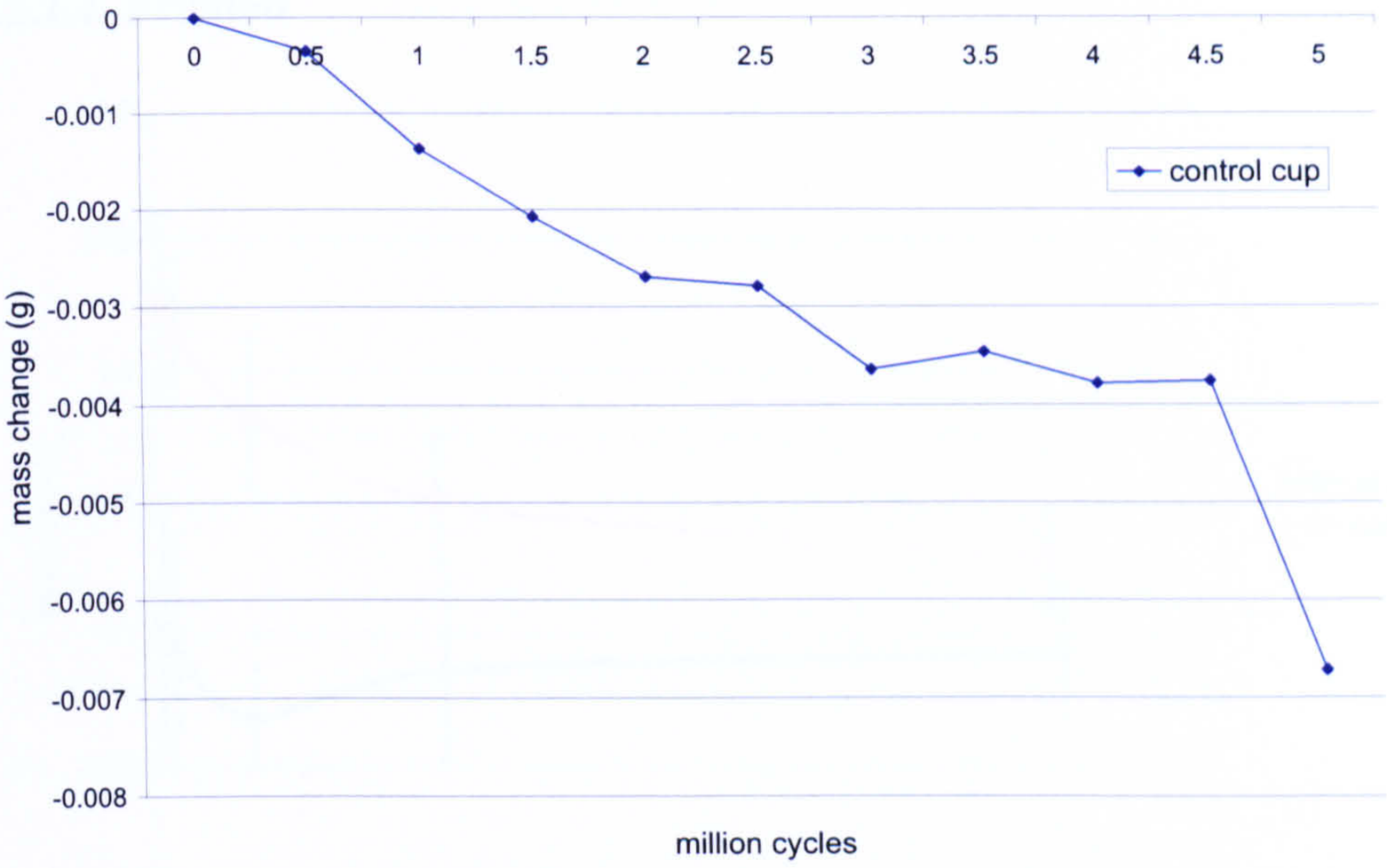

Figure 41 Mass change of control cup over the time taken for 5 million cycles

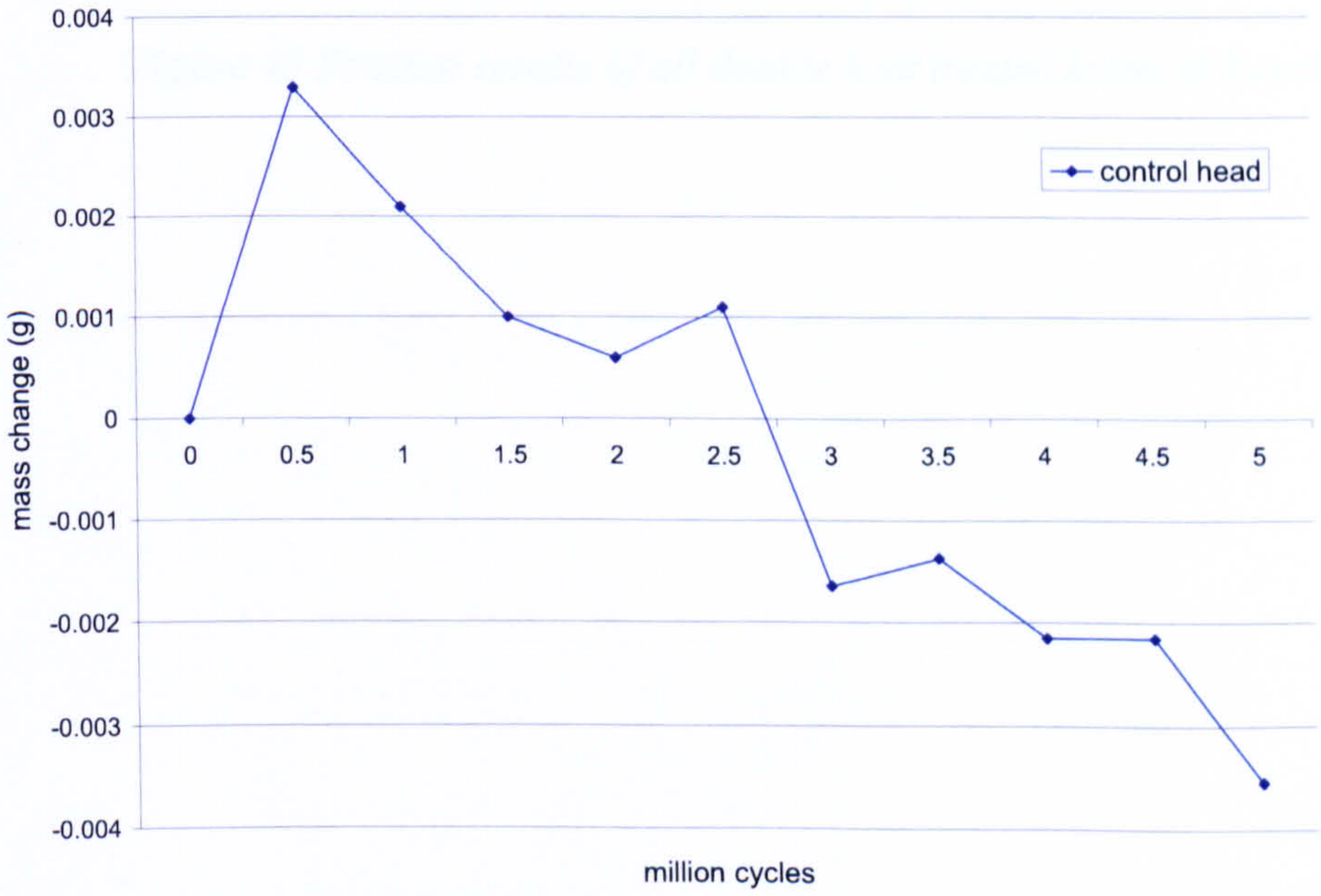

Figure 42 Mass change of the control head over the time taken for the 5 million cycles

Figure 41 and Figure 42 show the control joints mass change over the time taken to complete 5 million cycles and the joints appear to lose weight throughout. These mass changes are 2 orders of magnitude smaller than the wear rates seen in the articulating joints and therefore may be normal variation for these large components. However as such a large variation was seen in the data collected further tests would allow a fuller insight.

5.2.1.2. Friction

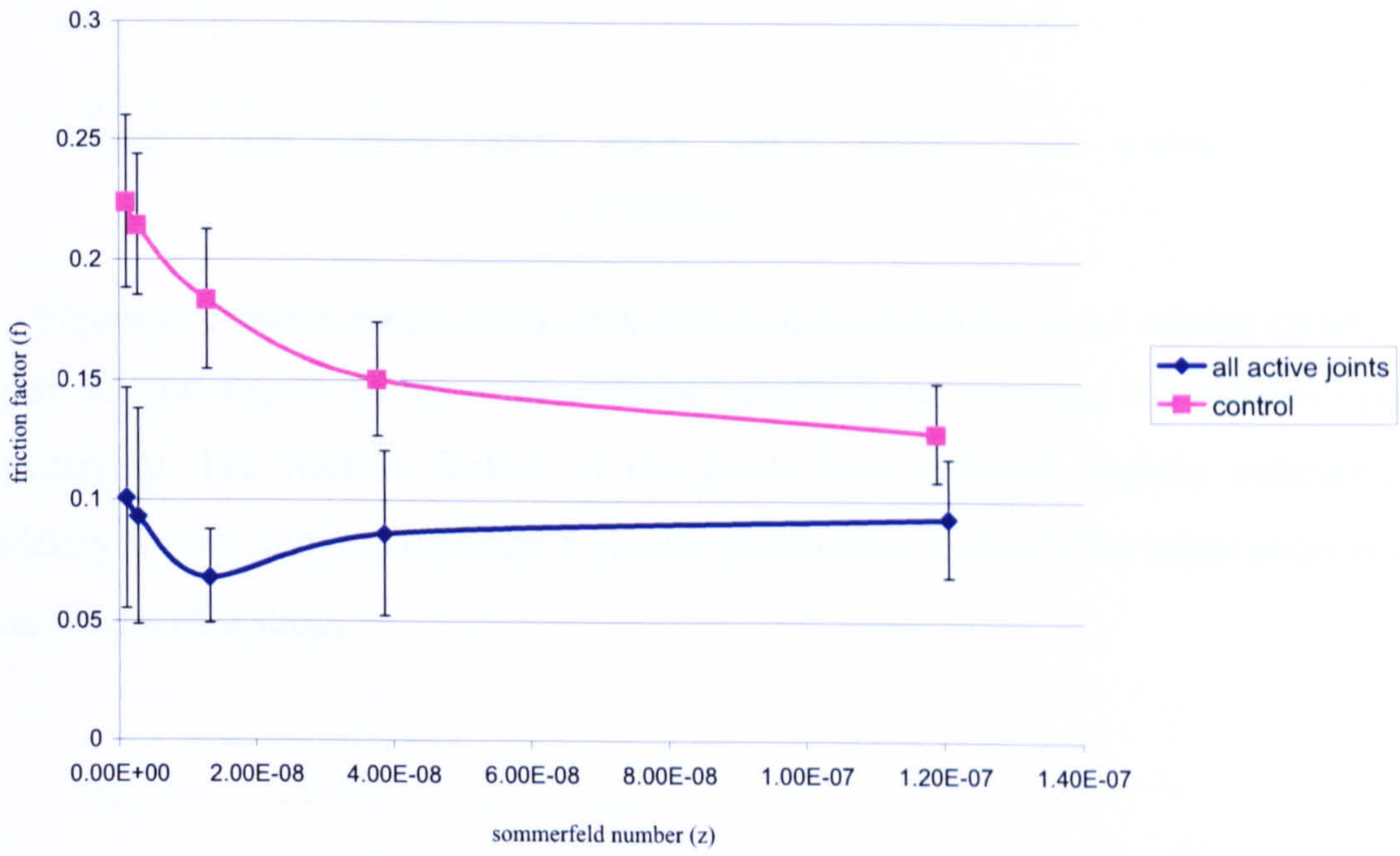

Figure 43 Friction results of all double heat treated joints at 0 cycles

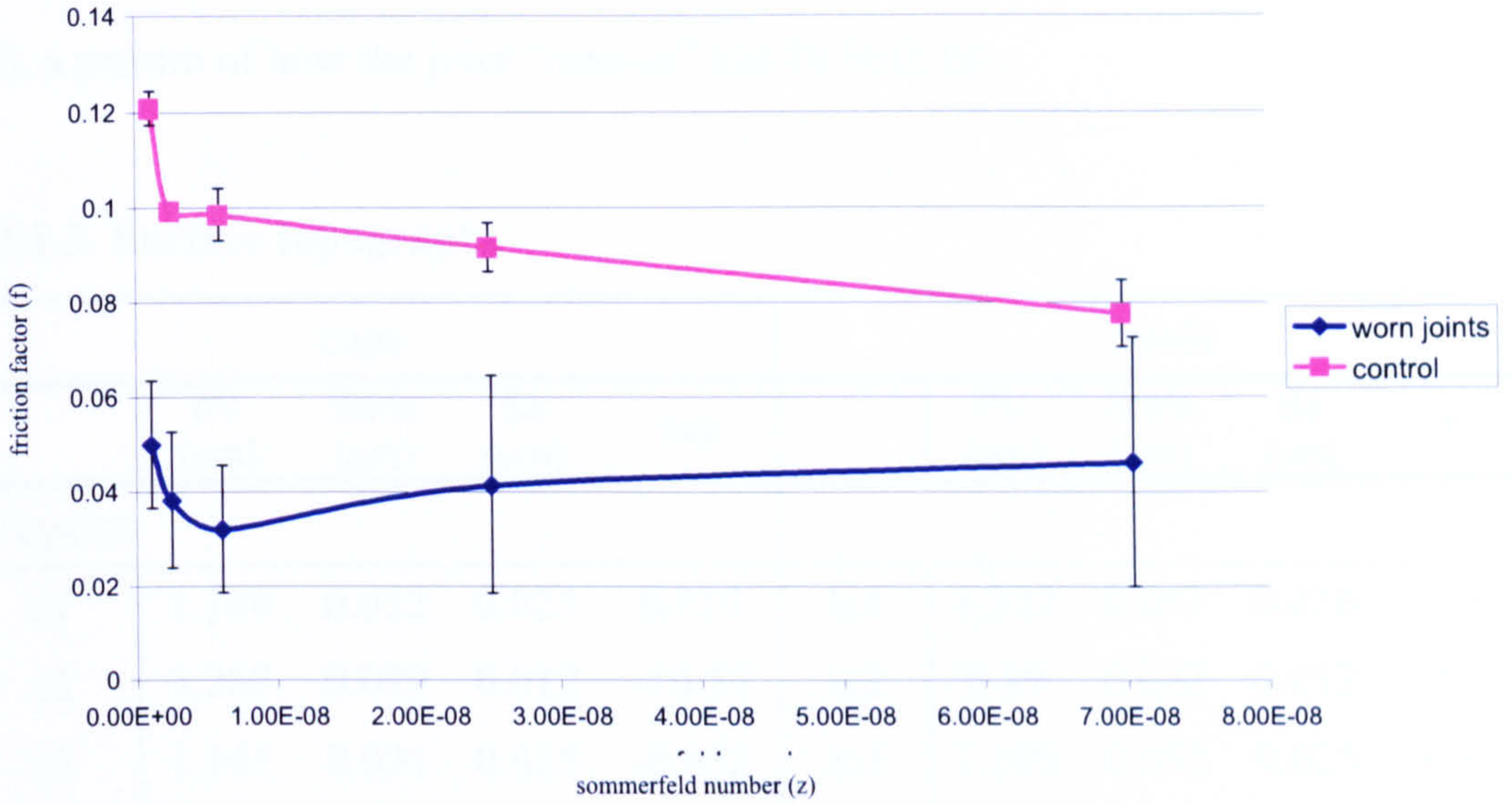

Figure 44 Friction results from all double heat treated joints at 3.5 million cycles

Figure 43 and Figure 44 show the friction results from zero and 3.5 million cycles respectively. The friction factors of the joints have reduced slightly indicating a tendency for the joints to undergo a greater proportion of fluid film lubrication in the latter stages of testing.

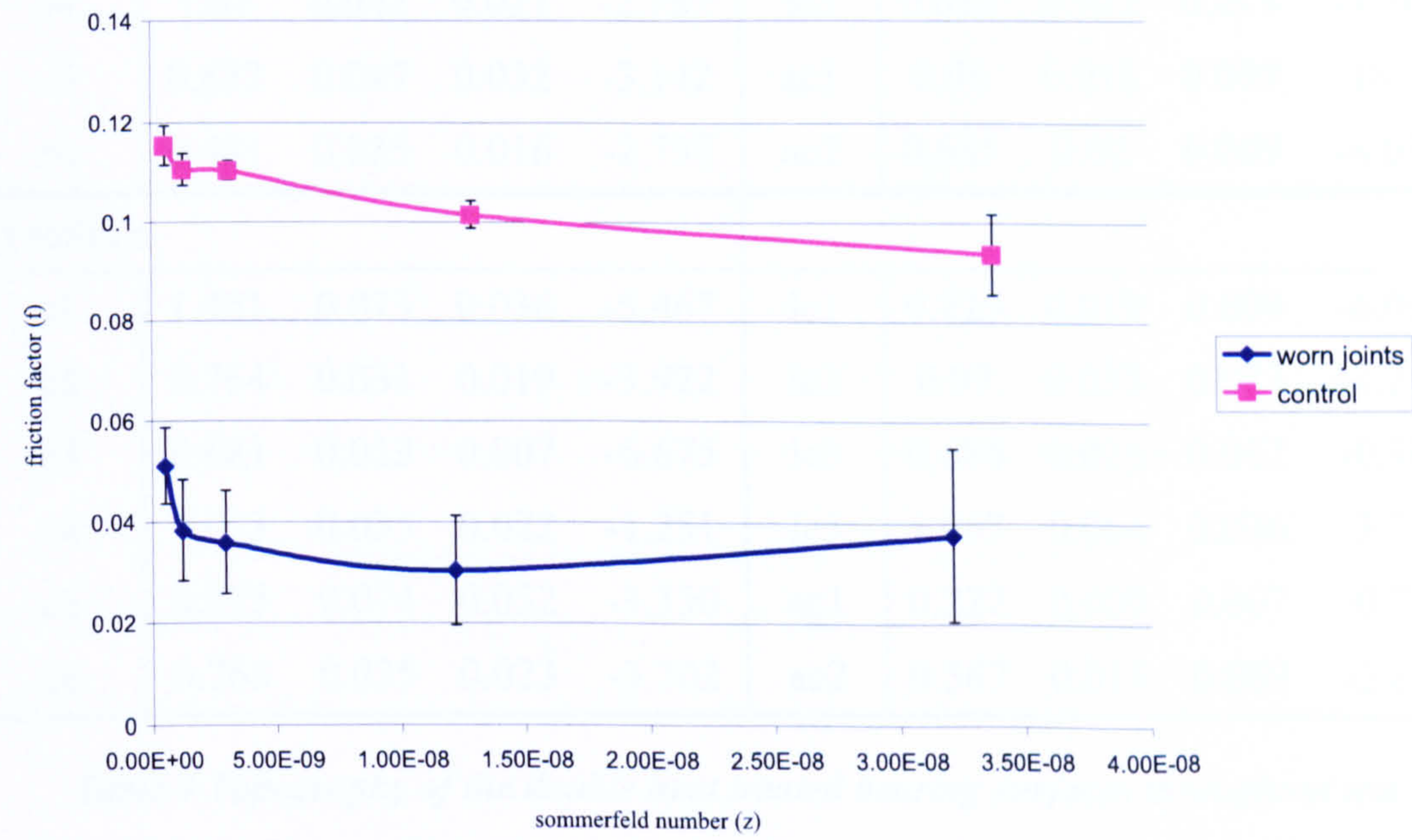

Figure 45 Friction results from all double heat treated joints at 5 million cycles

Figure 45 shows the friction results at 5 million cycles. This indicates the lubrication regime in the swing phase of the cycle at the end of the test. From the above 3

figures the progression of the joint lubrication improvement can be seen over the course of the 5 million cycles of wear. Coupled with the volumetric wear (Figure 38), a picture of how the joint "runs-in" can be built up.

5.2.1.3. Surface topography

cups					heads				
	PV (μm)	Srms (μm)	Sa (μm)	Ssk		PV (μm)	Srms (μm)	Sa (μm)	Ssk
0 cycles									
c1	1.109	0.052	0.025	0.810	lc1	1.323	0.051	0.026	-2.343
c2	1.268	0.029	0.012	-10.57	lc2	0.89	0.022	0.012	-5.787
c3	1.161	0.031	0.015	-6.652	lc3	1.109	0.052	0.025	0.810
c4	1.302	0.034	0.013	-8.967	lc5	1.183	0.048	0.025	-3.525
c5	1.272	0.041	0.017	-5.258	ac1	0.566	0.034	0.024	1.770
c6	1.331	0.03	0.013	-9.414	ac2	0.577	0.031	0.021	1.841
3 million cycles									
c1	0.926	0.042	0.024	-4.591	lc1	0.336	0.008	0.006	-2.022
c2	0.585	0.034	0.021	-3.210	lc2	1.154	0.089	0.045	-4.747
c3	0.693	0.027	0.014	-5.188	lc3	0.402	0.015	0.008	-3.059
c4	1.07	0.042	0.027	-2.787	lc5	0.688	0.032	0.018	-4.562
c5	0.633	0.047	0.032	-3.142	ac1	0.96	0.018	0.008	-18.17
c6	0.481	0.025	0.016	-2.757	ac2	0.685	0.02	0.009	-8.035
5 million									
c1	1.461	0.073	0.036	-5.467	lc1	0.725	0.019	0.009	-6.019
c2	0.764	0.031	0.019	-3.922	lc2	0.97	0.035	0.023	-1.215
c3	0.681	0.013	0.007	-6.675	lc3	0.684	0.026	0.017	-0.901
c4	1.033	0.035	0.022	-1.251	lc5	1.067	0.064	0.036	-3.202
c5	0.975	0.074	0.052	-3.350	ac1	0.227	0.009	0.007	-0.720
c6	0.768	0.035	0.023	-3.702	ac2	0.587	0.015	0.009	-2.845

Table 9 Topography of the double heat treated bearing surfaces throughout test

Table 9 shows the roughness, skewness and peak to valley height results of surface topography analysis from the initial, 3 million and final surface analysis. There appears to be very little trend in these data. Cup 1 starts off as the roughest surface but by 3 million cycles cups 4 and 5 are of similar Sa and Srms to cup 1. The two as-

cast heads start with a positive skewness and by 3 million have the largest negative skewnesses.

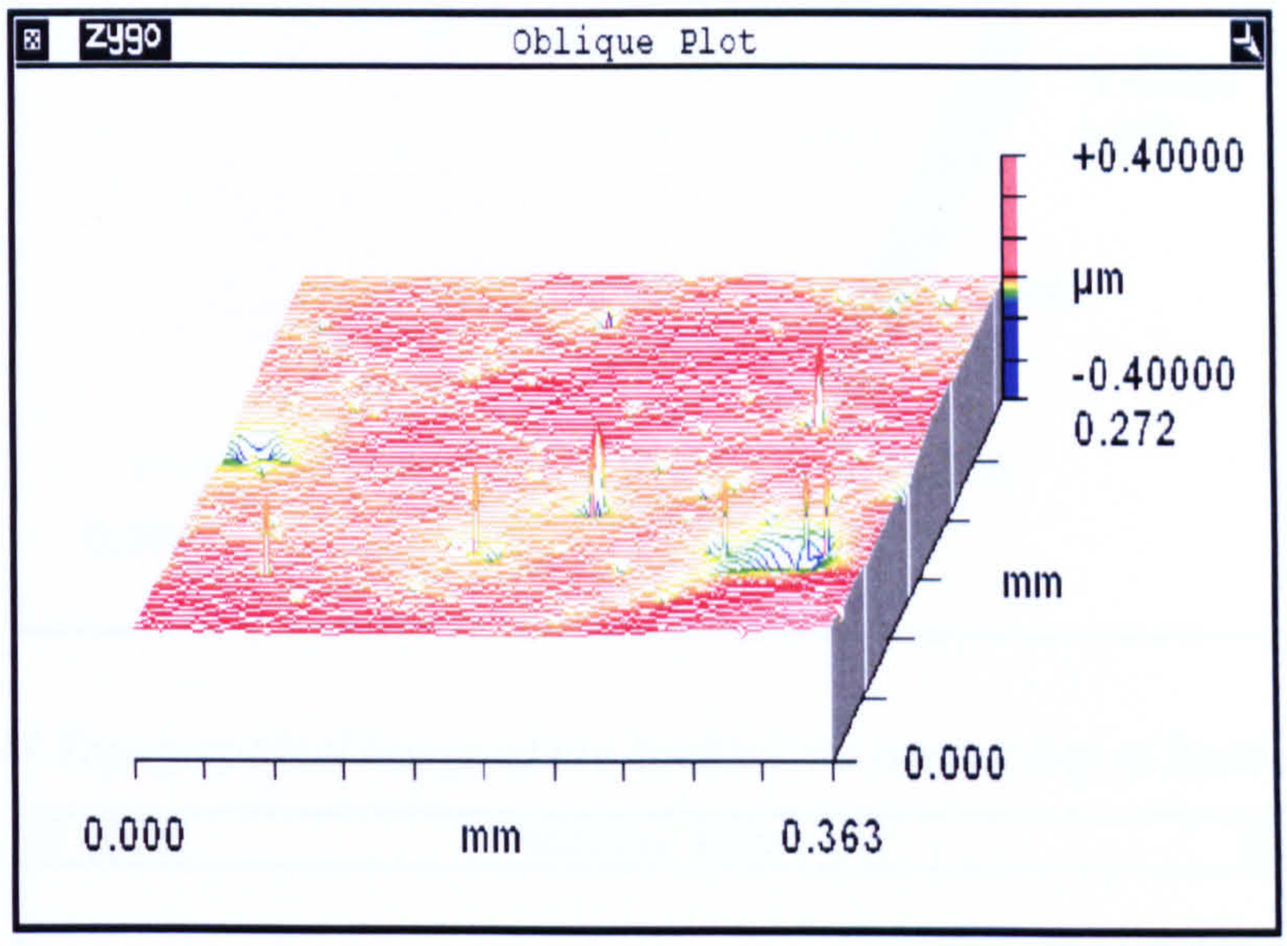

Figure 46 Topographical image of the double heat treated head at 0 cycles

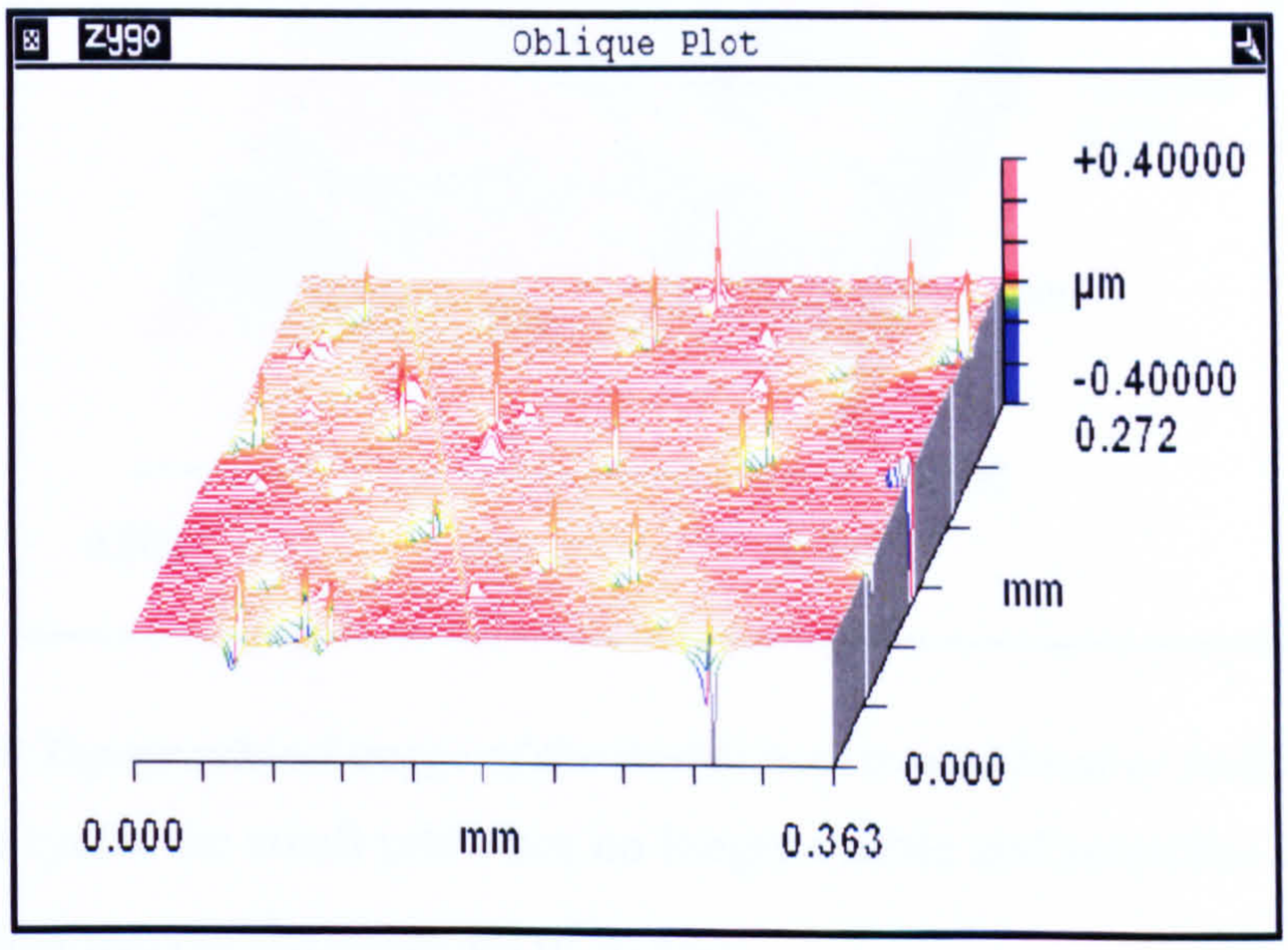

Figure 47 Topographical image of the double heat treated cup at 0 cycles

The head and cup surface topography at the initiation of the test were similar, there are few carbide protrusions out of the surface and several small pits in the surfaces.

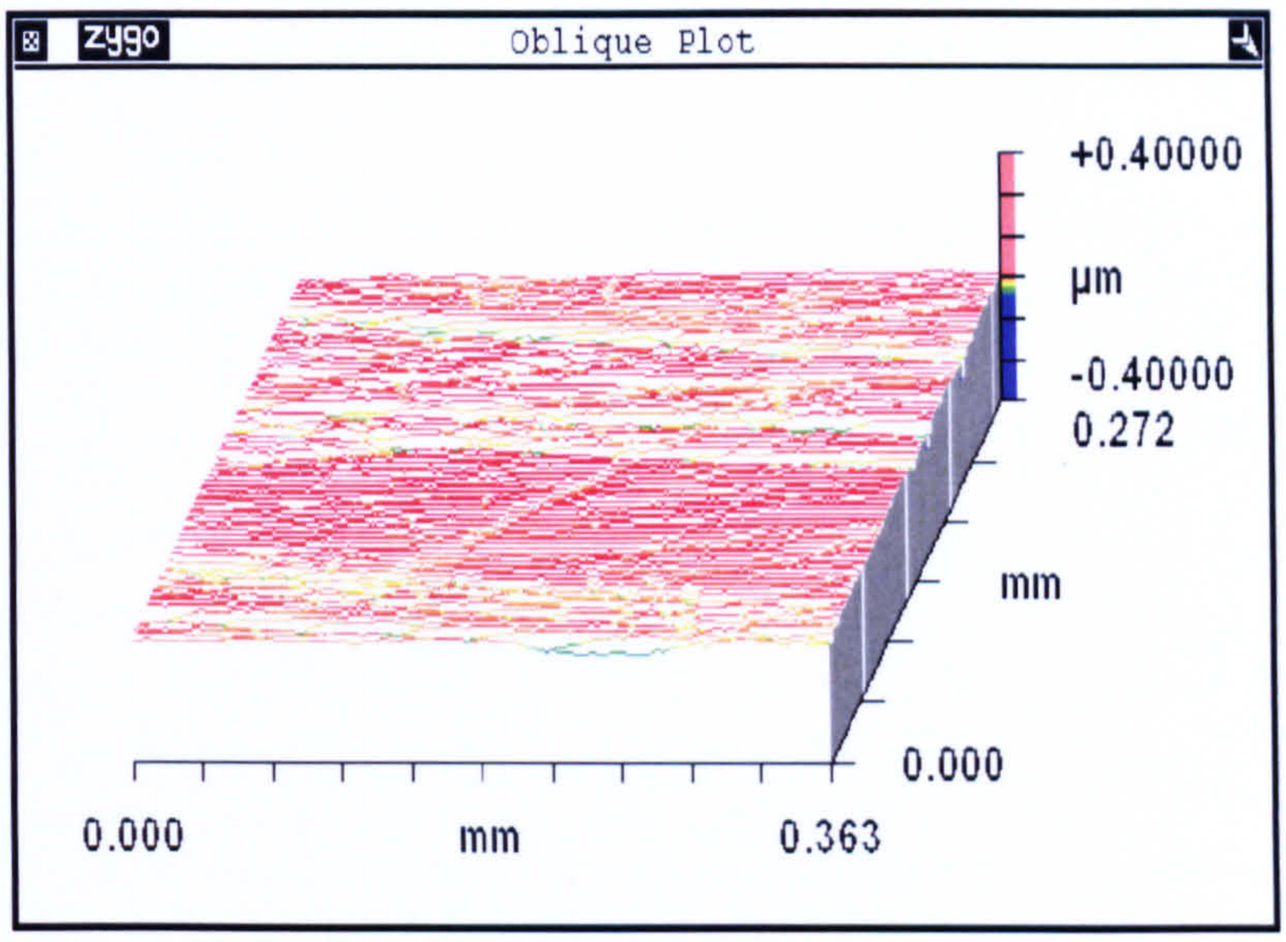

Figure 48 Topographical image of the double heat treated cup at 3million cycles

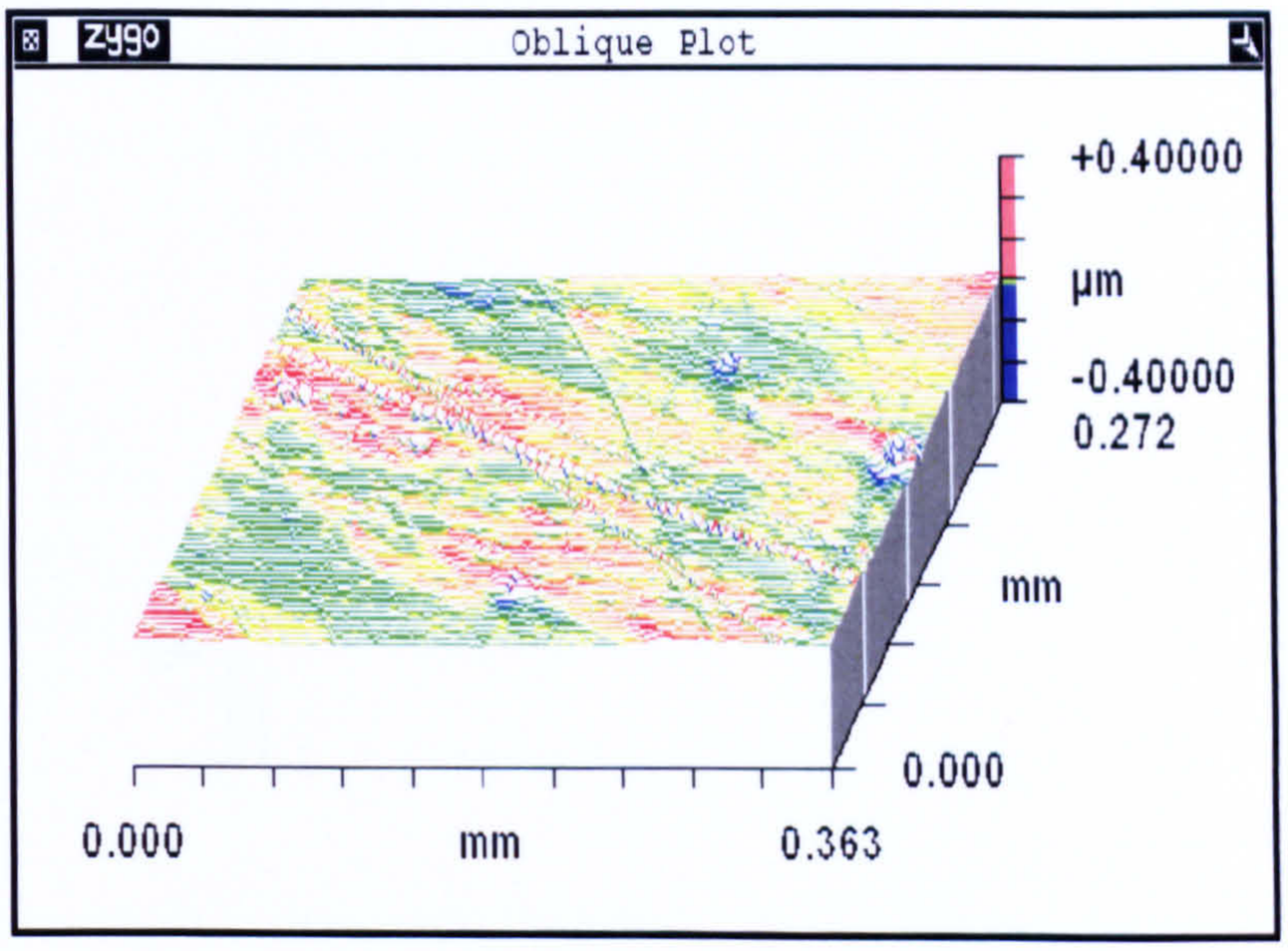

Figure 49 Topographical image of the double heat treated head at 3million cycles

By 3 million cycles the small pits were no longer visible and scratches could be seen across the specimens in the direction of motion.

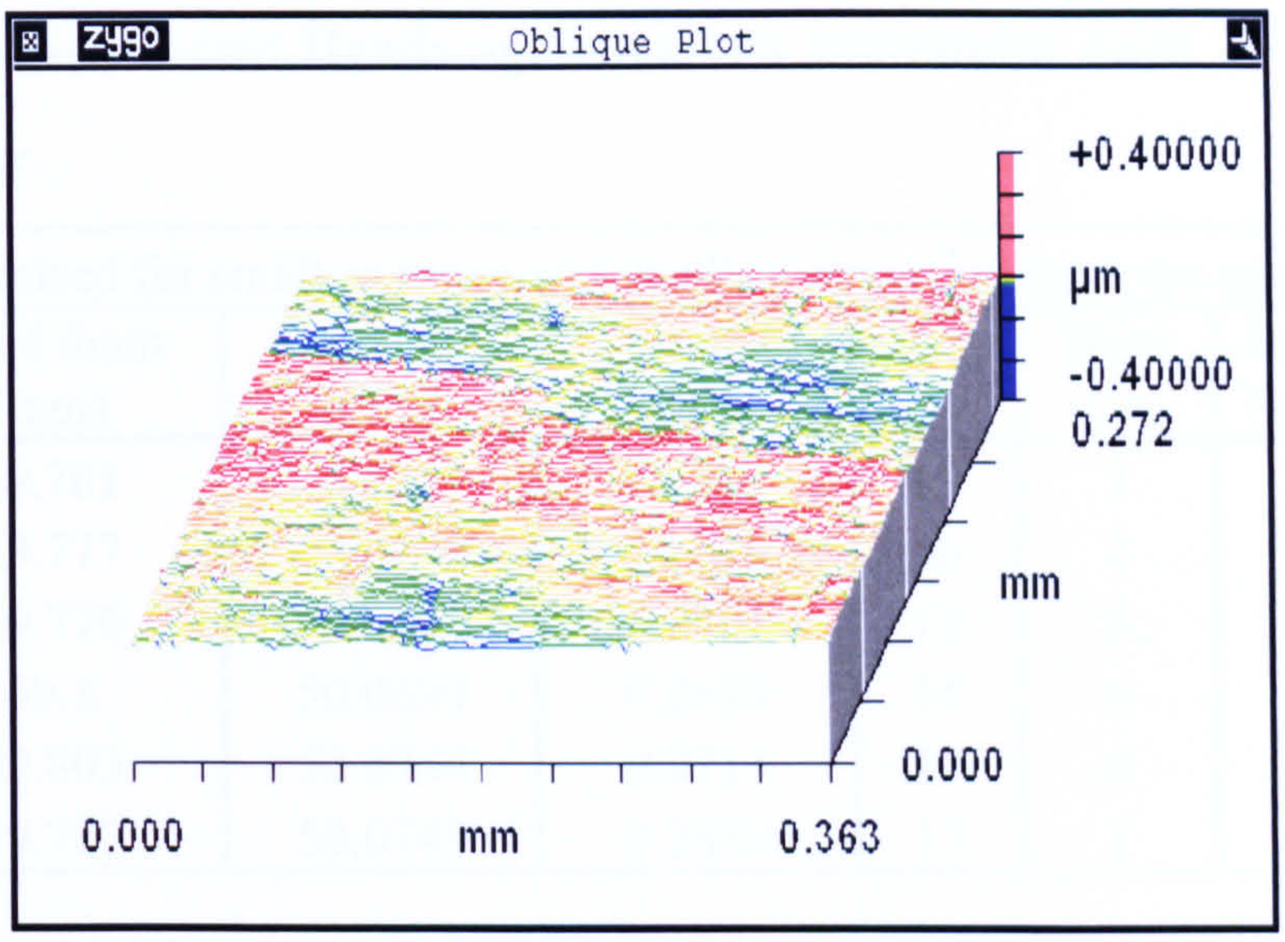

Figure 50 Topographical image of the double heat treated cup at 5million cycles

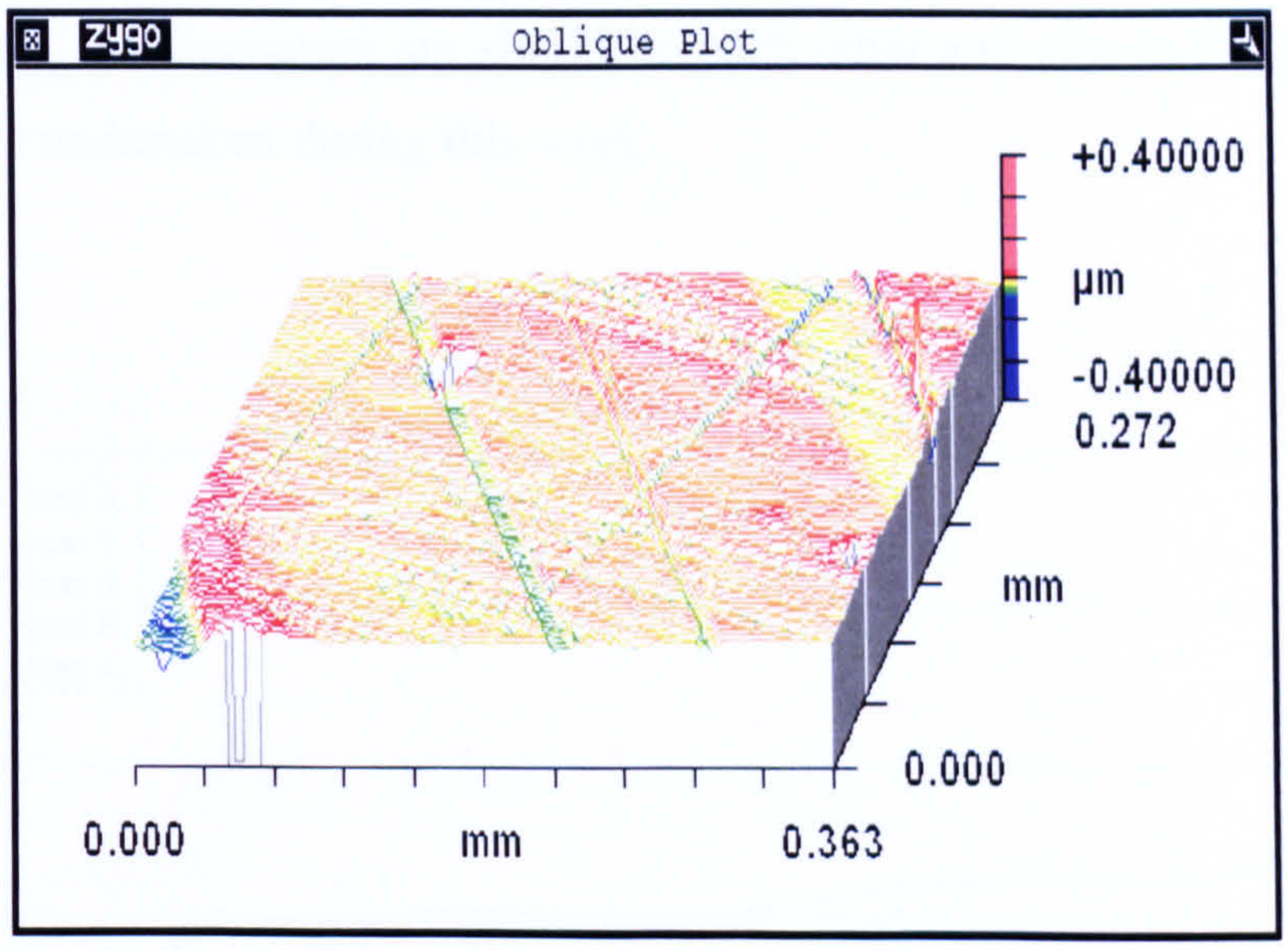

Figure 51 topographical image of the double heat treated head at 5 million cycles

The cup surfaces at 5 million cycles appeared smoother, however the head had deep scratches and some large pits visible.

5.2.2. Modular As-cast Heads against worn acetabular cups

5.2.2.1. Wear

Optimised for smallest range and smallest deviation from the mean					
Head diam (mm)	Cup diam (mm)	Clearance (mm)	cup No	Head No	Joint No
49.781	50.0253	0.2443	19	3	1
49.777	50.0296	0.2526	16	2	2
49.776	50.0321	0.2561	18	5	3
49.8	50.0639	0.2639	15	6	4
49.803	50.0744	0.2714	14	4	5
49.787	50.0749	0.2879	17	1	ctrl

Table 10 Clearances for the modular heads joints

Table 10 shows the head and cup diameter and the clearance for each joint that has been paired up, the clearances are similar to each other and also to the clearances of the other tests undertaken during this work.

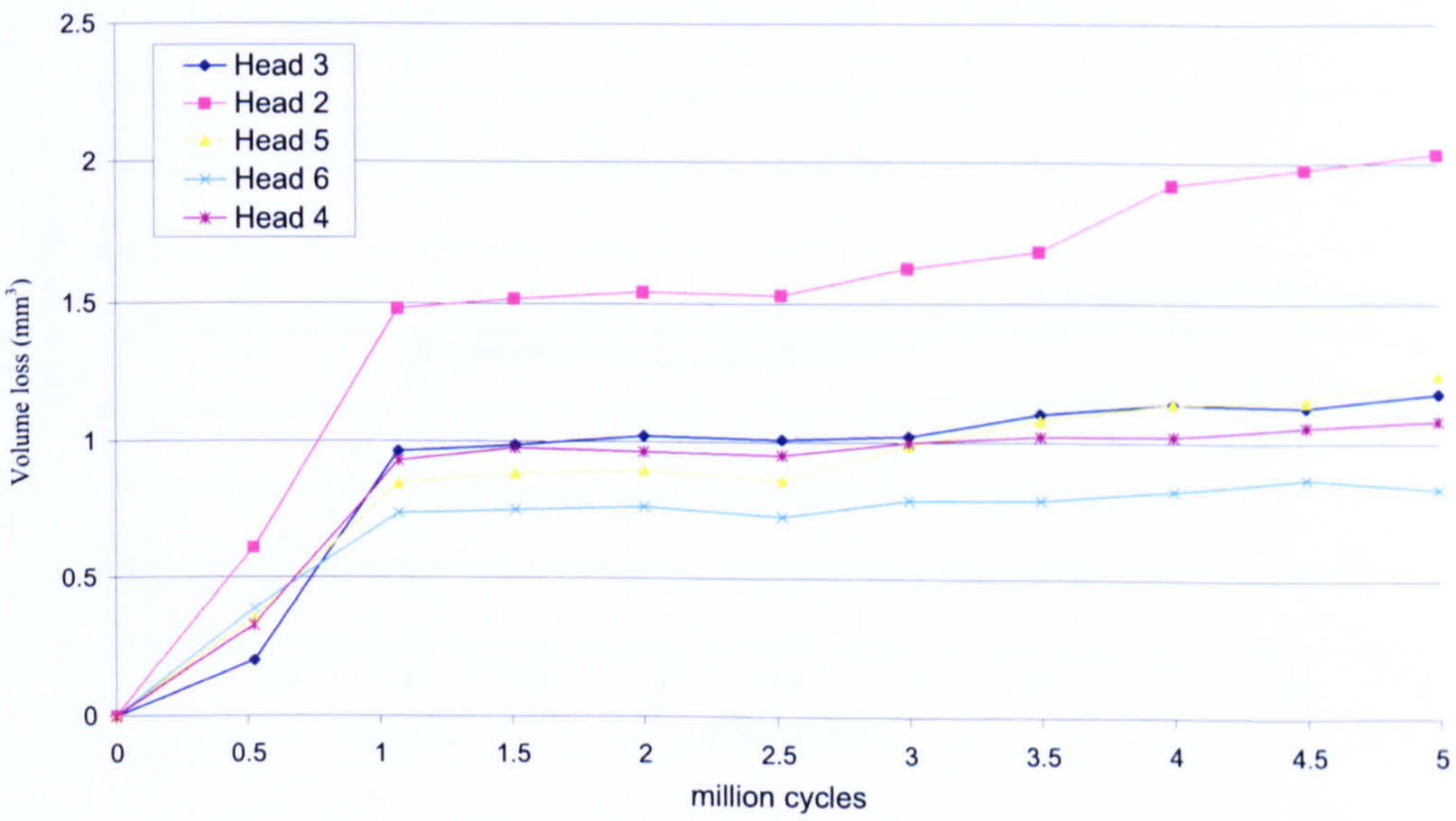

Figure 52 Volume loss vs number of cycles for head wear of as-cast heads against worn acetabular cups

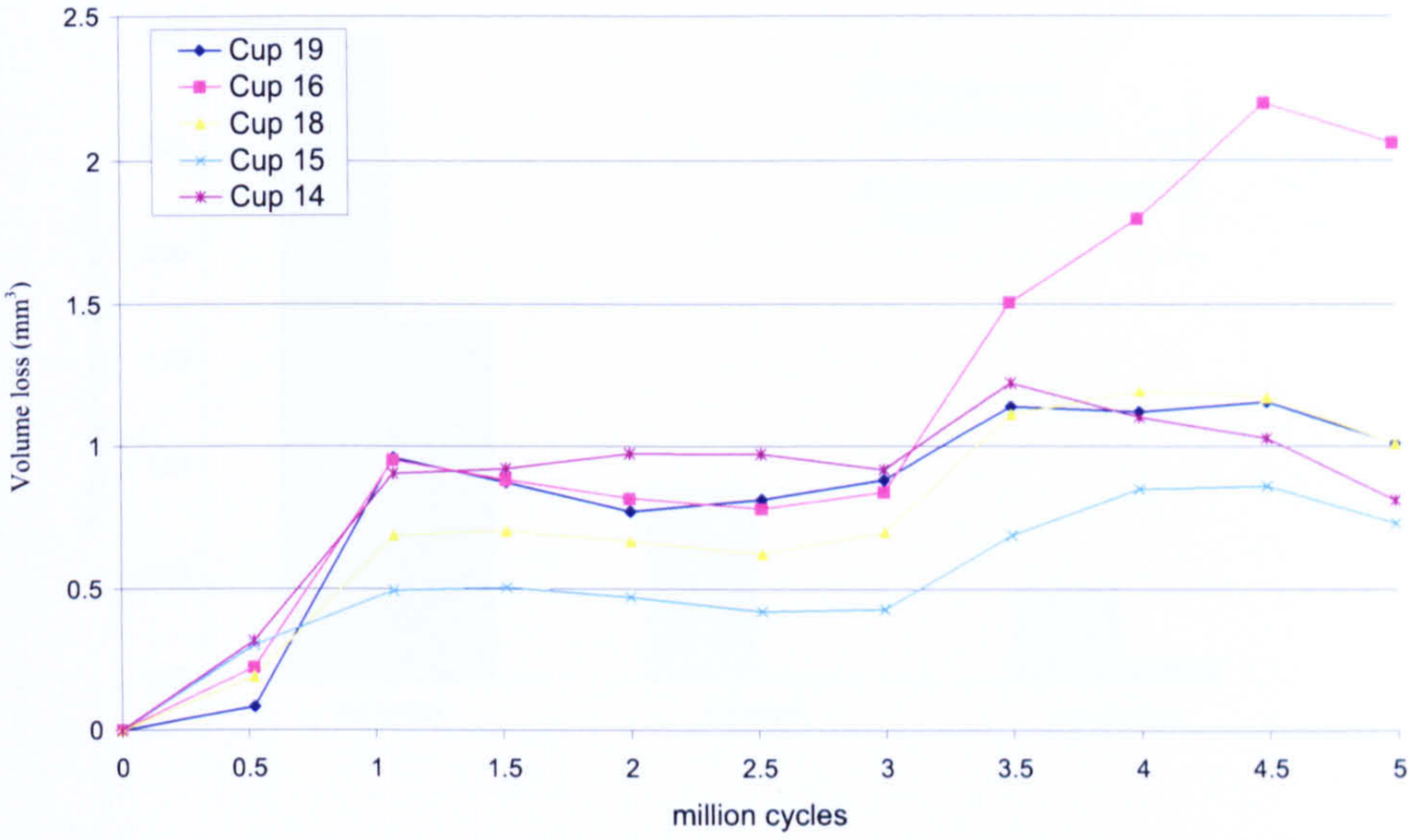

Figure 53 Volume loss vs number of cycles for the cups of as-cast heads against worn acetabular cups

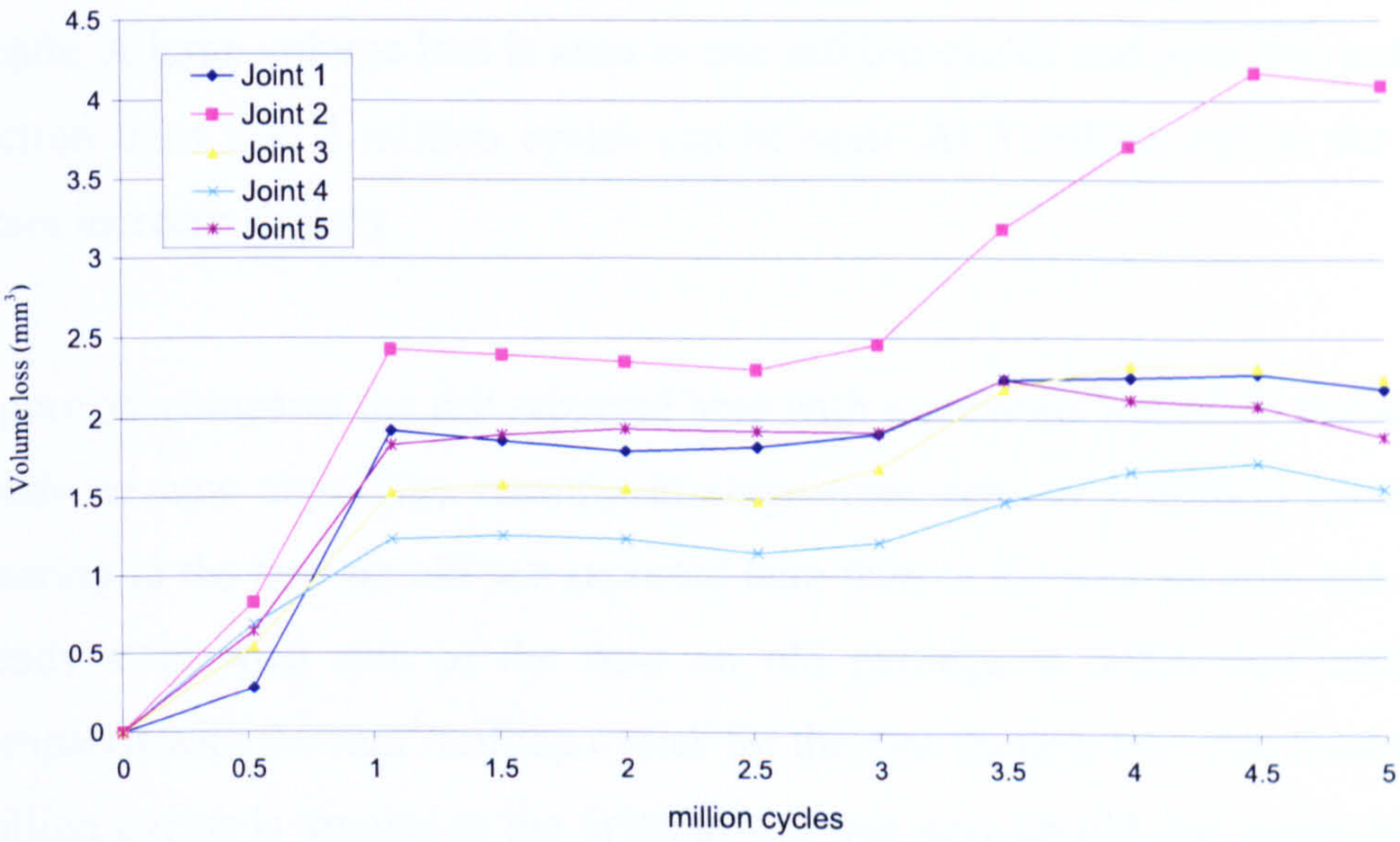

Figure 54 Combined wear data for all 5 joints of as-cast heads against worn acetabular cups

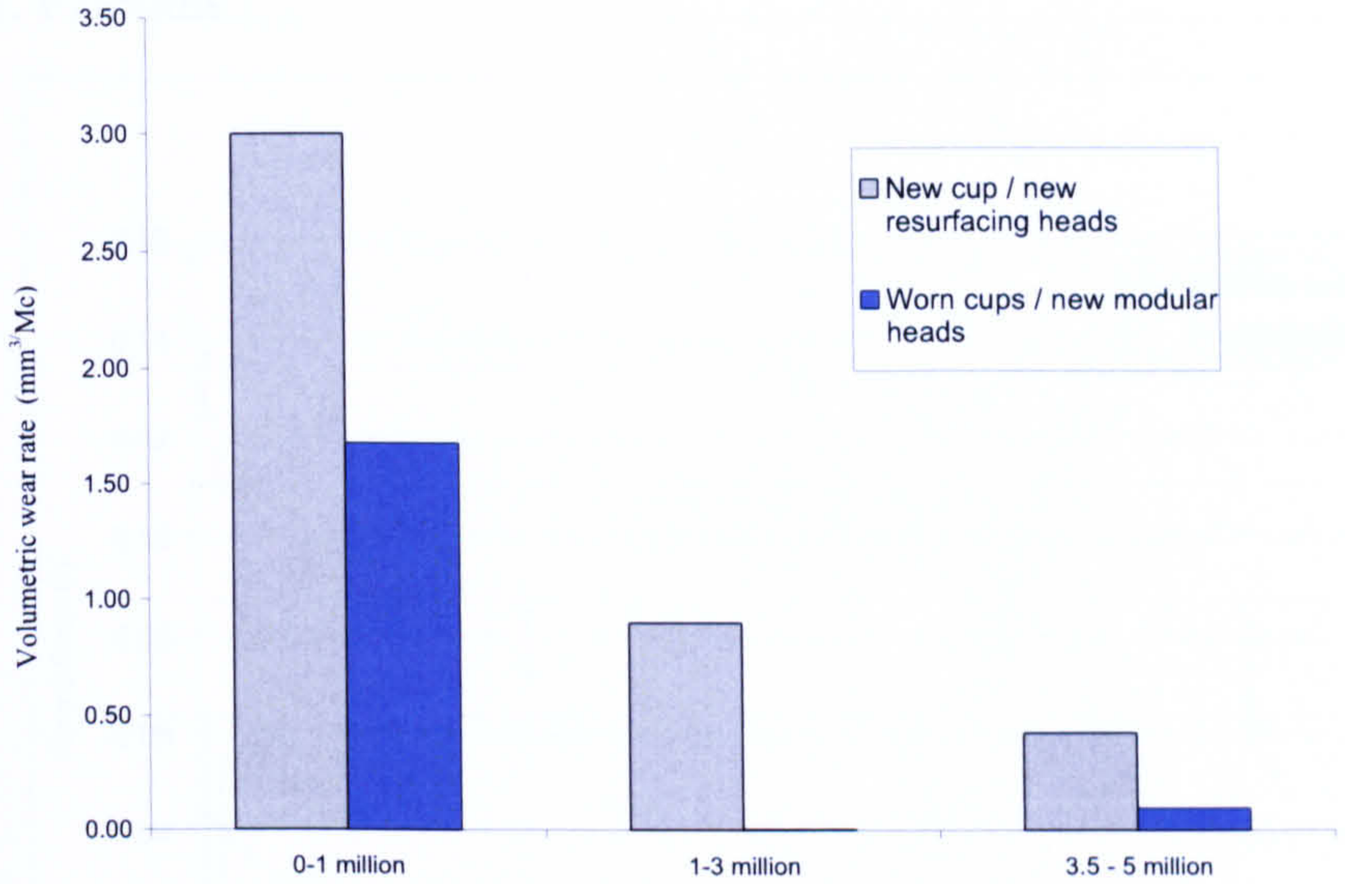

Figure 55 Comparison of wear rate for the new cups against new heads and old cups against new heads

Figure 52 and Figure 53 show the volume loss of the heads and cups against the number of cycles in the wear simulator. Both the heads and the cups show similar trends. A large volume loss is seen to one million cycles and after this period a level section from 1 to 3 million cycles can be seen. At 3 million cycles the wear rates again increase slightly.

Figure 55 compares the test reported here with a previous test of 50 mm as-cast new heads on new cups. The running in stage from zero to 1 million cycles is lower wearing in the new on old test reported here than in the new on new test. The initial steady state wear rate of the new on old pairings is 0.006 mm^3/million cycles compared with 0.9 mm^3/million cycles for the new on new test. The final stage 3 to 5 million cycles is similar to the original test, the new on old test wears slightly less. The heads and cups were analysed topographically with the non contacting white light profilometer at zero 3 and 5 million cycles the results can be seen at Figure 57, Figure 58, Figure 59, Figure 60, Figure 61 and Figure 62.

The frictional results can be seen below where the Stribeck plots indicate the lubrication regime.

5.2.2.2. Friction

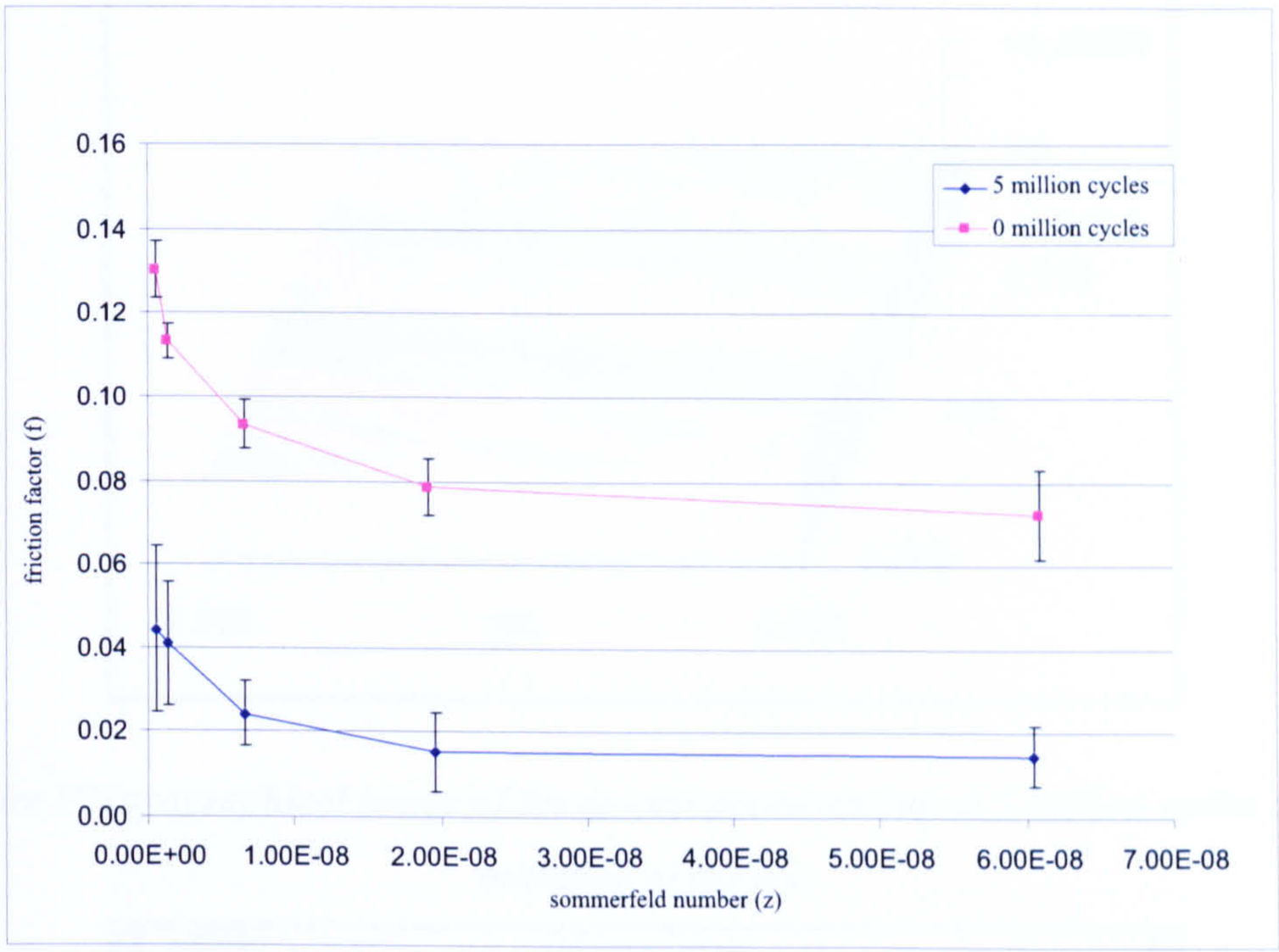

Figure 56 Friction results for the new on old modular device before and after the 5 million cycle test

5.2.2.3. Surface analysis

Figure 57 to Figure 62 shows the progression of the topography of the head and cup as the head wears from new to 5 million cycles the carbides are worn down and the surface gets smoother. The cup was worn from 5 to 10 million cycles the smooth initial surface appears to become scratched and re-polished again.

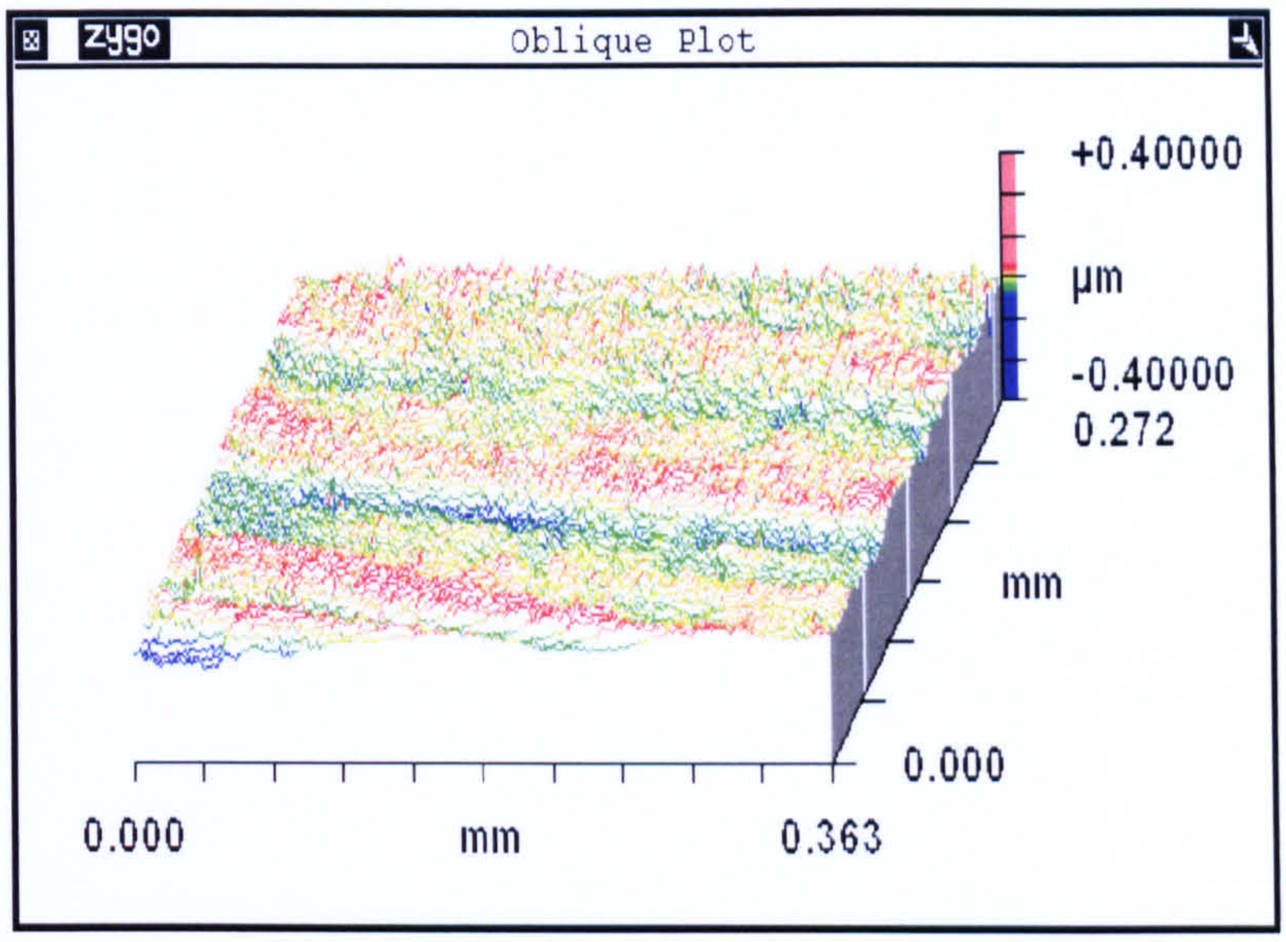

Figure 57Topographical image of the as-cast pre-worn cup at 5 million cycles at the initiation of the test

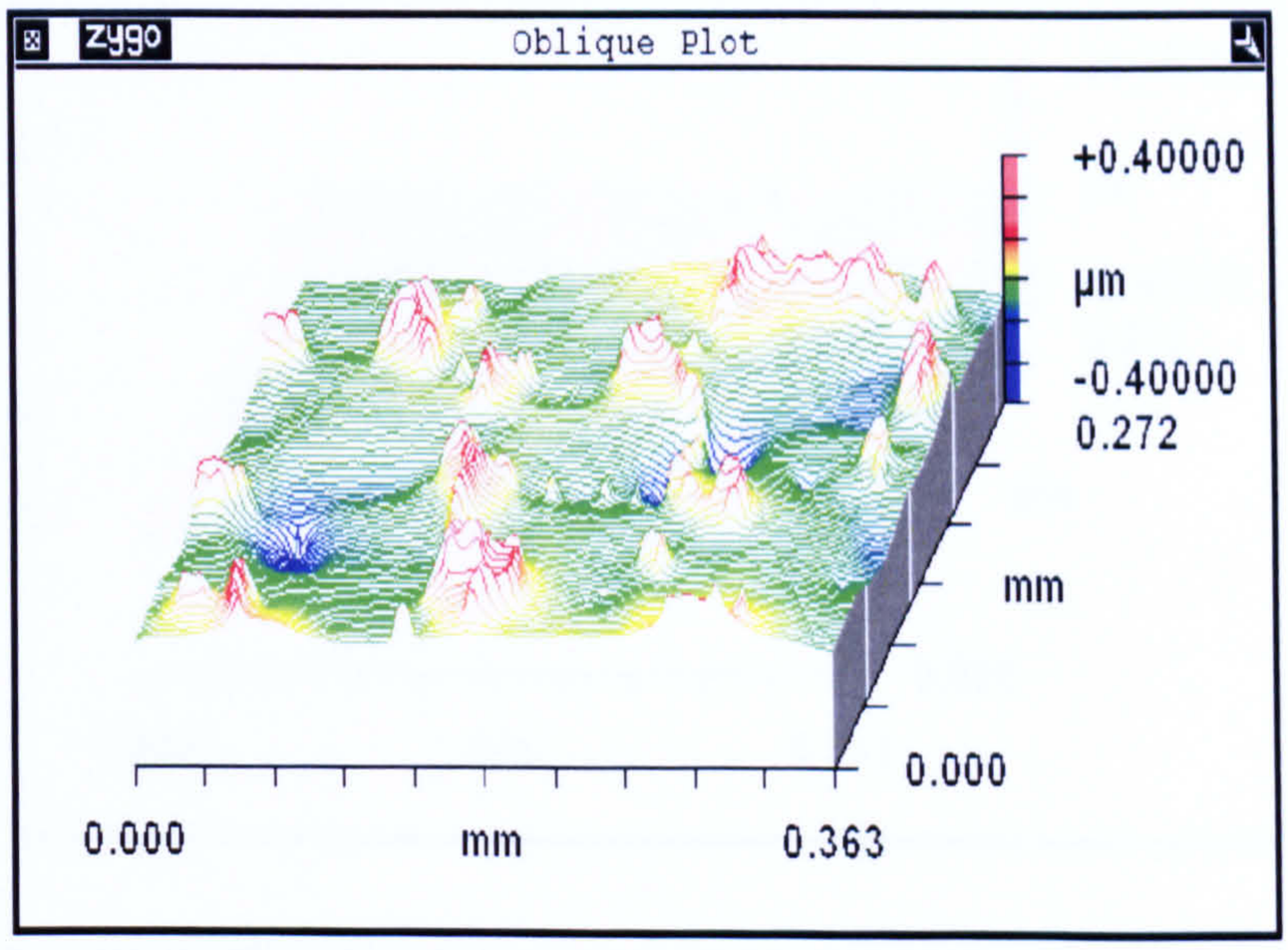

Figure 58 Topographical image of the as-cast new head at 0 cycles

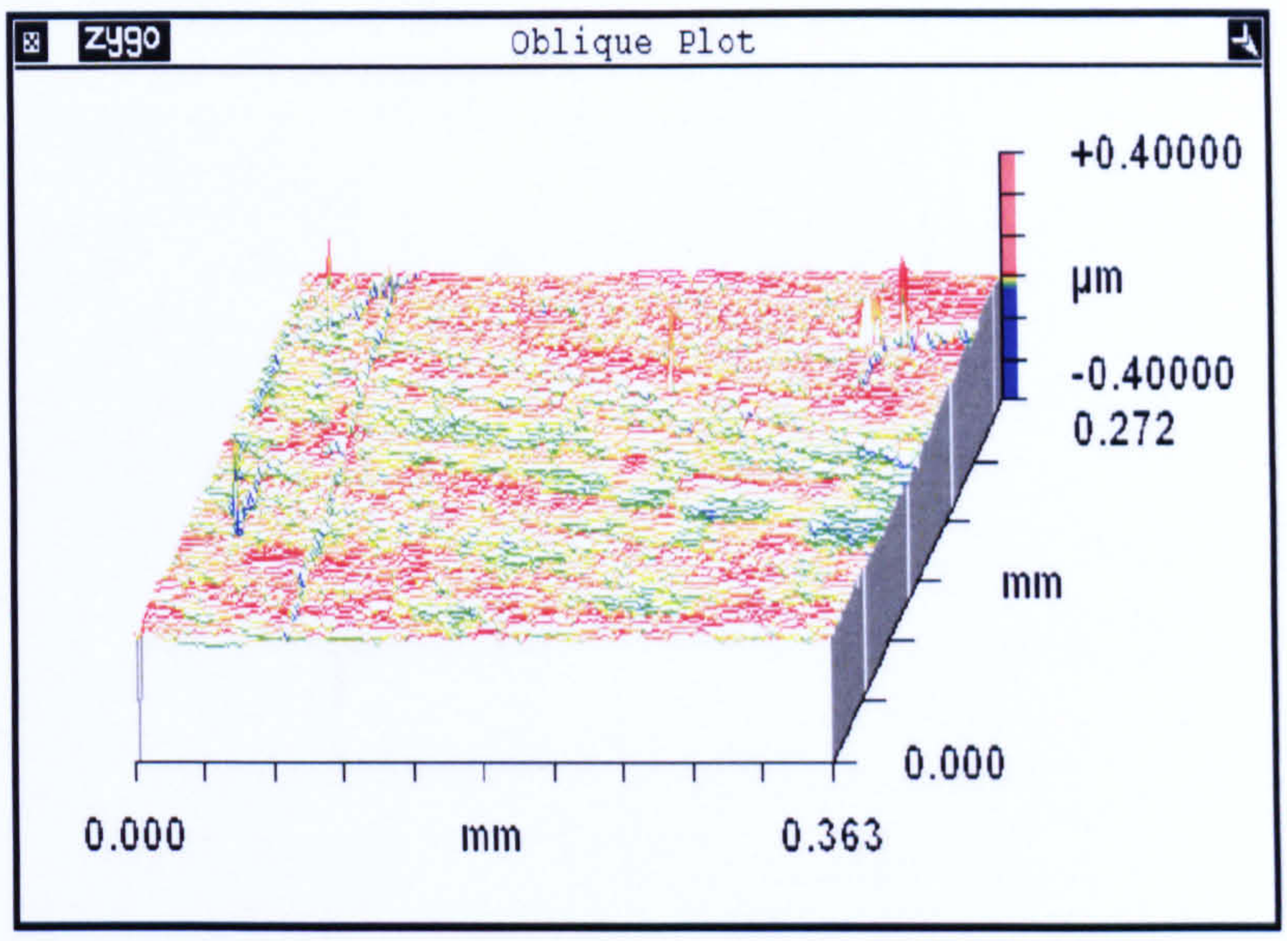

Figure 59 Topographical image of as-cast cup at 8 million cycles

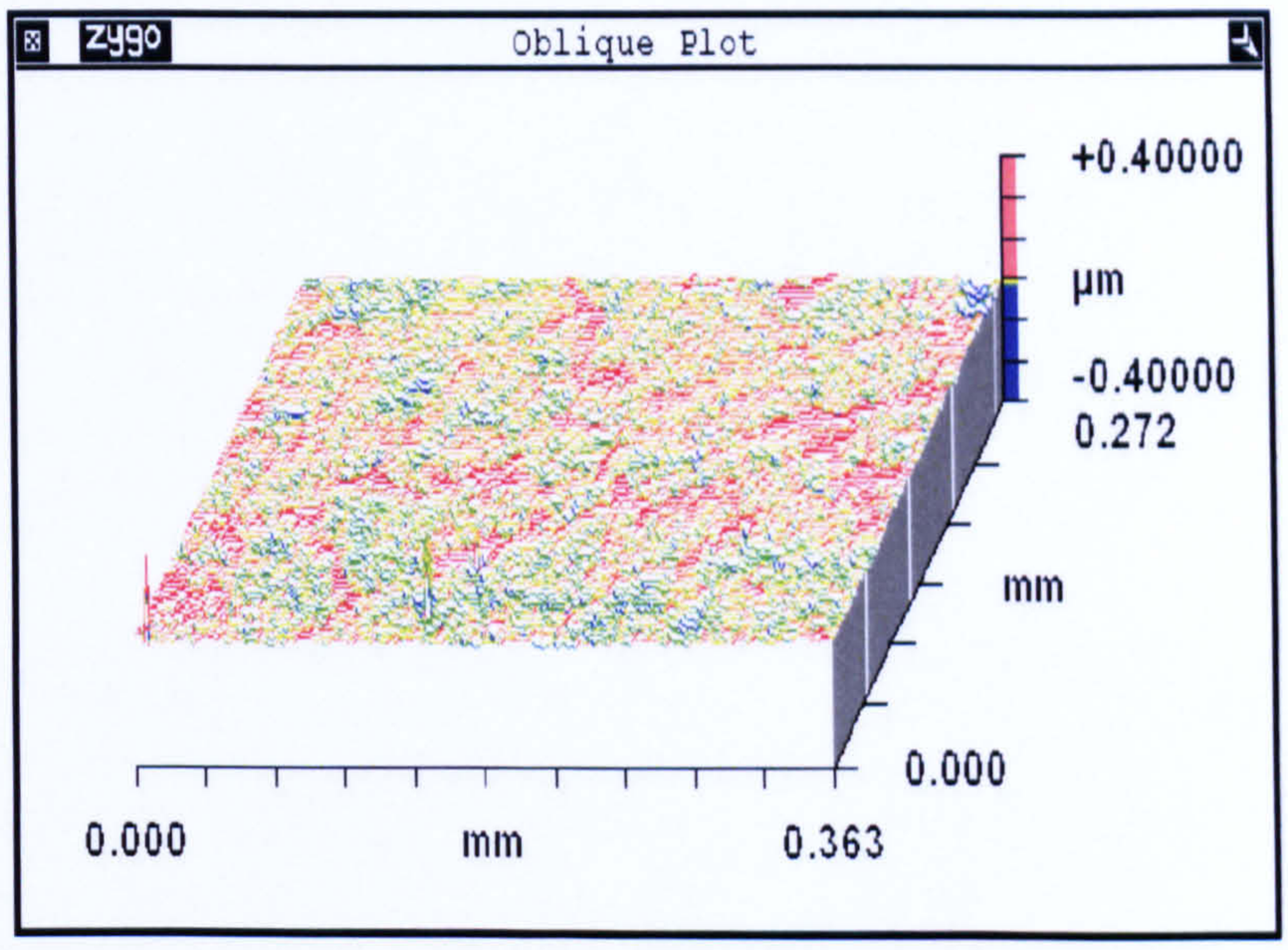

Figure 60 Topographical image of the as-cast head at 3 million cycles

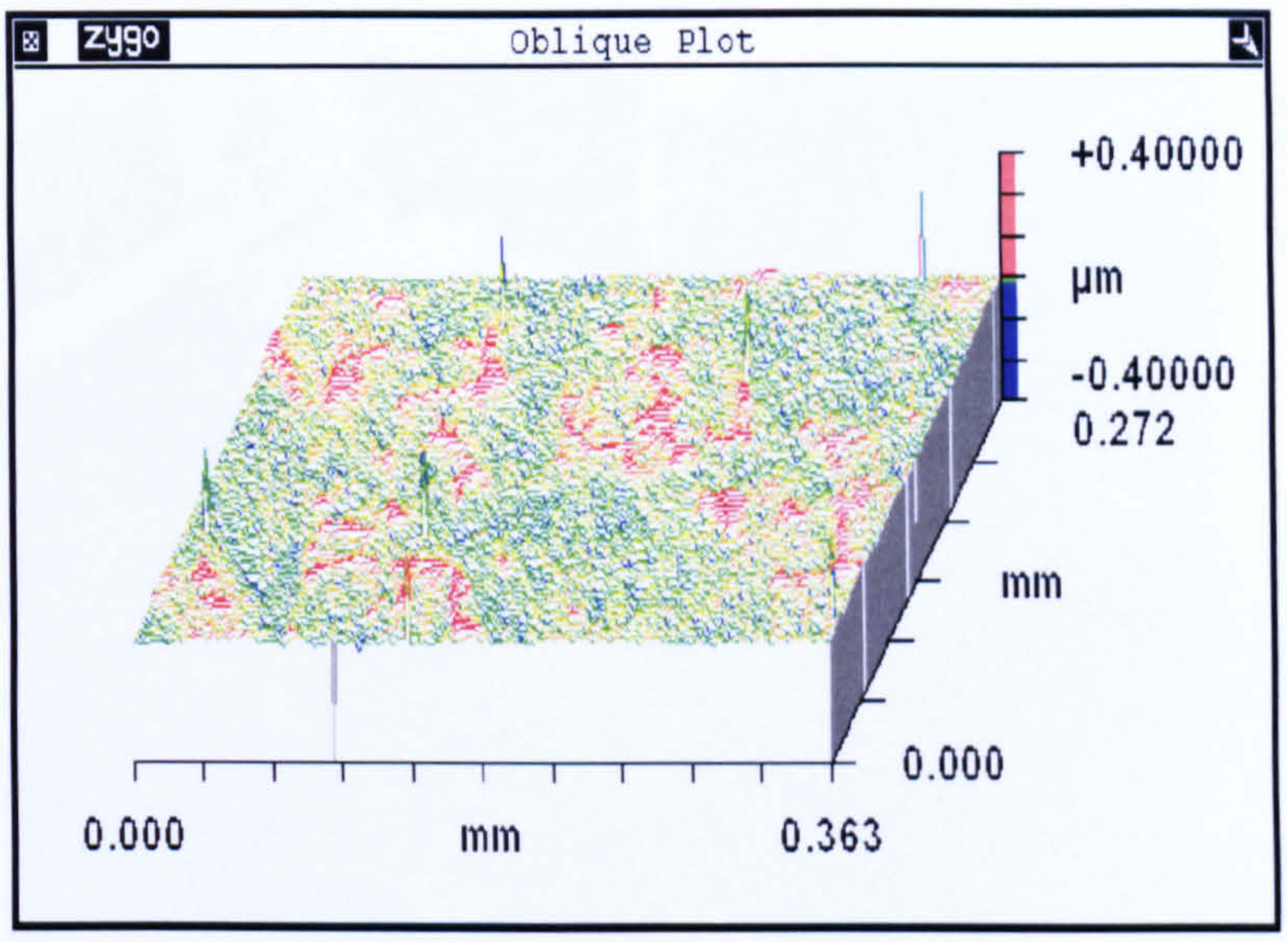

Figure 61Topographical image of the as-cast cup at 10 million cycles.

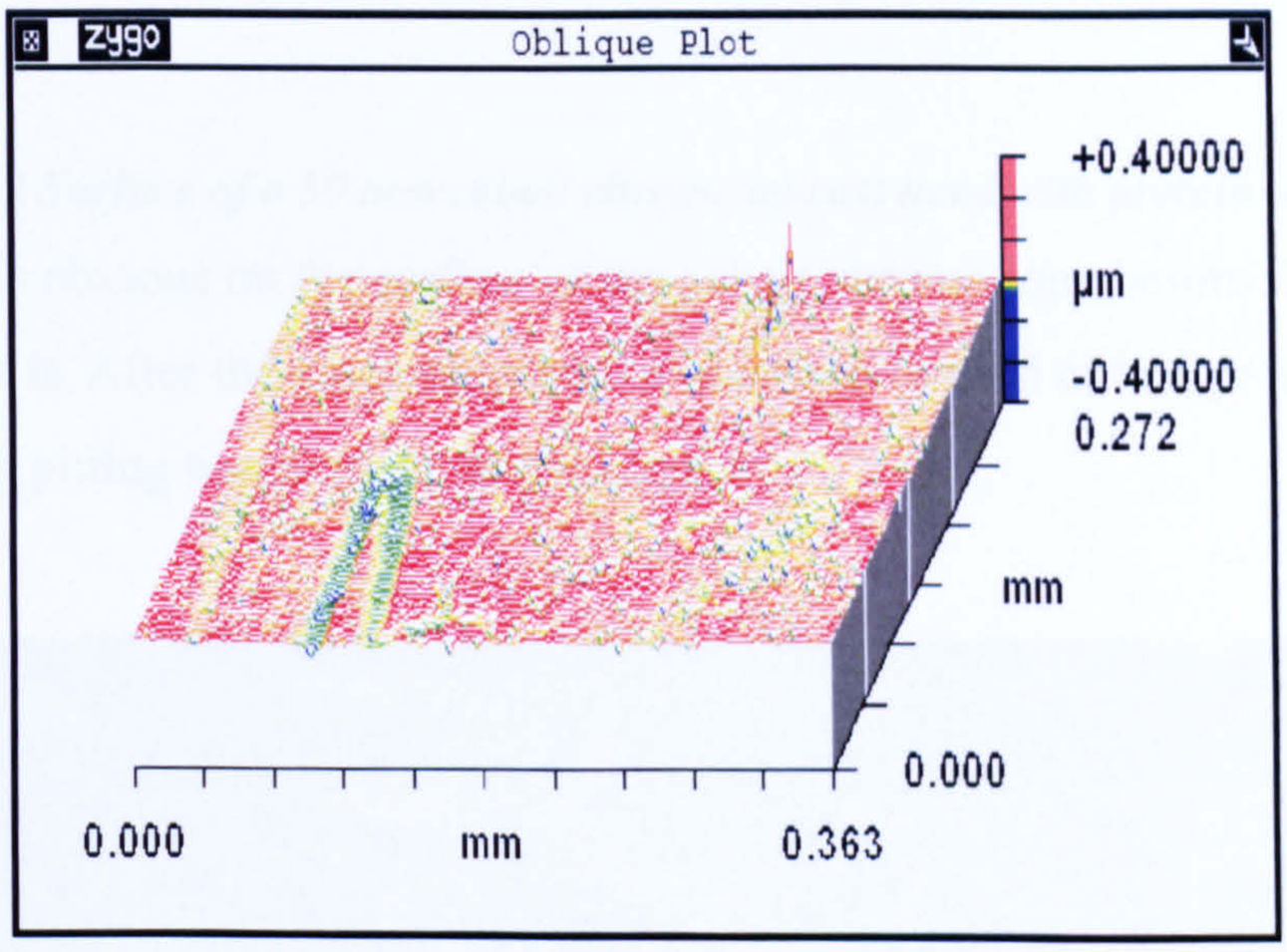

Figure 62 Topographical image of the as-cast head at 5 million cycles.

5.2.2.4. Protein removal

At 3 million cycles the joints appeared to be gaining weight and this was thought to be due to the deposition of protein on the surface of the joints. A 12M KOH solution was used for 24 hours to clean the joints of protein.

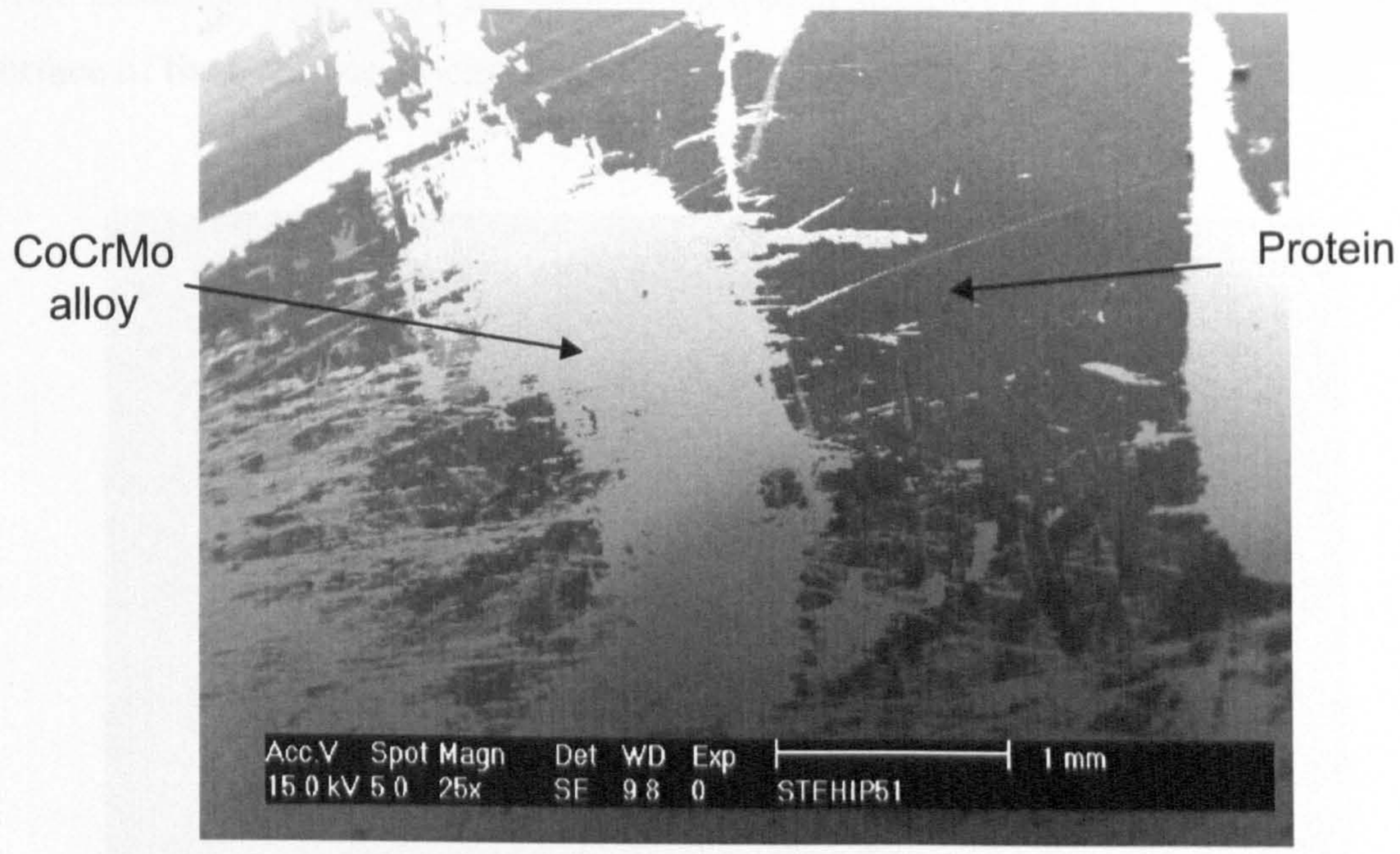

Figure 63 Surface of a 50 mm cobalt chrome as-cast head with protein adhesion.

The protein is obvious on the surface of the cobalt chrome joint before the KOH was used to clean it. After the cleaning protocol had been carried out no protein could be identified but pitting was evident on the surface.

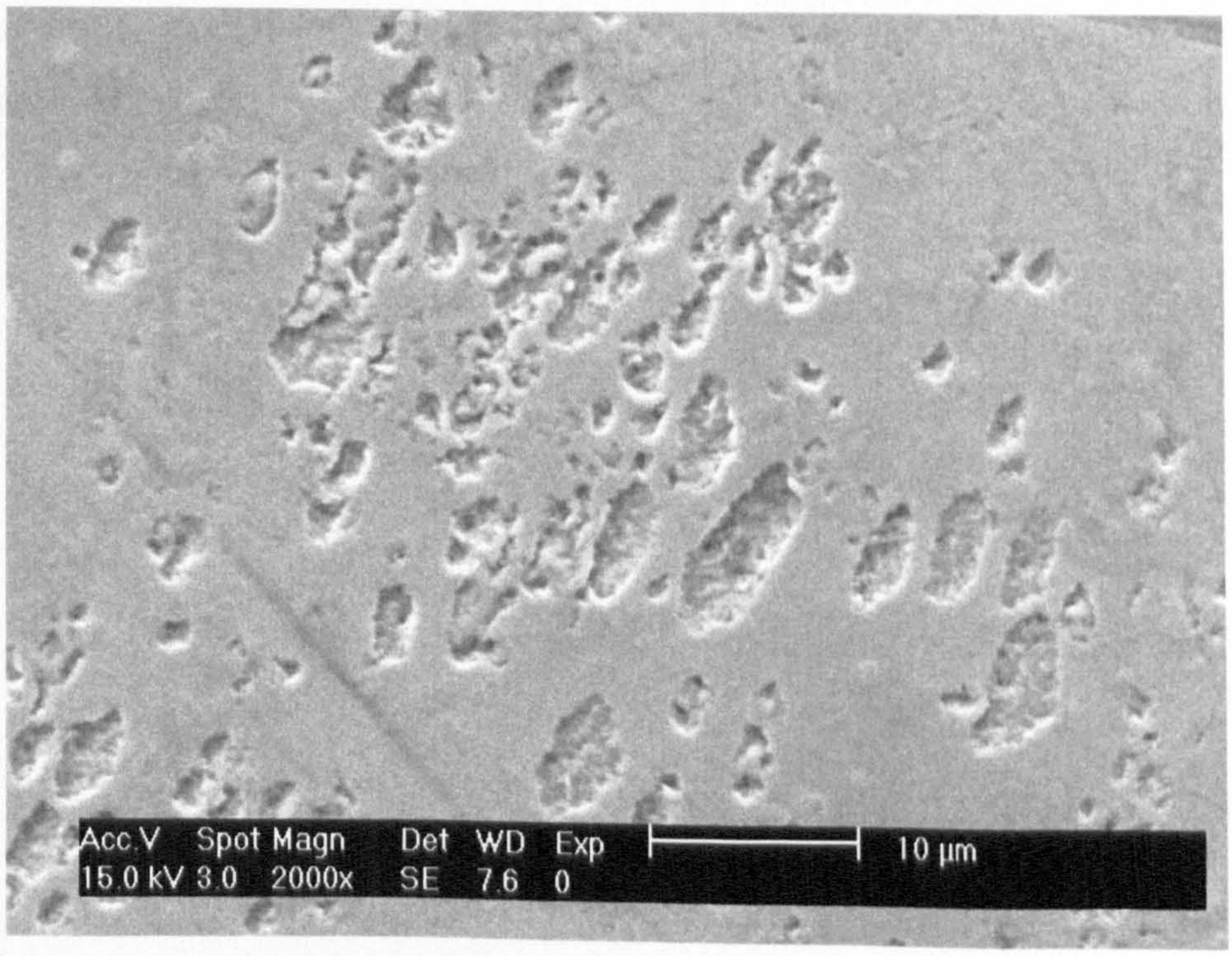

Figure 64 Surface of a cobalt chrome as-cast head after KOH cleaning

After cleaning with KOH the protein had been dissolved along with some of the surface of the CoCrMo as-cast joint

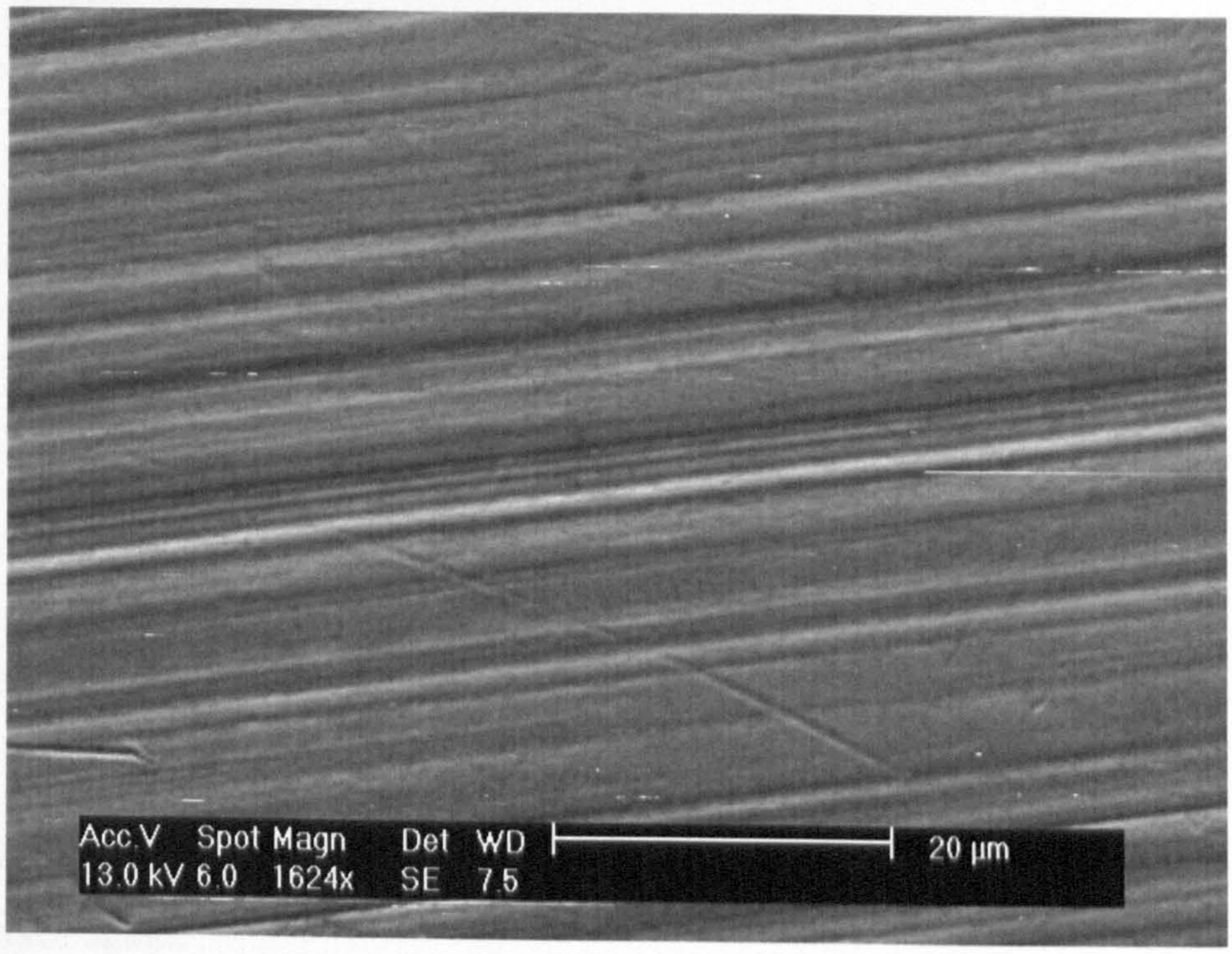

Figure 65 Surface of the wear patch of an as-cast joint after KOH cleaning and half a million cycles wearing

After wearing once more the wear patch appeared to have self polished and the corrosion was no longer visible.

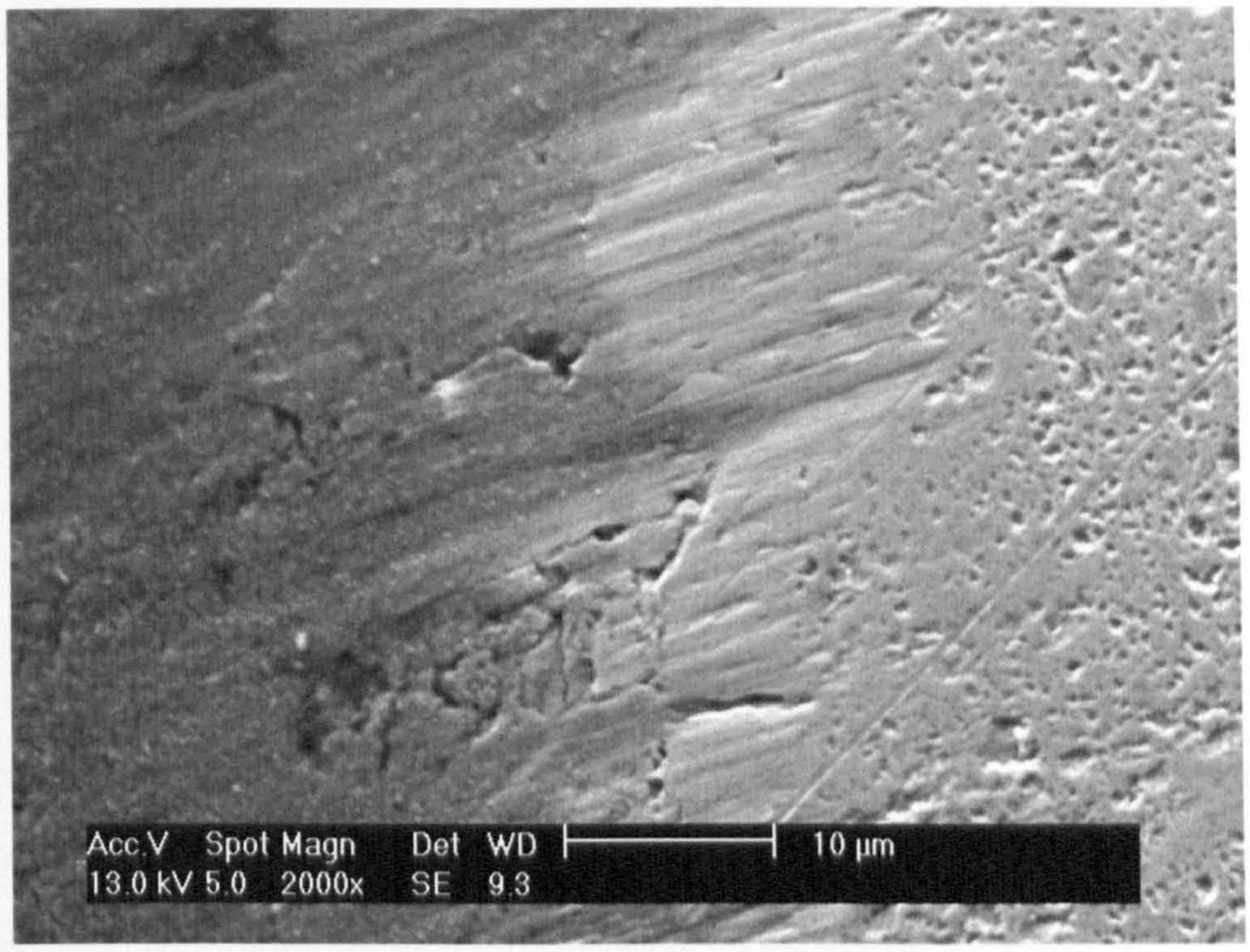

Figure 66 Surface image off the wear patch of the KOH cleaned, worn joint

However, off the wear patch the corrosion is still visible and protein has adhered to the surface again.

5.2.3. 38 mm As-Cast Prostheses

Simulator station	Head	Cup	Diametral Clearance (µm)
Joint 1	H2	C6	173
Joint 2	H3	C9	173
Joint 3	H4	C8	167
Joint 4	H5	C5	172
Joint 5	H6	C7	165
Joint 6 (Ctrl)	H1	C4	177

Table 11. Component pairs for testing in hip wear simulator

Table 11 shows the joint pairings arranged to give the best combination of similar clearances to each other within this test, these components are 38 mm diameter. The clearances are smaller than those for the 50 mm joints reported above, this is due to

the availability of sizes of components from the manufacturer and the fact that clearance should be a function of diameter.

5.2.3.1. Wear Results

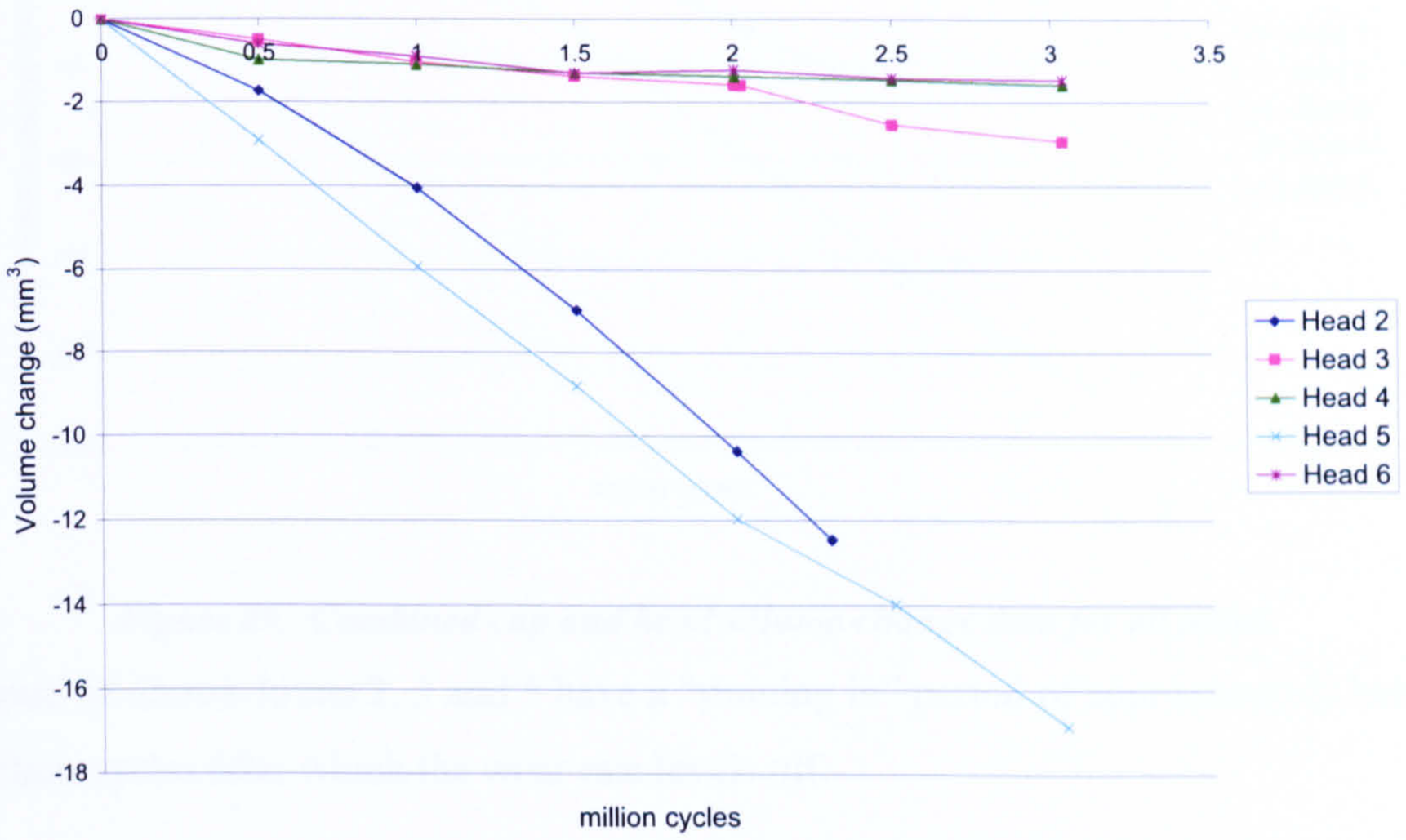

Figure 67. Volume change over the 3 million cycle test for all heads

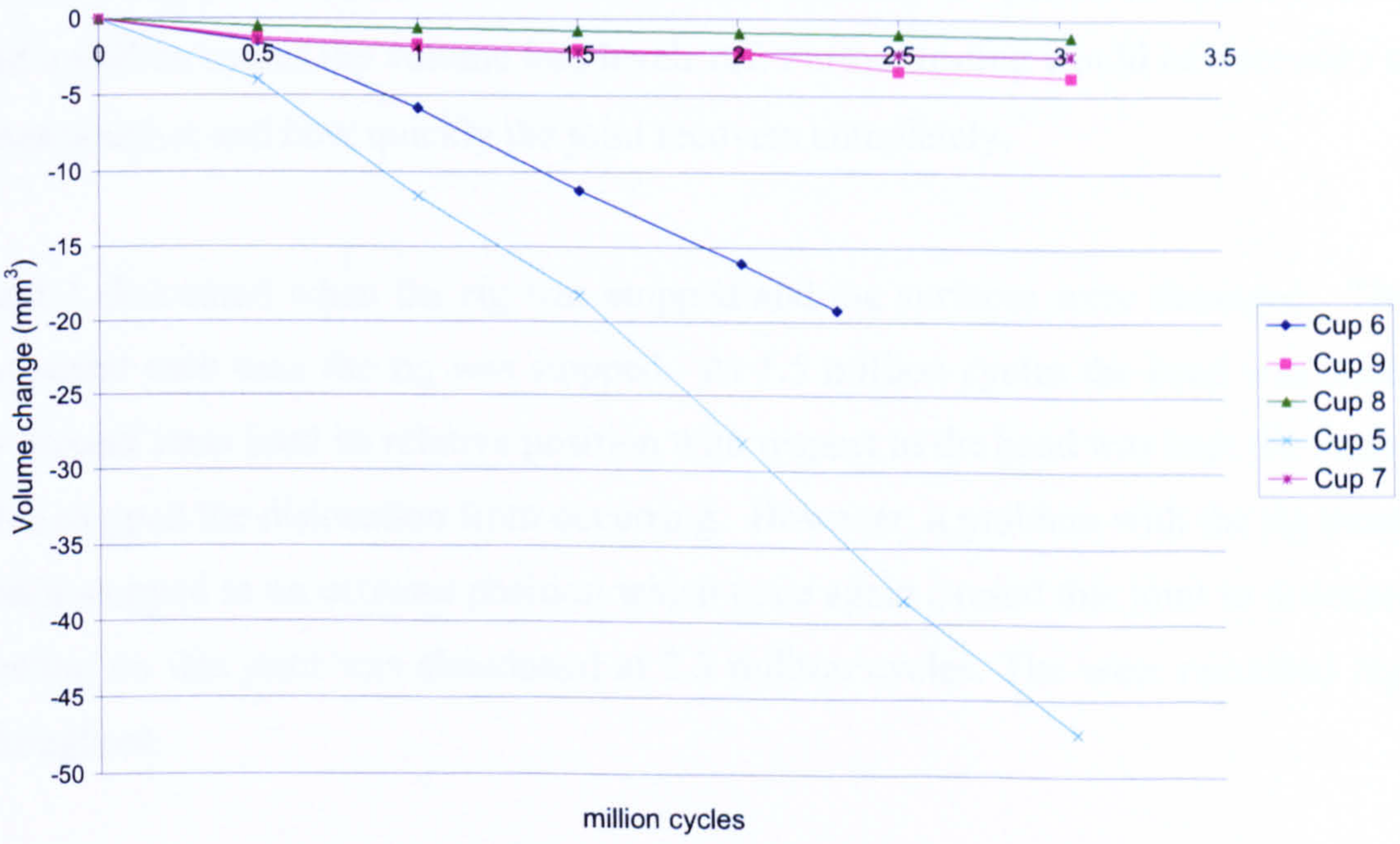

Figure 68. Volume change for all cups over the 3 million cycle wear test

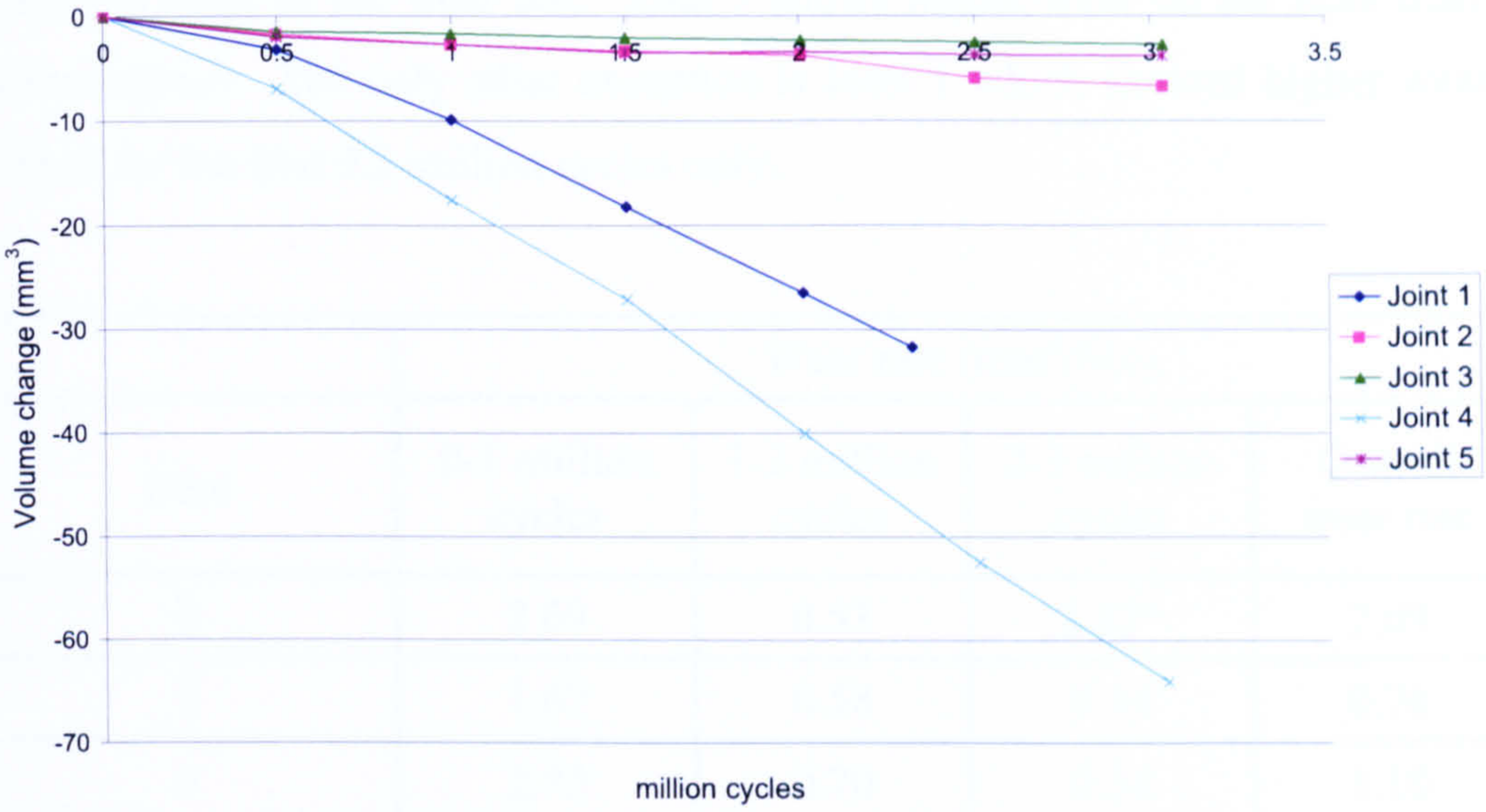

Figure 69. Combined cup and head volume change data for all joints.

Figure 69 shows Joints 2, 3 and 5 have a "running in" period of approximately half a million cycles after which the wear rate levels off.

Joint 2 shows an increase in wear at 2 million cycles. This was due to a mechanical error causing joint dislocation. After a further "running in" period of approximately half a million cycles the volume loss levels off. Further testing would be necessary to asses whether and how quickly the joint recovers completely.

Joint 1 dislocated when the rig was stopped and the surfaces were damaged. This happened each time the rig was stopped. At 1.5 million cycles the head was raised by around 1mm (and its relative position with respect to the head was kept the same). This stopped the dislocation from occurring. However, a problem with the rig meant that it stopped in an extreme position which once again caused this joint to dislocate. Testing on this joint was abandoned at 2.3 million cycles. The wear remained high throughout.

Joint 4 ran dry just before 1 million cycles due to the connecting tubing coming loose from the cup holder. The lubricant was topped up and the joint was replaced in the simulator. Although the wear rate increased after this event, the wear of this joint had been initially higher than that seen on other joints.

All joints except Joint 3 show a higher wear on the cup rather than the head throughout most of the wear test. Joint 3 shows higher wear on the head than the cup throughout. The only other exception is Joint 1 which showed higher wear on the head for the first 0.5 million cycles only.

	Wear rate (mm^3/Mc)			
Joint	0-1 million cycles	1-2 million cycles	2-3 million cycles	Overall wear rate
2	2.69	0.53	2.82*	2.09
3	1.67	0.58	0.44	0.76
5	2.72	0.70	0.38	1.10
Average from present study	2.36	0.60	1.21	1.32
Average from 50mm joint study Vassiliou [50]	1.83	1.06	0.34	1.08

Table 12 Summary of wear rates for various portions of the wear test.

*Joint 2 dislocated during this period.

Table 12 summarises the wear rates of the 38 mm diameter test and shows a comparison to a 50 mm diameter test performed previously [50]. If joint 2 is discounted very little difference can be seen. The "running in" wear of the 38 mm joints is higher but after 1 million cycles the wear rates are similar.

5.2.3.2. Friction Results

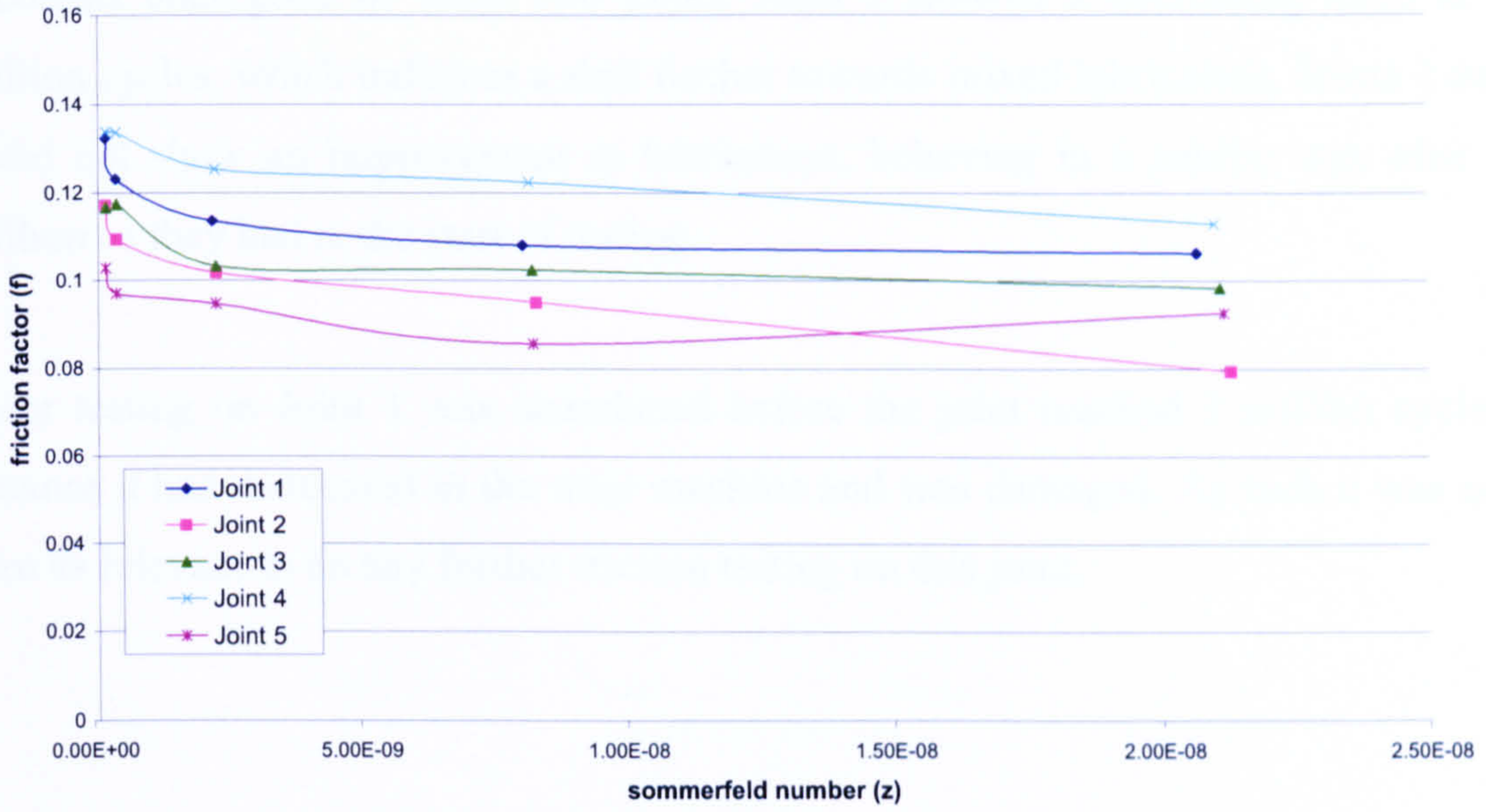

Figure 70. Friction results for all 38 mm diameter as-cast joints tested before the wear test began.

All joints showed mixed/boundary lubrication initially (Figure 70). Friction values were in the region of 0.06-0.14 for all joints at all viscosities.

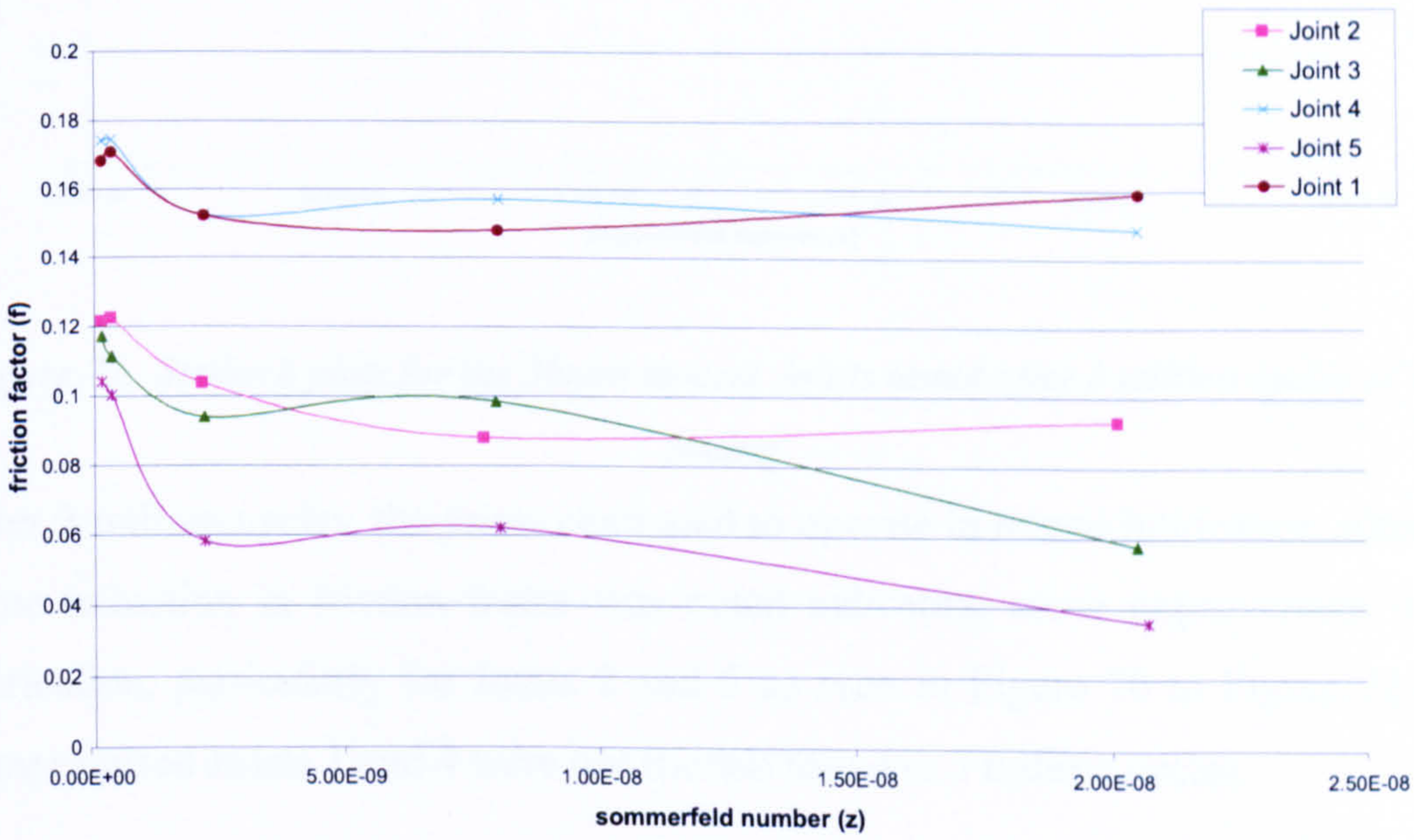

Figure 71. Friction results for all 38 mm as-cast joints tested after 1 million cycles of wear testing. Joint 1 was repeated due to its very high friction.

After 1 million cycles the joints were friction tested again. Joint 1 showed an increase in friction factor as did Joint 4. This is likely to be due to the specific testing problems undergone by these two joints. Joint 5 showed a decreasing trend at 1 million cycles, which indicates a shift further towards mixed lubrication. Joints 2 and 3 did not show an improvement in lubrication, behaving in a similar way after 1 million as they had at the start of testing.

Wear testing on Joint 1 was abandoned before the joint reached 3 million cycles, because it had dislocated in the wear machine and was damaged. As such it was not seen as relevant to do any further friction testing on this joint.

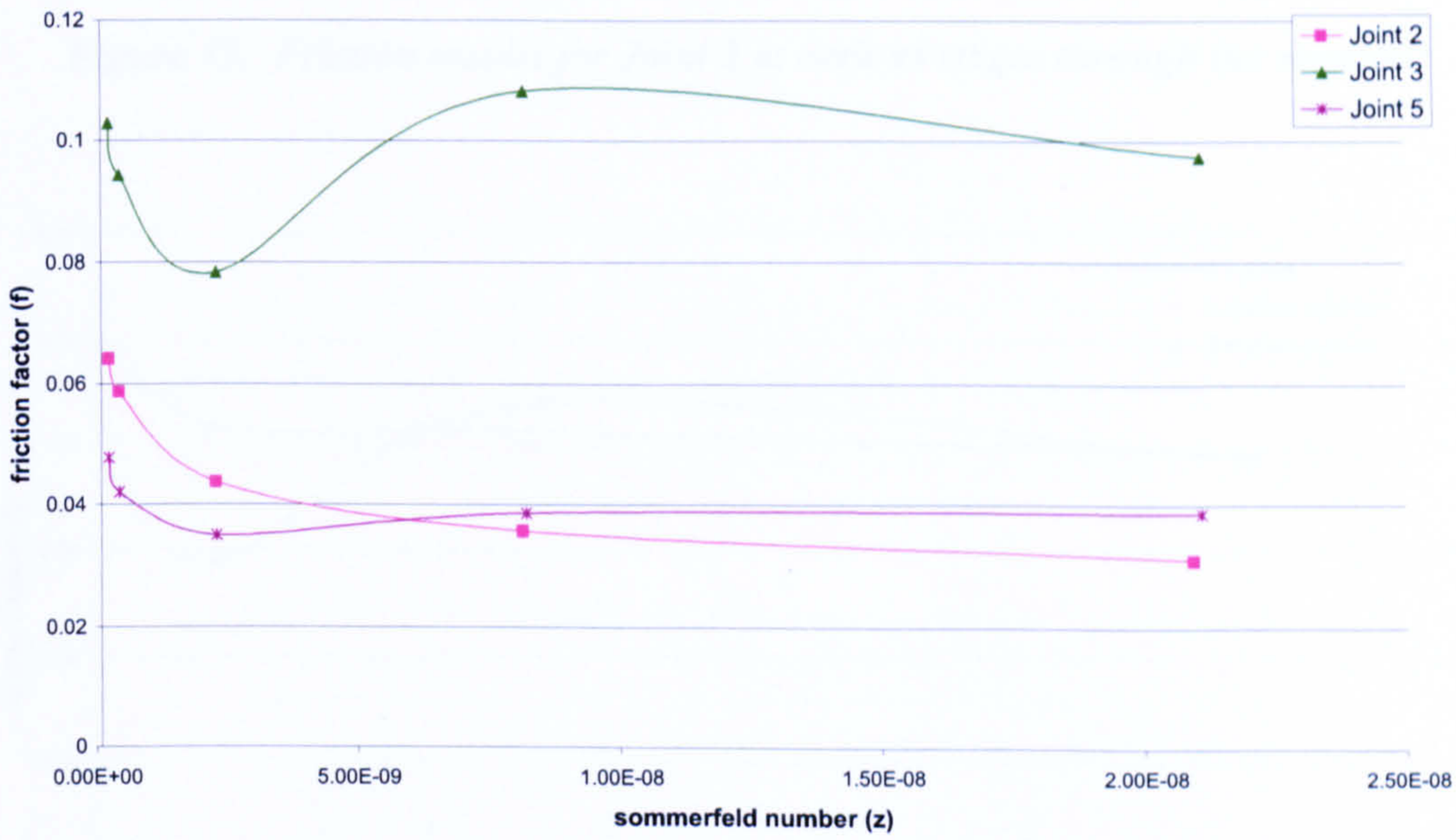

Figure 72. Stribeck plots for the 38mm as-cast joints tested after 3 million cycles of wear testing

After 3 million cycles, the joints continued to operate in mixed lubrication, although some reduction in friction factor was noted indicating some improvement in the lubrication, particularly for Joints 2 and 5 as seen in Figure 70 to Figure 72. The compromised Joints 1 and 4 were not friction tested at 3 million cycles.

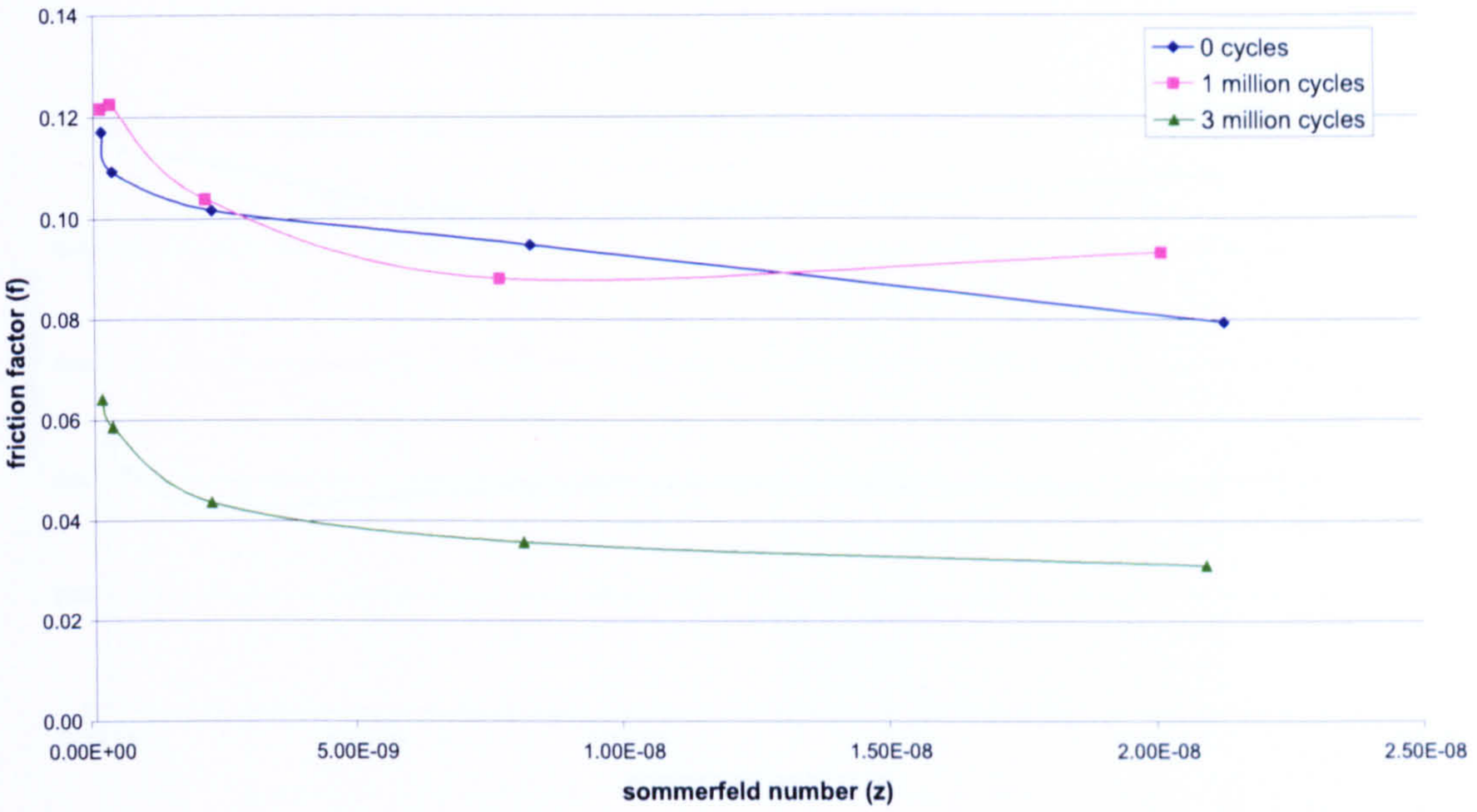

Figure 73. Friction results for Joint 2 at various stages through the wear test

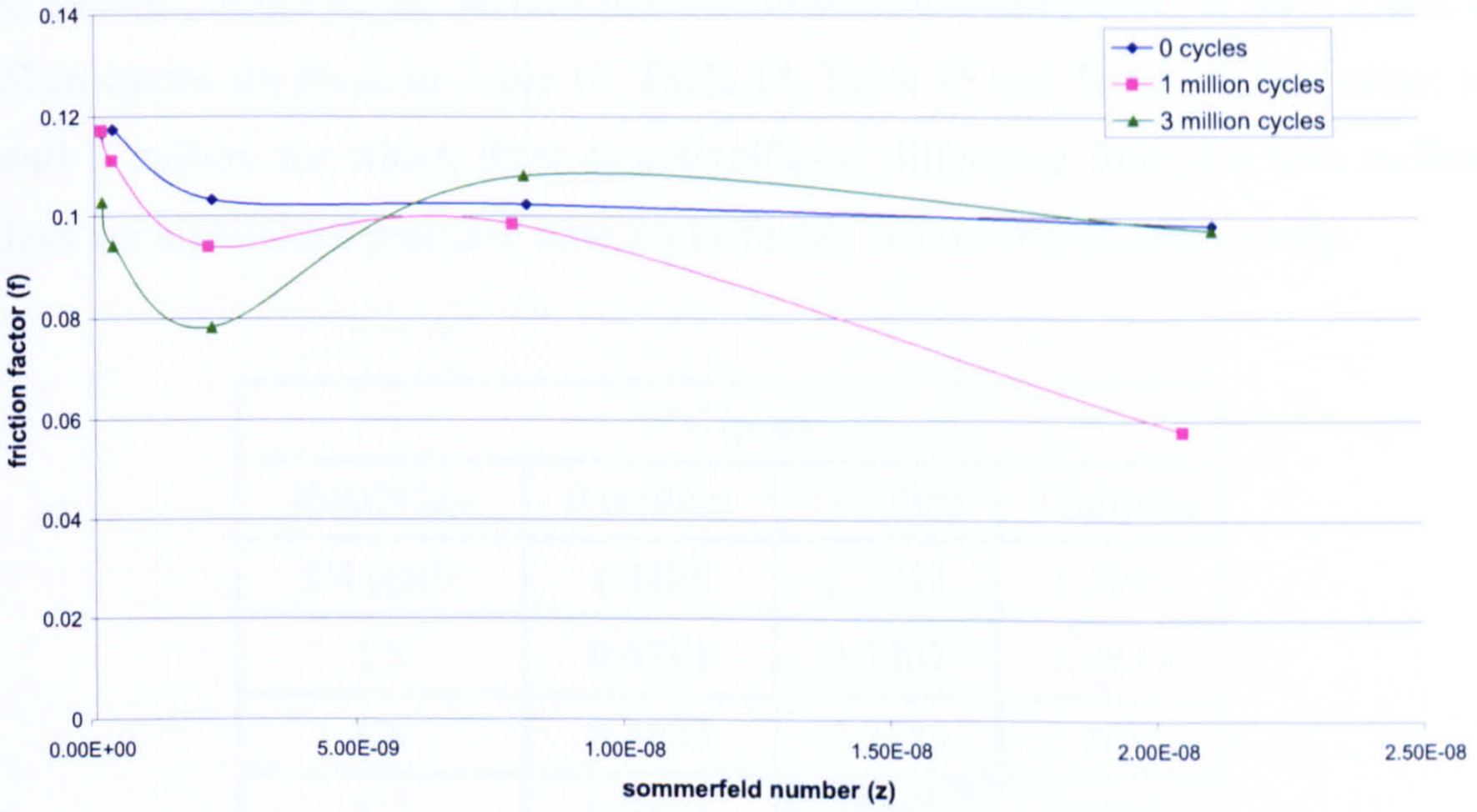

Figure 74. Friction results for Joint 3 at various stages through the wear test

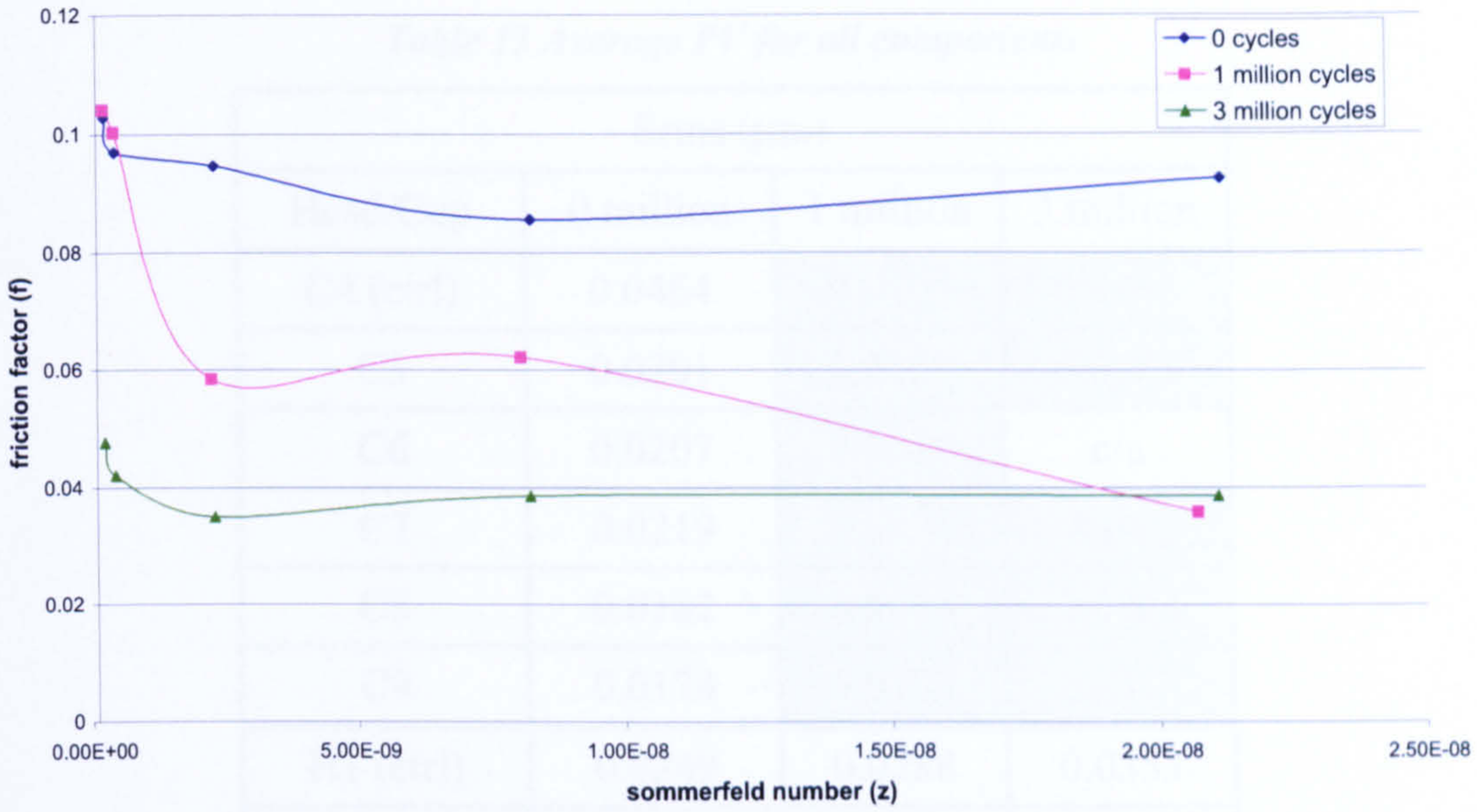

Figure 75. Friction results for Joint 5 at various stages of wear testing

5.2.3.3. Surface analysis

The average values of the surface parameters for each component at zero, 1 and 3 million cycles are given in Table 13, Table 14, Table 15 and Table 16. The values at 1 and 3 million for which there is a significant difference from the zero million values are highlighted pink and blue for increases and decreases respectively.

PV (μm)			
Head/Cup	0 million	1 million	3 million
C4 (ctrl)	1.3488	1.3842	1.5015
C5	0.4781	0.4407	1.0849
C6	0.3655	0.2233	n/a
C7	0.5621	0.0853	0.644
C8	0.3171	0.1504	0.6908
C9	0.2541	0.1827	0.9067
H1 (ctrl)	0.3419	0.9614	0.7195
H2	0.2838	1.3372	n/a
H3	0.2385	0.7371	1.5449
H4	0.2335	0.58	2.4463
H5	0.453	0.9944	2.1827

H6	0.369	0.857	1.3205

Table 13 Average PV for all components

Srms (μm)			
Head/Cup	0 million	1 million	3 million
C4 (ctrl)	0.0464	0.0405	0.0898
C5	0.0201	0.0168	0.0811
C6	0.0207	0.0089	n/a
C7	0.0219	0.0076	0.015
C8	0.0182	0.0074	0.0245
C9	0.0174	0.0102	0.0313
H1 (ctrl)	0.0249	0.0288	0.0353
H2	0.0222	0.0521	n/a
H3	0.0198	0.0138	0.0294
H4	0.0188	0.0245	0.1155
H5	0.0183	0.0392	0.2469
H6	0.0183	0.0103	0.0709

Table 14 Average Srms for all components

	Sa (μm)		
Head/Cup	0 million	1 million	3 million
C4 (ctrl)	0.0234	0.0228	0.0598
C5	0.0114	0.0116	0.0627
C6	0.0121	0.0062	n/a
C7	0.0129	0.0057	0.011
C8	0.0109	0.0055	0.0114
C9	0.0100	0.0074	0.0143
H1 (ctrl)	0.0145	0.0153	0.0238
H2	0.0132	0.0317	n/a
H3	0.0117	0.0077	0.016
H4	0.0112	0.0147	0.084
H5	0.0106	0.0238	0.1969
H6	0.0109	0.0043	0.0485

Table 15 Average Sa for all components

	Ssk		
Head/Cup	0 million	1 million	3 million
C4 (ctrl)	-4.5873	-4.6591	-2.5523
C5	-0.0148	0.6951	0.2608
C6	1.7122	0.2068	n/a
C7	0.6542	0.2514	-3.100
C8	2.6011	-0.9704	7.4739
C9	2.6703	0.6833	5.8159
H1 (ctrl)	2.2472	-0.6997	1.8982
H2	2.3389	-0.9136	n/a
H3	2.4925	-4.9256	-9.5542
H4	2.4421	-3.098	-12.1293
H5	1.921	0.5446	-0.5997
H6	1.9854	-12.5231	-1.1008

Table 16 Average Ssk for all components

Anova statistical testing was used on the raw values of the surface parameters. There was no significant change in surface roughness (Sa and Sq) of any of the heads between zero and 1 million cycles. The Sa showed an increase in roughness of heads 4 and 5 after 3 million cycles of wearing. This was not seen in the Sq results. All the cups significantly decreased in roughness between 0 and 1 and 3 million cycles. At 1 million cycles only the PV of cup 7 decreased. Heads 1 and 2 increased. Cups 5, 8 and 9 and head 3, 4, 5 and 6 all increased in PV after 3 million cycles of wearing due to scratching. Head 3 and cups 8 and 9 all decreased in skewness after 1 million cycles, however, cups 8 and 9 also showed an increase in skewness after 3 million cycles.

The surface images revealed a raised carbide structure as seen on this material for 50 mm joints in an earlier study. In agreement with the previous study, the carbide structure was diminished after 1 million cycles.

In addition some deep hollows were observed on some of the cups initially, were not evident after 1 million cycles (except on C4 which is the Ctrl). This feature was not evident on the heads.

Deep directional scratches were seen on H2 at 1 million cycles. This may have been caused by the crash after dislocation of the joint. Some scratching is seen on other components, although not as deep as can be seen in Figure 76.

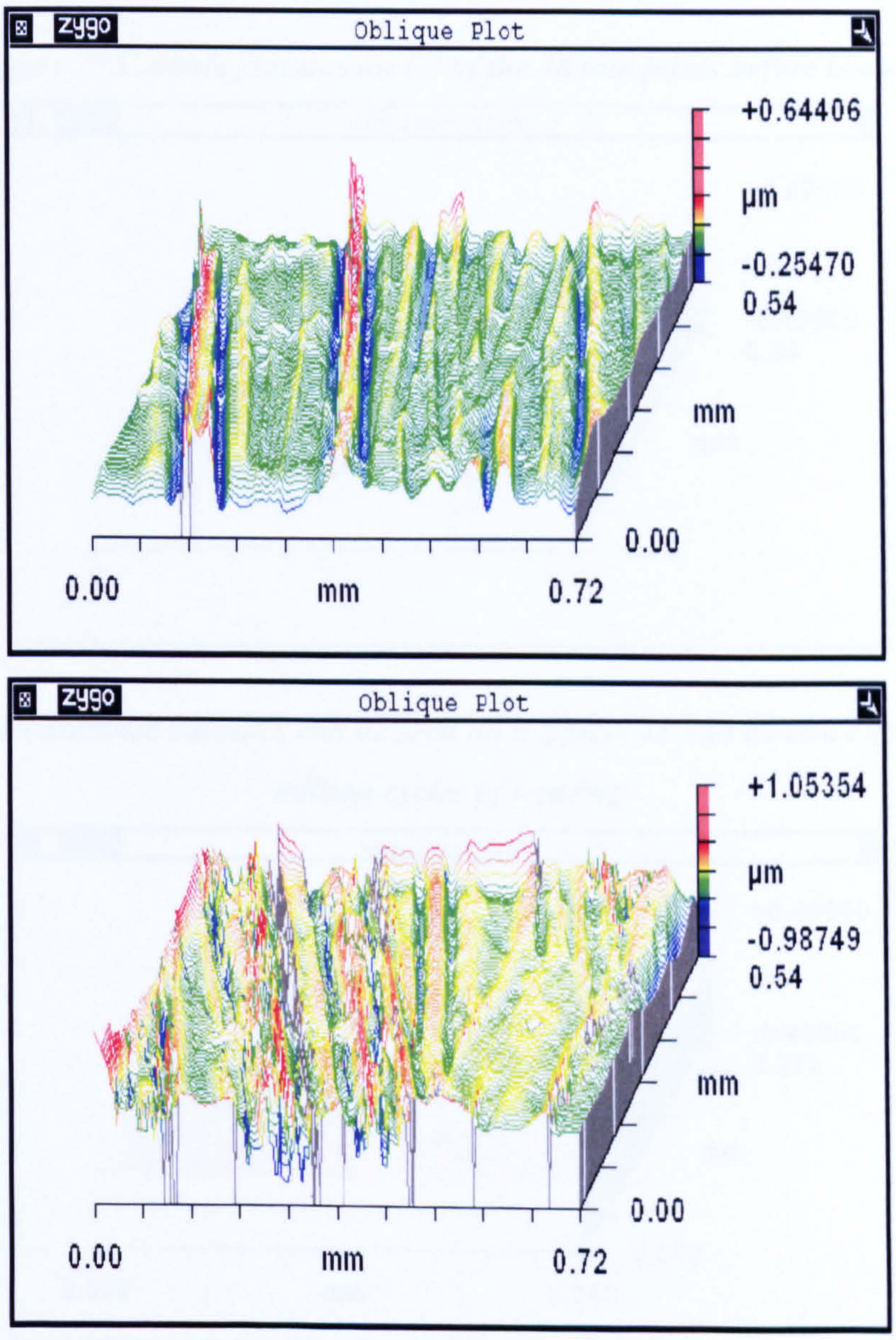

Figure 76 Directional scratches on areas of H2 of the 38 mm as-cast joints after 1 million cycles.

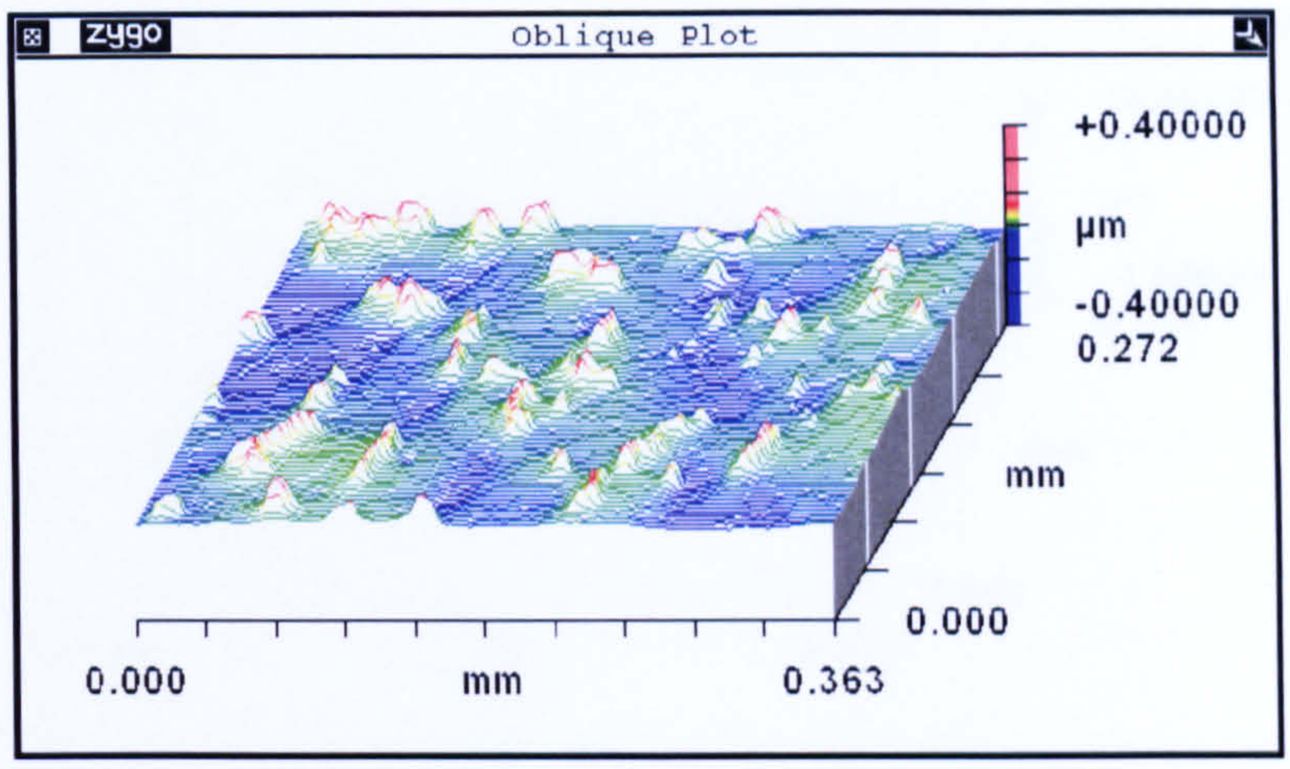

Figure 77 Carbide features on C9 of the 38 mm joints before testing

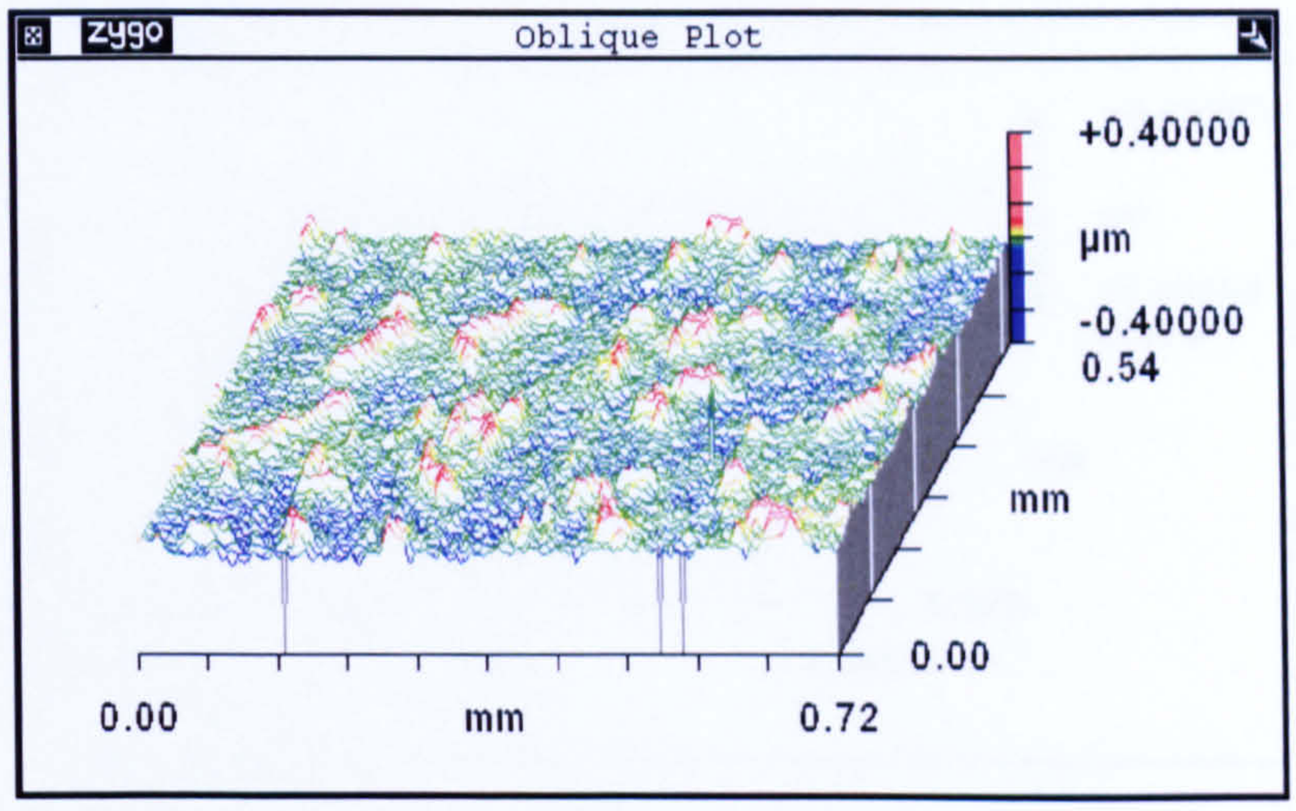

Figure 78 Diminished carbides can be seen on a typical 38 mm as-cast cup (5) after 1 million cycles of wearing

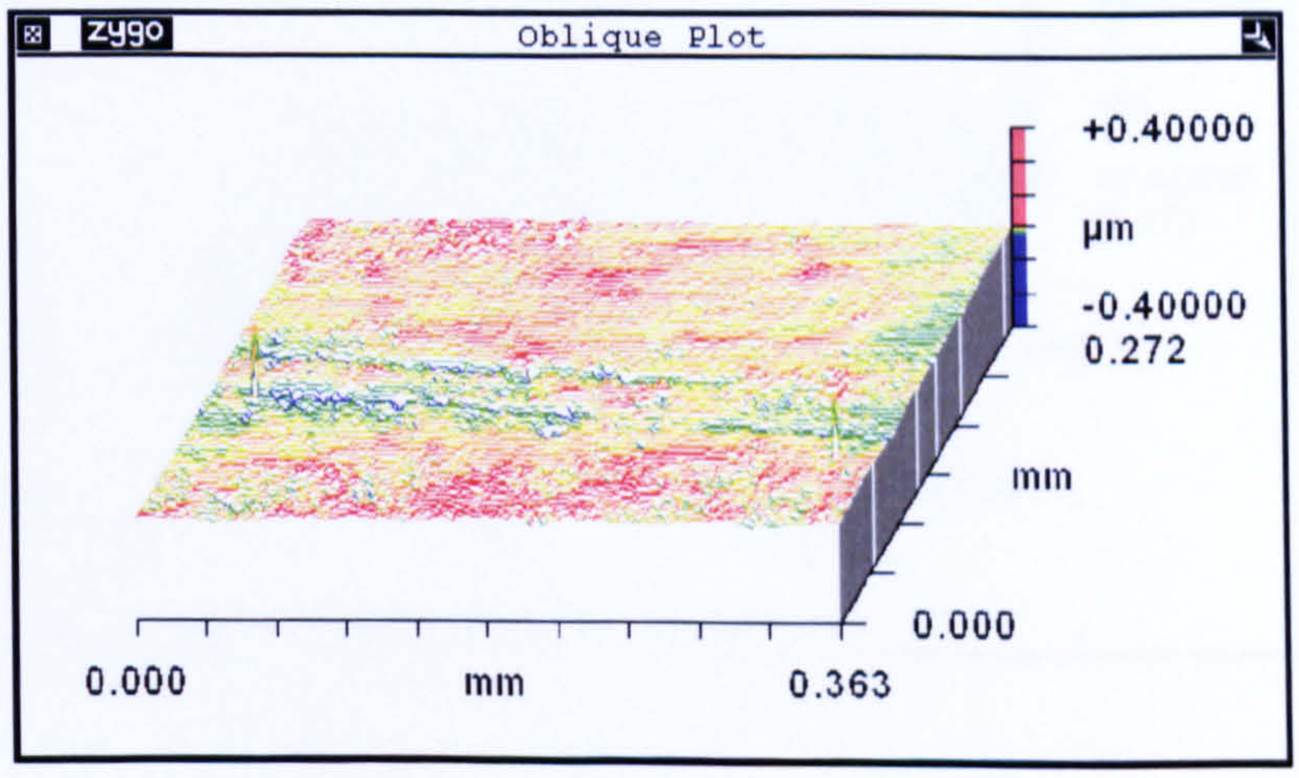

Figure 79 No carbides can be seen on a typical 38 mm as-cast cup (7) after 3million cycles of wearing

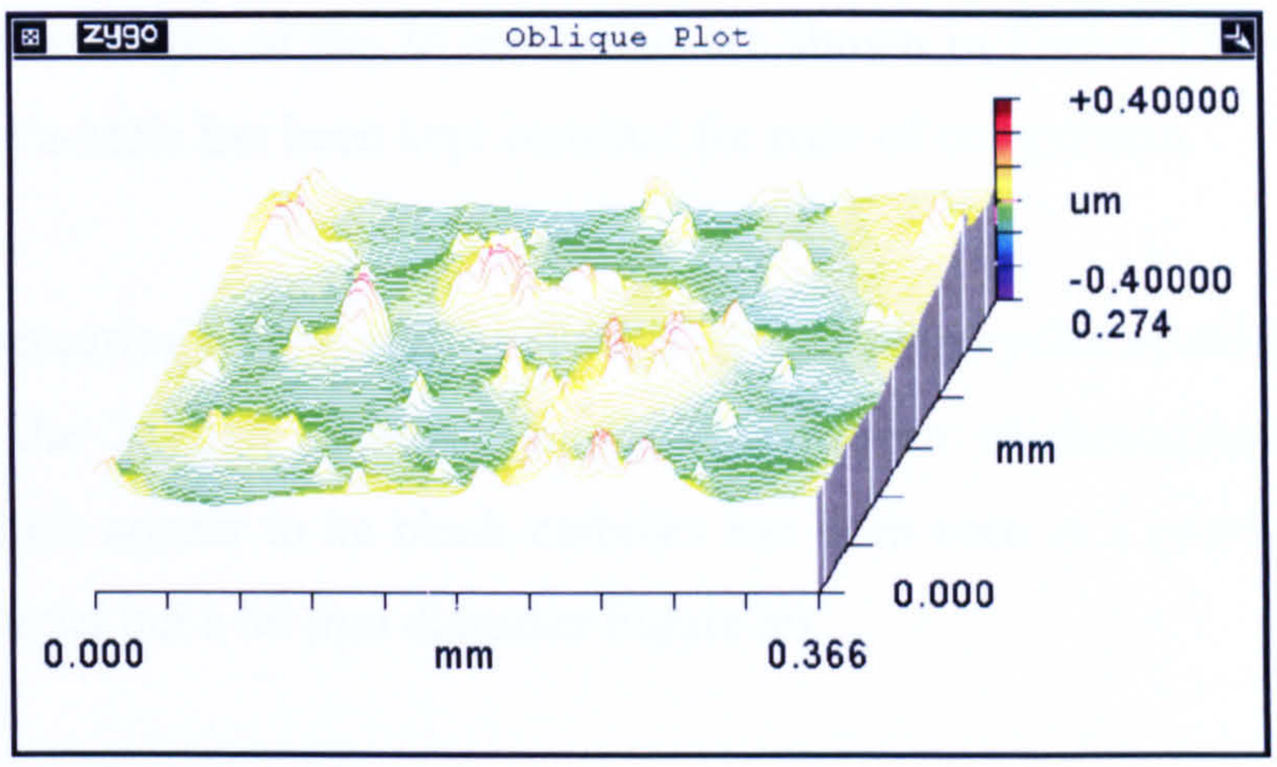

a)

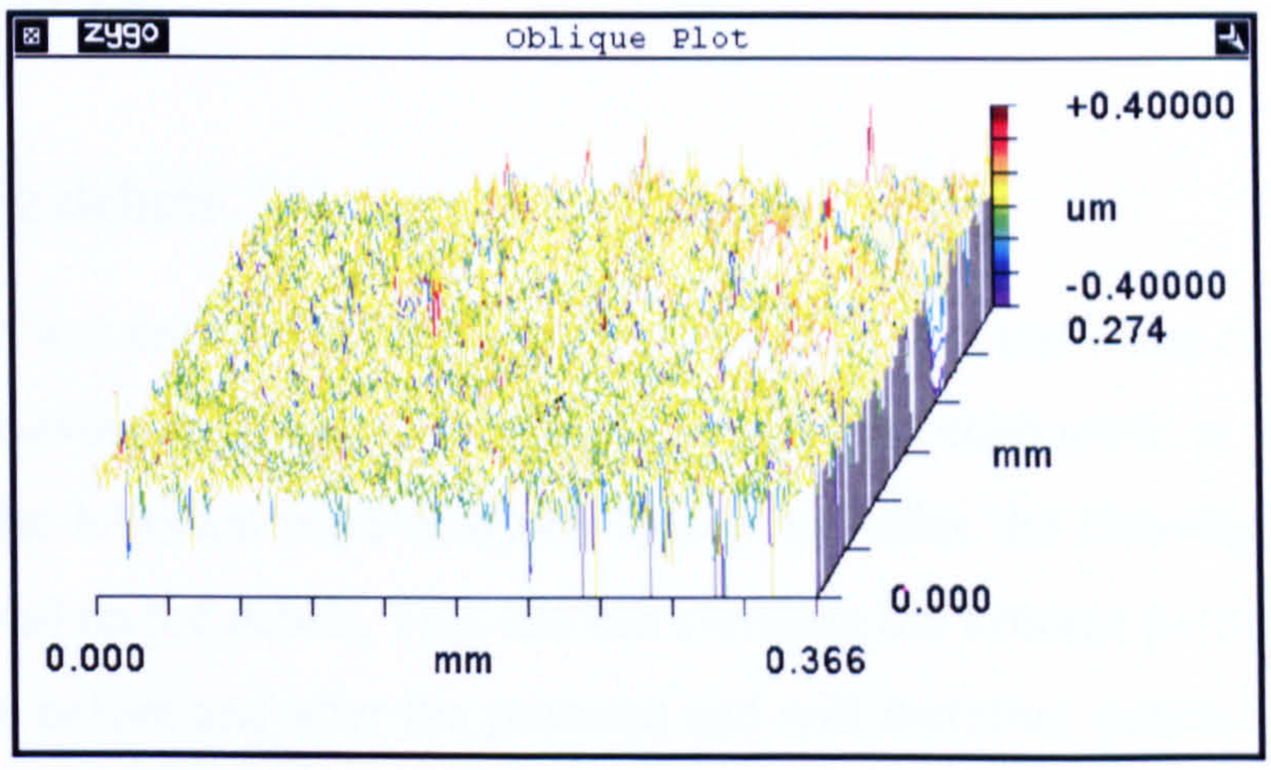

b)

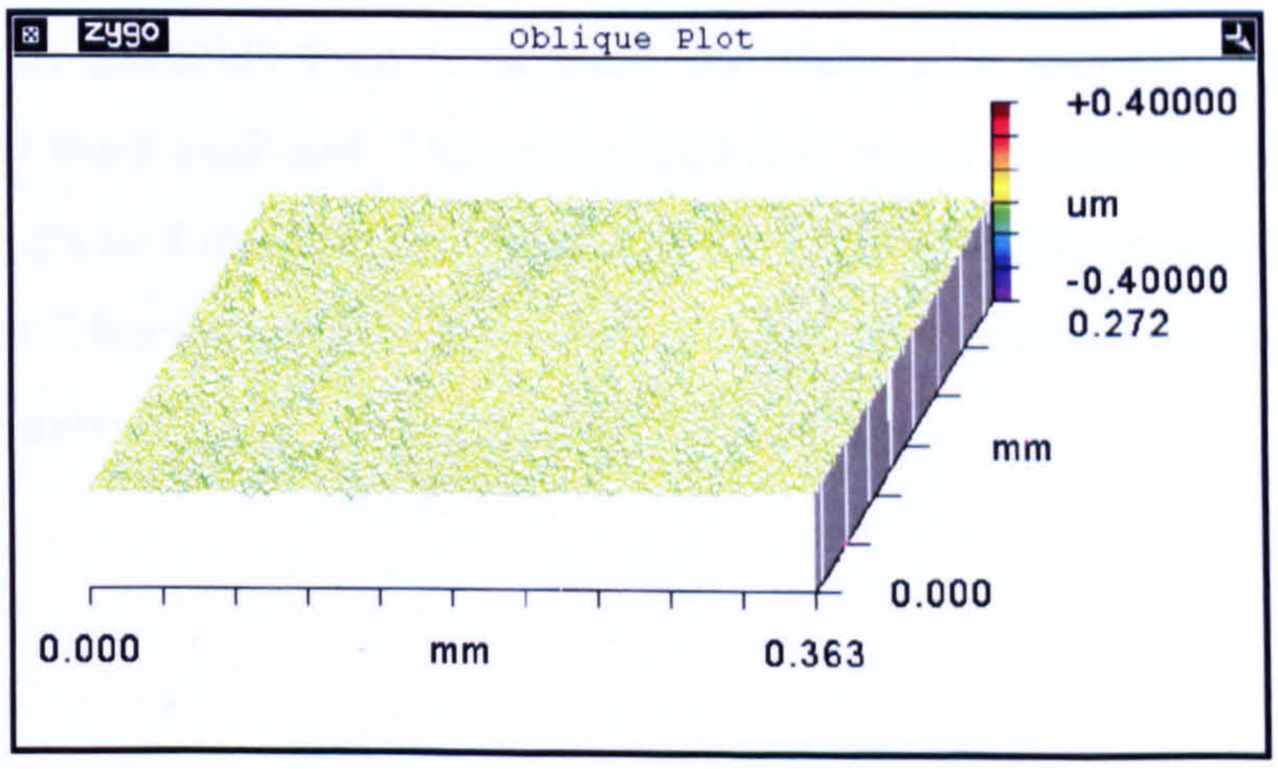

c)

Figure 80 surface images from a previous test (50 mm As-cast) showing a) initial surface, b) after 1 million cycles and c) after 3 million cycles (Vassiliou et al [50])

Typical surface images of the 38 mm joints are shown in Figure 77, Figure 78 and Figure 79, the z-scale has been kept constant for ease of comparison.

No Carbide smearing can be seen at either 1 or 3 million cycles in either the head or the cup for the 38 mm diameter joints. This pattern of diminishing protruding structures which appear to be block carbides has been seen in a previous test using the same material but a 50 mm diameter Figure 80.

A white deposit, presumed to be a protein layer, was found on all components after 1 and 3 million cycles.

5.3. Particle debris

An initial test was carried out to make sure the debris was not being corroded by the enzymatic cleaving protocol. A pin-on-plate test was conducted in water and the particles in the lubricant were analysed before and after the cleaving protocol had been performed on the debris. This test can compare the average particle size for the metal particle before and after the protocol and will therefore indicate if any severe damage is being done to the particles during the protocol. Data labelled digested 1 and digested 2 were particles created in the pin-on-plate machine with a water lubricant, these particles then underwent the enzymatic particle digestion, once complete they were analysed. The undigested data was the control. All particles in this test were created in water, not bovine serum, therefore no protein has contacted these particles. This test was used to asses the digestion protocol for its effect on the particles themselves.

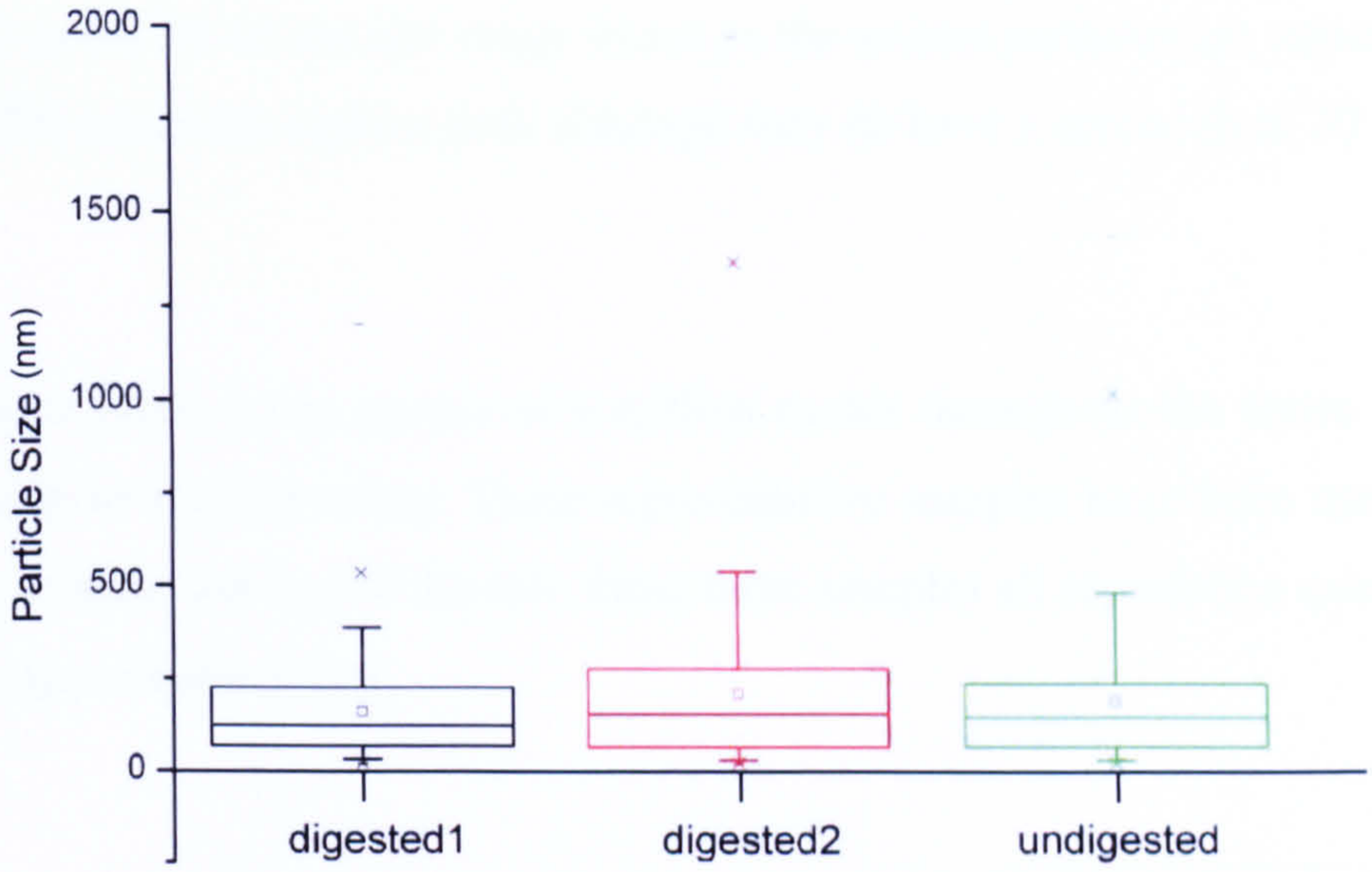

Figure 81 Particle debris from a control sample, before and after enzymatic digestion took place

5.3.1. Pin-on-plate debris

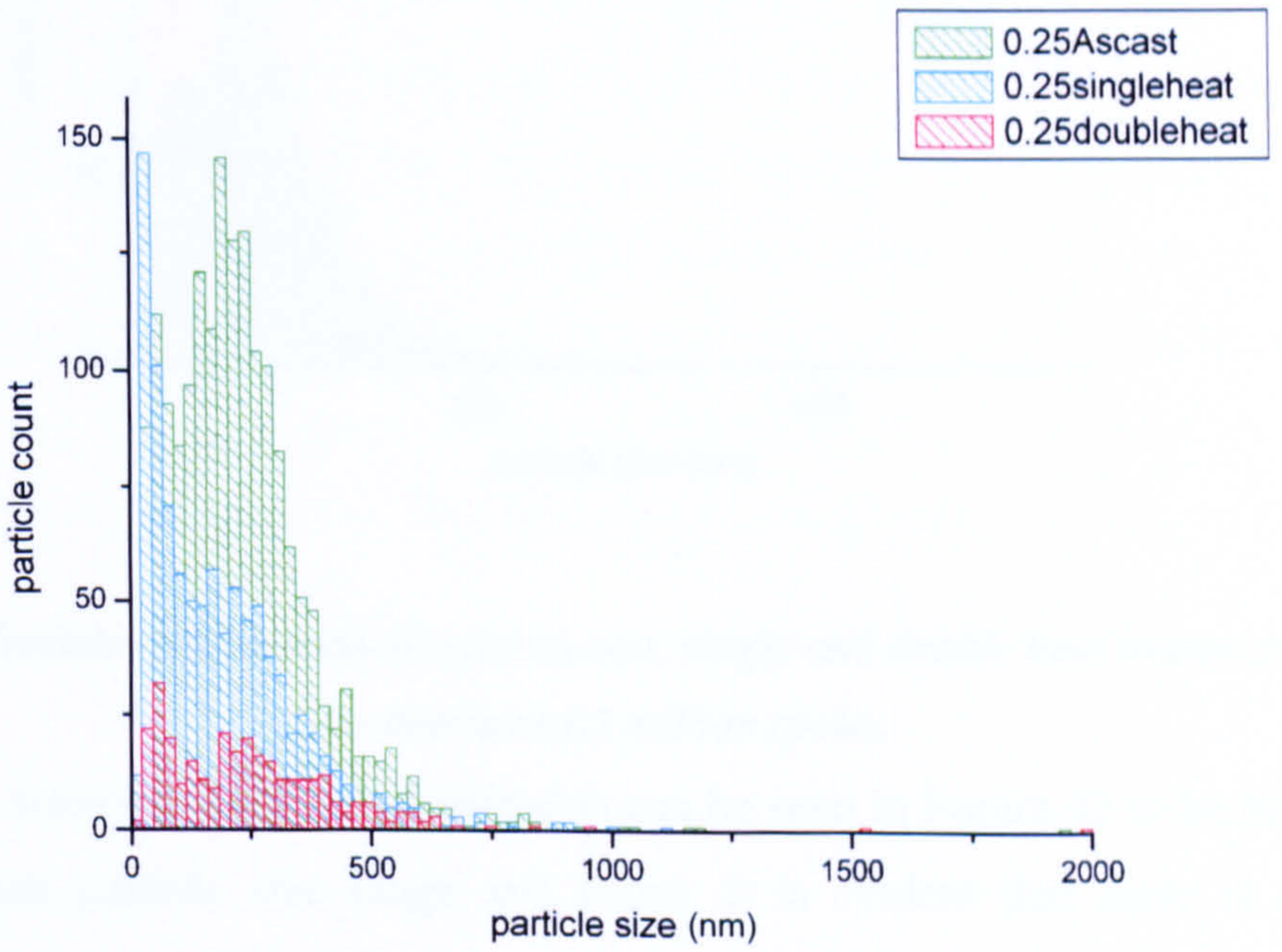

Figure 82 Count versus particle size for the as-cast, single and double heat treated pin-on-plate samples at the first sampling interval 0.25 million cycles.

Figure 82 shows the average of 5 analyses taken from a single protein digestion of lubricant from the 4 station pin-on-plate rig. The graph above shows that both single heat treated and as-cast have a count of about 150 particles per ml but the double heat treated has a much smaller count, the single heat treated also has a large number

of particles in the 20-40 nm size range where as the as-cast particles are rather bigger at around 200 nm at the highest peak although they do have a spread from 20 nm to 1 micron.

Samples were taken every quarter of a million cycles throughout the entire test and replaced with new clean serum. Three representative samples have been used at the beginning, middle and end of the test, these three samples all represent a quarter of a million cycles of wear debris.

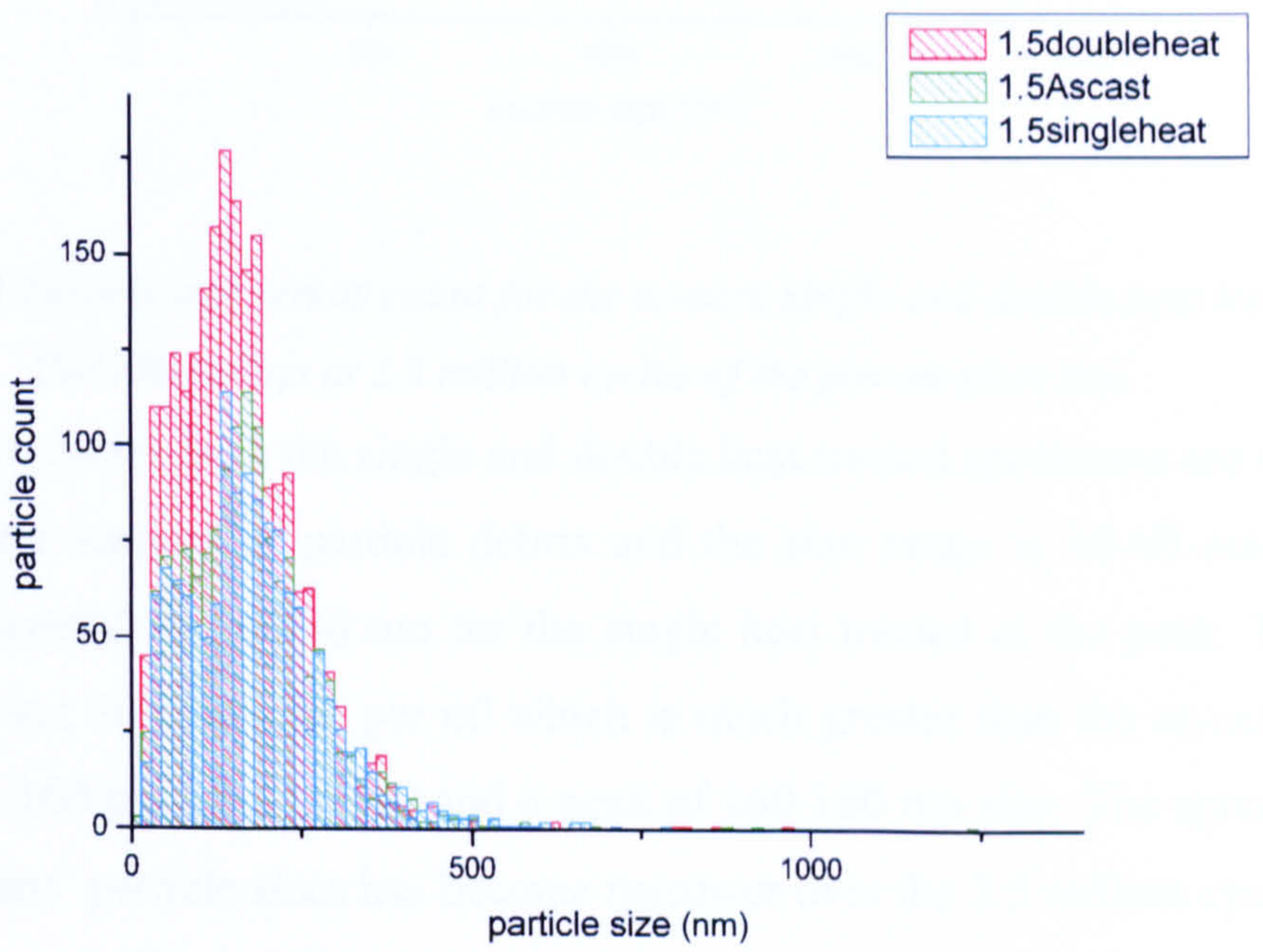

Figure 83 Particle count versus size for as-cast, single and double heat treated pin-on-plate debris at 1.5 million cycles.

The particles from the three heat treatments can be seen in Figure 83 to be becoming similar in their particle size range and count. It is evident that there is a larger volume of double heat treated particles at this point.

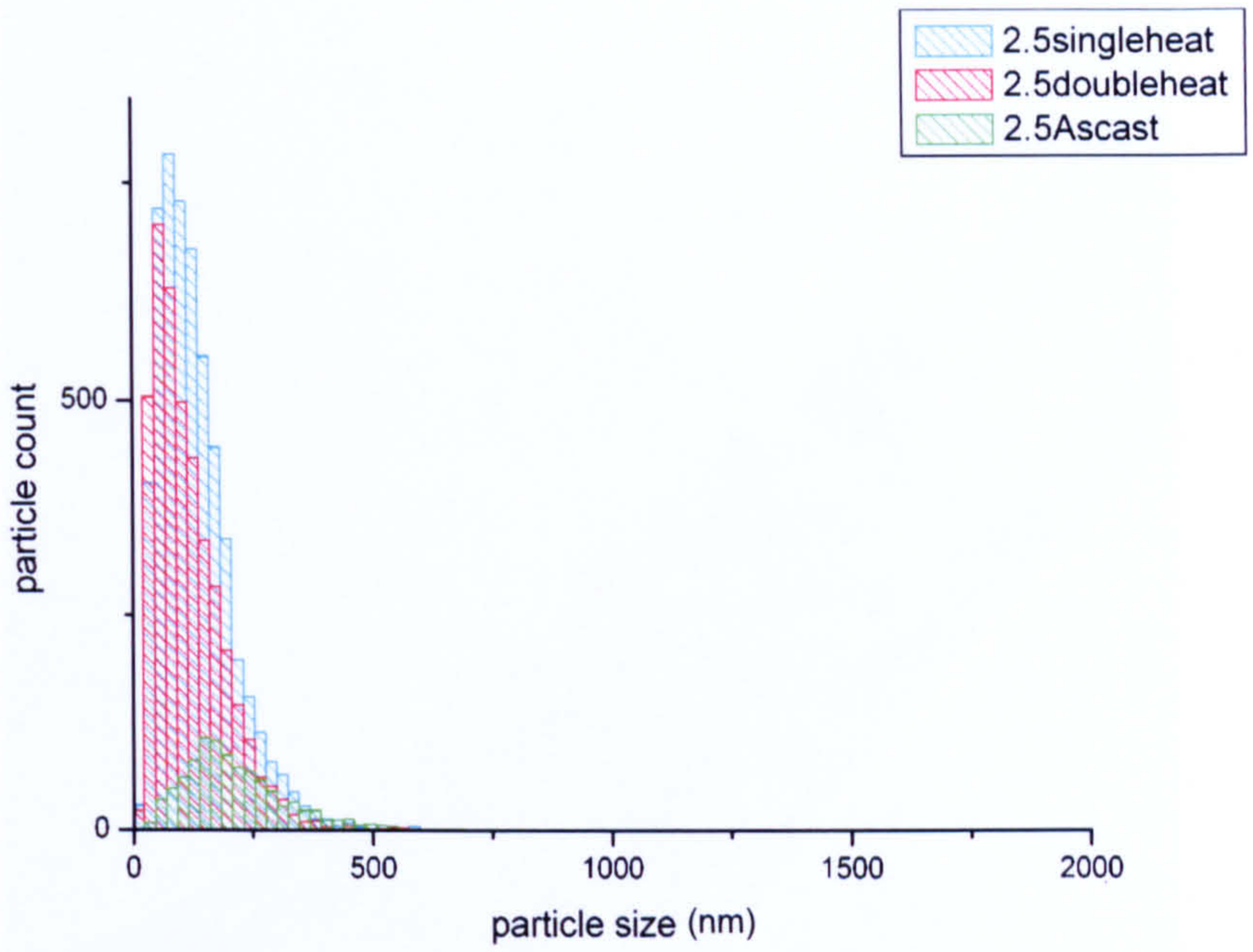

Figure 84 Particle size versus count for the as-cast, single and double heat treated CoCrMo alloys at 2.5 million cycles of the pin-on-plate test.

By 2.5 million cycles both the single and double heat treated specimens are showing a much greater amount of particle debris and the size range is 40-60 nm for the double heat treated and 60-80 nm for the single heat treated at the peak. The data shows well over 500 particles per ml which is much greater than the as-cast debris which shows 100 particles per ml and a peak of 160-180 nm size. The spread of all three specimens' particle sizes has become narrower over the 2.5 million cycles. The y-scale is larger on Figure 84 as the particle count was greater.

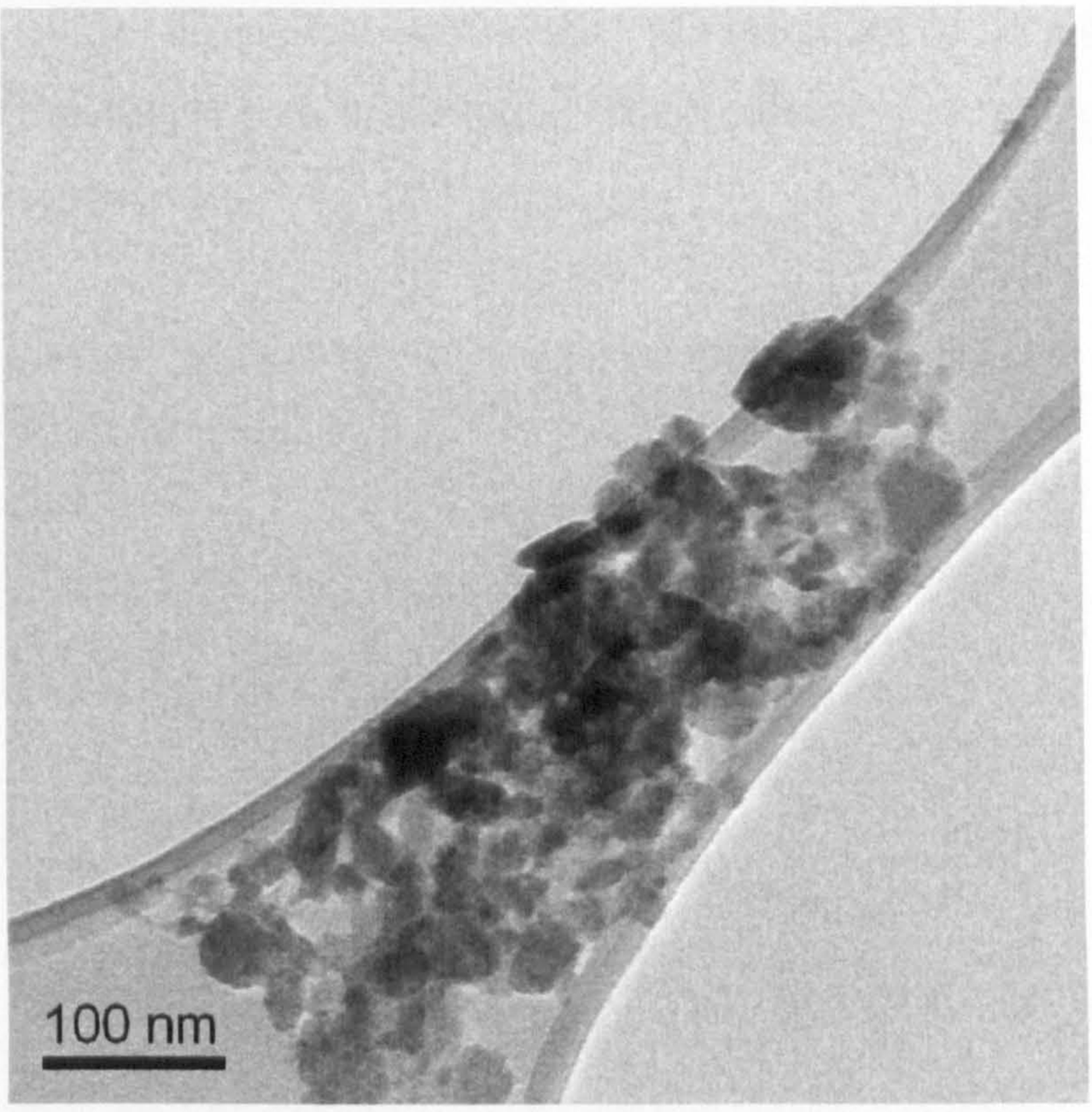

Figure 85 TEM image of the as-cast particles during the pin-on-plate test.

As can be seen the particles shown in Figure 85, resting on a carbon mesh, are agglomerated. They range in shape from needle shaped to round and the different thicknesses can be identified by the colour intensity. EDX has shown that these particles are made from the bulk cobalt chrome alloy tested in the pin-on-plate rig.

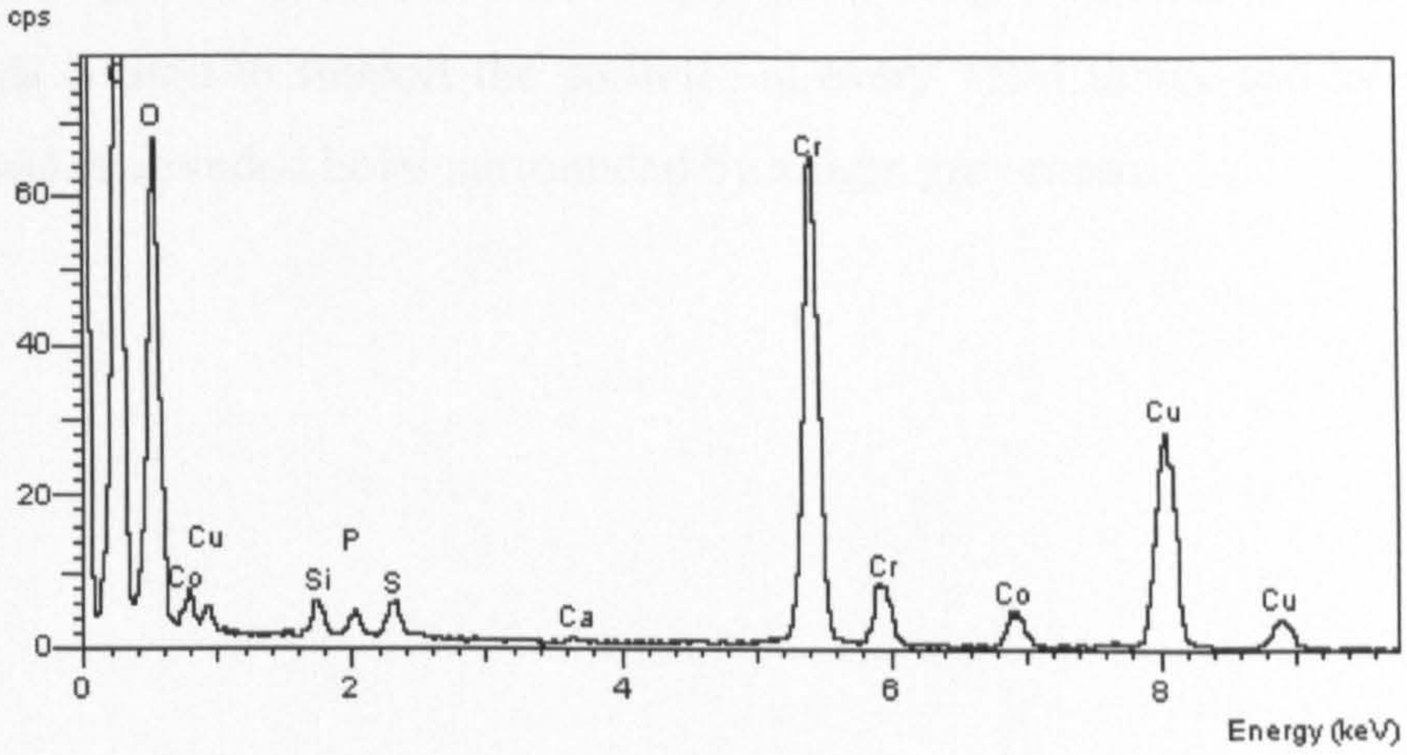

Figure 86 Shows an energy dispersive x-ray analysis (EDXA) of as-cast pin-on-plate particulate debris, the graph shows energy in kiloelectronvolts (keV) against counts per second (cps)

Figure 86 shows that the particles seen in the TEM image above are made of cobalt chrome alloy, the copper peak is due to the carbon coated copper grid on which the sample was imaged.

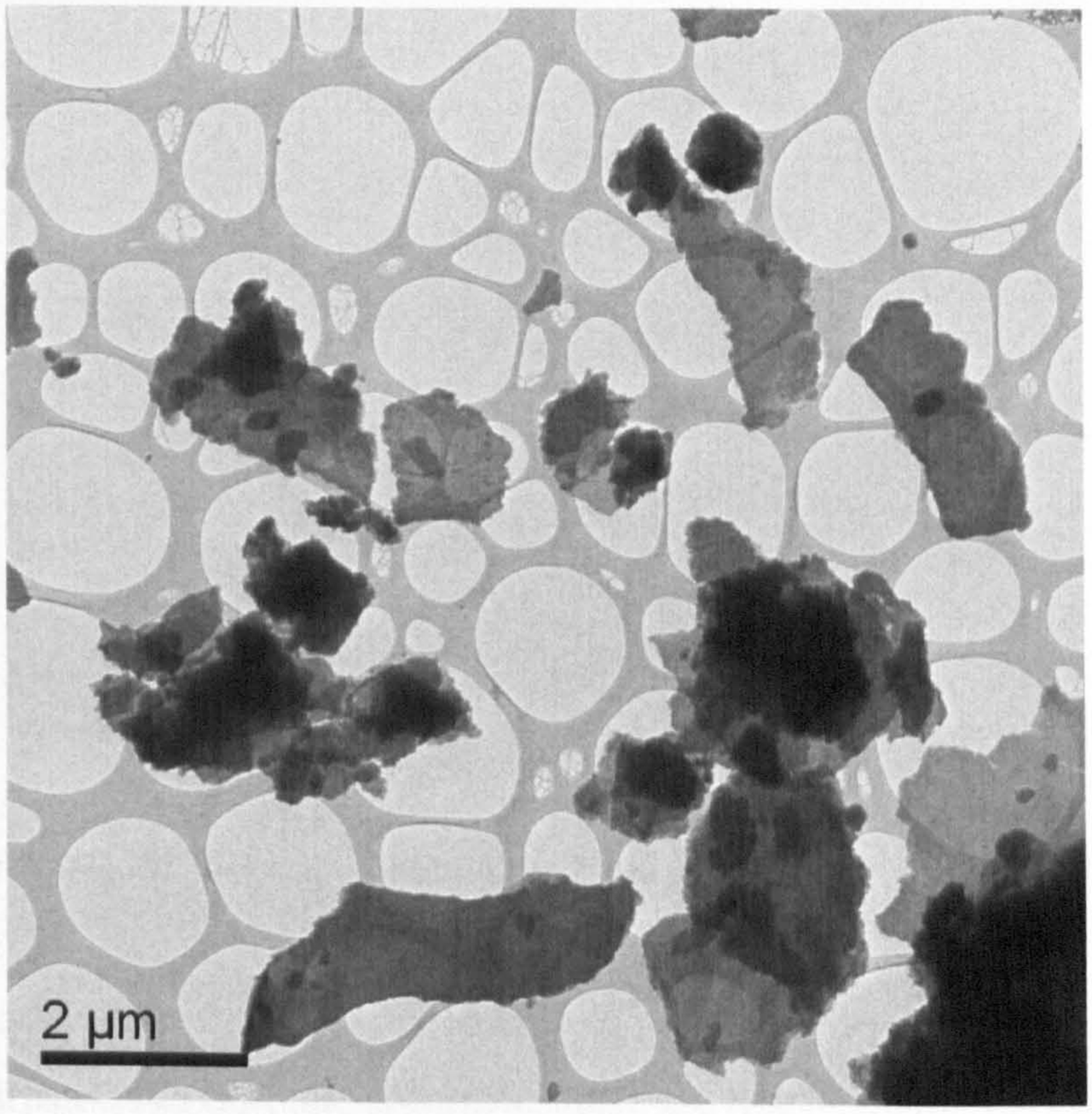

Figure 87 Double heat treated pin-on-plate particles at a low magnification

The image above shows flake like particles from the double heat treated pin-on-plate specimen which are between 1 and 2 microns in length. The carbon coated copper grid which is used to support the particles in every TEM image can be seen in the background as rounded holes surrounded by a light grey mesh.

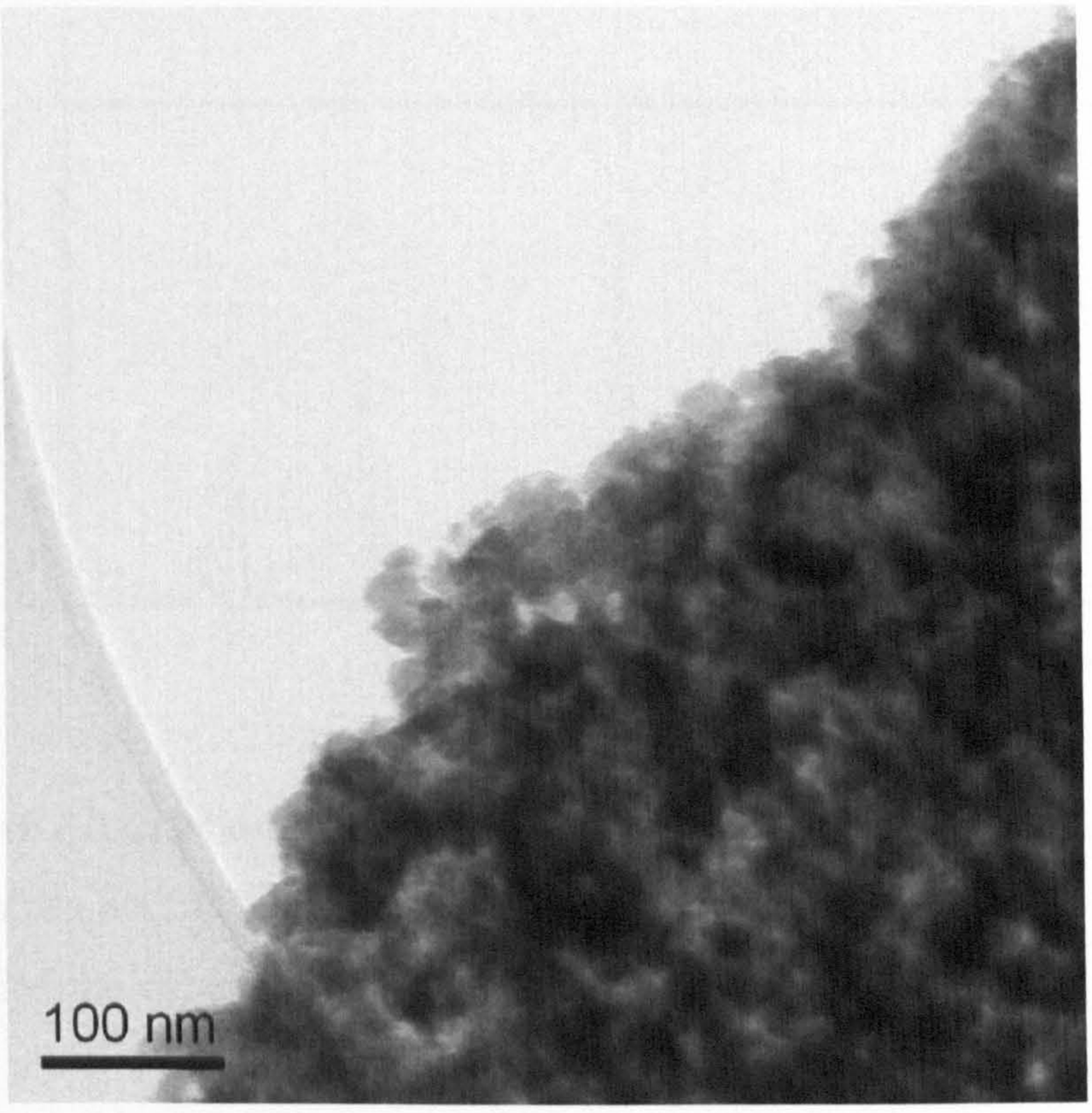

Figure 88 Double heat treated particles from pin-on-plate specimen at a high magnification

Figure 87 and Figure 88 show the different particles that were created from the double heat treated pin-on-plate specimen these are much smaller particles of around 10 nm. The small particles seen in Figure 88 are those seen in the particle size data as the NanoSight would not be able to detect the particles seen in Figure 87. The particles at low magnification are generally larger than 2 μm and will make up the majority of the wear debris due to their larger volume.

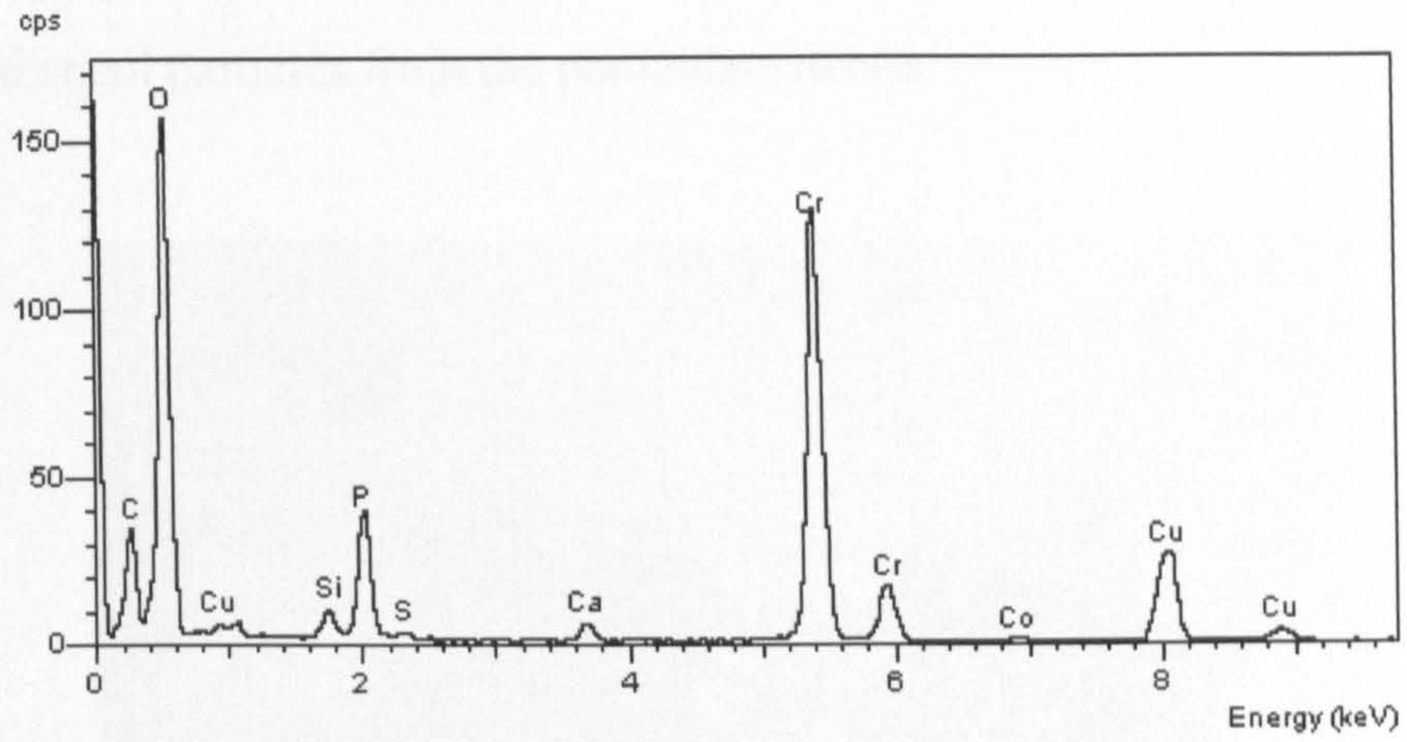

Figure 89 An EDXA of double heat treated particulate debris from a pin-on-plate test

Figure 89 shows an EDXA of the double heat treated particles that were studied under the TEM the cobalt and chromium peaks again confirm that the particles are the CoCrMo alloy. The diffraction also shows a phosphor spike, this may have been due to the sodium doedecyle phosphate that the particles were rinsed in to separate them from the protein chains.

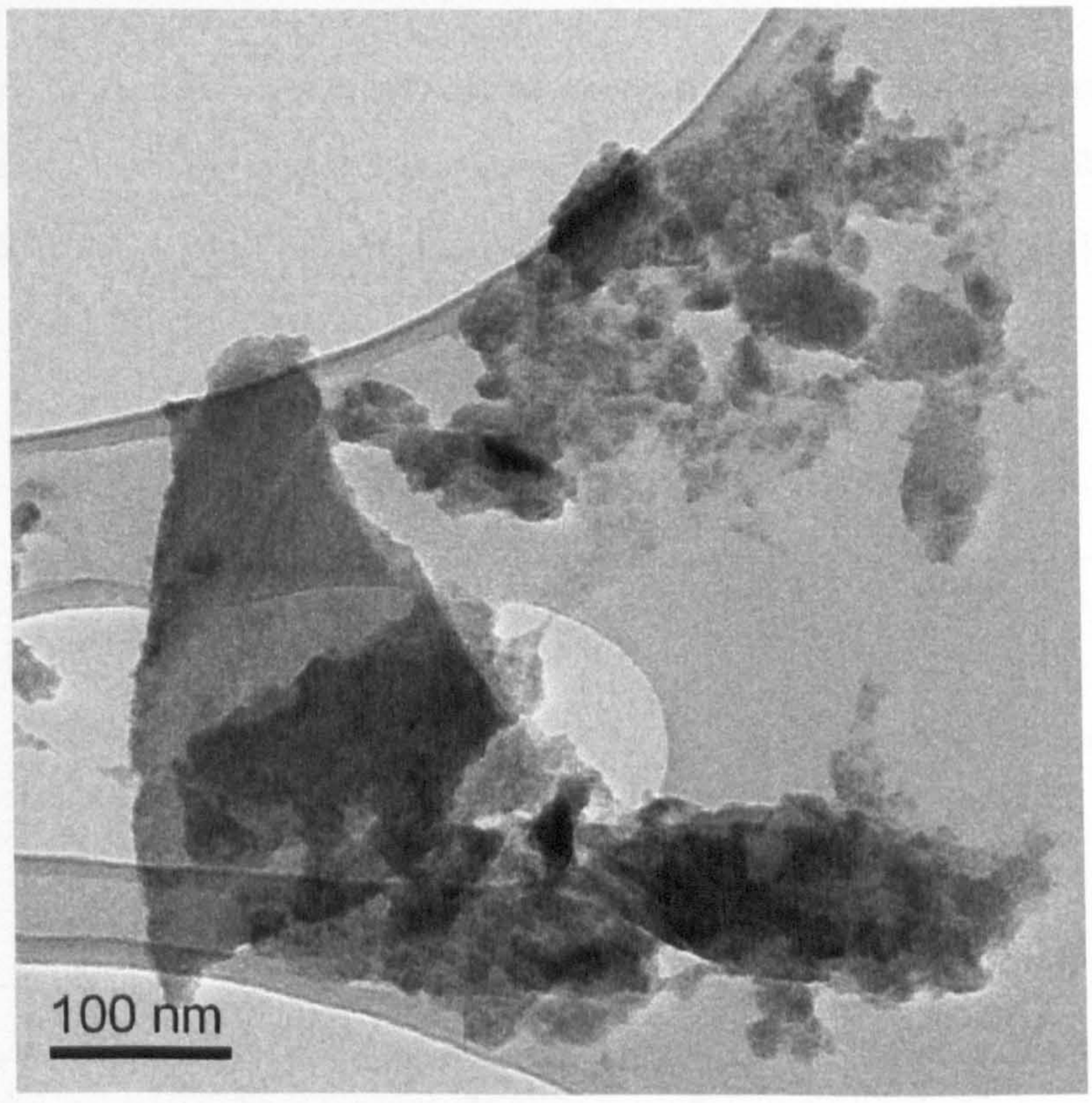

Figure 90 Single heat treated particle debris from a pin-on-plate specimen

This high magnification image of the single heat treated particles shows both large plates and small particles from the particulate debris.

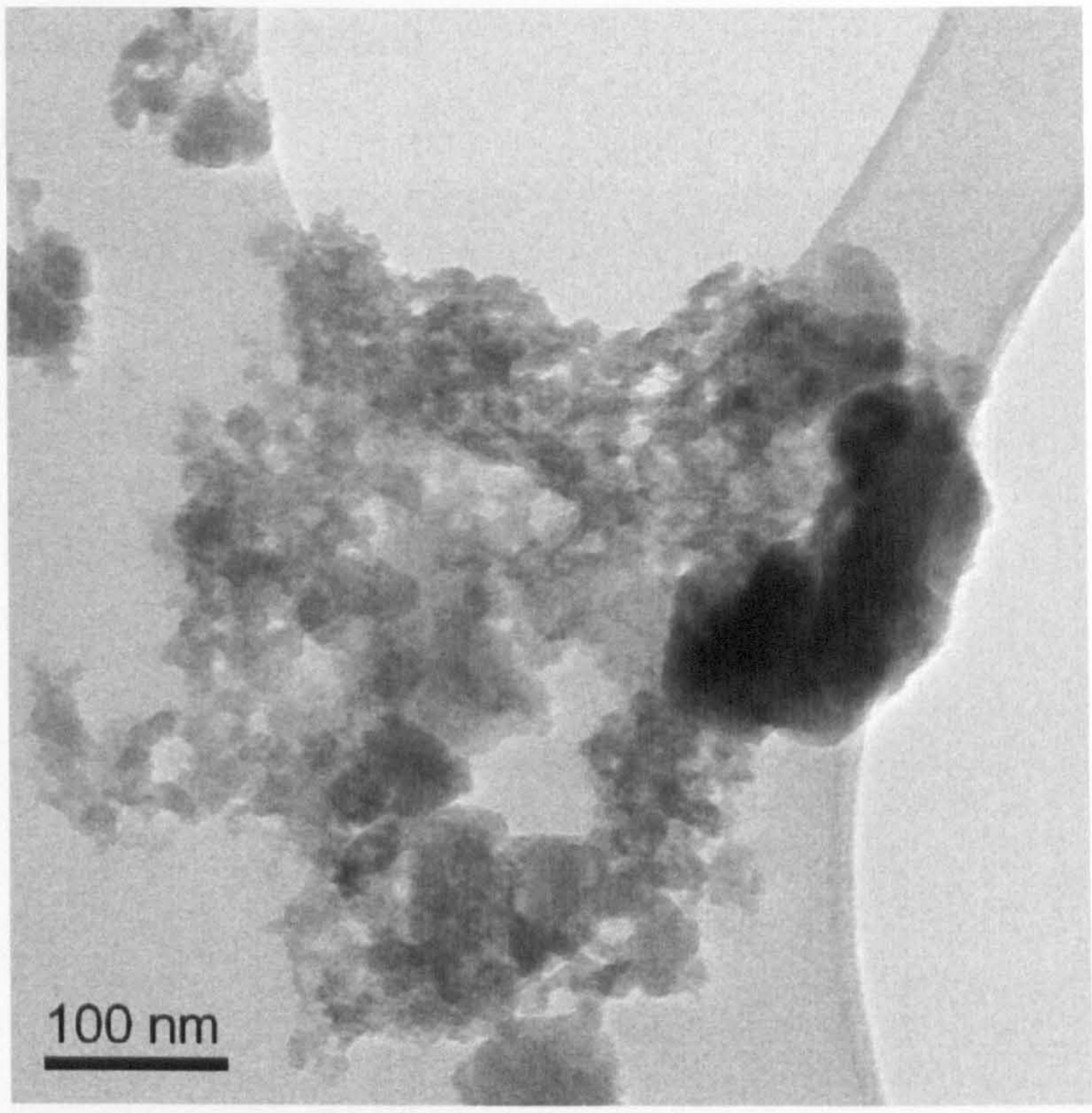

Figure 91 Single heat treated particle debris from a pin-on-plate specimen

The small debris from the single heat treated specimens was seen more than the large plate like particles, all the debris agglomerated when dried onto the carbon coated copper grids used for imaging.

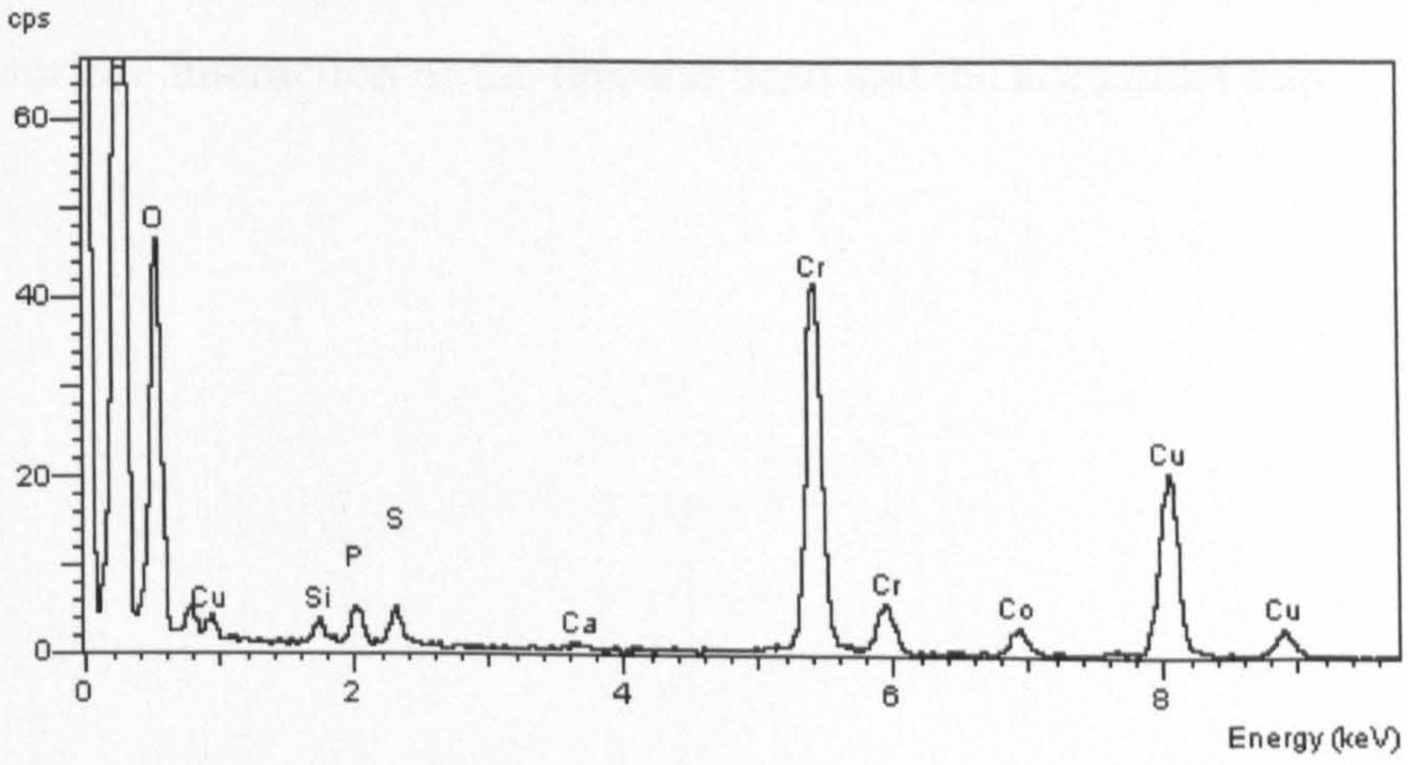

Figure 92 An EDX of single heat treated particulate debris from a pin-on-plate test

An EDX revealed that the particles were made from cobalt chrome and yet again a small phosphor spike can be seen due to the cleaning protocol.

5.3.2. Simulator Particle Debris

5.3.2.1. Double heat treated

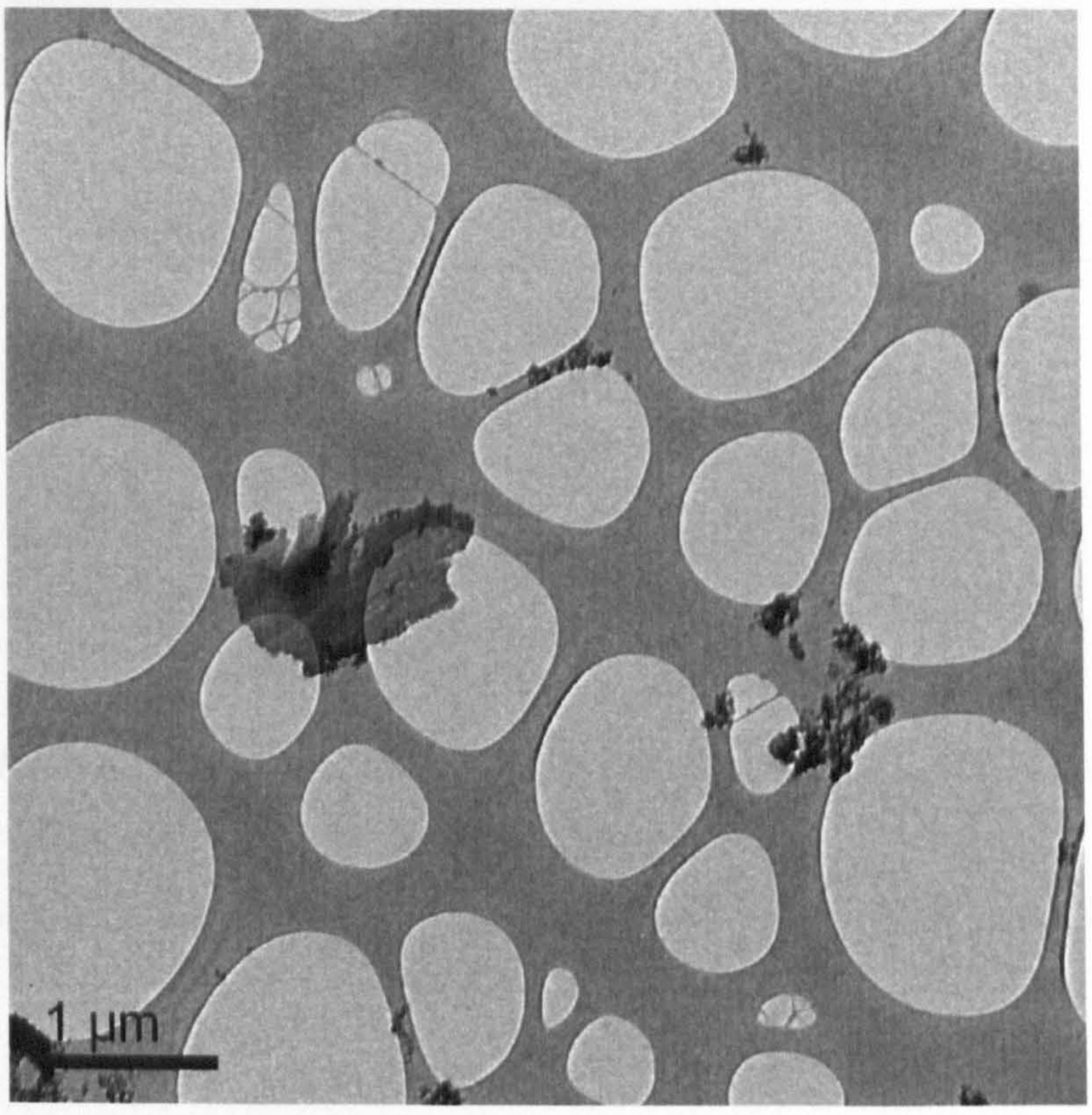

Figure 93 Low magnification image of particulate debris from a 50 mm double heat treated simulator test

This low magnification image of the double heat treated debris from a simulator wear test shows that large flakes of material as well as smaller particles are produced from the surface interaction of the femoral head and the acetabular cup.

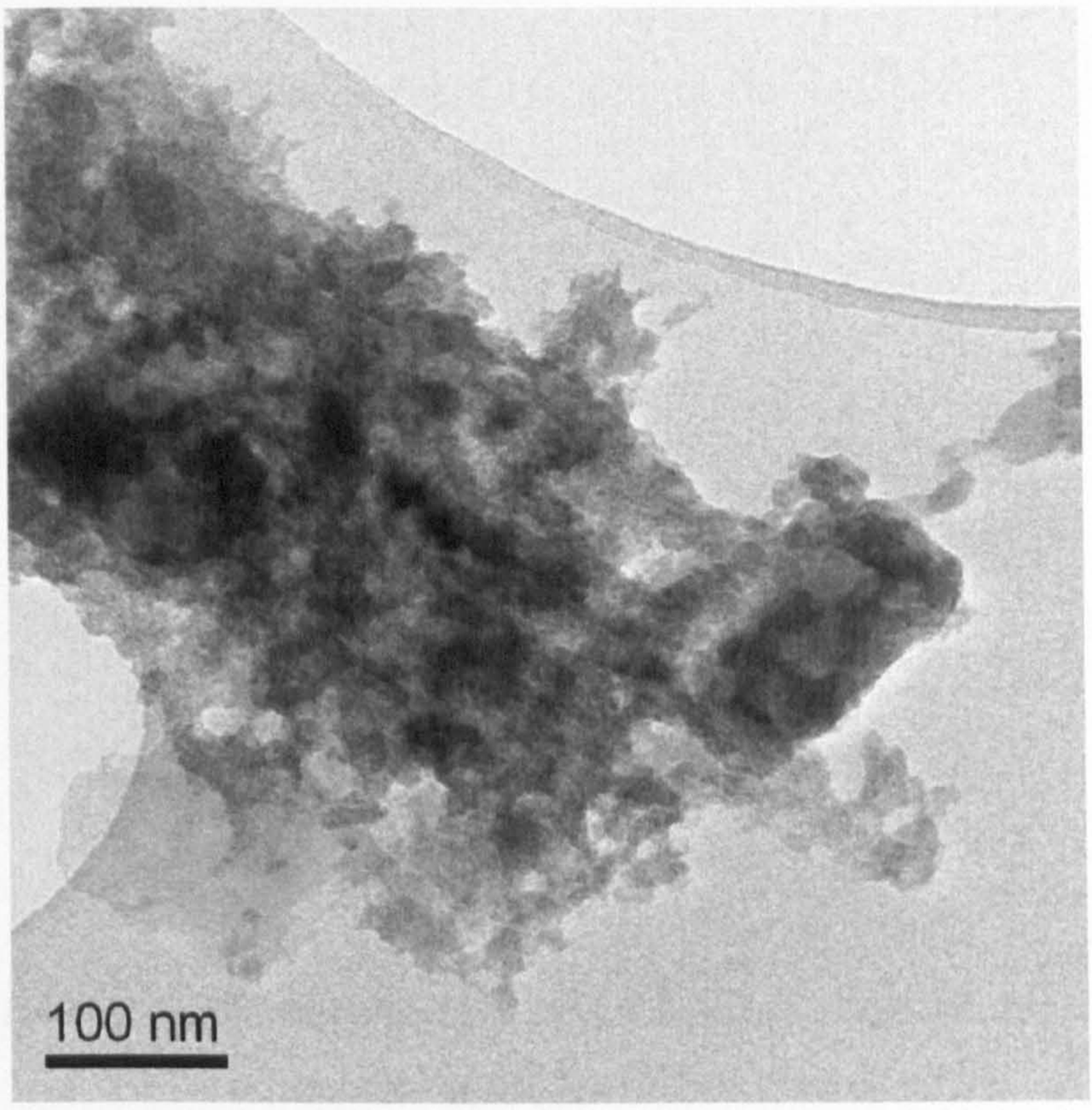

Figure 94 High magnification image of particulate debris from a double heat treated 50 mm simulator test

This high magnification images shows the smaller particles in more detail.

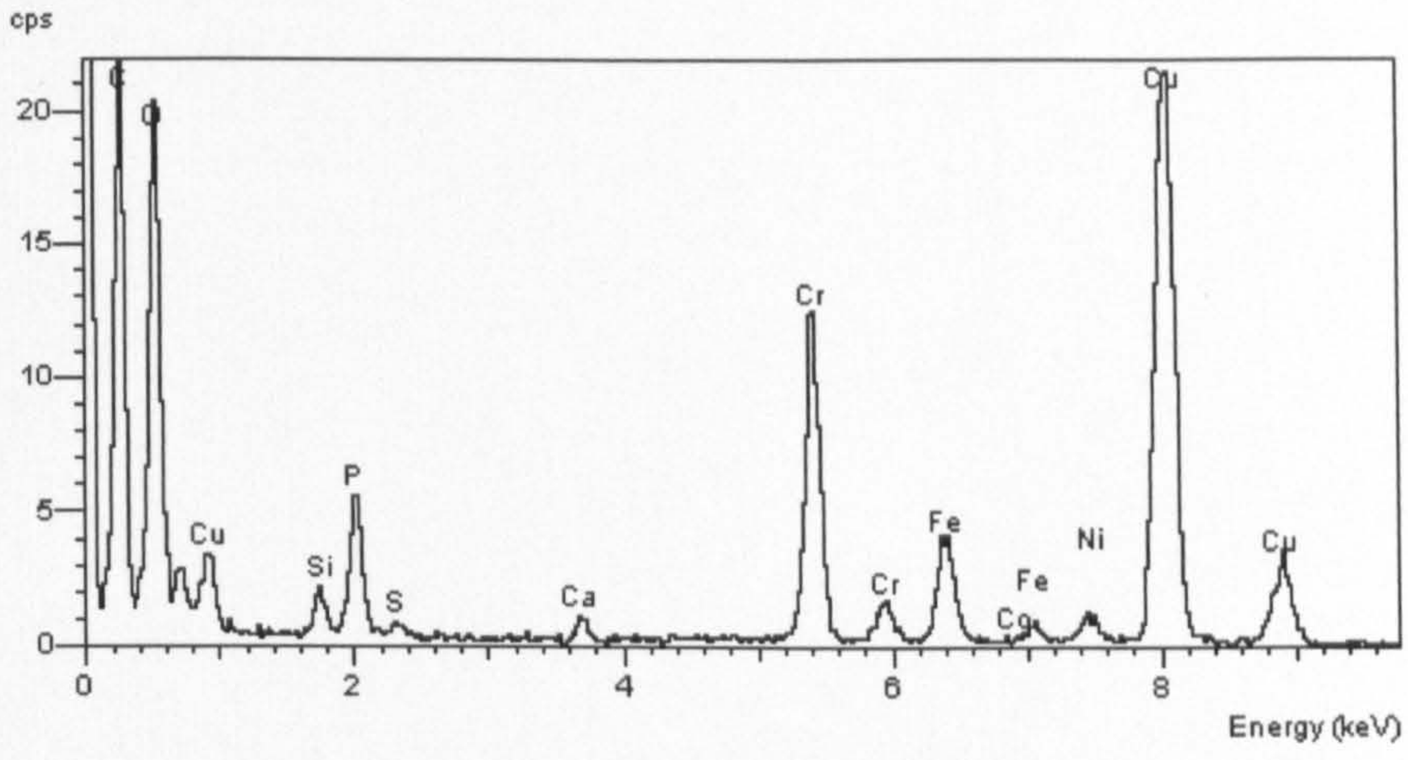

Figure 95 An EDXA of double heat treated CoCrMo particle debris from a hip wear simulator test

The xray diffraction indicated that although the cobalt chrome alloy is present there is also iron and nickel in the particle debris, the phosphorus spike is also identified as is a silicon spike.

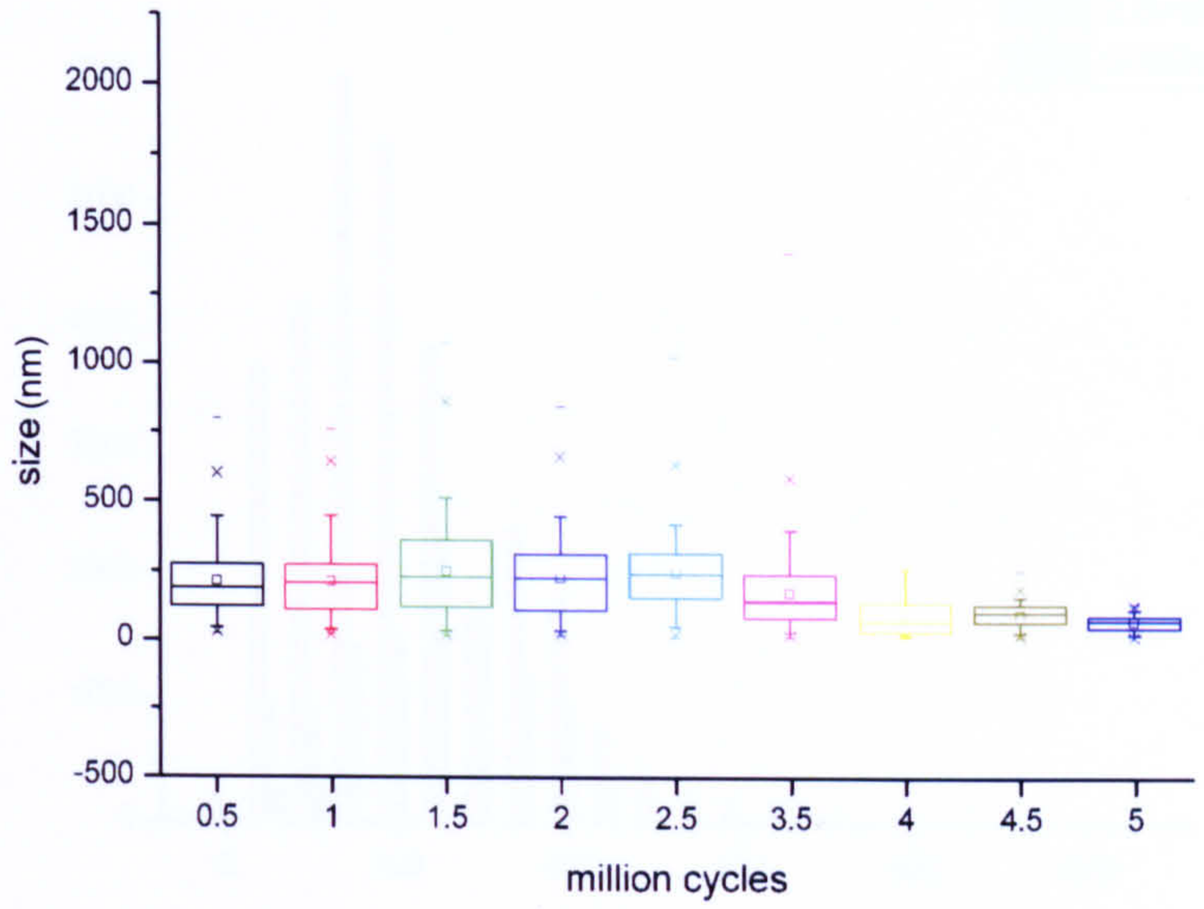

Figure 96 Particle debris size distribution of a 5 million cycle simulator test of 50 mm double heat treated CoCrMo

The particle size of each half million cycle period over the 5 million cycle test was recorded for the double heat treated simulator specimens. The particle spread seems to increase to a maximum at 1.5 million cycles and then decrease, ending at 5 million with a very narrow spread centred at 100 nm.

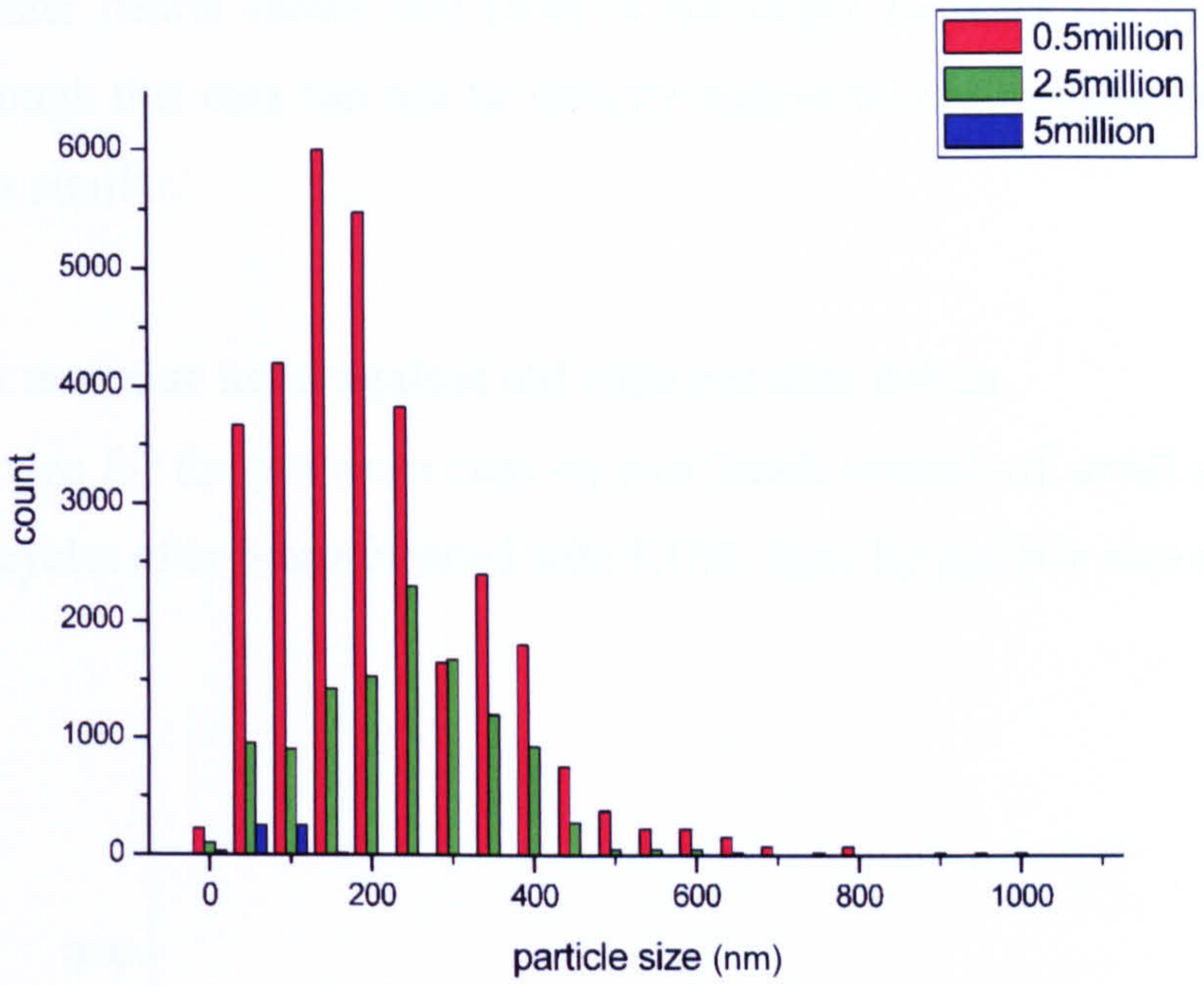

Figure 97 Particle size vs count of double heat treated particles at intervals through the simulator test

The particle count against particle size indicated the volume of particle debris. The volume of debris created decreases over the 5 million cycles as well as the particle size decreasing and becoming a smaller distribution.

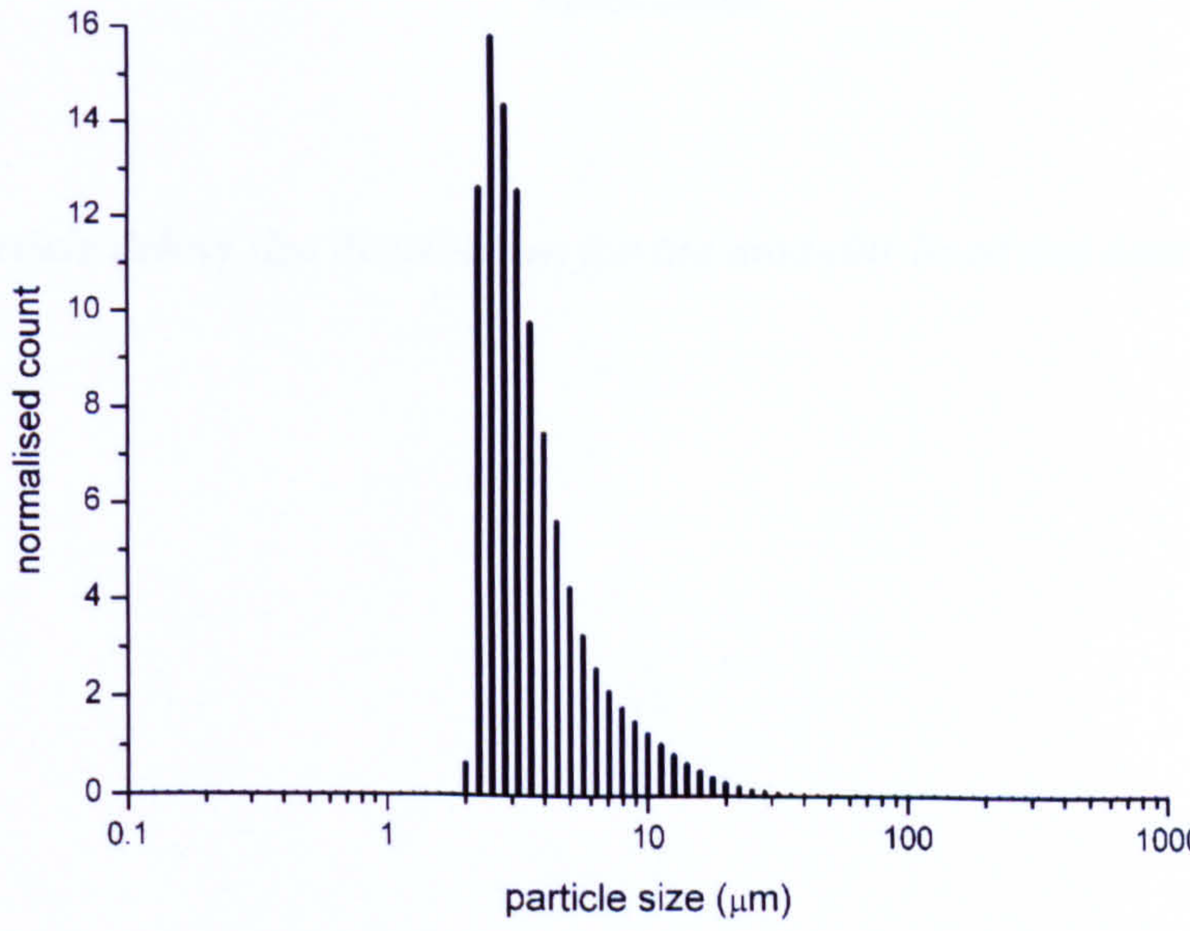

Figure 98 Mastersizer data indicating the larger particulate debris from the double heat treated joints at 0.5 million cycles

The Mastersizer debris shows that most of the larger particles are between 1 and 10 μm. Although this data can not be directly compared to the TEM image the size of particles is similar.

5.3.2.2. New modular head against old cups particle debris

The particle size for the pre worn cups on new heads started off small and increased at 3 million cycles after being cleaned with KOH, then the particle size decreased.

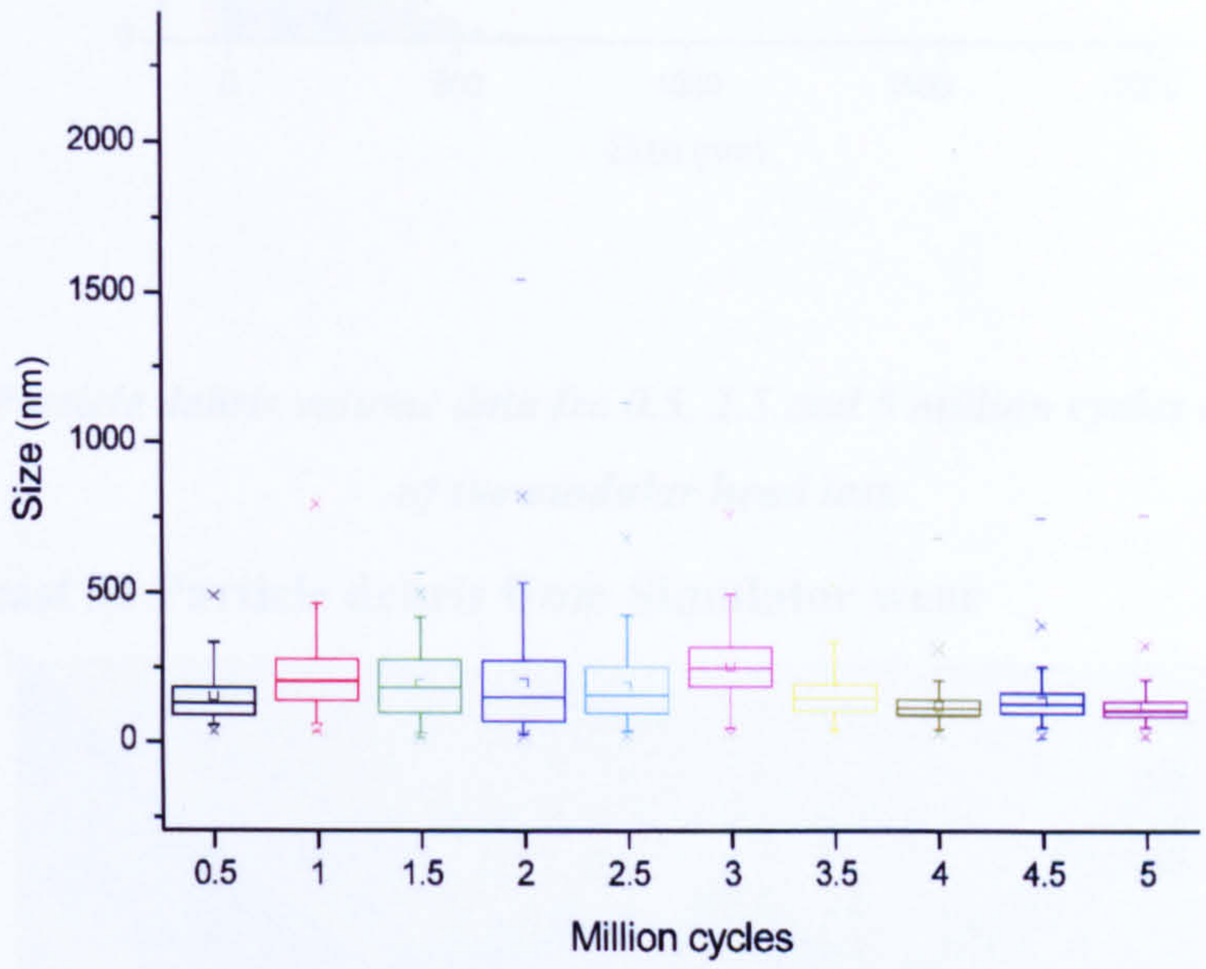

Figure 99 Particle debris size distribution for the modular head test over 5 million cycles

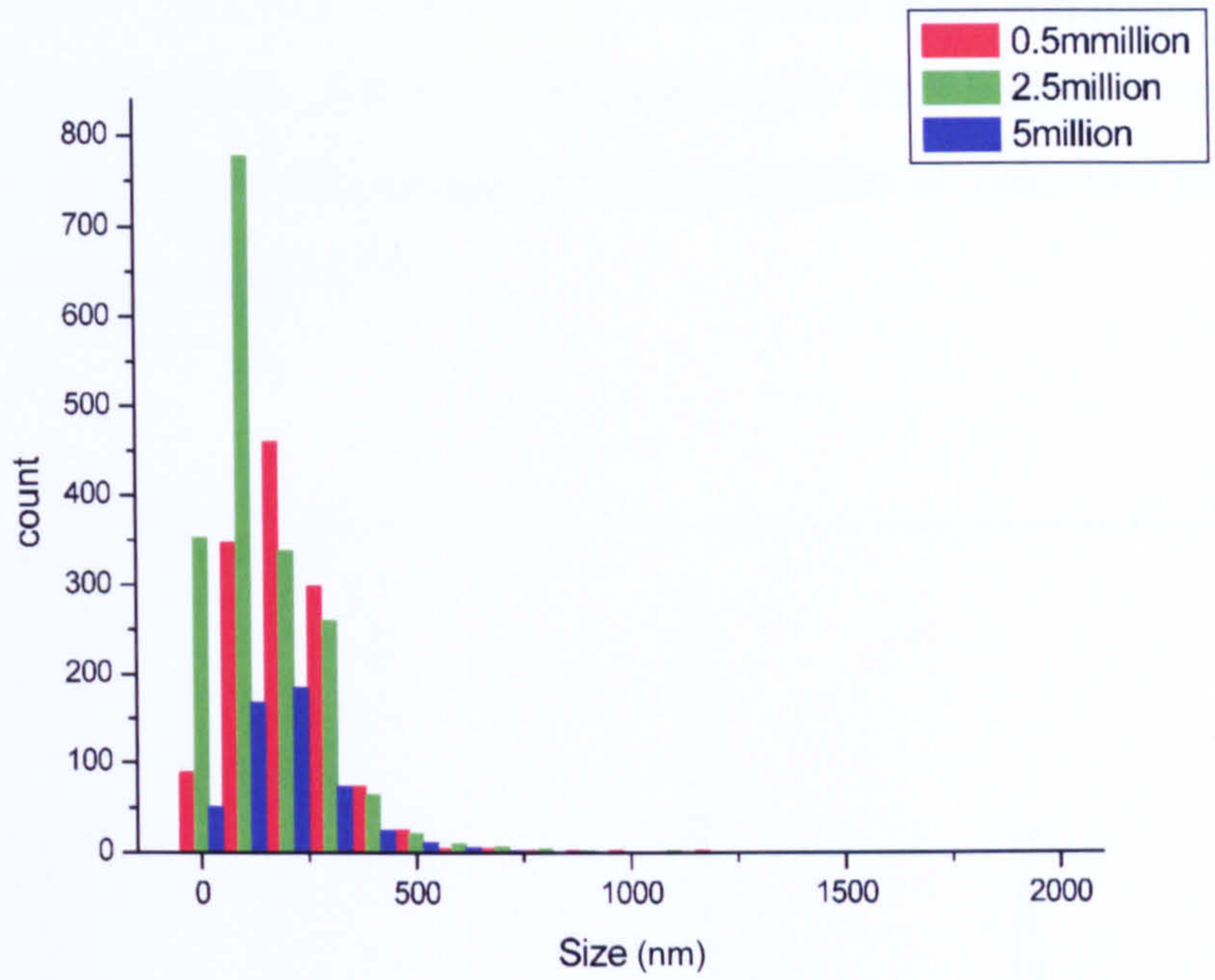

Figure 100 Particle debris volume data fro 0.5, 2.5 and 5 million cycles over the duration of the modular head test.

5.3.2.3. As cast 38 Particle debris from Simulator wear

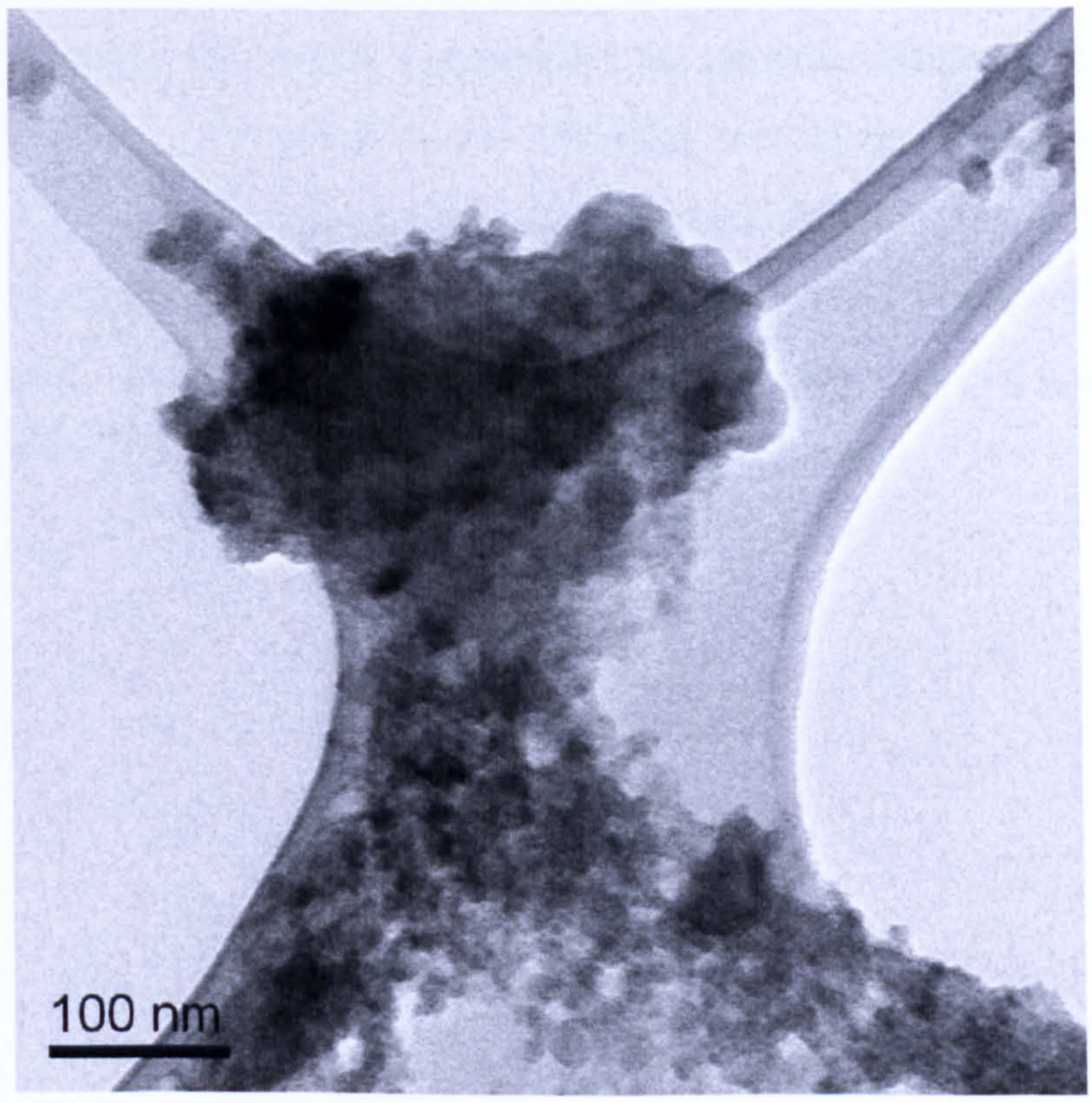

Figure 101 Particulate debris from the 38 mm diameter joints which underwent simulator testing

The particle debris produced from the 38 mm joints from simulator testing was imaged using a TEM on a carbon coated copper grid. This sample is representative of all the particles seen in this sample, no large particles or flake like particles were seen in this specimen (Figure 101).

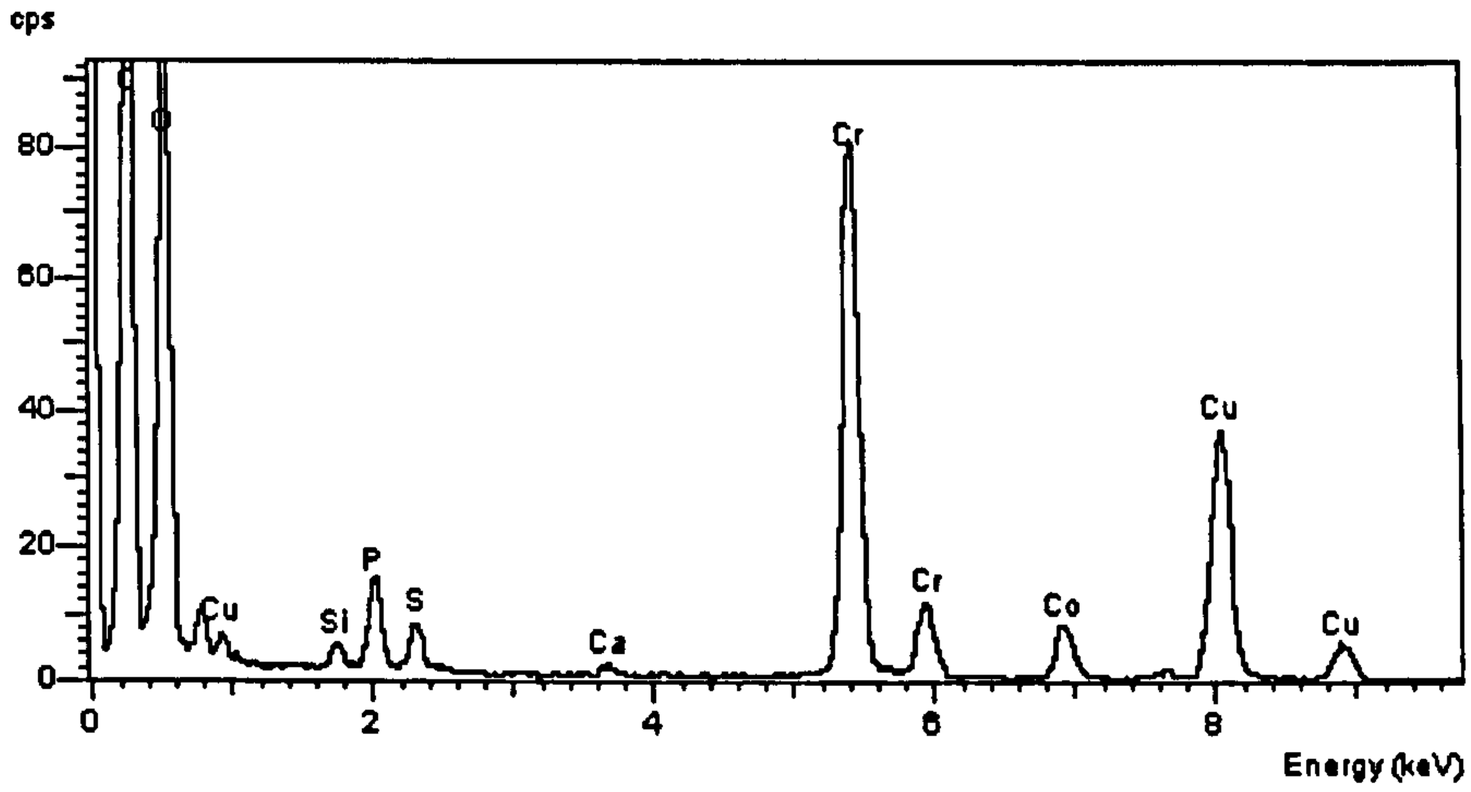

Figure 102 An EDX of particulate debris from a 38 mm as-cast CoCrMo hip wear simulator test

The x-ray diffraction was used to confirm that the particles imaged in the TEM were CoCrMo alloy as can be seen in Figure 102 there is a strong chromium peak and a cobalt peak indicating that the particles are made of CoCrMo alloy. Again there is a phosphor peak from the sodium doedecyle phosphate used to cleave the particles from the protein. The copper and carbon are from the carbon coated copper grid that is used to support the particles whilst imaging is undertaken.

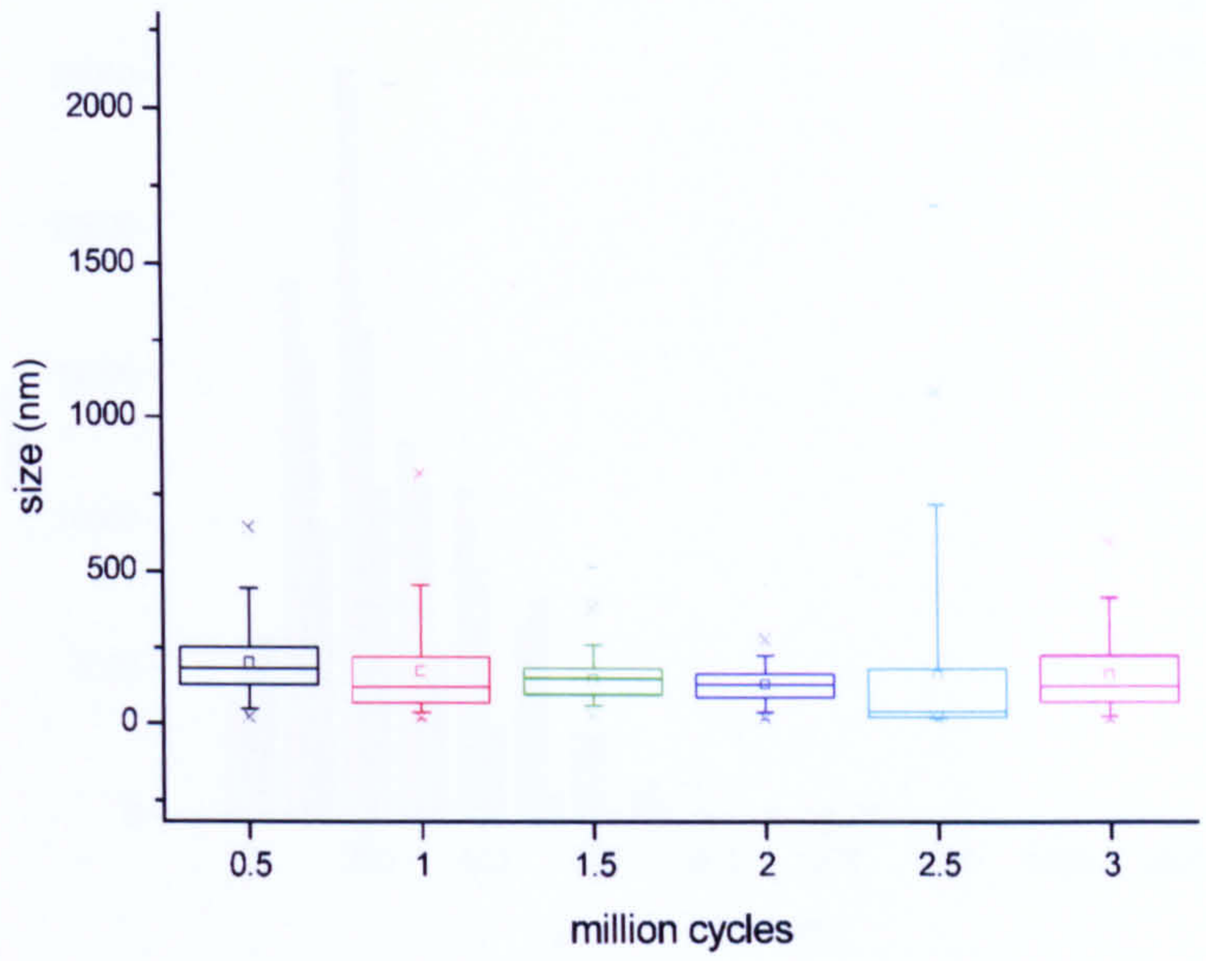

Figure 103 Size distribution of particulate debris over a 3 million as-cast 38 mm simulator test

The size of the particles is slightly higher at half a million cycles than elsewhere over the test although this is not statistically significant the average particle size is larger. The ninety fifth percentile of all particulate debris was below 250 nm in this 38 mm as-cast test.

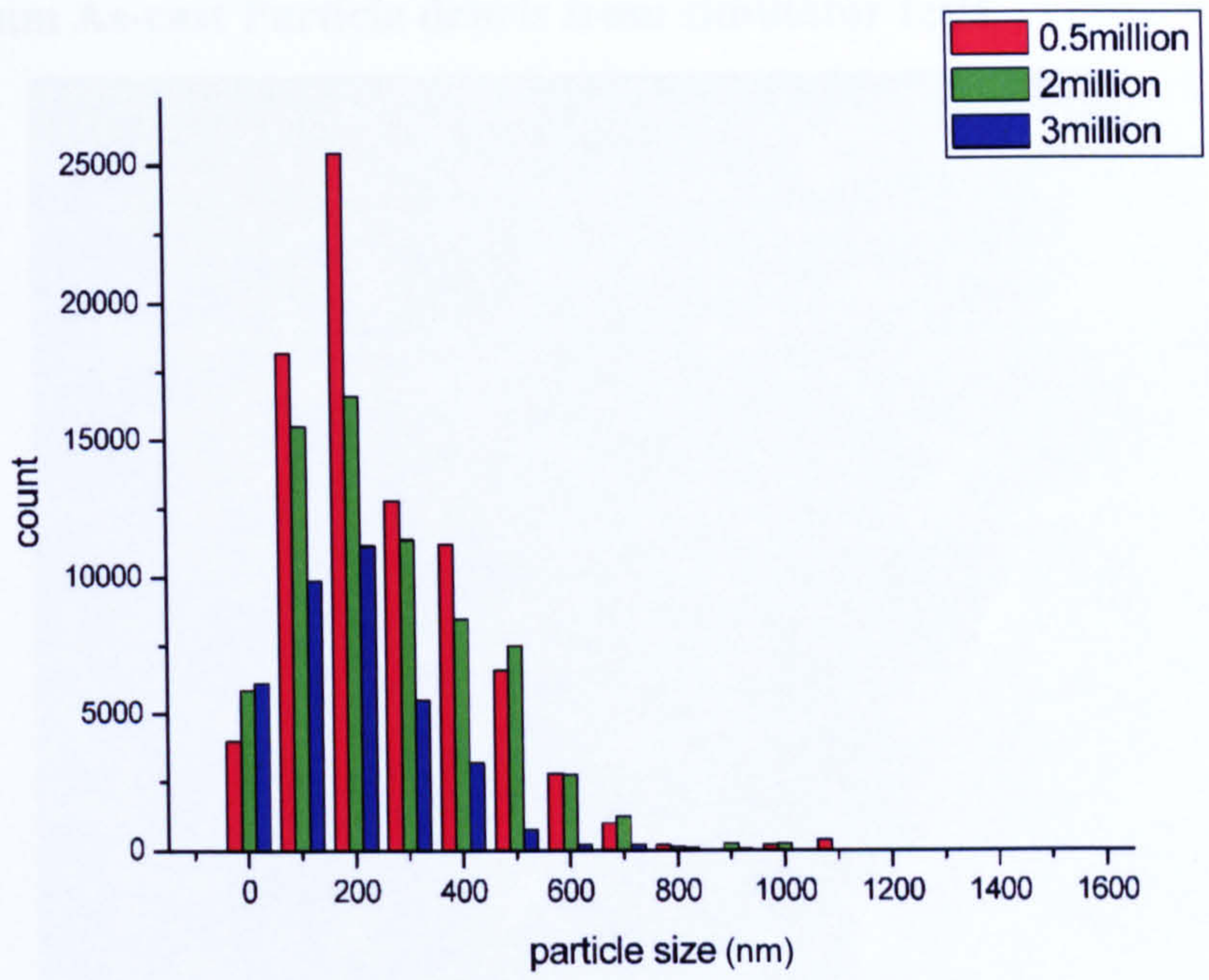

Figure 104 Shows the particle count against size for half, two and three million cycles.

Each half million cycle the bovine serum lubricant was taken out, saved and replaced with fresh bovine serum. Representative data from the beginning, middle and end of the test have been plotted together here to show the trend of particle size over the length of the test. Each data set represents half a million cycles of particle debris.

The number of particles decreases over the 3 million cycles. There are more particles in the 1-100 nm group and fewer in all the other groups as the test continues. Showing a trend towards smaller particles.

5.3.2.4. 50mm As-cast Particle debris from simulator tests

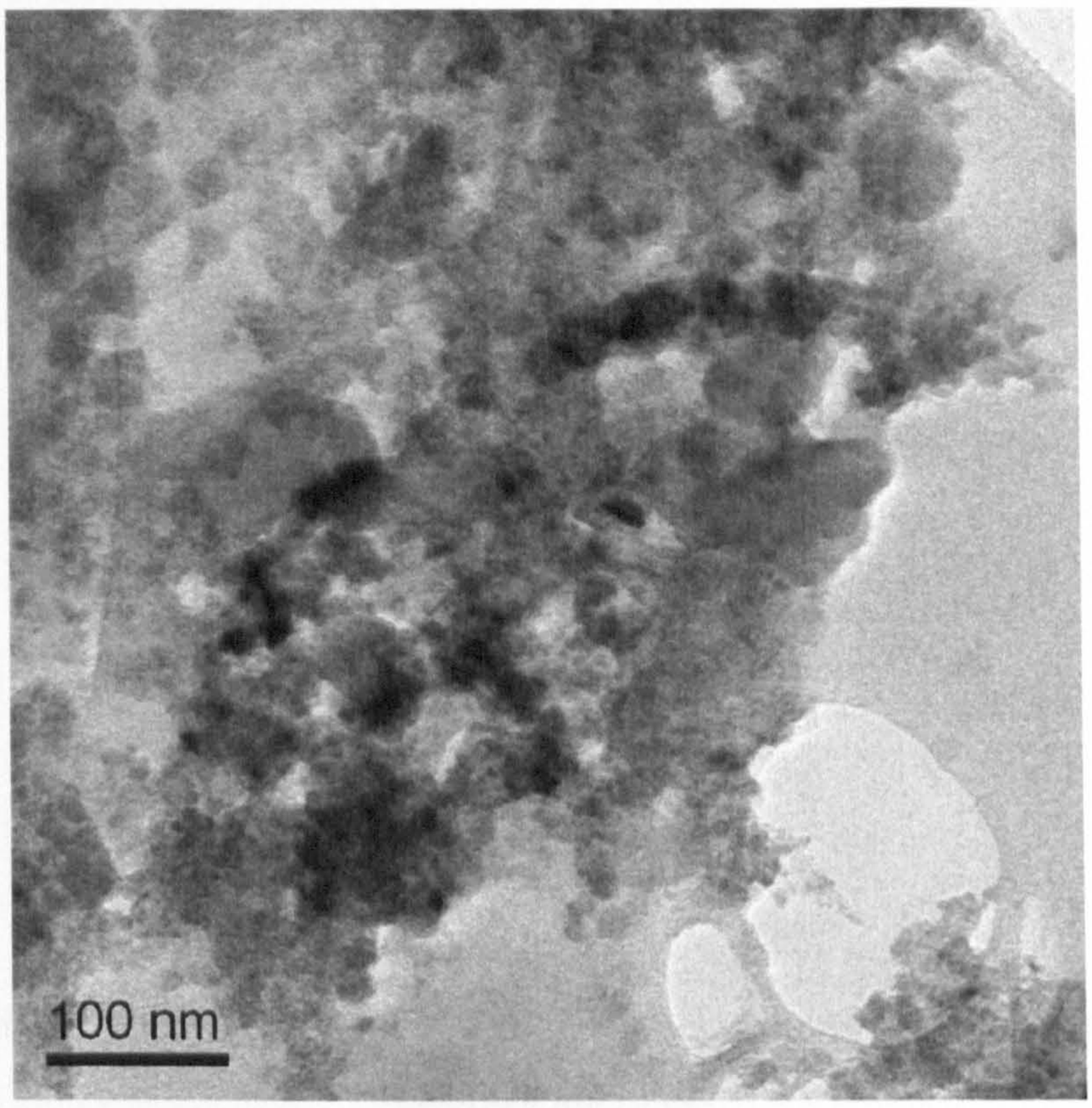

Figure 105 An image of particulate debris from a 50 mm as-cast CoCrMo simulator test

A TEM of the as-cast particles from the 50 mm simulator test shows a range of particle sizes, however no large flakes of material were found within the sample.

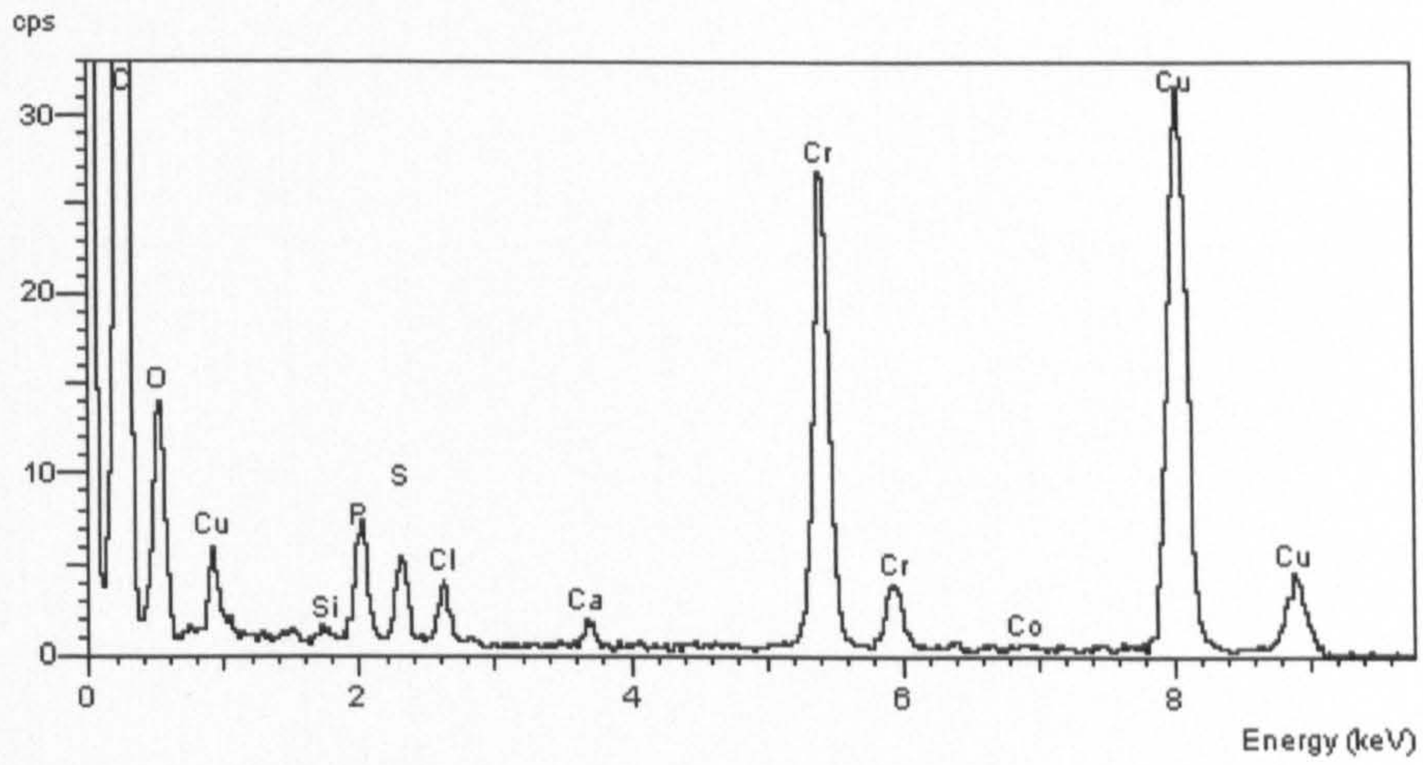

Figure 106 An EDX of particulate debris from 50 mm as-cast CoCrMo hips in a wear simulator test

An x-ray diffraction of the particles indicates that the bulk material is CoCrMo alloy but phosphorus, sulphur and chlorine are also present.

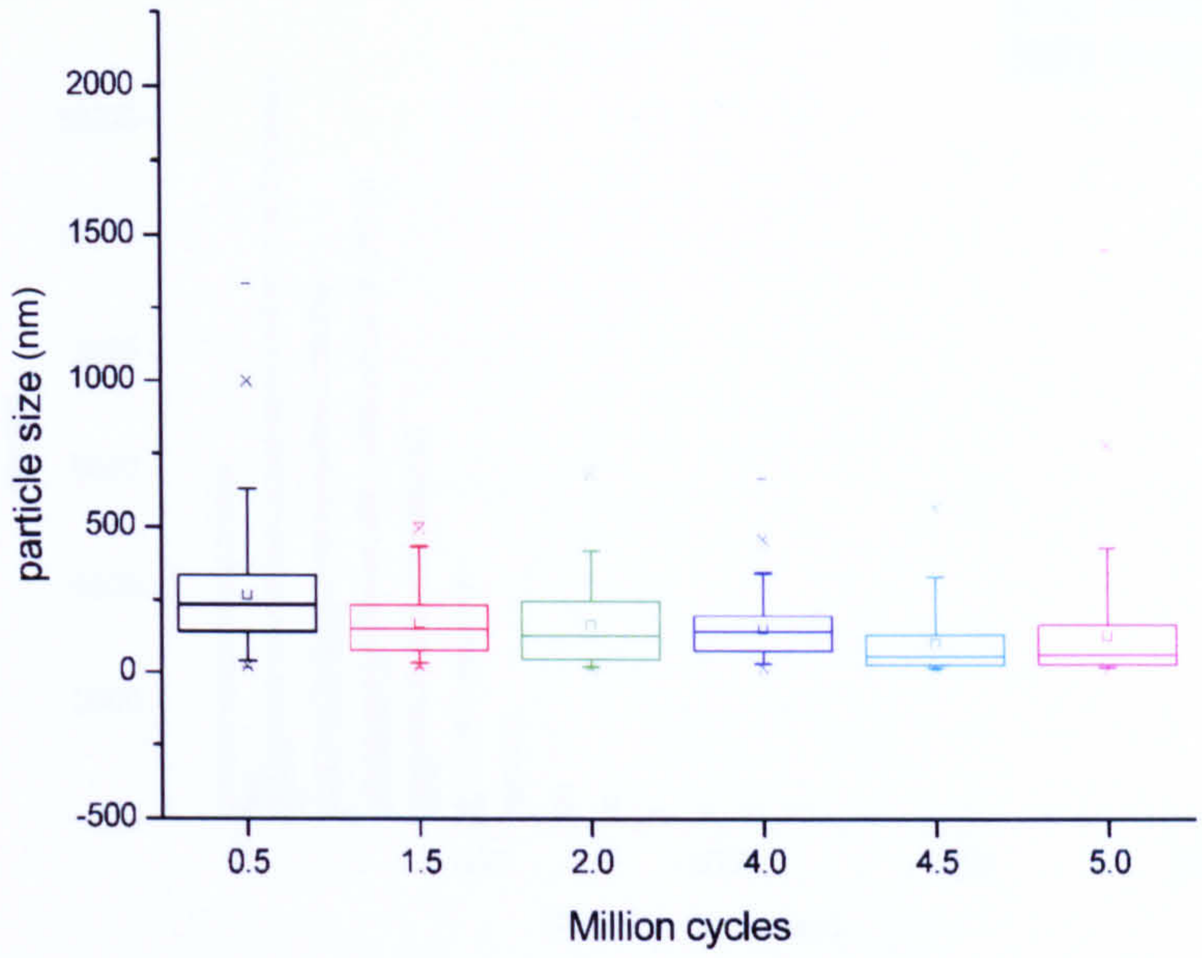

Figure 107 Size distribution over a 5 million cycle simulator test of 50 mm as-cast CoCrMo hip joints

The sizes of the particles over the course of a 5 million cycle test are shown above. The first half million cycles appear to produce slightly although not statistically significantly larger particles than the rest of the test. The spread of the particle size over the course does not alter, however the modal average size of the particle does decrease on average.

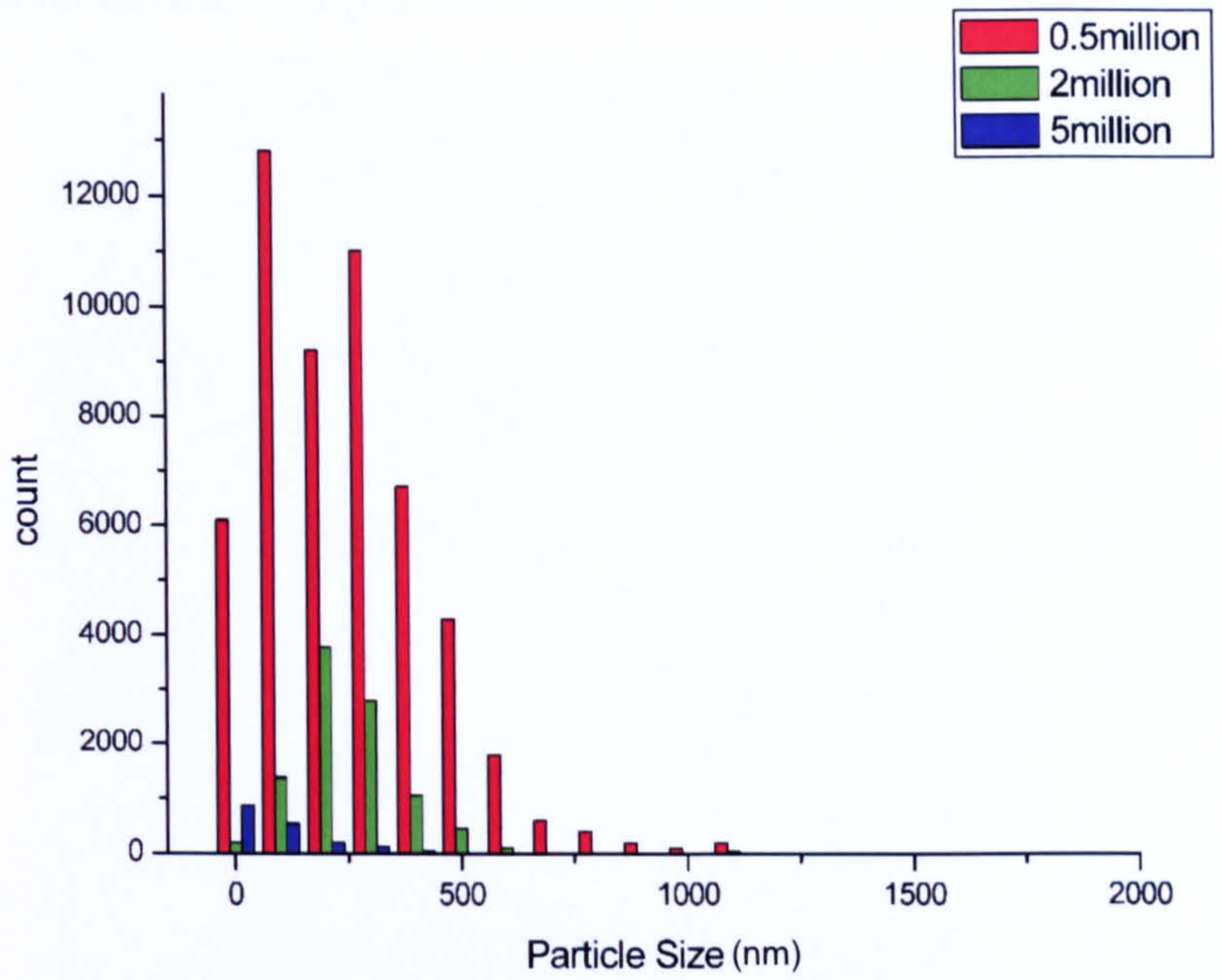

Figure 108 Particle size vs count for the 50 mm as-cast simulator test as the test progressed

The volume of particles over the course of the 5 million cycles decreased notably. The size also altered from peaking at 100 to 200 nm to peaking below 100 nm.

5.3.2.5. Plasma carburised particle debris from simulator wear tests

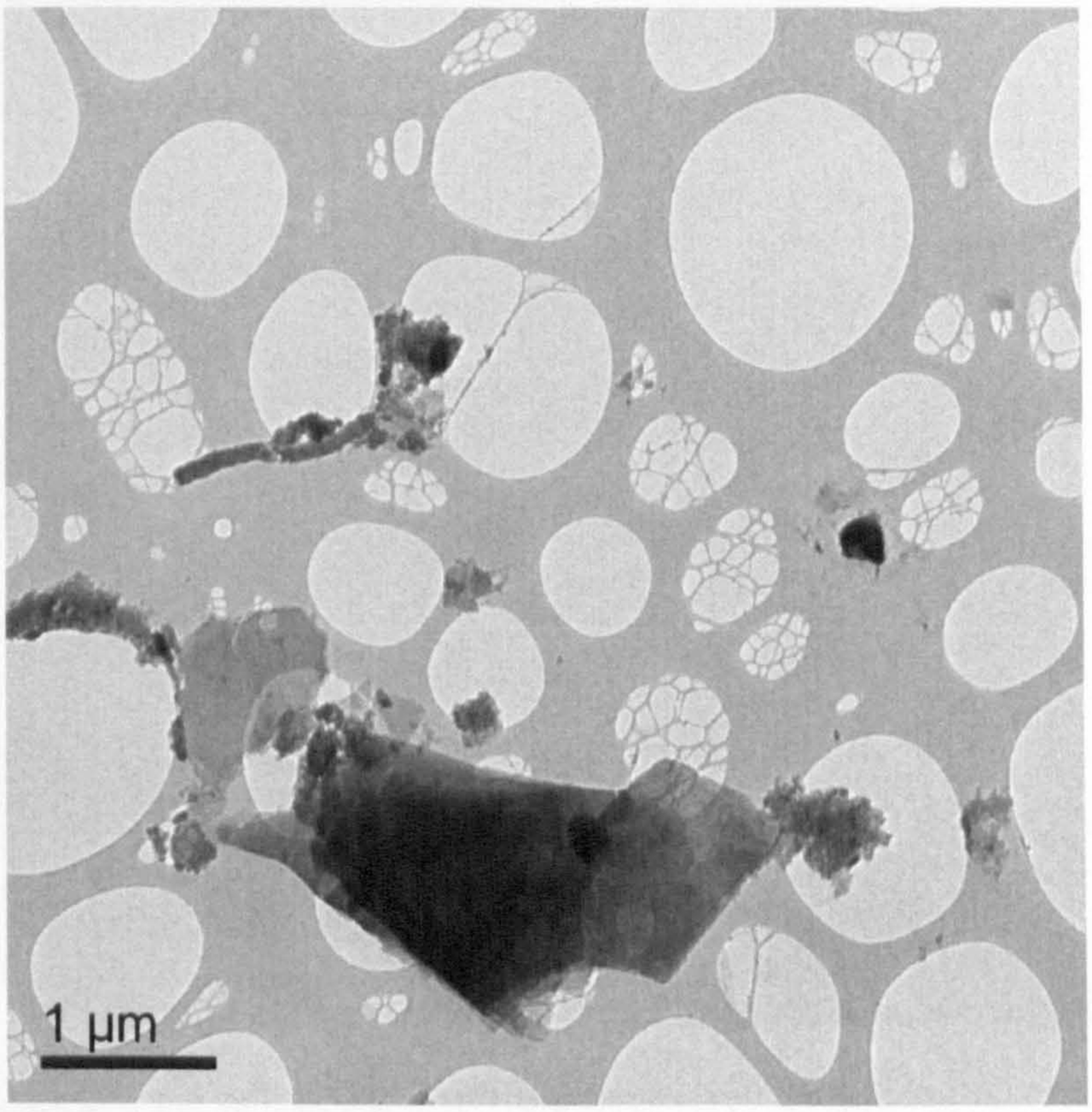

Figure 109 low magnification image of particulate debris from plasma carburised 50 mm simulator test.

Particulate debris from the plasma carburised cobalt chrome was seen to have both large and small particles.

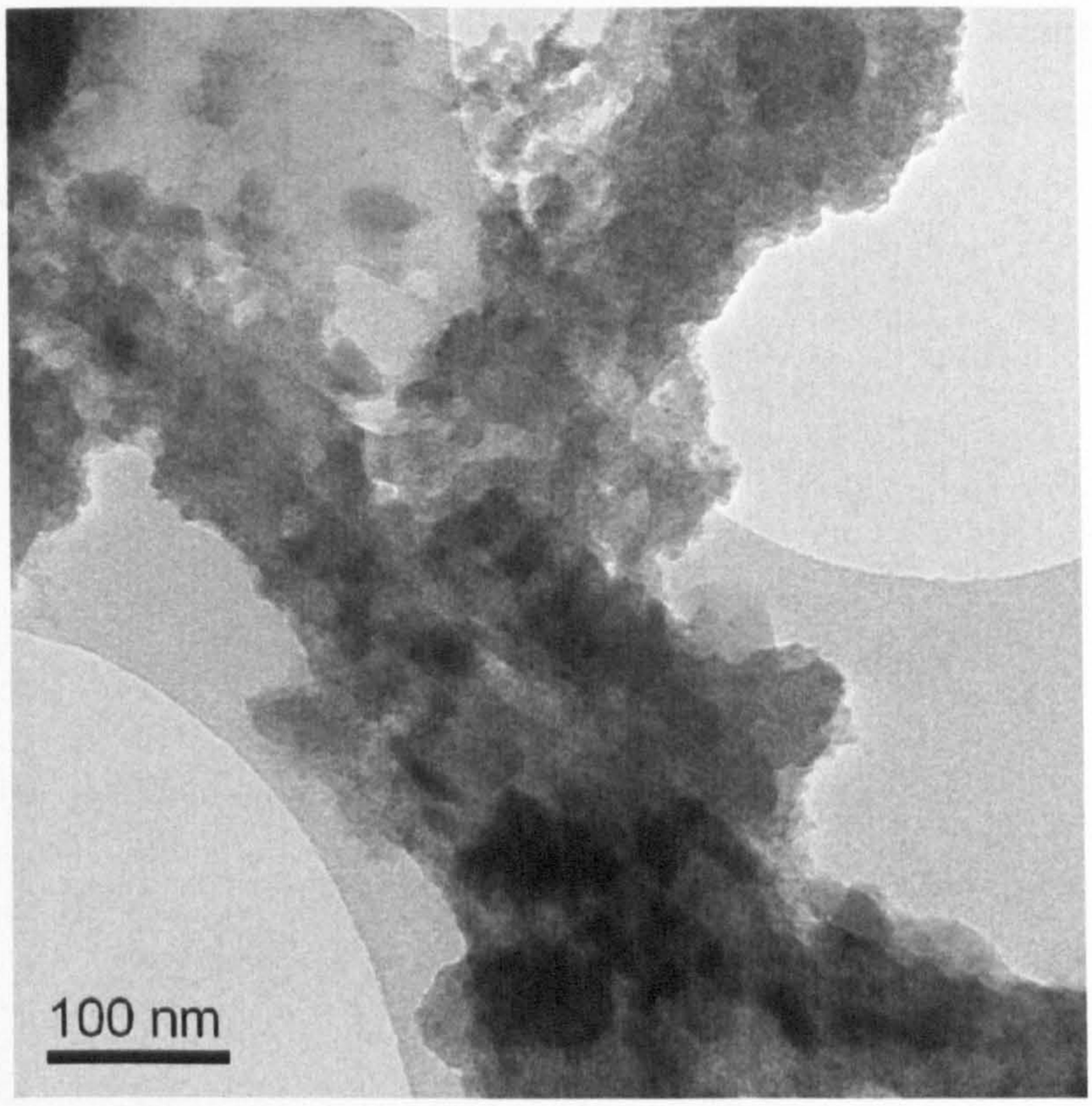

Figure 110 High magnification image of plasma carburised particulate debris from a simulator test

A higher magnification image showed the detail of the smaller particles from the plasma carburised cobalt chrome.

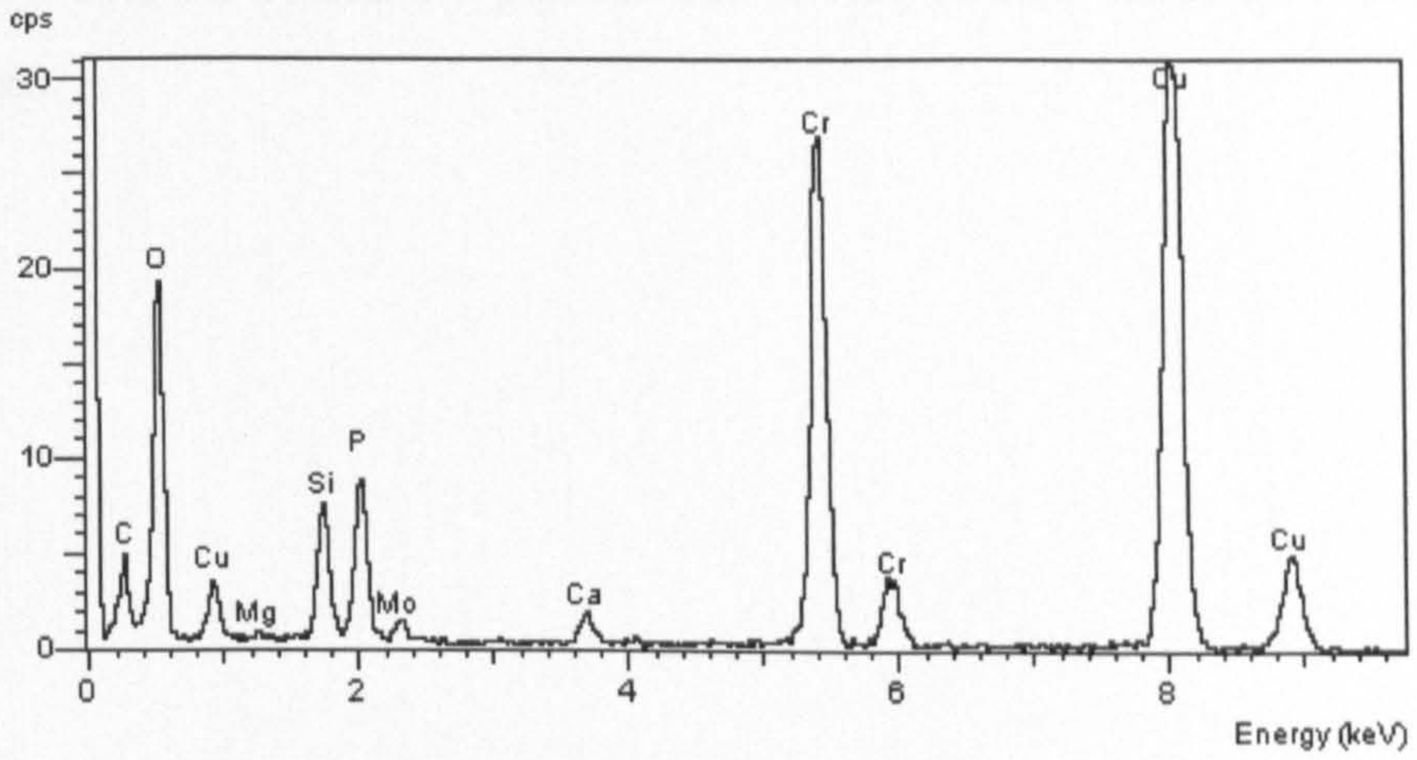

Figure 111 An EDXA of particulate debris from a hip joint wear simulator test of 50 mm plasma carburised CoCrMo.

An x-ray diffraction for the plasma carburised particles revealed a chromium spike but no cobalt, however there was an indication of molybdenum. Silicon and phosphorus were also present.

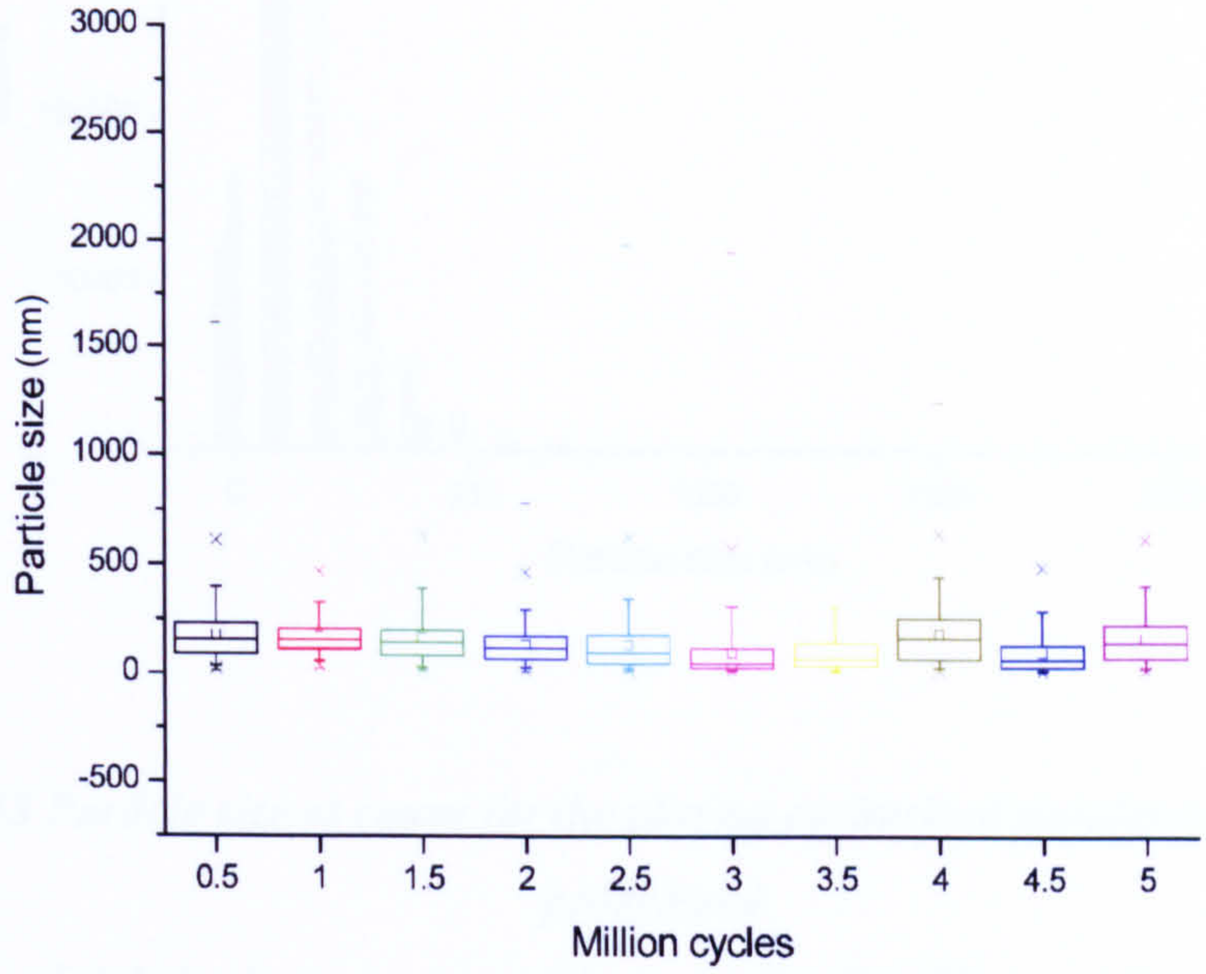

Figure 112 Size distribution of particulate debris from a plasma carburised CoCrMo hip wear simulator test over 5 million cycles

Over the 5 million cycles the particle size of the plasma carburised debris altered very little.

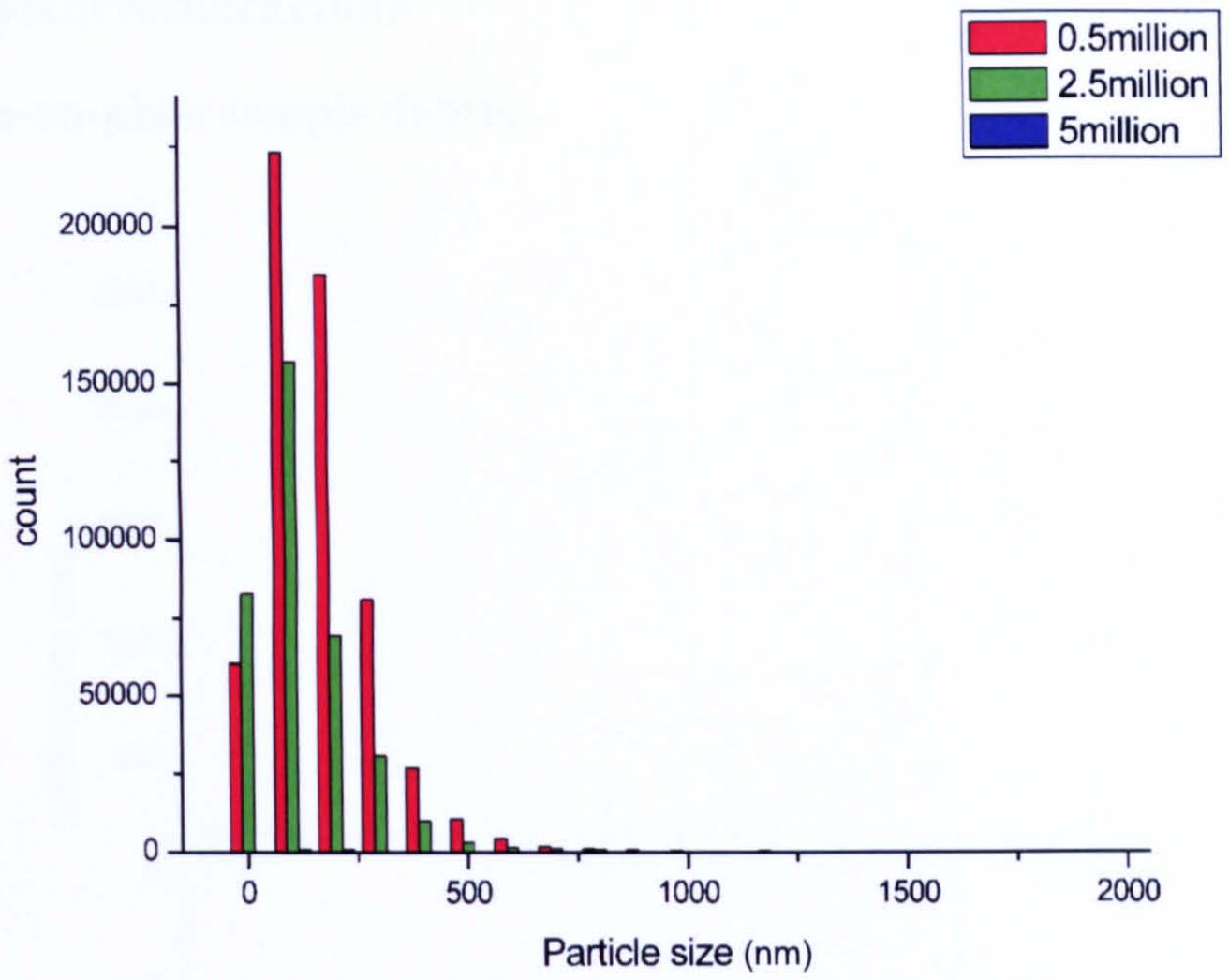

Figure 113 Particle size vs count for the plasma carburised simulator test as the test progressed

The volume of debris decreased notably over the 5 million cycles. However it was not noted that the size of the particulate debris changed over the 5 million cycle test.

5.3.3. Polyetheretherketone

5.3.3.1. Pin-on-plate sample debris

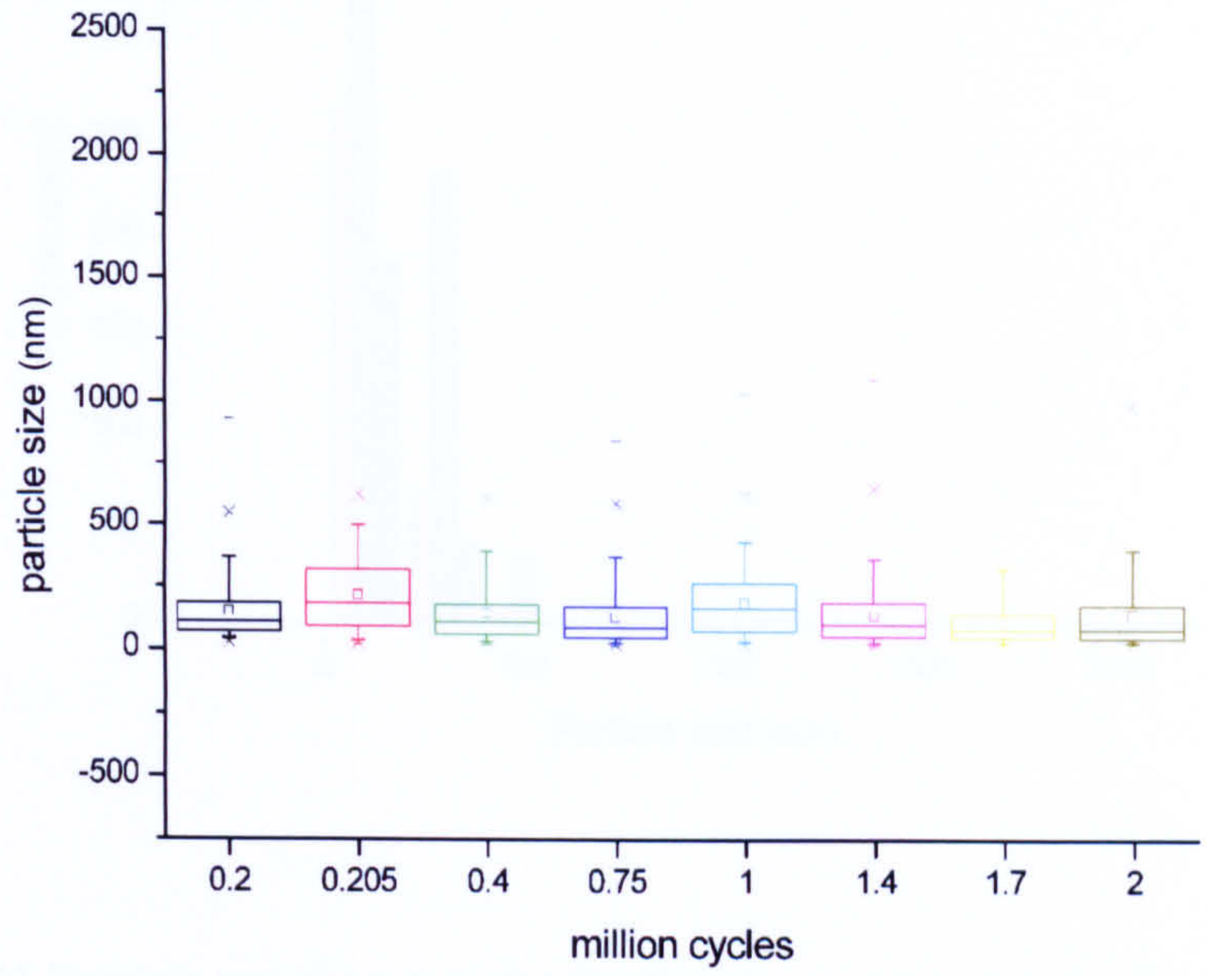

Figure 114 Particle size distribution for pin-on-plate test samples of PEEK on ceramic over a 2 million cycle test

Figure 114 shows a similar size range for all particles measured during the 2 million cycle pin-on-plate test. The test ran dry at 0.205 million cycles and it can be seen that the average particle size increased at this point but by 0.4 million the average size had lowered again.

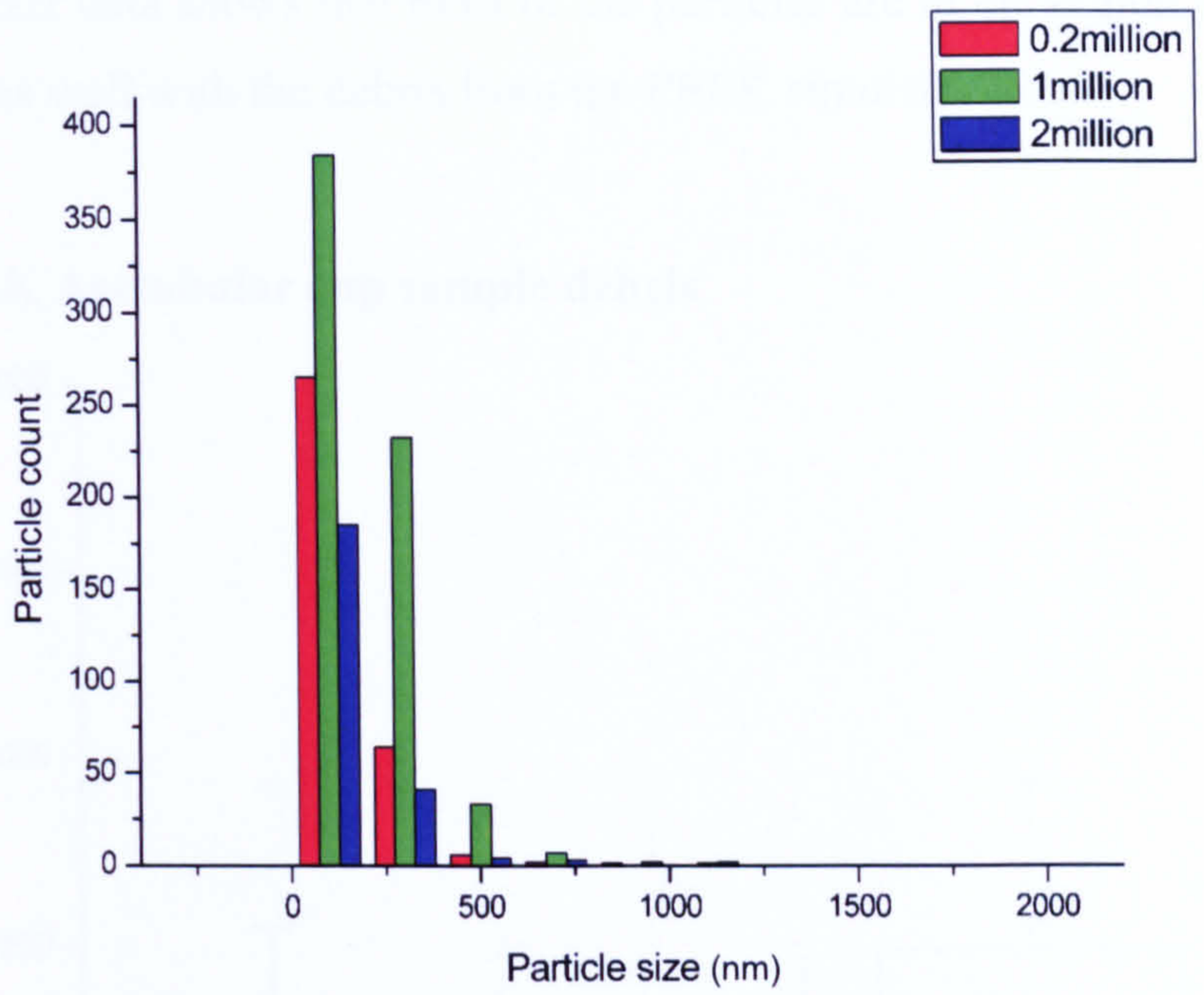

Figure 115 Particle count versus size for the pin-on-plate debris of a PEEK pin on a ceramic plate at 0.2, 1 and 2m cycles.

Figure 115 can be used to indicate volume change in the particle debris over the two million cycle pin-on-plate test. The change in volume is small over the test.

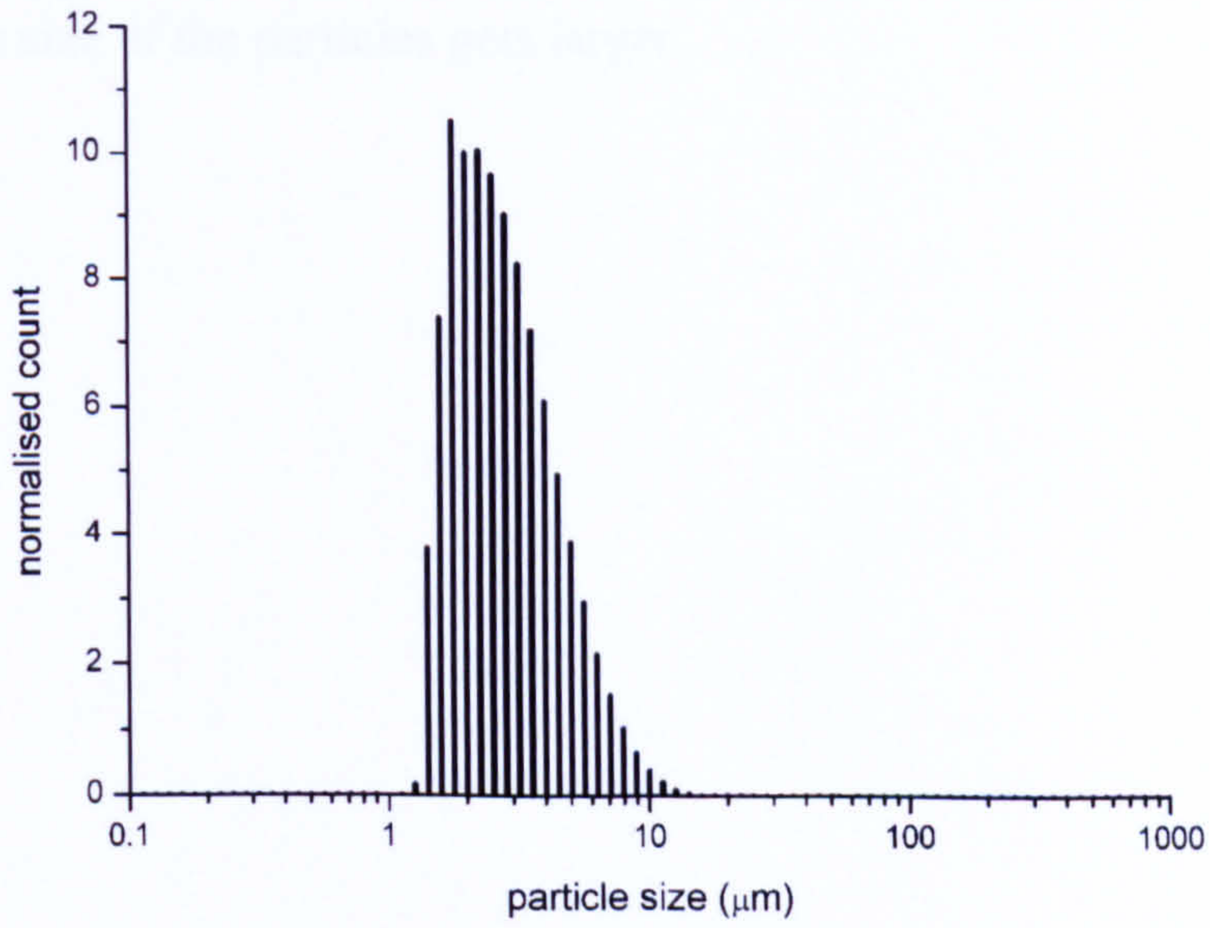

Figure 116 Mastersizer data showing the larger debris from the pin-on-plate PEEK on ceramic tests

The Mastersizer data shows that most of the particles are in the region of 2 to 5 μm. This correlates well with the debris from the PEEK simulator tests.

5.3.3.2. PEEK Acetabular cup sample debris

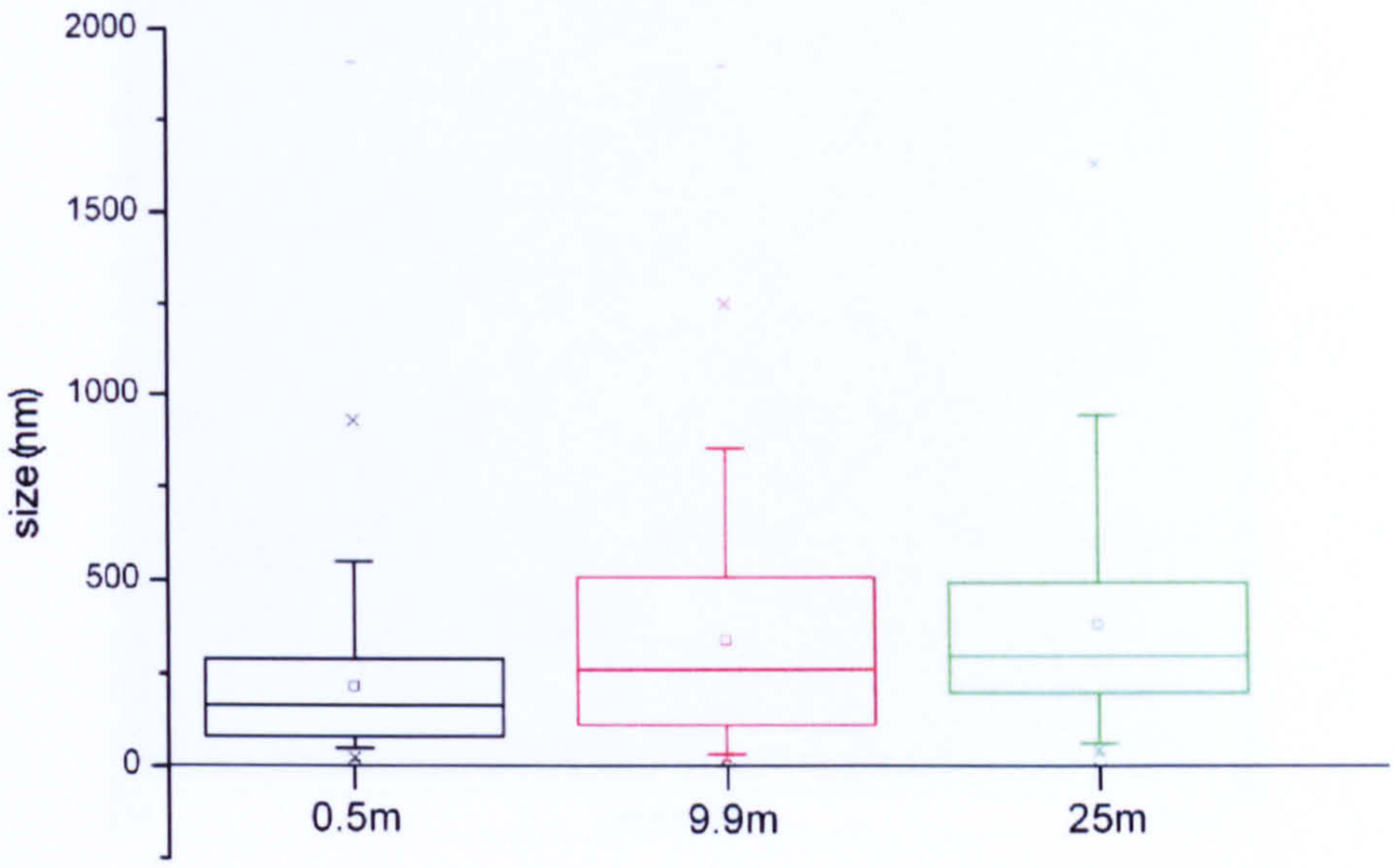

Figure 117 Particle size distribution for sample debris from PEEK acetabular cups on ceramic femoral heads.

Figure 117 shows the particle distribution of the peek debris from the simulator PEEK on ceramic 25 million cycle test. The trend appears to be that as the test progresses the size of the particles gets larger.

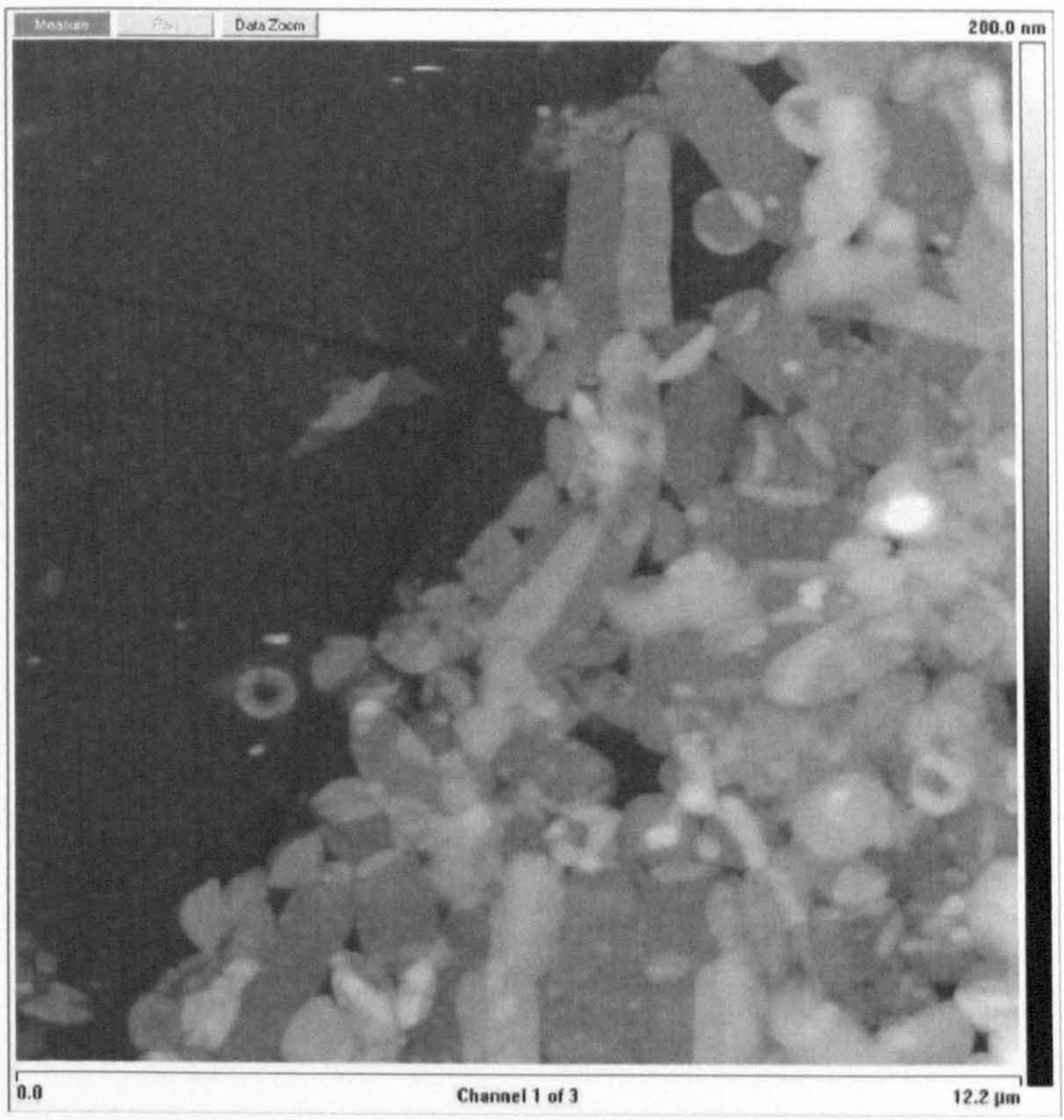

Figure 118 an afm image of PEEK particles from the PEEK on ceramic simulator test

An AFM image of the particulate debris revealed two different types of particles, tubes of material and much smaller round particles. Figure 119 revealed more detail about the smaller round particles.

Figure 119 a high magnification image of the PEEK particles from the PEEK on ceramic simulator test

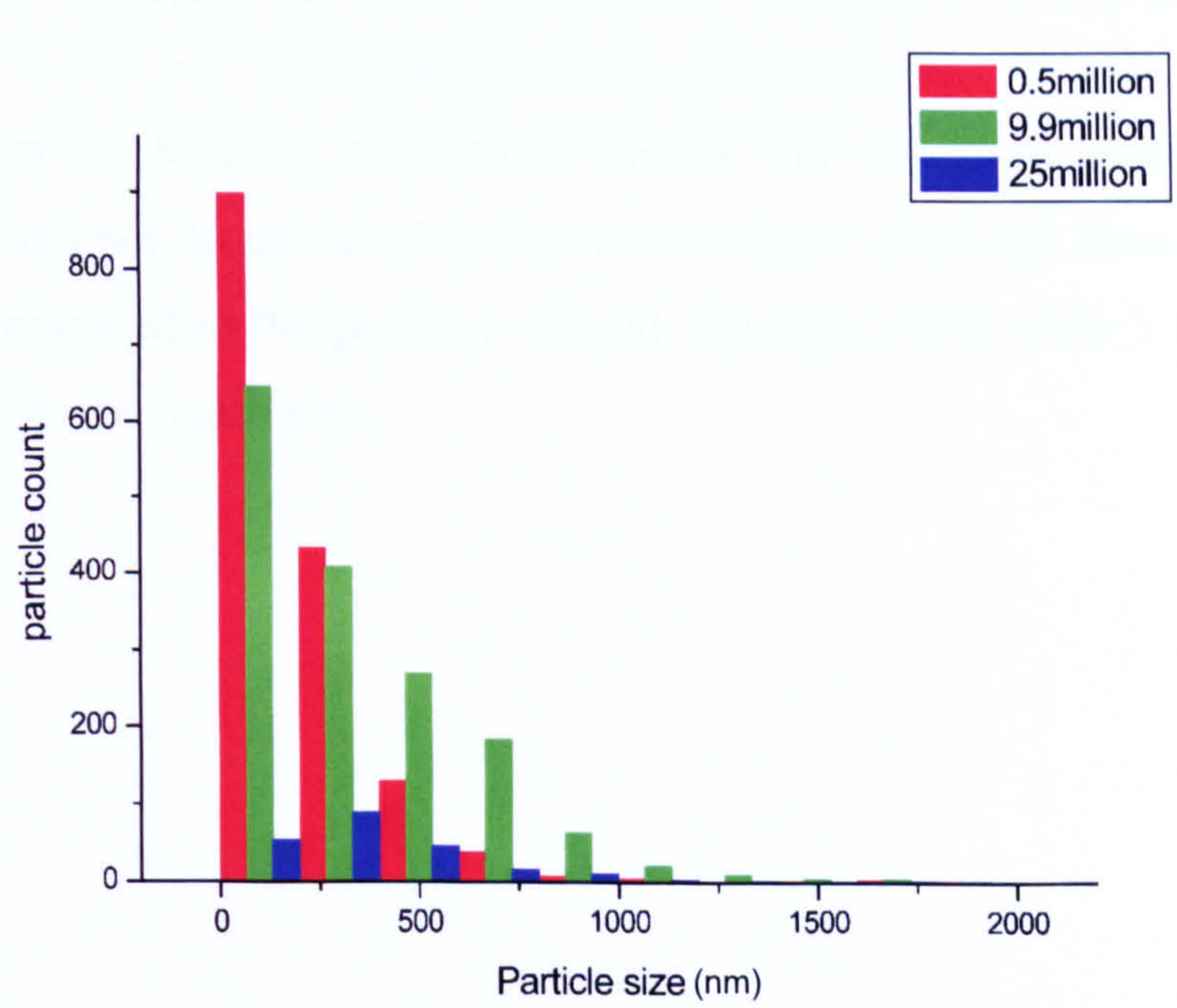

Figure 120 Particle count versus size for the particle debris from a PEEK acetabular cup against a ceramic femoral head.

Figure 120 can be used to indicate the volume change in the particle debris over the 25 million cycle test. The debris indicates that less wear debris is produced as the test

continues. It can be seen that this data corresponds to Figure 117 and shows that as the test continues to 25 million cycles the particle debris gets larger in size.

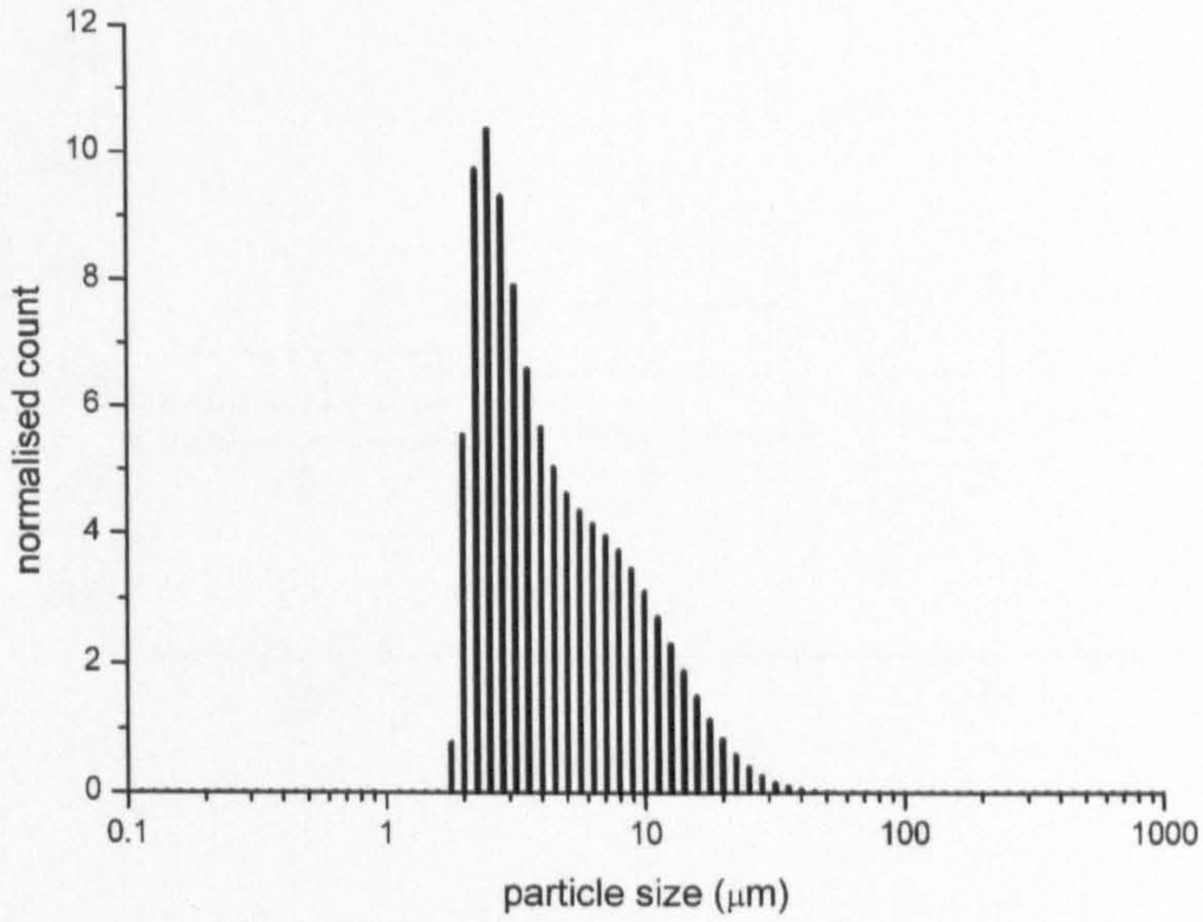

Figure 121 Mastersizer data showing the larger debris from the PEEK on ceramic simulator tests at 9.9 million cycles

The data from the Malvern Mastersizer showed that the larger particles that the NanoSight could not detect were between 2 and 10 μm. Although these data can not be directly compared to the particles viewed under the AFM were 3 to 5 microns long which is in the same range.

5.3.4. Polycarbonateurethane Knee sample debris

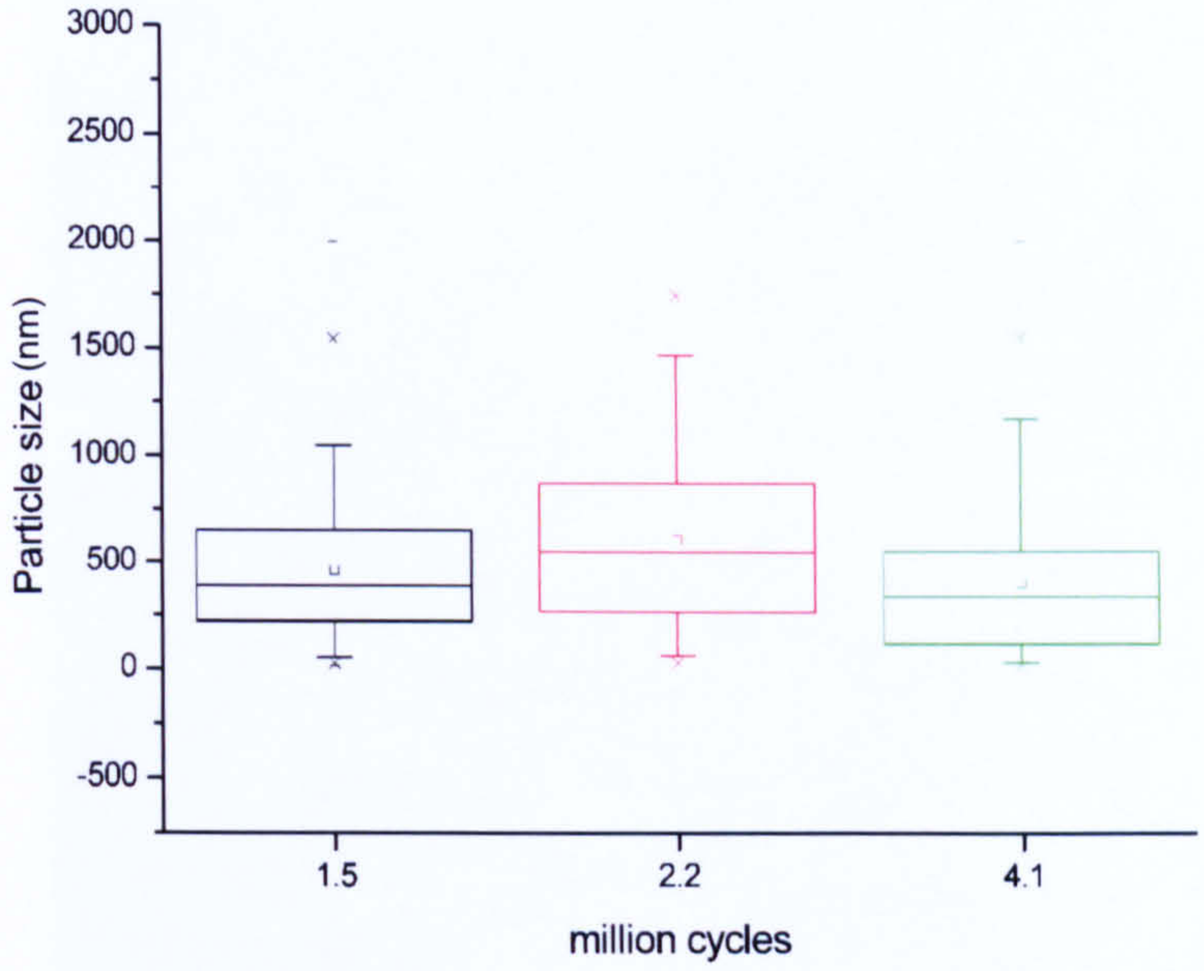

Figure 122 Particle size distribution for particle debris from a 5 million cycle Polycarbonateurthane unicondylar knee test

Figure 122 shows the size distribution of the polyurethane knee debris over the 5 million cycle test. The debris shows little size change as the test progresses.

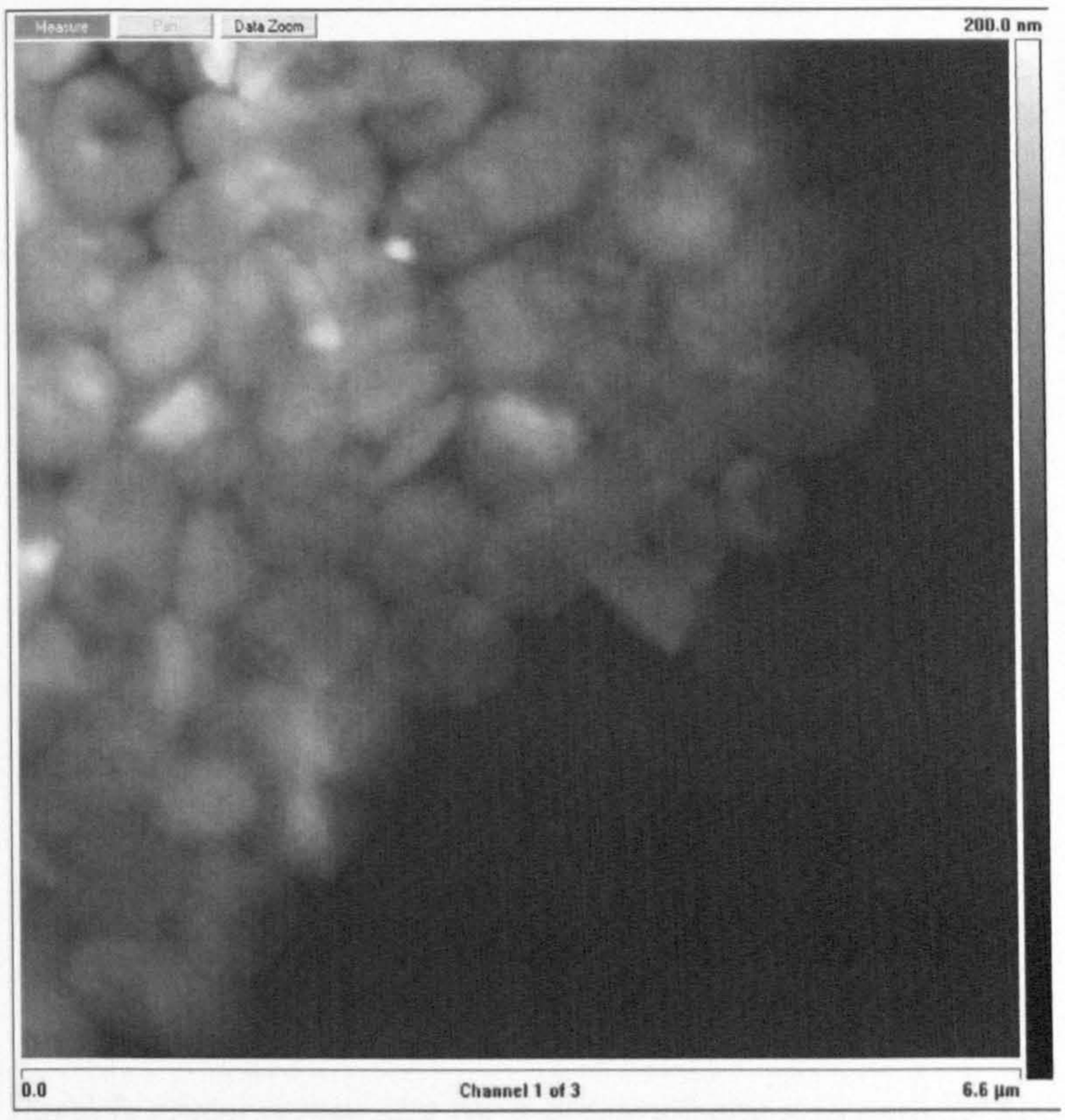

Figure 123 an AFM image of polyurethane particles from a unicondylar knee test

An AFM image shows more detail about the particles, these polyurethane particles appear as flat discs, they have agglomerated on drying.

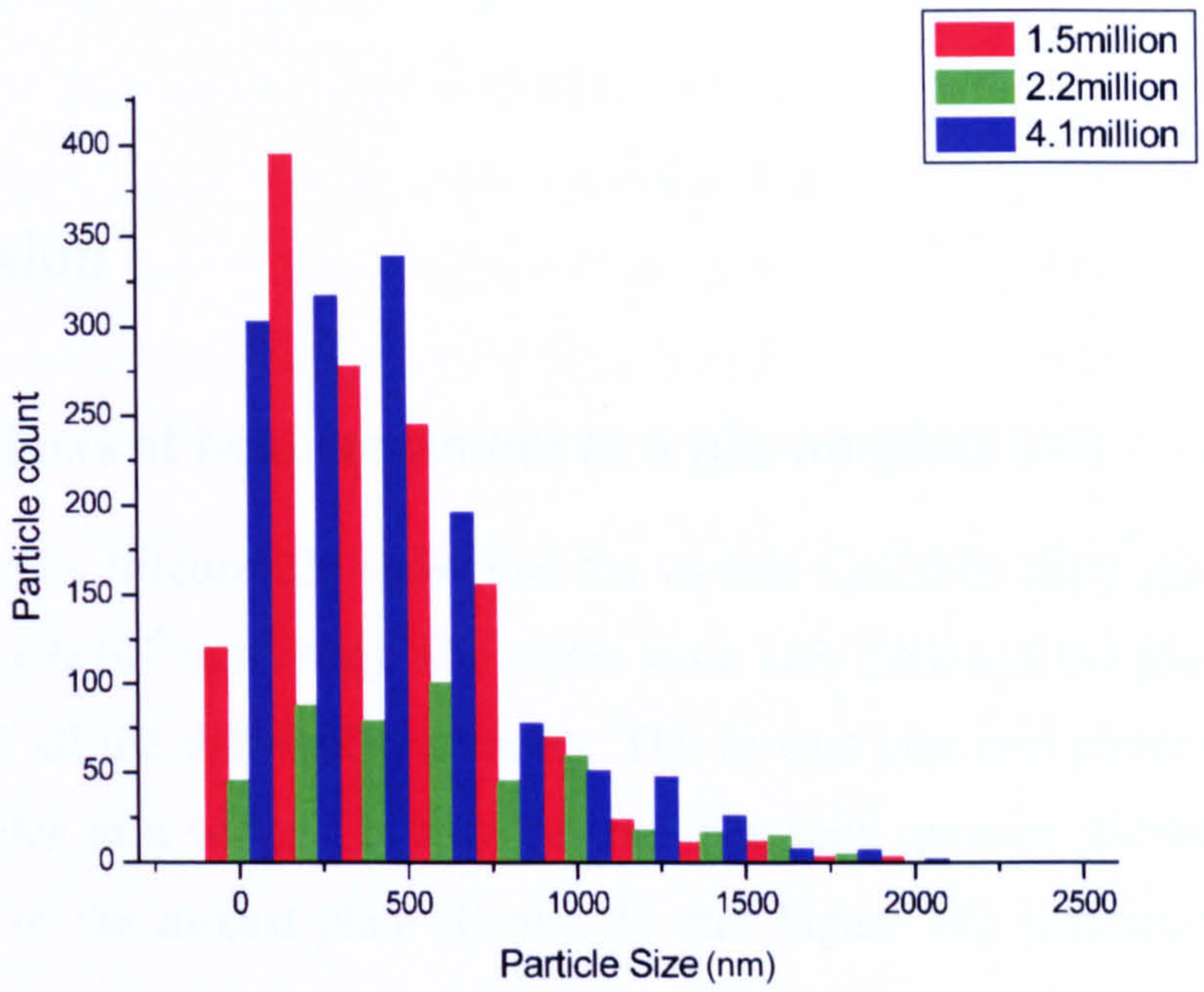

Figure 124 Particle count versus size for a polyurethane unicondylar knee during a 5 million cycle test.

Figure 124 can be used to indicate the volume change in the debris collected during the 5 million cycle polyurethane unicondylar on CoCrMo test. The results indicate that the joints underwent severe wear at 2.2 million cycles but by 4 million had returned to the same levels as at 1.5 million cycles.

6. Discussion

6.1. The effects of heat treatment in a pin-on-plate test

The wear results (Figure 23) show that the as-cast CoCrMo alloy gave the lowest total wear ($1.69x10^{-6}$ mm^3/Nm). The plates wore very little and the pins showed the least wear of all the different treatments. The as-cast pins and plates contain hard blocky carbides in a softer CoCrMo matrix. The long grooves shown in the final SEM image of the as-cast plate (Figure 33 and Figure 34) indicate that the hard carbides of the pin cut grooves into the softer matrix material on the opposing bearing surface. The large protruding carbides of the pins and plates are also evident in the surface topography images (Figure 28). These show that the softer matrix material surrounding the carbides was smeared in the direction of motion. This provides evidence of the contrasting hardness of the carbide and matrix material. Due to the differing scales of the two imaging techniques, the grooves that can be seen in the final SEM images are not apparent in the surface topography analysis (Figure 29). The results are indicative of the bearing surfaces wearing through abrasion. The small variation in wear (Figure 17) between the four as-cast specimens indicated good reproducibility of the experimental results.

The pins wore more than the plates in the as-cast test as can be seen by comparing Figure 15 and Figure 16. This may be due to the frictional heating of the pin as the bearing end is always in contact with the plate, however, the wear area of the plate is not always in contact with the pin. Varano *et al* [120] suggested that a phase change from FCC to HCP was undertaken in CoCrMo alloys caused by stress. The pin wear may be higher as the FCC surface is constantly being lost and therefore a harder HCP phase has no chance to form, where as the plate has time to form a harder HCP phase.

The single heat treated material showed similar plate wear but slightly higher pin wear compared with the as-cast specimens (Figure 19 and Figure 20). The surface

topography, after three million cycles (Figure 32) showed an increase in surface roughness and small pits thought to be due to a combination of carbide pullout and surface adhesion. Single heat treatment resulted in smaller and fewer carbides due to partial solution of the carbon into the matrix lattice. The remaining carbides cause abrasive wear seen as scratching on the apposing surface of the bearing material. The reduced size of the carbides resulted in smaller holes compared with the as-cast specimens. Decreasing the percentage of carbides on the bearing surfaces led to an increased chance of intimate contact of identical phase material. A proportion of the holes shown in the single heat treated specimen are due to adhesive wear caused by this intimate contact. This adhesive wear results in small, shallow areas of material removal in the wear area compared with large deep carbide removal and particles produced from this type of wear appeared as large flakes of material. The peak to valley distance was initially large due to a proportion of carbides being pulled out during the polishing process. However, after three million cycles a significant ($p=<0.001$) decrease was observed in 3 out of the 4 specimens due to large amounts of bulk matrix wear reducing the peak to valley distance.

Again the single heat treated plate wear was much smaller than the pin wear (Figure 19 and Figure 20). One plate gained in weight possibly due to material transfer from the pin (Figure 20). The combined pin and plate wear (Figure 21) shows a wear rate similar to the other pairs implying that the material from the pin was transferred to the plate.

The greatest amount of wear was found in the double heat treated material. The block carbides initially formed during casting were completely diffused into the matrix due to the double heat treatment. Upon inspection of the unworn surface, a very low surface roughness was found, and no carbides were visible. This structure resulted in adhesion being the primary method of wear, due to intimate contact of identical matrix material. The final SEM image of the double heat treated specimen (Figure 31 and Figure 32) showed large pits approximately 20 μm across where material may have been adhesively worn from the surface. In contrast the single heat treated material showed an average pit size in the region of 5 μm. The absence of carbides in the double heat treated structure allows large volumes of material to be

removed. The presence of carbides (as seen in as-cast and single heat treated material) interrupts the matrix structure hindering the propagation of crack growth through the material. A smaller volume of material is therefore removed from the surface on every occasion of intimate contact. The topographical image of the final double heat treated sample (Figure 26) shows an increased roughness compared with the unworn surface. The large pits shown in the SEM image (Figure 31 and Figure 32) can not be identified using this profilometer technique. Both the average roughness and the root mean square roughness of the plates indicate that the surface was significantly ($p=<0.001$) rougher after 3 million cycles, for all 4 specimens, however the pins became smoother. Self polishing of the surface does not occur due to the continuous material removal resulting in a high proportion of the surface being pitted at all times. Again the pins show more wear than the plates over the test duration.

Due to the nature of pin-on-plate testing, the lubrication regime is likely to differ from that of a prosthetic joint. Previous authors [114] show no statistical difference in wear rates between as-cast and solution annealed or HIPed materials when testing large diameter hip prostheses in joint simulators. This is likely to be because the geometry of *in vitro* hip joint simulation allows fluid film lubrication to be generated [50]. In contrast the contact of pin-on-plate machines due to the specimen geometry and testing conditions will eliminate any fluid film lubrication, therefore the effects of material properties and any possible boundary lubrication can be tested.

Varano *et al* [120] examined the effect of microstructure on the wear of cobalt based alloys. A high carbon as-cast and solution annealed specimen were among the test specimens. The unworn surfaces showed similar results to those shown in this study with larger carbides visible at the surface of the as-cast specimen and smaller, sparser carbides visible after a single annealing treatment. Using reciprocating pin-on-plate apparatus, wear results showed $0.25mm^3$/million cycles for the solution annealed and $0.05mm^3$/million cycles for the as-cast. These results show similar trends to those obtained in this study.

Bowsher *et al* [185] also compared as-cast CoCrMo joints with a double heat treated specimen using large diameter hip bearings. The double heat treated material was both HIPed and solution annealed resulting in a different material structure to the study reported here. An orbital simulator was used. Bowsher *et al* showed that the wear rates during running in, steady state and jogging were statistically similar between the as-cast and the heat treated specimens. However additional walking after the jogging cycles found as-cast wear to be statistically higher than the heat treated specimens. The wear rate of 0.25mm^3/million cycles for the double heat treated specimens agrees with both the results obtained here and those of Varano *et al.*

6.2. Simulator Tests

6.2.1. Double heat treated heads and cups

Problems to be noted

The double heat treated specimens had a number of manufacturing problems which were brought to the attention of Smith and Nephew but we were asked to continue testing in spite of the fact that there was a substantial crack in one of the stems and the grain boundaries were visible to the naked eye in all of the heat treated heads. These open boundaries and cracks were problematic due to the water ingress changing the weight of the specimens.

6.2.1.1. Wear

The wear rates of joints 4 and 5 (Figure 38) where both the head and the cup were double heat treated gave low average wear of 0.0008 mm^3/Mc (volume loss) however joint 3 (head lc5) had a large crack in the stem where water could easily have become trapped. The wear rate when allowing for the control (which was the same material combination) was -0.0005 mm^3/Mc which was calculated from a linear regression performed on the data. As discussed the results obtained from lc5 are unreliable due to a crack in the stem and therefore the results from joint 3 should be discounted. If joint 3 is not included in the data set then the new calculated value of wear rate is 0.0008 mm^3/Mc for heat treated CoCrMo on itself and

0.00065 mm^3/Mc for heat treated CoCrMo on as-cast CoCrMo, these results are not statistically different. These are extremely low wear rates. Bowsher *et al* also reported low wear rates when testing heat treated CoCrMo joints in the Queen Mary's MTS elliptical testing simulator [115, 185].

Both the control head and cup have lost weight over the course of the 5 million cycles this suggests some corrosive effects on the specimens, however this was two orders of magnitude lower than the wear observed. The loss could be fluctuation in the results as it is so small compared with the wear observed. An initial study has shown the lubricant to be pH 6 and therefore slightly acidic, which is unlikely to be a strong enough acid to affect the surface of CoCrMo alloy. Further work on the effects of the 25% bovine serum with added EDTA and sodium azide on double heat treated CoCrMo would perhaps lead to an explanation, or negative results would lead to the conclusion that the trend seen was random.

In comparison with the simple material testing carried out on the pin-on-plate machine using the identical materials, the results above have extremely low wear. This may be due to the poor quality specimens and large grain boundaries which were identified before the test. These defects may have absorbed water making the gravimetric results false. This may also be due to the initially negatively skewed smooth surfaces and shape of the prosthesis promoting fluid film lubrication in the wear simulator. If the majority of the contact is fluid film lubricated then wear will have been prevented in these cases, however *in vivo* where there is much more stopping, starting, sitting, tripping and other activities which are not accounted for in the simulator, more serious wear may occur as demonstrated in the simple material testing using pin-on-plate machines. A further study using a wear pattern including everyday walking patterns like stopping, starting, sitting and even tripping or stair climbing may reveal different results using this double heat treated material, the particle debris from the test could then be compared to *ex vivo* particle debris.

6.2.1.2. Friction

The friction results Figure 43, Figure 44 and Figure 45 show a Stribeck plot indicating boundary lubrication at 0 cycles, the friction factor falls over the 5 million

cycles, but the shape of the graph stays constant. This is supported by the wear results where there is very little running in evident.

Vassiliou *et al* showed the friction results of the as-cast material on the same simulator with the same size joints [50]. If the results that were obtained during the double heat treated test are compared with this as-cast high carbon test of the same diameter joint, using the same Durham wear and friction simulators, it can be seen that by 3 million cycles the as-cast joints had reached 0.015 friction factor at $1.0x10^{-8}$ Sommerfeld number which has not been reached by 5 million cycles in the double heat treated test. The lowest friction factor by 5 million cycles was 0.02 friction factor at $1.5x10^{-8}$ Sommerfeld number. This indicated that the as-cast 50 mm joints ran in and provided more effective lubrication by 3 million cycles than the double heat treated joints did by 5 million cycles. This contradicts the wear results which show a lower wear for the double heat treated than for the as-cast, however the erratic weight gain and loss from the double heat treated joints indicate that water may have been gained and lost into and out of the large grain boundaries formed by the heat treatment.

6.2.1.3. Surface topography

The surface roughness analysis showed little significance. The skewnesses of the as-cast joints were positive at the start indicating that carbides were protruding from the surface, by 3 million cycles the skewnesses of the as-cast heads were the most negative indicating that some shallow blocks of carbide may have been pulled out of the surface.

When compared with the results previously obtained on the same simulator at Durham University (Figure 125) the gravimetric results show that as-cast 50 mm joints wore more than these double heat treated 50 mm results. The linear measurements previously conducted by Finsbury for the as-cast specimens, Figure 126, also show higher linear wear than the measurements taken by Smith and Nephew during this test.

Joint no.	Cup	Head	Diameter (mm)		Diametral clearance (μm)
			Cup	Head	
1	10	8	49.947	49.711	236
2	9	6	49.963	49.762	201
3	13	5	49.949	49.731	218
4	12	7	49.959	49.742	217
5	11	10	49.965	49.789	176
6 (Control)	7	9	50.011	49.810	201

Table 17 clearances of previous as-cast 50 mm test [50]

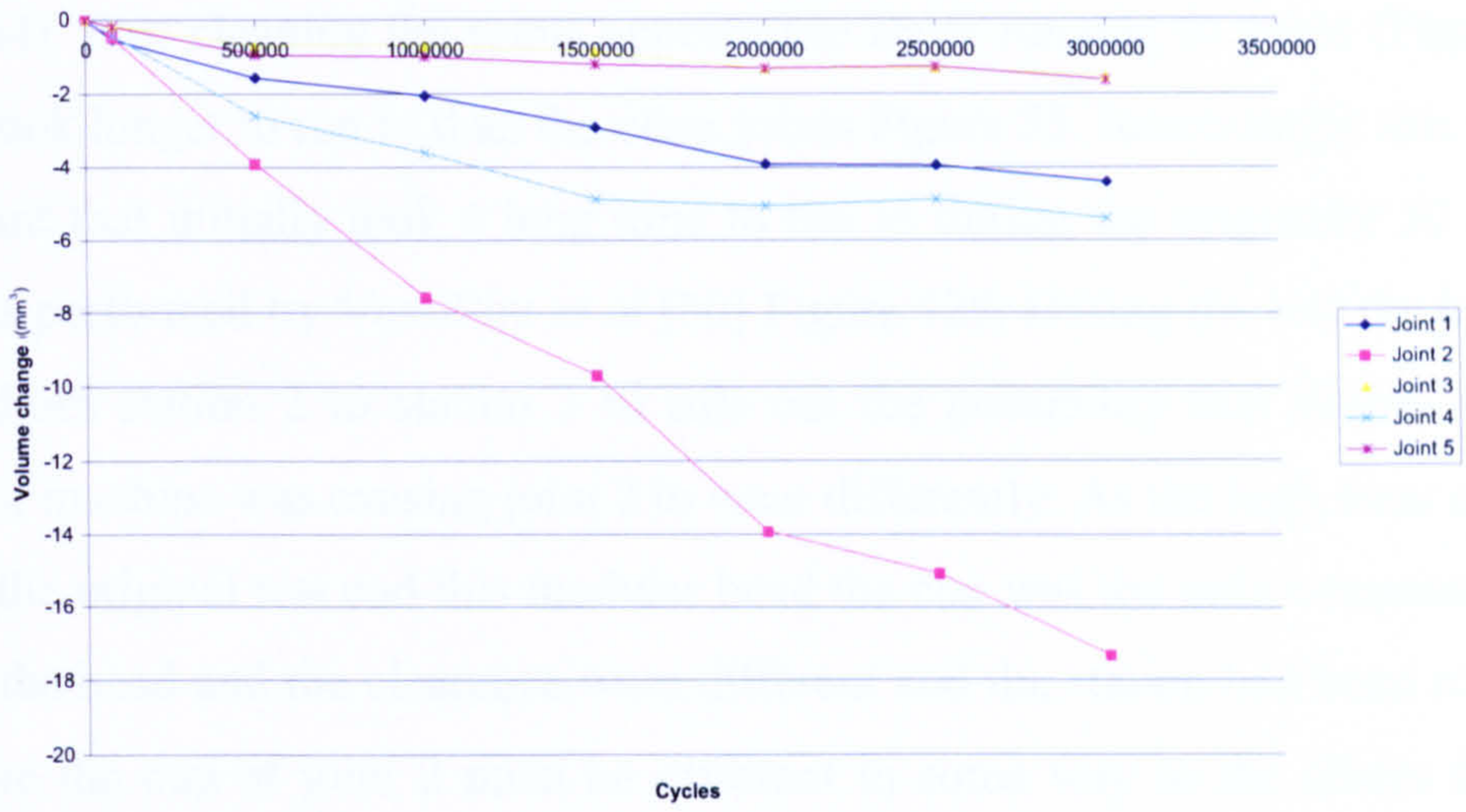

Figure 125 Previous test results using a 50 mm diameter as-cast joint [50]

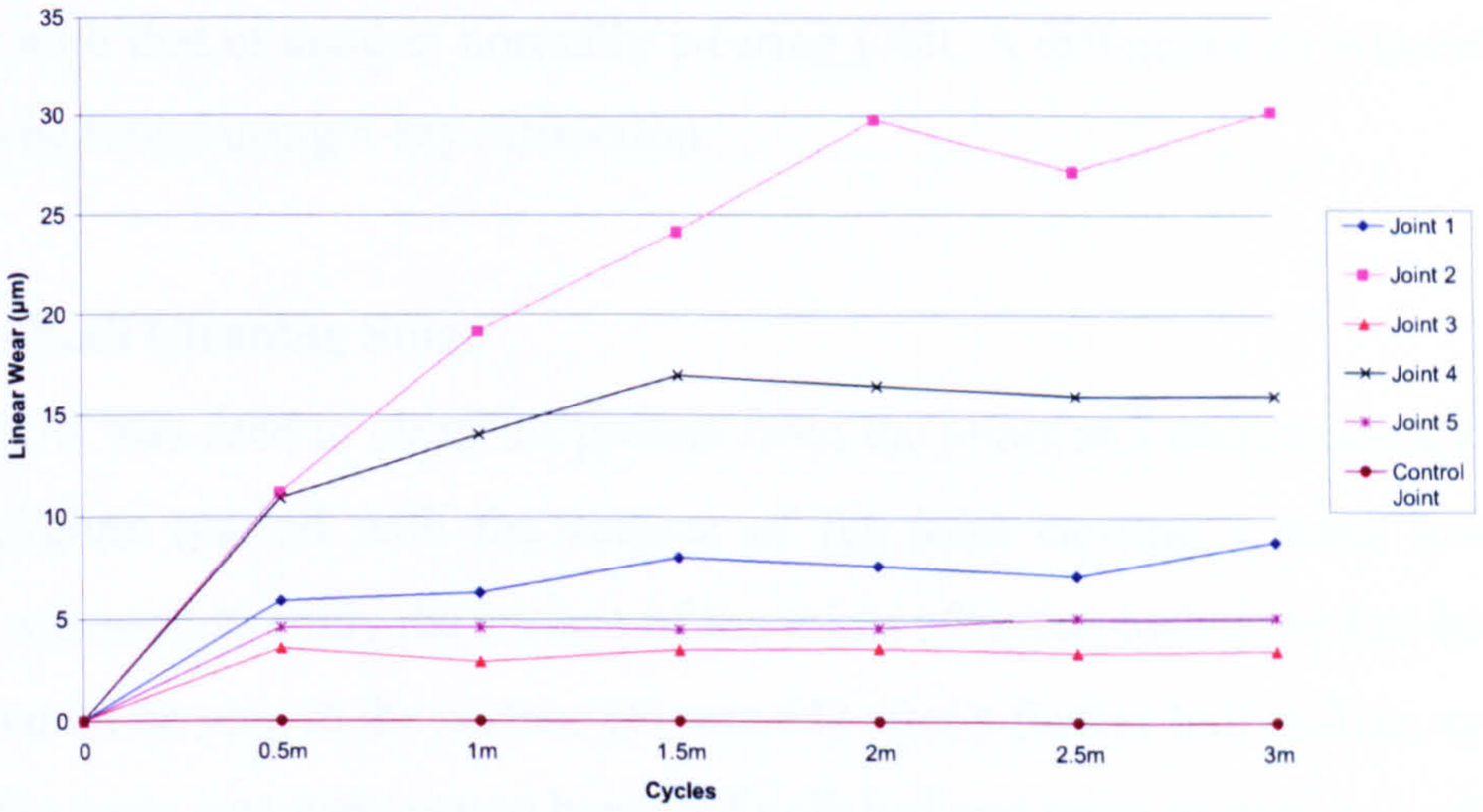

Figure 126 Linear results conducted by Finsbury orthopaedics on the 50 mm as-cast test [50]

6.2.2. New as-cast Modular heads on Pre-worn cups

This test was undertaken to ascertain if a new modular head could replace an existing damaged or worn component within the body without having to replace the acetabular cup if it is well positioned and well fixed.

6.2.2.1. Wear

The results were seen to show a running in period over one million cycles and a steady state wear rate from one to three million cycles. At the three million cycle point a different method was used to clean the protein from the joints. This method damaged the surface of the joints whilst cleaning the protein off (Figure 63 and Figure 64). Post cleaning the joints appeared to show running in again (Figure 65). Joint 2 took longer to run in than the other joints Figure 55. Interestingly this was the same joint that initially took a long time to run in during the originally 50 mm as-cast tests performed by Vassiliou *et al* [50] Figure 125. During the test the joint was moved from station 2 to station 3 to rule out the possibility that station 2 of the simulator machine was causing joint 2 to wear differently. As the high wear occurred in both the original test and this modular head the cup was the only common feature as both the head and the clearance were different and the station had been ruled out. Therefore the cup of joint 2 must be different in some way to the others from the batch. This must cause running in to last longer for this particular joint. An interesting further study would be to section the cup and compare the internal structure with that of another normally wearing joint. A difference in material phase may also be found using x-ray diffraction.

6.2.2.2. Alkali Cleaning Stage

Strong KOH was used to clean the protein from the joints at 3 million cycles and the strong alkaline reacted with the surface of the joint causing a mass loss. SEM analysis was used to study the surface of the joints after this technique had been used and pits could be seen in the surface (Figure 64) after a further half million cycles the edge of the wear area was seen to have self polished and more protein had adhered to the surface, however the non contacting bearing surface was still pitted (Figure 64,Figure 65 and Figure 66). This technique was not used again.

6.2.2.3. Friction

Overall the wear rate of a new head on an old cup showed less wear over 5 million cycles than a new head on a new cup. The friction indicated mixed lubrication, the friction factor fell from 0.14 to 0.04 over the 5 million cycle test but mixed lubrication persisted.

6.2.2.4. Surface analysis

Figure 57 shows the pre-worn cups are smooth having been polished by the 5 million cycle test previously completed. Figure 58 shows the new as-cast heads start off with large protruding carbides on the surface. At 3 million cycles (Figure 59 and Figure 60) the pre-worn cups are similar to the topographical analysis at the initiation of the test. The head appears much smoother, the large protruding carbides have gone. There is very little change between 3 and 5 million cycles (Figure 61 and Figure 62) indicating that the surfaces have worn in by 3 million cycles. This is corroborated by the wear results which show a rapid wearing in followed by a steady state phase (Figure 54).

6.2.3. 38mm As-Cast Simulator wear tests

6.2.3.1. Wear

Initial average wear rate was 2.36 mm^3/million cycles. This reduced substantially towards the end of the test as is expected due to the phenomenon of "running in". This is commonly seen in metal-on-metal joints [23, 116, 186]. The compromised joints (Joints 1 and 4) did not show improvement in wear rate over the course of the test.

In the 50 mm BHR wear test conducted previously Vassiliou *et al* [50], an average "running in" wear rate of 1.83 mm^3/million cycles was seen. This is lower than that seen in this test. Reiker *et al* [187] found similar linear running in wear on the 38 mm and 50 mm joints. Bowsher *et al* [178] found running in wear did not correlate with joint diameter (with 40 mm diameter showing lowest wear).

The average steady state wear on the 50 mm joints over 1 to 2 million cycles was 1.06 mm^3/million cycles. This is higher than the corresponding wear seen in this

study (0.60 mm^3/million cycles). Over the 2-3 million cycle interval the wear rates for Joints 3 and 5 are similar, but slightly higher than the 50 mm average wear rate. Bowsher *et al* [178] demonstrated that for normal walking, larger diameter joints show lower steady state wear rates, although there is not a large variation in steady state wear rates between the different diameters. Overall wear rates are similar to those seen by the 50 mm joints tested previously.

Joint 2 showed a comparable wear factor to that of joints 3 and 5 when analysed between 1 and 2 million cycles. After joint 2 dislocated, a small increase in volume loss was observed. For the first half million cycles after the dislocation there was a volume loss of 2.15 mm^3, the joint then showed good recovery losing only 0.78 mm^3 in the next half million cycles. Further testing would be necessary to determine whether a steady state wear rate similar to that before the dislocation could be attained i.e. 0.42 mm^3 per half million cycles. This contrasts with Joint 1 which after initial dislocation did not recover. However, Joint 1 had multiple dislocations.

These results are in agreement with theoretical considerations. Where a larger (50 mm) diameter joint has been used the surface will have travelled faster than that of the 38 mm joint causing a thicker fluid film to have been developed. Fluid film lubrication will prevent asperities touching and therefore little wear will be accumulated. With the smaller diameter joint (38 mm) a thinner fluid film will be generated, as the surface will move more slowly, however there will be less wear due to the shorter sliding distance of the smaller diameter head.

6.2.3.2. Friction

Initially all joints operate in mixed lubrication. Joints 2 and 3 continued to show similar frictional behaviour after one million cycles. Joint 5 shows an improvement in lubrication condition with a larger decrease in friction factor with higher viscosities than initially. Joints 1 and 4 both showed an increase in friction factor over the entire range of viscosities. Joint 4 had run dry during the second half million cycles, and this may have adversely affected the surface. Joint 1 dislocated when the rig was stopped and the head crashed into the rim of the cup. The friction

factor was not as low as the pre-wear test levels. Joint 1 was not friction tested at the end of the test.

The initial friction factors for the 38 mm joints were higher than those seen for the 50 mm joint of the same type tested in an earlier test (Vassiliou *et al* [50]). However, just as in the 50 mm test, an improvement in lubrication was seen in this study as wear testing progressed. Joint 5 from this study behaved in a very similar fashion to the friction tested joint in the 50 mm study, even down to similar friction factor values. Joints 2 and 3 also showed an improvement in lubrication regime, although slightly later than seen on 38 mm Joint 5 and 50 mm Joint 1. These joints are clearly "running-in" as had been noted in the 50 mm study, and as is confirmed by the reduction in the wear rate over the course of the test.

6.2.3.3. Surface analysis

Figure 76 to Figure 80 show that both the 38 mm diameter and the 50 mm diameter joints made of the same as-cast material are worn away in similar fashions. The initial images show block carbides protruding from the surface. The images taken after 1 million cycles differ slightly as the 38 mm diameter joints show some remaining carbide structures where as the 50 mm joints show a rough surface. The final images at 3 million cycles again show a similar pattern, no carbides can easily be identified and the surface appears less rough than the 1 million images in both diameter joints.

As with the 50 mm diameter joints test [50], the surface roughness of the cups continued to decrease from initiation of the test to 1 million and then 3 million cycles. The 38 mm diameter cups showed the majority of the change in roughness, only two heads significantly increased at 3 million cycles.

6.3. Particle Debris

6.3.1. Pin-on-plate Wear Debris

As-cast, single heat treated and double heat treated pin and plate sample debris was analysed using the NanoSight LM10. Initial samples Figure 82 at 0.25 million cycles revealed that the double heat treated material showed the least wear and that as-cast showed the highest wear. However when double checking the results using a TEM and EDXA the reason for this small amount of debris was explained. The debris from the double heat treated samples had been created by mainly adhesive wear and this had produced large flakes of material often larger than 2 microns in diameter Figure 87. The limit of the LM10 for sizing particles is 2 microns as after this threshold the particles tend to sink within the chamber and can not be analysed. It was also noted that some of the single heat treated particles were also large on the TEM images Figure 90, this indicated that the severe wear causing the large particle debris in the double heat treated specimens was happening to a lesser extent in the single heat treated specimens as well. However, none of the as-cast particles were large Figure 85. This explained the discrepancy in the data from the gravimetric results and the particulate results. The majority of the mass of the debris had been in the large particles which could not be identified by the LM10. The SEM images of the surfaces confirmed that the primary form of wear was adhesive and that the wear had caused large pieces of the plate to be pulled from the surface. Catelas *et al* [23, 24] analysed particulate metal debris using an enzymatic protocol and found the particles to be round to oval in shape the average size found was below 100 nm and the analysis technique involved using a TEM to image the particles which had been set in epoxy resin and sectioned. Tipper *et al* [27] and Firkins *et al* [177] both looked at the metal particles from metal-on-metal articulations using a filtration method and an SEM technique. To the authors knowledge there has been no mass identification technique such as has been conducted in this work published up to this date (2008).

The particle analysis from 1.5 million cycles shows that the as-cast particulate debris has stayed constant in volume and size whereas the double heat treated particulate debris appeared to create more debris, this does not agree with the gravimetric results as the wear rate for the double heat treated pin-on-plate specimen was linear. The result can be partially explained by the larger flakes of material found using the

TEM. There may be more, smaller particles at 1.5 million cycles due to the surface roughness of the plate, as the test progressed the adhesive wear tore pieces of the highly polished surface from the specimen, this manner of wear leaves a rougher surface. A rougher surface results in less surface area being in intimate contact, therefore fewer large particles can be pulled from the surface and more smaller particles are created, these particles can be identified in the NanoSight LM10.

The final particle debris analysis took place at 2.5 million cycles and both the single and double heat treated debris showed large volumes of particles in the smaller size ranges 40-100 nm. The as-cast debris stayed constant from the 0.25 million cycle debris analysis with a maximum count at 150 particles. It should also be noted that while the particles for the double heat treated CoCrMo alloy and single heat treated CoCrMo alloy have become smaller in size the as-cast particles have stayed constant. The results indicate that the single and double heat treated materials alter how they perform according to their surface roughness' while the as-cast material will wear consistently, both in the amount and type of particles produced, even during large roughness variation of the surface. This may be due to the primary type of wear that takes place for the materials. Initially the highly polished double and single heat treated specimens come into intimate contact over large flat areas and therefore large flakes of material are detached from the homogenous materials. This form of wear makes the surfaces rougher and therefore the next time that specific part of the specimen comes into contact the areas which are in intimate contact are smaller and therefore smaller particles are produced from this wear. The as-cast specimen has large block carbides which prevent large amounts of material adhering to the apposing surface. This encourages the wear to be mainly abrasive, the hard block carbides create grooves in the apposing surface and smaller debris is produced. This type of wear is not affected substantially by the roughness of the surfaces and therefore a much more consistent particle distribution is created from this type of wear. To the authors knowledge no study of particulate debris from differently annealed cast CoCrMo alloy has taken place before this study.

The TEM analysis (Figure 101) showed that the particles were round to needle shaped, this agreed with Catelas *et al* [23] who found 50% round, 37% oval and 13%

needle shaped. From the as-cast debris the particles are shown in the TEM images to be slightly smaller than the NanoSight results. The NanoSight gives a sphere equivalent diameter whereas the TEM can only show a 2 dimensional image, this means that the results are not directly comparable. The depth of the particles are not known from the TEM image and the edges of the particles may have been thin enough to not produce an image from TEM analysis. While it is possible to get an idea of relative thickness from the depth of colour of the image an exact depth is not possible. The EDX analysis indicates that the particles that were seen in the TEM images were made from the CoCrMo specimens. A large chromium peek and a smaller cobalt peek can be identified. The copper, carbon and oxygen peaks can be attributed to the particle surroundings. A silicon, phosphor and sulphur peak can be identified in most of the EDX analysis from the particles analysed, these may be remnants of the phosphate buffered saline used in the washing protocol, the silicon may have come from the manufacturing process as it can be identified in all particulate debris. In some cases a calcium peek can be identified, this comes from the bovine serum lubricant that the tests were lubricated with, EDTA was used to retard calcium phosphate formation of the surface of the specimens.

The double heat treated particles appear to have two different types of particle, large flake like material generally 2 microns in diameter and above Figure 93 and small particles which agglomerate under the TEM analysis conditions. These are much smaller generally less than 100 nm. If these data are compared with the NanoSight data, again the two measurement techniques can not be directly compared, however the NanoSight does show a large peek at 40 nm (Figure 97) which coincides with the size of the smaller particles which can be seen in the TEM image Figure 94. UHMWPE particles of a larger size have previously been analysed using a Malvern Mastersizer Elfick *et al* [188], however these smaller particles were too small to be identified using this technique.

The single heat treated specimen shows smaller flakes of material around 0.5 microns in diameter Figure 90, these were rare and the majority of material seen under the TEM conditions are around 100 nm Figure 91.

6.3.2. Double Heat Treated Simulator Wear Particles

The particles in Figure 93 show that at low magnification both small and large particles can be seen. A large flake of around one micron diameter can be identified, however also there are agglomerations of smaller particles Tipper *et al* [27] also found agglomerates of small particles when analysing a dried sample on an electron microscope. Figure 94 shows a higher magnification image of the small particles. It is hard to identify individual particles from the agglomeration. The particle data from the NanoSight indicated that the particles are on average 120 nm initially, by 2.5 million cycles the average size has increased to 220 nm and after this peak the average fell to 50 nm. From Figure 96 it is evident that not only the average particle size but also the distribution of the range of particle size gets smaller over the 5 million cycles. As the test progressed the surfaces became rougher, scratches appeared which may have been caused by 3 body wear of the roughened surfaces, however there was no change in wear rates over the 5 million cycles. The surfaces may have had protein adhering to them causing the gravimetric results to be anomalous. Also large grain boundaries and cracks may have had water absorbed to them making the gravimetric measurements false. Over the course of the test the particles from the serum decreased in number indicating that less wear was occurring, however this was not corroborated by the wear rates, however, Bowsher *et al* [115] also found low wear rates of heat treated large diameter joints. The friction factor of the joints became lower over the course of the test. The size of the particles increases to a peak at 1.5 million cycles and then starts to decrease, large flake like particles could be identified using the TEM, however, they were beyond the limits of the NanoSight LM10 instrument. The change in the particle size may be explained by an initially bimodal distribution. The larger flakes can not be identified, so initially the particles look small, once the surface has become rougher due to the adhesive action of the wear the large flakes are no longer created, smaller flakes may be created in the place of the larger flakes as smaller particles, these particles could be identified by the NanoSight and therefore increase the modal average size. Once this has started to occur, smaller and smaller particles will be created as the intimate contact of the surface becomes smaller and smaller due to the increasingly rougher surfaces.

The EDX analysis revealed that there was iron in the particles and calcium phosphate which may have been deposited on the surface of the head and cup during wear simulator testing. Silicon is apparent this may be partially from the silicon gaiter which contains the joint and lubricant while testing, however, it was also seen in the pin-on-plate tests, this indicated that the metal is contaminated during a common process e.g. manufacturing process. Nickel and sulphur can also be identified in the spectrum the nickel may be from the CoCrMo which contains 0.36% nickel and the sulphur may be from the sodium doedcyle sulphate (SDS) in which the particles were washed during a cleaning step of the protein cleavage protocol. Alternatively sulphur has a very similar EDX peak to Mo and could have been mistaken for the Mo peak. The large chromium peak indicated that the particles are made of the CoCrMo material, however, it would appear that the cobalt has leached out of the particles during the protein cleavage. This was also noted by Catelas *et al* [24] when using a similar double enzymatic protocol.

The Mastersizer data of the double heat treated particle debris indicated that there were larger particles of around 1 to 10 microns, this coincides with the size of the flake like particles seen under the TEM, however, a direct comparison can not be made as the TEM shows a 2 dimensional image and the Mastersizer gives a sphere equivalent diameter.

6.3.3. As-cast Modular heads (Particles)

Modular heads showed a low average particle size for the first half million cycles. The particle size and standard deviation then became larger until 3 million cycles. At three million cycles, when the KOH was used to clean the protein off the joints, the particle size jumped to its highest average over the whole 5 million cycles. After this, the average and standard deviation of the particles decreased until 5 million cycles. This could be due to the cups already having a highly polished wear area, only the heads have to be self polished, this would produce less wear and fewer particles. Once self polishing has begun mixed lubrication causes a consistent particle count.

The volume of particle debris that was imaged by the NanoSight gradually decreased over the 5 million cycles. This indicated that as the test went on the lubrication

generated became closer and closer to full fluid film lubrication. The friction results indicate that full fluid film lubrication was not reached in the 5 million cycles, however, the friction factor did decrease over the period.

After the joints were cleaned with potassium hydroxide the surfaces were roughened by the corrosion causing more wear to occur as can be seen in the wear results and at this point larger particles were detected. As the test continued and the potassium hydroxide was no longer used self polishing continued leading to a smoother wear area and therefore fewer and fewer particles and smaller and smaller sized particulate debris.

6.3.4. 38 mm As-cast Simulator Test Particle Debris

The particles from the 38 mm as-cast simulator test showed an average size of 200 nm. The range of particle size was consistent from 0 to 1 micron over the 3 million cycles. The volume of the particles fell slightly over the three million cycles, however, the modal average remained the same throughout. The TEM analysis indicated a range of particles from round to needle shaped and in the size range indicated by the NanoSight results. Catelas *et al* [23] also reported a range of particle shapes from round to needle shaped, which may be due to 3 body wear. Some of the particles became trapped between the bearing surfaces either rolling or sliding along causing scratching and changing the third body's shape. The particles appear to be smaller from the TEM analysis but they have agglomerated so it is difficult to identify individual particles. The TEM only looks at a cross section of the particles where as the NanoSight uses Brownian motion to detect the mass of the particle and therefore its volume and gives an equivalent sphere diameter, these two methods can not be directly compared. Another important point is that the TEM may not recognise the thinner edges of the particles if they are very thin they may blend into the background making the particle appear smaller.

The EDX analysis indicated that the particles are made from the CoCrMo with a calcium phosphate deposit and some silicon. The cobalt has not been completely leeched in these as-cast particles and a small cobalt peek can be seen.

From Figure 67 there is no identifiable running in phase and this agrees with the particle debris. There is no step change in volume in the particle debris. The volume decreases slowly over the 3 million cycles. This also agrees with the friction results since the joint continues to operate in mixed lubrication through out the test.

The particle, wear and friction data all indicate that the 38 mm prostheses do not perform as well as the 50 mm components. This agrees with the theory as the entraining velocity of a smaller joint will be lower and therefore fluid film lubrication is less likely to occur.

6.3.5. 50 mm As-cast Simulator Test Particle Debris

The particle debris from the 50 mm as-cast wear test reported previously by Vassiliou *et al* [50] was digested and analysed. The data indicated that the particles were on average 100 nm. The volume of the wear particles in the case of this joint do not make a step change until 3 million cycles and if this is compared with Vassiliou's results there is an obvious step change in the wear rate at 3 million cycles. The friction of joint 1 was analysed by Vassiliou *et al* and shows that a change from boundary to fluid film lubrication takes place over the 5 million cycles, this will account for the step change in particle debris as, if the surfaces are touching less and less regularly fewer and fewer particles will be created. The image from the TEM showed particles that vary in size from 10 to 200 nm. This is also evident using the NanoSight data. The EDX analysis confirmed that these particles were made from the CoCrMo material, as well as showing calcium phosphate deposition.

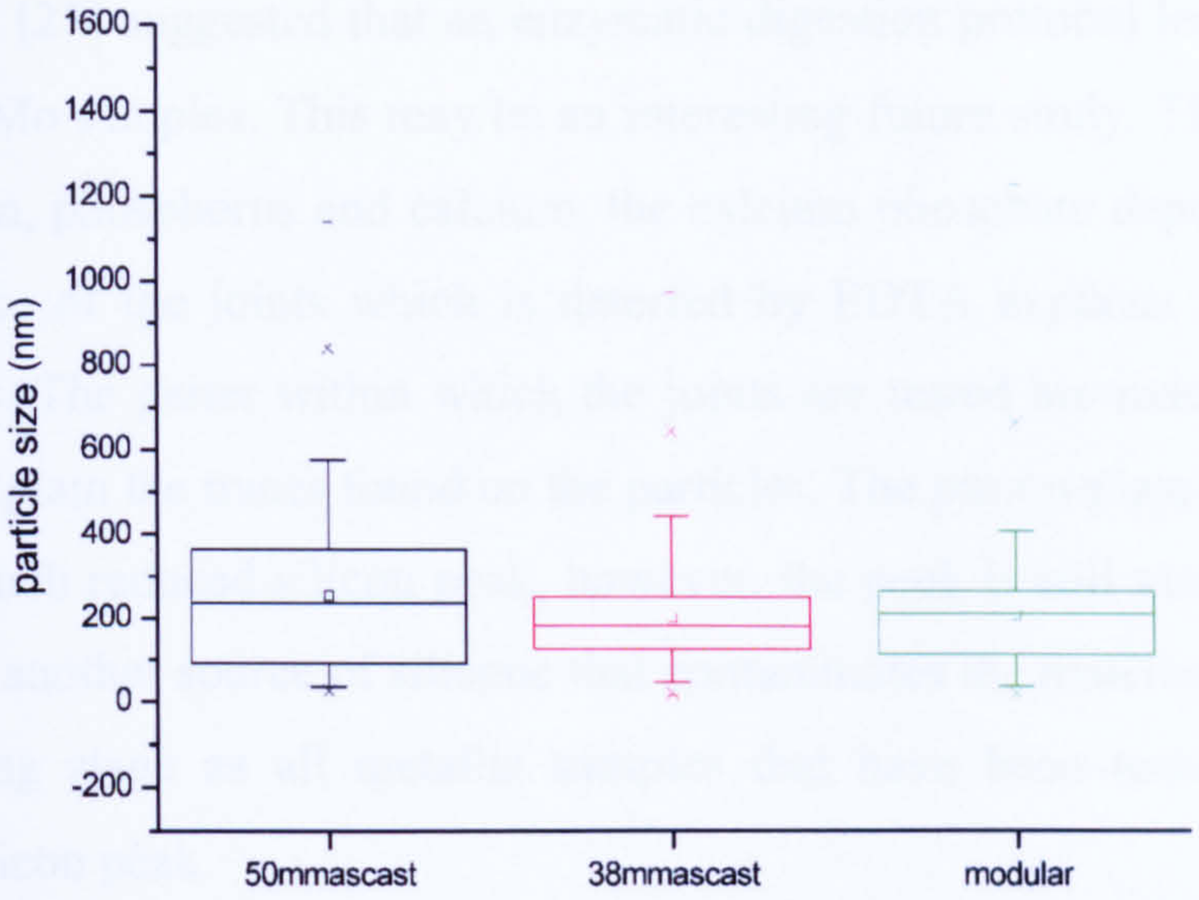

Figure 127 Comparison between the as-cast particle debris at 0.5 million cycles

The particles from the as-cast 50 mm, 38 mm and modular components were very similar. From the EDX analysis they all showed a similar elemental analysis indicating that they were made from the same material. From the TEM analysis the particles looked of similar size and from the NanoSight analysis the distribution of particle size was similar. This indicated that it is not the specific design of the heads that determined the particle size but the material and its treatment prior to testing or implantation. Further evidence to support this theory is the particle debris size from the as-cast pin-on-plate specimens. Although much more wear occurred and therefore there was a lot more debris, the size of the debris coincided with that of the 38 and 50 as-cast prostheses. All the debris ranged from 10 to 200 nm in size, and all the debris from the prostheses show a decrease in both the average and the standard deviation of the particle size over the duration of the testing.

6.3.6. Plasma Carburised Simulator Test Particle Debris

Vassiliou conducted simulator tests in 2004 which tested plasma carburised heads against as-cast cups. The lubricant was saved and stored at -20°C until it could be analysed for the size of the particle debris. Plasma carburised particles consisted of large flakes of material as with the double heat treated material and smaller particles which looked round under the TEM. The EDX analysis showed a large chromium

peak and a small molybdenum peek but the cobalt peak had completely disappeared. Catelas *et al* [23] suggested that an enzymatic digestion protocol leached cobalt out of the CoCrMo samples. This may be an interesting future study. The spectrum also shows silicon, phosphorus and calcium, the calcium phosphate deposit that attaches to the surface of the joints which is deterred by EDTA explains the calcium and phosphorous. The gaiter within which the joints are tested are made from silicone, this could explain the traces found on the particles. The pin-on-plate particle analysis showed a much reduced silicon peak, however, the peek is still visible. There must therefore be another source of silicone that contaminates the material, possibly in the manufacturing stage as all metallic samples that have been tested in this series showed a silicon peak.

The plasma carburisation technique disseminated carbon less than one micron into the surface of the prosthesis. This layer was harder than the substrate material, the difference in properties of the materials may have caused delamination of the harder carburised layer causing larger flake like particles to be produced. Smaller particles may have been broken off the carbides on the surface of the non carburised component causing the bimodal particle distribution seen.

If the wear behaviour (Report for S&N BHR 04/2 September 2005) is compared with the particle size and distribution, the change in wear rate is easily identifiable as a change in slope on the wear graph and corresponds to the 4 million cycle point, where from figure 103 it can be seen that the average size of the particles show a step increase following a downward trend and the size distribution of the particles at this point is increased. This may have been the point at which the thin layer of carburised material was worn away exposing the subsurface layer to contact with the apposing bearing surface. As this subsurface layer was predominantly as-cast these particles seen at 4 million cycles should coincide with the particles seen from the 50 mm as-cast test. If the particles from the 4 million cycles of the plasma carburised test are compared with the particles from the 0.5 million cycles of the 50 mm as-cast test the distribution is similar Figure 128. The volume of particles is vastly different, however, the very small particles which were also present in the heat treated particle results can be seen along side larger particles. These larger particles show a peak just

larger than the modal average for the as-cast particle debris. It is possible that this peak is from the substrate as-cast material articulating against the untreated as-cast cups.

Both the double heat treated and the plasma carburised specimens have produced large flake like particles along side very small particles. These larger particles are fragile as they are very thin and therefore if they are trapped in between the bearing surfaces they may be torn apart producing the very small particles also seen in these situations.

Cell lines have been introduced to different sized particles in other work [169, 171] and indicate that smaller particle produces a greater biological reaction. However, this work does not take account of the full immune response especially with metals where ions can be leeched out and carried away to different parts of the body. Particle debris from periprosthetic tissue from these patients would be an interesting further study.

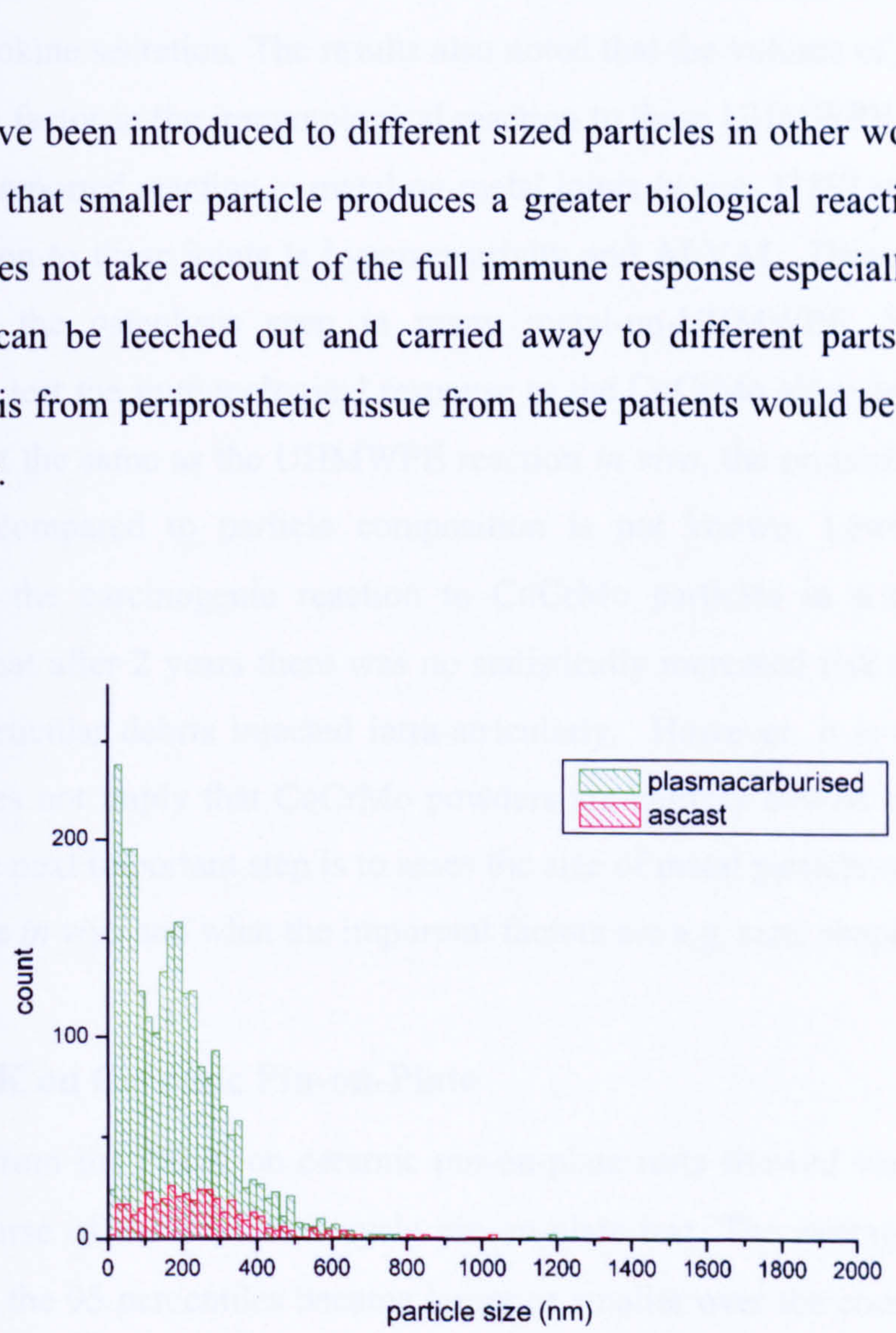

Figure 128 Plasma carburised component debris from a hip wear simulator at 4 million cycles compared with an as-cast 50 mm component debris from a hip wear simulator at 0.5 million cycles.

Firkins *et al* [26] analysed clinically relevant particulate debris from 28 mm Cobalt chrome prostheses tested in the Leeds Mk 1 physiological simulator from high and low carbon content alloys. The method used was 12 M KOH at 60°C for 48 hours. Given how strong an alkali 12 M KOH is there may have been some corrosion of the metal particles. The results showed small particle of diameter 25-35 nm measured on a TEM and an SEM. This is smaller than was found in this study.

Matthews *et al* [169, 171] studied the response to UHMWPE debris of varying sizes. *The results indicated that particles smaller the 7.6 microns resulted in enhanced levels of cytokine secretion. The results also noted that the volume of the debris was* an important factor in the immunological reaction to these UHMWPE particles. Few papers have reported reaction to metal-on-metal joints *in vivo*, [189] and the majority of the reaction to these joints is hypersensitivity and ALVAL. These responses are different to the osteolysis seen in many metal-on-UHMWPE. It is therefore important to test the immunological response to the CoCrMo alloy particles, as it is evidently not the same as the UHMWPE reaction *in vivo*, the proportion of reaction to volume compared to particle composition is not known. Lewis *et al* [190] investigated the carcinogenic reaction to CoCrMo particles in a rat model and concluded that after 2 years there was no statistically increased risk of cancer from CoCrMo particular debris injected intra-atricularly. However, it is noted that this outcome does not imply that CoCrMo powders are entirely devoid of carcinogenic activity. The next important step is to asses the size of metal particle which cause the most damage *in vivo* and what the important factors are e.g. size, shape or volume.

6.3.7. PEEK on Ceramic Pin-on-Plate

The debris from the PEEK on ceramic pin-on-plate tests showed very little change over the course of the 2 million cycle pin-on-plate test. The average stayed fairly constant but the 95 percentiles became larger or smaller over the course Figure 117. The particle debris data was compared with the wear rates over the course of the test [191].

The wear rates [191] were linear. The particle debris reported was from the biolox forte against CFR-PEEK pan two million cycle pin-on-plate wear test. The wear

graph shows linear wear for both pin and plate of all 4 active test samples up to 2 million cycles. The particle size changed very little over the course of the wear test. The volume also changed a small amount over the 2 million cycles and the variation shown could be due to natural variation in particle debris from one quarter of a million cycle to the next.

As this was a pin-on-plate test the lubrication was boundary and did not change over the course of the test. The particle debris and the wear rates corroborate this. No change in the wear rate or particle debris volume or size was detected over the 2 million cycle test. The Mastersizer data confirmed that large particles were being produced as well as small ones.

6.3.8. PEEK on ceramic acetabular cups

The particle size for the acetabular cups made from PEEK articulating against ceramic heads increased over the 25 million cycle test. The AFM images indicate that there is a bimodal distribution of particles, some very small particles are shown on the AFM as white specks, the long thin tubes are much larger and may be to do with the carbon fibres. There is no evidence that these tubes have carbon in them but they may have done so. Figure 120 corresponds to Figure 117 and corroborates that the average size of the wear particles from the PEEK acetabular cups shows an increasing trend over the 25 million cycle test. The wear rate can be seen in [8] , the wear was linear. Over time the smaller particles that were identified using the NanoSight technique become fewer, which therefore means that larger particles must be created as the total volume of the wear was the same. This would also explain the increase in the particle size distribution over time. The Mastersizer data shows a peak at 3 microns. This correlates well with not only the AFM images taken but also the pin-on-plate debris from the PEEK on ceramic pin-on-plate tests.

The AFM was used to identify the particles in this instance as the particles can charge in an electron microscope, this means that if a TEM is to be used a coating of gold or another metal would have to be used which may impair the resolution of the particle debris. Using an AFM meant that EDXA could not be used to identify the composition of the particles

Howling *et al* [192] studied the particle debris from a pin-on-plate CFR-PEEK against ceramic using a 6 M KOH protocol and resin embedded TEM analysis. This method only allowed around 100 particles to be imaged at a time. An image of the particles is shown , however no size distribution is mentioned. These CFR-PEEK particles were cultured with U937 monocytic cells, cell viability tests were undertaken after with different particle volume to cell number ratio's. The results showed these wear particle had no cytotoxic effects indicating that these particles may not cause adverse tissue reactions such as necrosis. However, no *in vivo* results have been reported, as yet, and therefore it is unknown whether osteolysis will occur in the medium term.

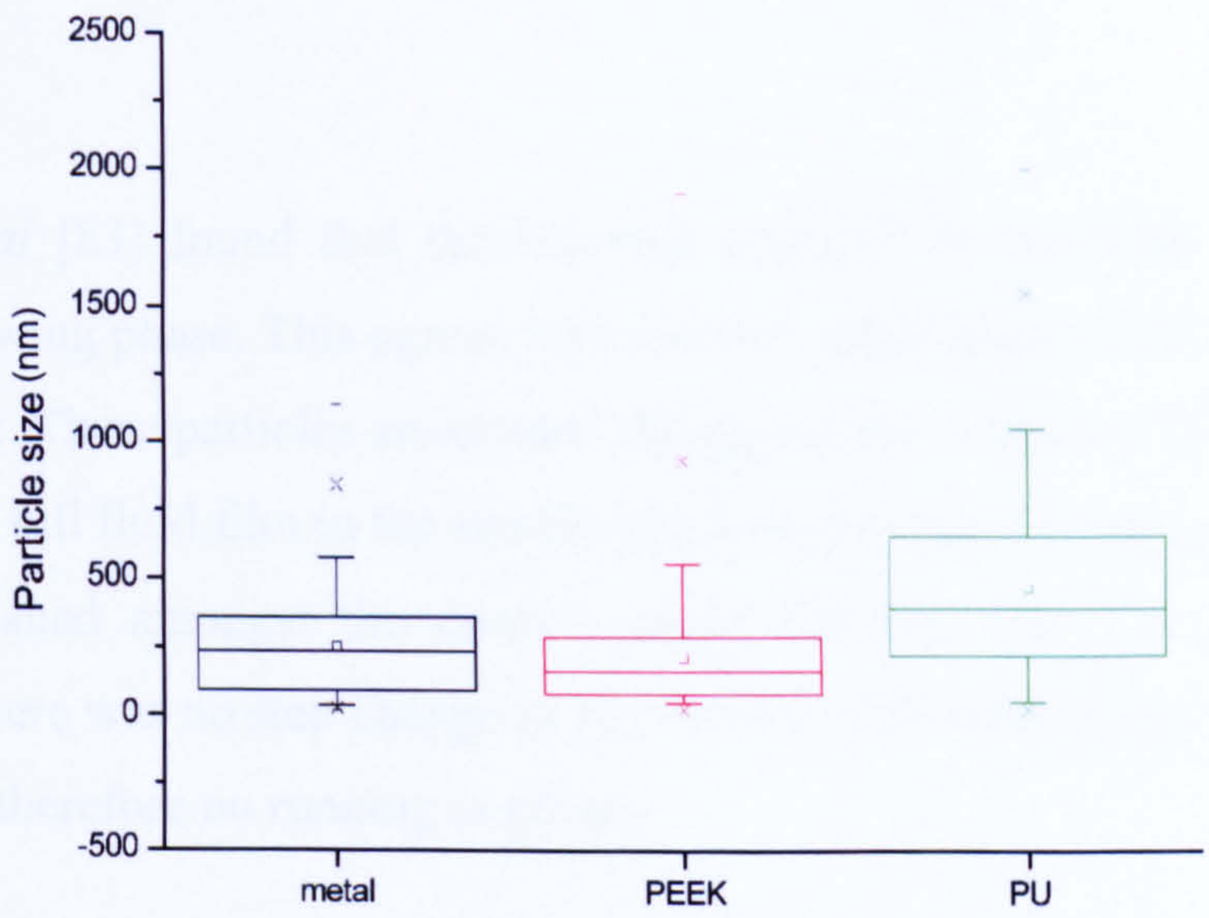

Figure 129 Comparison between the different materials of particulate debris at 0.5 million cycles

The comparison between the material types shows that the polyurethane has the largest particles, however many of the PEEK particles were not detected by the NanoSight method and are therefore not represented on this graph. The metal particles are the smallest particles as the PEEK particles showed a bimodal distribution of which, only the smallest particles are shown above..

6.3.9. Polyurethane on cobalt chrome unicondylar knee

The debris from the polyurethane knee experiment showed very little change in particle size over the 4 million cycles of test duration. The 95th percentile and modal average of all the particles altered very little over the duration. These data can be compared with the wear data [83] which shows small changes in volume over the 5 million cycle test. The particle count is very low and the 2.2 million cycle particle debris coincides with a small downward trend in the wear graph. The AFM image corroborates the particle NanoSight data that the particles are on average 100 nm Figure 123. However, these two methods can not be directly compared as one gives the sphere equivalent diameter and the other a cross sectional diameter. From the AFM the particles appear to be small flat disks of about equal size. The tiny amount of wear and number of particles indicate that the polyurethane is a good bearing surface.

Scholes *et al* [83] found that the bearings operated in full fluid film lubrication during the swing phase. This agrees with the very small number of particles found in the lubricant. These particles are created during the few occasions that the joint is not operating in full fluid film in the simulator e.g. at start up. No running in phase could be distinguished amongst the erratic weight changes, this was mirrored by the particles. There was no step change in the volume of the particles at any point during the test and therefore no running in phase.

Kahn *et al* [81] tested the biocompatibility of the polycarbonate urethane used in this test. Corethane 80A proved to be biostable, however, the effects of the particles *in vivo* are not yet fully known. Further work on the effect of particles isolated in this work on human cells would be of great interest.

7. Conclusion

The pin-on-plate tests of identical material differently heat treated revealed a great deal about the wear process for each of the differently heat treated materials. These tests were specifically performed on a pin-on-plate apparatus in order to separate the effects of the material wear from the effects of lubrication. The results therefore showed the worst case scenario.

The as-cast specimens withstood the wear the best. The surface topography images indicated that the primary form of wear was abrasive indicted by the grooves running in the direction of the motion along the wear path. These grooves were created by the harder carbides ploughing through the softer matrix material.

The double heat treatment caused the carbides fully to disperse into the matrix material. This created the opportunity for the surfaces to be finished more smoothly. Whilst in a prosthetic head and cup simulation a small roughness would be a positive step towards fluid film lubrication, in a pin-on-plate test where only boundary lubrication can be achieved a smoother surface has no advantage and in this case actually caused large flakes of material to be created by adhesion. These flakes of material were large as there were no carbides in the matrix structure to interrupt the formation and propagation of a crack.

The single heat treated material showed a mixture of adhesive and abrasive wear the diminished carbides from the heat treatment cause abrasive wearing but also stop crack progression limiting the size of the wear particles caused by the adhesive wear.

When as-cast joints were tested in a wear simulator the results indicated an initial period of wearing in for around 1 million cycles where the wear rate was higher (1-3 mm^3/ million cycles) subsequently a period of lower wear occurred (0.006-0.4 mm^3/million cycles). The friction results indicated that initially the wear was mixed lubrication, moving towards fluid film lubrication in most cases as the test progressed. These two results indicate that an initial period where the surface is rougher corresponding with more wear and mixed lubrication is succeeded by a

period where the surface is smoother the wear is less and the lubrication is more likely to be fluid film. It is thought that self polishing brings about this change.

The double heat treated prostheses when worn in the hip simulator showed very little wear, the dispersion of the carbide into the matrix material enabled a smoother finish to be gained and therefore a smaller depth of lubricant would have been needed to create fluid film lubrication. As these are 50 mm joints a higher entraining velocity was created enabling the fluid film lubrication to be created at the initiation of the test. The wear graph showed little evidence of wearing in and the friction graph, although the friction factor reduced over the 5 million cycles, did not change shape and even at the beginning of the test indicated that fluid film lubrication may have been achieved. However this is unlikely when the values of friction factor are examined. The specimens tested appeared to have large grain boundaries and cracks on the reverse of the bearing surface which may have allowed water absorption, making the gravimetric results inaccurate.

An existing enzymatic digestion technique was altered and a new particle analysing technique was developed to analyse the particle debris from pin-on-plate and simulator wear tests. The as-cast particles from the pin-on-plate test were between 40 to 200 nm and needle to round in shape. These were very similar to the particles from both the 38 and 50 mm as-cast simulator wear debris although the volume of debris from the different testing methods were different as would be expected given the different lubrication regimes. This also coincided with the results of Catelas [23]. This indicated that a pin-on-plate test is a good approximation to the wear simulation of a full hip joint, but a pin-on-plate test creates more wear as the lubrication is always boundary. The as-cast particles from the pin-on-plate debris were consistent over the 2.5 million cycle test indicating that the form of wear developed from as-cast against itself is stable over time if mixed or fluid film lubrication is not developed.

The particles from the double heat treated pin-on-plate debris appeared to be very small using the NanoSight technique, when the technique was verified using a transmission electron microscope, very large particles as well as agglomerations of

the smaller particles could be identified. These particles were so big that they were beyond the limits of the NanoSight. These larger flake like particles corroborate the theory that the heat treatment disperses the carbides and allows crack propagation through the material causing large adhesively worn areas. There are no carbides to prevent the crack growth through the material. When these particles from the pin-on-plate tests are compared with those from the simulator tests, similarities are seen. Again there are two types of particle, smaller particles and larger flake like particles, although there are fewer particles created in the simulator test. This indicates that although fluid film lubrication is occurring in many instances during this test when it does not occur the wear mechanism seen in the pin-on-plate test is taking place and large amounts of wear could occur if a fluid film was unable to form. Again these similar particles indicate that a pin-on-plate test is a valid comparison to simulator tests when the lubrication is ignored.

Simulator tests took place for 50 mm as-cast old (pre worn to 5 million cycles) cups on new heads and 38 mm as-cast Birmingham Hip Resurfacing components. These can also be compared to previous work on the same Durham hip wear simulator on 50 mm as-cast Birmingham Hip Resurfacing prostheses. All three sets of joints followed the same trend showing a large wear rate for the first million cycles whilst the joints ran in. The next 2 to 4 million cycles show lower wear rates, the modular heads showed a change in wear rate once they had been cleaned of protein with potassium hydroxide. The friction results indicate a trend towards fluid film lubrication over the test, however unlike Vassiliou [50] there was no definite fluid film lubrication evident by the end of the tests.

The initial trial of cleaning the protein from the components during the old cups on new heads test revealed that potassium hydroxide corrodes the surface of the cobalt chrome molybdenum component whilst cleaning the protein off it. The result is a pitted surface that causes the component to have to re-self polish during a small running in phase. The component is also left with pitting corrosion over the main body of the component where contact has not occurred.

The particles from the 38 mm 50 mm and modular tests were compared and reveal that the particle size from all these as-cast components were similar the 50 mm as-cast and the 38 mm as-cast were around 200 nm modal average and the modular heads started off smaller at around 100 nm and increased after the potassium hydroxide had damaged the surface. The modal average sizes of these particles, with the exception of the 3 million cycle modular heads particles, were consistent over the course of the tests. If the particle size is compared to the heat treated data, it can be seen that the modal average of the heat treated particles decreases from 2.5 million cycles as does the spread of the particle size data. This indicated that there is a change in wear pattern at this point, the as-cast components show no evidence this.

In both the pin-on-plate testing and the simulator testing the heat treated debris created large flake like particles. These larger particles were thin and appeared to be fragile. These particles come from the intimate contact of the smooth surfaces to the uninterrupted homogenous surface of the heat treated materials. The fragile particles may be broken up easily within the joint space creating many small particles to be created.

PEEK particles that have been analysed showed larger debris as the test continued. This was evident in the 25 million cycle test. The ceramic on PEEK pin-on-plate studies showed a consistent wear rate over the 2 million cycles, and the particles corroborated this, however, this is such a small percentage of 25 million cycles that it would be difficult to identify the same upward trend. The PU particles were flat oval disks and the particles appeared a consistent size over the course of the 4 million cycle test.

- Pin-on-plate tests indicated that heat treatment had a detrimental effect on wear rate

- The particles produces in the pin-on-plate tests were found to be larger for heat treated samples than as-cast materials. This was found to be due to a dominance of adhesive wear over abrasive wear in heat treated materials.

- Simulator tests demonstrated low wear rates for both as-cast and heat treated hip joints. The material processing of the heat treated simulator joints resulted in a structure which had large grain boundaries. It has been proposed that these boundaries allow the absorption of water during testing leading to unreliable analysis of wear from gravimetric assessment.

- The size of debris produces in simulator tests was comparible to that produced in pin-on-plate tests with heat treated again showing larger particles.

- Pin-on-plate tests produce similar wear particles to simulator tests and therefore offer an economical experimental procedure for the study of particle size distribution and wear regime. However pin-on-plate wear rates do not reflect wear simulator wear rates due to differing lubrication behaviour.

- Particle analysis of debris from simulator tests of plasma carburised femoral heads against as-cast cups showed few large particles to begin with followed by smaller particles. The transition in particle size behaviour corresponded to a transition in wear rate from an initial low value to a higher one.

- Particle analysis of PEEK debris from both a pin-on-plate and a simulator test demonstrated similar wear particle size results. Both showed a bimodal distribution of particles. When image analysed the larger particles appeared as tube shapes.

- Particle analysis of P.U. debris from a 4 million cycle knee wear simulator test showed few particles of consistent shape. Over the course of the test the particle size changed very little. When imaged the particles appeared as flat disks.

8. Further Work

An in depth study into the FCC to HCP phase transformation of CoCrMo alloy under stress and after heat treatment may explain some of the differences found in the wear properties of the different specimens used in this study.

Further work into why the pin wears more rapidly in the pin-on-plate tests would be a useful study to allow more insight into how the materials are wearing against one another.

As the control of the twice annealed test slowly lost weight an interesting study would be to investigate the effects of the 25% bovine serum with added EDTA and sodium azide on this alloy and would perhaps give an explanation for these results.

A further study into the wear patterns including everyday walking patterns of different ages of the population would allow a better simulation of real life simulation to be demonstrated *in vitro*.

Ex vivo particles from similar prostheses to those tested in the laboratory could be compared to those analysed in this study, this would allow an assessment of the simulator wear and its ability to simulate everyday gait.

The sectioning of a high wearing metal cup and analysis of the internal material structure in comparison to that of a lower wearing metal cup may provide further insight into why some metal components wear more than others.

The first step of the protein cleavage technique separates the solid matter from the supernatant, it would be interesting to analyse the supernatant, not only for particulate debris that may be too small for the 16000g to pull down but also look at the ions within that supernatant and find out if the cobalt has been leeched into the serum.

Further work on the particle size of different novel materials such as PEEK and Polycarbonate urethane as seen in this study would allow further insight into whether these novel materials will be well accepted in the body.

9. References

1 **Back D. L., Dalziel R., Young D. and Shimmin A.** Early results of primary Birmingham Hip Resurfacings. *Journal of Bone and Joint Surgery*, 2005, **87-B**(3), 324-329.

2 **Daniel J., Pynsent P.B. and McMinn D.** Metal on metal resurfacing of the hip in patients under the age of 55 years with osteoarthritis *Journal of Bone and Joint Surgery- British*, 2004, **86-B**(2), 117-184.

3 **Itayem R., Arndt A., Nistor L., McMinn D. and Lundberg A.** Stability of the Birmingham Hip Resurfacing arthroplasty at two years. A radiostereophotogrammetric analysis study. *Journal of Bone and Joint Surgery-British*, 2005, **87B**(185-162).

4 **Jacobsson S., Djerf K. and Wahlstron O.** 20-year results of McKee-Farrar versus Charnley prosthesis. *Clinical Orthopaedics and Related Research*, 1996, **329S**, S60-S68.

5 **Schmalzried T. P., Peters P. C., Maurer B. T., Bragdon C. R. and Harris W. H.** Long duration metal-on-metal total hip arthroplasties with low wear of the articulating surfaces. *Journal of Arthroplasty*, 1996, **11**(3), 322-331.

6 **Schmalzried T. P., Szuszczewicz E. S., Akizuki K. H., Petersen T. D. and Amstutz H. C.** Factors correlating with long term survival of McKee-Farrar total hip prostheses. *Clinical Orthopaedics and Related Research*, 1996(329), S48-S59.

7 **Unsworth A., Roberts B. J. and Thompson J.C.** The application of soft layer lubrication to hip prostheses. *Journal of Bone and Joint Surgery- British*, 1981, **36B**, 297.

8 **Scholes, S.C., Inman, I.A., Unsworth, A. and Jones, E.** Tribological assesment of a flexible carbon-fibre-reinforced poly(ether-ether-keytone) acetabular cup articulating against an alumina femoral head. *Proc. I MechE J. Engineering in Medicine Part H*, 2008, **222**(H3), 273-283.

9 **Walker P.S. and Gold B. L.** The tribology (friction, lubrication and wear) of all-metal artificial hip joints. *Wear*, 1971, **17**, 285-299.

10 **Charnley J.** Arthroplasty of the hip. *The Lancet*, 1961, 1129-1132.

11 **Schmalzried T. P., Jasty M. and Harris W. H.** Periprosthetic Bone Loss in Total Hip-Arthroplasty - Polyethylene Wear Debris and the Concept of the Effective Joint Space. *Journal of Bone and Joint Surgery-American Volume*, 1992, **74A**(6), 849-863.

12 **Murray, D.W. and Rushton, N.** Macrophages stimulate bone resorbtion when they phagocytose particles. *Journal of Bone and Joint Surgery- British*, 1990, **72-B**, 988-992.

13 **Wroblewski B. M. and Siney P.D.** Charnley low-friction arthroplasty of the hip. *Clinical Orthopaedics and Related Research*, 1993, **292**, 191-201.

14 **Willert H. G. and Semlitsch M.** Reaction of the articular capsule to plastic and metalic wear products from joint endoprostheses. *Congress of dutch-swiss orhtopaedic societies*, 1974, 119-131.

15 **Harris W. H.** Osteolysis and particle disease in hip replacement. *Acta. Orhtop. Scand.*, 1994, **65**(1), 113-123.

16 **Harris W. H.** The problem is osteolysis. *Clinical Orthopaedics and Related Research*, 1995, **311**, 46-53.

17 **Essner A., Sutton K. and Wang A.** Hip simulator wear comparison of metal-on-metal, ceramic-on-ceramic and crosslinked UHMWPE bearings. *Wear*, 2005, **259**, 992-995.
18 **Tipper, J.L., Firkins, P.J., Besong, A.A., Barbour, P.S.M., Nevelos, J., Stone, M.H., Ingham, E. and Fisher, J.** Characterisation of wear debris from UHMWPE on zirconia ceramic, metal-on-metal and alumina ceramic-on-ceramic hip prostheses generated in a physiological anatomical hip joint simulator. *Wear*, 2001, **250**, 120-128.
19 **Wilson-Macdonald J., Morscher E. and Z., M.** Cementless uncoated polyethylene acetabular components in total hip replacement. *Journal of Bone and Joint Surgery- British*, 1990, **72**(B), 423-430.
20 **Besong A. A., Tipper J. L., Ingham E., Stone M. H., Wroblewski B. M. and Fisher J.** Quantitative comparison of wear debris from UHMWPE that has and has not been sterilised by gamma irradiation. *Journal of Bone and Joint Surgery-British Volume*, 1998, **80B**(2), 340-344.
21 **DeHeer, D.H., Engels, J.A., DeVries, A.S., Knapp, R.H. and Beebe, J.D.** In situ complement activation by polyethylene wear debris. *Journal of Biomedical Materials Research*, 2001, **54**(1), 12-19.
22 **Green T. R., Fisher J., Stone M., Wroblewski B. M. and Ingham E.** Polyethylene particles of a "critical size" are necessary for the induction of cytokines by macrophages in vitro. *Biomaterials*, 1988, **19**, 2297-2302.
23 **Catelas I., Bobyn J. D., Medley J. B., Krygier J. J., Zukor D. J., Petit A. and Huk O. L.** Effects of digestion protocols on the isolation and characterization of metal-metal wear particles. I. Analysis of particle size and shape. *Journal of Biomedical Materials Research*, 2001, **55**(3), 320-329.
24 **Catelas I., Bobyn J. D., Medley J. J., Zukor D. J., Petit A. and Huk O. L.** Effects of digestion protocols on the isolation and characterization of metal-metal wear particles. II. Analysis of ion release and particle composition. *Journal of Biomedical Materials Research*, 2001, **55**(3), 330-337.
25 **Doorn P. F., Campbell P. A., Worrall J., Benya P. D., McKellop H. A. and Amstutz H. C.** Metal wear particle characterization from metal on metal total hip replacements: Transmission electron microscopy study of periprosthetic tissues and isolated particles. *Journal of Biomedical Materials Research*, 1998, **42**(1), 103-111.
26 **Firkins P. J., Tipper J. L., Saadatzadeh M. R., Ingham E., Stone M. H., Farrar R. and J., F.** Quantitive analysis of wear and wear debris from metal-on-metal hip prostheses tested in a physiological hip joint simulator. *Bio-Medical Materials and Engineering*, 2001, **11**, 143-157.
27 **Tipper, J.L., Firkins, P.J., Ingham, E., Fisher, J., Stone, M.H. and Farrar, R.** Quantitative analysis of the wear and wear debris from low and high carbon content cobalt chrome alloys used in metal on metal total hip replacements. *Journal of Materials Science-Materials in Medicine*, 1999, **10**(6), 353-362.
28 **Gray H.** *Greys Anatomy Masterclass edition*. (Chancellor Press, London, 1985).
29 **Cook A. F., Dowson D. and Wright V.** The rheology of synovial fluid and some potential synthetic lubricants for degenerate synovial joints. *Proceedings of the Institute of Mechanical Engineers Part H-Engineering in Medicine*, 1978, **7**(H2), 66-72.
30 **Paul J. P.** Forces Transmitted by joints in the human body. *Proc. Instn. Mech. Engrs.*, 1966, **181**(37), 8-15.

31 **English T.A. and Kilvington M.** In vivo records of hip forces using a femoral implant with telemetric output. *Journal of biomedical engineering*, 1979, **1**(2), 111-115.
32 **Paul, J.P.** Analysis of loading of the hip Joint. *Sngineers and Surgeons-Joined at the hip*, p. C601/076/2002London, 2002).
33 **Hollander, J.L. and Jr., M.D.** *Arthritis and allied conditions*. (Lea and Febiger, Philadelphia, 1972).
34 **Kelly, W., Harris, E.D., Ruddy, S. and Sledge, C.B.** *Text book of Rheumatology section xxi Medical Orthopedics and rehabilitation, chapter 99 biomechanics of joints*. (Saunders, Philadelphia, 1993).
35 **Johnson K. L.** One hundred years of hertzian contact. *Proc. IMechE J. Engineering in Medicine*, 1982, **196**, 363-378.
36 **Jacobson B.** The strybeck Memorial lecture. *Tribology international*, 2003, **36**, 781-789.
37 **Charnley, J.** Total hip replacement. *American Medical Association*, 1974, **230**(7), 1025-1028.
38 **Semlitsch, M.** Technical progress in artificial hip joints. *J. Engineering in Medicine*, 1974, **3**(4), 10-19.
39 **Unsworth A., Pearcy M. J., White E. F. T. and White G.** Frictional properties of artificial hip joints. *Proceedings of the Institution of Mechanical Engineering - Part H Journal of Engineering in Medicine* 1988, **17**(3), 101-104.
40 **Archard J. F.** Contact and Rubbing Of flat Surfaces. *Journal Of Applied Physics*, 1953, **24**(3), 981 - 988.
41 **Unsworth A., Dowson D. and Wright V.** Some new evidence on human joint lubrication. *Ann. Rheum. Dis.*, 1975, **34**, 277-285.
42 **Unsworth A., Dowson D. and Wright V.** The frictional behaviour of human synovial joints. *Trans. ASME Journal of lubrication Technology* 1975, 369-376.
43 **Unsworth A., Pearcy M. J., White E. F. T. and White G.** The effects of lubrication in hip joint prostheses. *Physics in Medicine and Biology*, 1978, **23**(2), 253-268.
44 **Unsworth A.** Frictional resistance of new and explanted artificial hip joints. *International Tribology conference* pp. 383-390Perth Australia, 1994).
45 **Hall R. M., Unsworth A. and Wroblewski B. M.** Frictional characterisation of explanted charnley hip prostheses *Wear*, 1994, **175**(1-2), 159-166.
46 **Unsworth A., Hall R. M. and Burgess I. C.** Frictional resistance of new and explanted artificial hip joints. *Wear*, 1995, **190**(2), 226-231.
47 **Hall R.M. and Unsworth A.** Friction in hip prostheses. *Journal of biomaterilas*, 1997, **18**(15), 1017-1026.
48 **Scholes S. C. and Unsworth A.** Comparison of friction and lubrication of different hip prostheses. *Proceedings of the Institution of Mechanical Engineering - Part H Journal of Engineering in Medicine* 2000, **214**(Part H), 49-57.
49 **Scholes S. C. and Unsworth A.** The tribology of metal-on-metal total hip replacements. *Proceedings of the Institution of Mechanical Engineering - Part H Journal of Engineering in Medicine* 2006, **220**(H2), 183-194.
50 **Vassiliou K., Elfick A. P. D., Scholes S. C. and Unsworth A.** The effect of 'running-in' on the tribology and surface morphology of metal-on-metal birmingham hip resurfacing device in simulator studies. *Proceedings of the Institution of Mechanical Engineering - Part H Journal of Engineering in Medicine* 2006, **220**, 269-277.

51 Dowson D., McNie C. M. and Goldsmith A. A. J. Direct experimental evidence of lubrication in a metal-on-metal total hip replacement tested in a joint simulator. *Proceedings of the Institution of Mechanical Engineering - Part C*, 2000, **214**(1), 75-86.
52 Smith S. L., Dowson D. and Goldsmith A. A. J. The lubrication of metal-on-metal total hip joints: a slide down the Stribeck curve *Proceedings of the Institution of Mechanical Engineering - Part J* 2001, **215**(J5), 483-493.
53 Yan Y., Neville A. and Dowson D. Biotribocorrosion of CoCrMo orthopaedic implant materials- assesing the formatin and effect of the biofilm. *Tribology international*, 2006, **40**, 1492-1499.
54 Rabinowicz, E. *Friction and wear of materials*. (Wiley, 1965).
55 Burwell J. T. and Strang C. D. On the emperical law of adhesive wear. *J. Appl. Phys.*, 1952, **23**, 18-28.
56 Joyce, T.J., Thompson, P. and Unsworth, A. The wear of PTFE against stainless steel in a multi-directional pin-on-plate wear device. *Wear*, 2003, **255**, 1030-1033.
57 Scholes S. C., Green S. M. and Unsworth A. The wear of metal-on-metal total hip prostheses measured in a hip simulator. *Proc. IMechE J. Engineering in Medicine*, 2001, **215**(Part H), 523-530.
58 Unsworth A. Tribology of human and artificial joints. *Proceedings of the Institution of Mechanical Engineering - Part H Journal of Engineering in Medicine* 1991, **205**, 163-172.
59 Jalali-Vahid D., Jagatia M., Jin ZM and Dowson D. Prediction of lubricating film thickness in UHMWPE hip joint replacements. *Journal Of Biomechanics*, 2000, **34**, 216-266.
60 Hou J. S., Holmes M. H., Lai W. M. and Mow V. C. *Squeese film lubrication for articular cartilage with synovial fluid* (Springer, Verlang New York, 1990).
61 Hamrock B. J. and Dowson D. Elastohydrodynamic lubrication of elliptical contacts for materials of low elastic modulus-fully flooded conjuction. *Transactions of ASME Journal of Lubrication Technology* 1978, **100**, 236-245.
62 MacConaill M. A. Function of intra-articular fibrocartilageges with special reference to the knee and inferior-radio-ulnar joints. *J Anatomy*, 1932, **66**, 210.
63 Jones E. S. Joint Lubrication. *Lancet*, 1934, **1**, 1426.
64 Jones, E.S. Joint Lubrication. *Lancet*, 1936, **1**, 1043.
65 Charnley, J. The lubrication of animal joints *Institute of mechanical Engineers Symposium Biomechanics*, 1959, 12.
66 Charnley, J. The lubrication of animal joints in relation to surgical reconstruction by arthroplasty. *Annals of Rheumatic Diesase*, 1960, **19**, 10.
67 McCutchen, C.W. Sponge-hydrostatic and weeping bearings. *nature*, 1959, **184**, 1284.
68 Walker P.S., Dowson D., Longfield M.D. and Wright V. "boosted lubrication"in synovial joints by fluid entrapment and enrichment. *Annals of Rheumatic Diesase*, 1968, **27**(512-520).
69 Longfield, M.D., Dowson, D., Walker, P.S. and Wright , V. boosted lubrication of human joints by fluid enrichment and entrapment. *Bio. Med. Eng.*, 1969, 517-522.
70 Ling, F.F. A new model of articular cartilage in human joints. *Trans ASME J. lubrication Technology*, 1974, 449-507.

71 Dintenfass, L. Lubrication in synovial joints: a theretical analysis-a rheological aproach to the problems of joint ovements and joint lubrication. *Journal of Bone and Joint Surgery*, 1963, **45-A**, 1241.
72 Tanner, R.I. An alternative mechanism for the lubrication of synovial joints. *Physics in medicine and Biology*, 1966, **11**, 119.
73 Higginson, G. and Unsworth, A. *The lubrication of natural joints.* (Elsevier, Amsterdam, 1981).
74 Dowson D. Modes of lubrication in human joints. *Proceedings of the Institution of Mechanical Engineering - Part H Journal of Engineering in Medicine* 1967, **181**, 45.
75 Linn F. C. and Radin E. L. Lubrication in animal joints III The effect of certian chemical alteration of te cartilage and lubricant. *Arthritis Rheum.*, 1968, **11**, 674.
76 Higginson, G.R. Elastohydrodynamic Lubrication in human joints. *Engineering in Medicine IMechE*, 1978, **7**(1), 35-41.
77 Bennett A. and Higginson G. R. Hydrodynamic lubrication of soft solids. *J. Mechanical Engineering Science*, 1970, **12**, 218-222.
78 Higginson G.R. and Norman R. The lubrication of porous elastic solids with reference to the functioning of human joints. *Journal Mechanical Engineering science*, 1974, **16**, 250-257.
79 Unsworth A., Pearcy M. J., White E. F. T. and White G. Lubrication of artificial hip joints. *Proceedings of the Institution of Mechanical Engineering - Part H Journal of Engineering in Medicine* 1987, 715-722.
80 Dowson D. and Jin Z. M. Microelastohydrodynamic lubrication of synovial joints. *Proceedings of the Institution of Mechanical Engineering - Part H Journal of Engineering in Medicine* 1986, **152**, 63-65.
81 Khan, I., Smith, N., Jones, E., Finch, D.S. and Cameron, R.E. Analysis and evolution of a biomedical polycarbonate urethane tested in an invitro study and an ovine arthroplasty model: Part I materials selection and evaluation. *J. Biomaterails*, 2005, **26**(6), 621-631.
82 Khan, I., Smith, N., Jones, E., Finch, D.S. and Cameron, R.E. Analysis and evaluation of a biomedical polycarbonate urethane tested in an invitro study and an ovine arthroplasty model Part II in vivo investigation. *J. Biomaterails*, 2005, **26**(6), 633-643.
83 Scholes, S.C., Unsworth, A. and Jones, E. Polyurethane unicondylar knee prostheses: simulator wear tests and lubrication studies. *Physics in medicine and Biology*, 2007, **52**, 197-212.
84 Unsworth A. The effects of lubrication in hip joint prostheses. *Physics in Medicine and Biology*, 1978, **23**(2), 253-268.
85 Itayem R., Arndt A., McMinn D., Daniel J. and Lundberg A. A five–year radiostereometric follow-up of the Birmingham Hip Resurfacing arthroplasty. *Journal of Bone and Joint Surgery- British*, 2006, **89B**, 1140-1143.
86 McKellop, H. Wear of artificial joint materials II Twelve channel wear-screening device: correlation of experimental and clinical results. *Proceedings of the Institution of Mechanical Engineering - Part H Journal of Engineering in Medicine* 1981, **10**(3), 123-136.
87 Smith S. L. and Unsworth A. A comparison between gravimetric and volumetric techniques of wear measurement of UHMWPE acetabular cups against zirconia and cobalt chromium molybdenum femoral heads in a hip simulator.

Proceedings of the Institution of Mechanical Engineering - Part H Journal of Engineering in Medicine 1999, **213**(Part H6), 475-483.

88 Kabo, J. In vivo wear of polyethylene acetabular components. *Journal of Bone and Joint surgery*, 1993, **75-B**(2), 254-258.

89 Firkins P.J., Tipper J.L., Ingham E., Stone M. H., Farrar R. and Fisher J. A novel low wearing differential hardness, ceramic on metal hip joint prosthesis. *Journal of biomechanics*, 2001, **34**, 1291-1298.

90 Berry D. J., Scott Harmsen W., Cabanela M. E. and Morrey B. F. Twenty-five-year survivorship of two thousand consecutive primary charnley total hip replacements. *Journal of Bone and Joint Surgery*, 2002, **84-A**(2), 171-177.

91 Derbyshire, B. and Porter, M.L. A study of the elite Plus femoral component using radiostereometric analysis. *Journal of bone and joint surgery*, 2007, **89-B**(6), 730-735.

92 Callaghan J. J., Forest E. E., Olejniczak J. P., Goetz D. D. and Johnston R. C. Charnley total hip arthroplasty in patients less than fifty years old. *Journal of Bone and Joint Surgery*, 1998, **80-A**(5), 704.

93 Amaral M., Abreu C. S., Oliveira F. J., Gomes J. R. and Silva R. F. Biotribological performance of NCD coated Si3N4-bioglass composites. *Diamond and Related Materials*, 2007, **16**, 790-795.

94 Bowsher J. and Shelton J. C. Hip simulator study of the influence of patient activity level on the wear of crosslinked polyethylene under smooth and roughened femoral conditions. *Wear*, 2001, **250**(1), 167-179.

95 Affatato S., Goldoni M., Testoni M. and Toni A. Mixed oxides prosthetic ceramic ball heads. Part 3: effect of the ZrO2 fraction on the wear of ceramic on ceramic hip joint prostheses. A long-term in vitro wear study. *Journal of Biomaterials*, 2001, **22**(7), 717-723.

96 Scholes S. C. and Unsworth A. Pin-On-Plate studies on the effect of rotationon the wear of metal-on-metal samples. *J. Mater. Sci. Mater. Med.*, 2001, **12**, 299-303.

97 Besong A.A., Jin Z. M. and Fisher J. Importance of pin geometry on pin-on-plate wear testing of hard-on-hard bearing materials for artificial hip joints, technical note. *Proceedings of the Institution of Mechanical Engineering - Part H Journal of Engineering in Medicine* 2001, **215**, 605-610.

98 Jin, Z.M., Firkins, P., Farrar, R. and Fisher, J. Analysis and modelling of wear of cobalt-chrome alloys in a pin-on-plate test for a metal on metal total hip replacement. *Proc. I MechE Engineering in Medicine Part H*, 2000, **214**, 559-568.

99 Cawley, J., Metcalf J. E. P., Jones A. H., Band T. D. and Skupien D. S. A tribological study of cobalt chromium molybdenum alloys used in metal-on-metal resurfacing hip arthroplasty. *Wear*, 2003, **255**, 999-1006.

100 Kinbrum, A. and Unsworth, A. The wear of high-carbon metal-on-metal bearings after different heat treatments. *Proc. I MechE Engineering in Medicine Part H*, 2008, **222**, in press.

101 Daniel J. and McMinn D. Metal ions and wear rates in Birmingham Hip Resurfacing. *Presented at the European Orthopaedic Research Society Meeting*Amsterdam, 2004).

102 August, Aldam and Pynsent. The Mckee-Farrah hip arthroplasty a long term study. *Journal of Bone and Joint Surgery- British*, 1986, **66-B**, 520.

103 Djerf and Wahlstrom. Total hip replacement comparison between the Mckee-Farrah and Charnley prostheses a 5 year follow up study *Arch Orhtop Trauma Surg*, 1986, **105**, 158.

104 Brown S.R., Davies W.A., DeHeer D.H. and Swanson A.B. Long-term survival of McKee-Farrar total hip prostheses. *Clin. Orthop. Related Res.*, 2002, **402**, 157-163.
105 Higuchi, F., Inoue, A. and Semlitsch, M. Metal-on-metal CoCrMo Mckee-Farrar total hip arthroplasty characteristics from a long term study. *Arch. Orthop Trauma Surg*, 1996, 116-121.
106 Zahiri C. A., Schmalzreid T. P. and Ebramzadeh E. Lessons learned from loosening of the Mckee-Farrar metal on metal total hip replacement. *Journal of Arthroplasty*, 1999, **14**, 326.
107 Anderw T. A., Berridge D. and Thomas A. Long term review of a Ring total hip arthroplasty. *Clinical Orthopaedics and Related Research*, 1985, **201**, 111.
108 Bryant M.J., Mollan R.A.B. and Nixon J.R. Survivorship analysis of the Ring hip arthroplasty. *Journal of Arthroplasty*, 1991, **6**(Suppl 1), s5-s10.
109 Willert H.G. and Buchhorn G.H. *Retrieval Studdies on classic cemented metal on metal hip endoprostheses* (Hans Huber, Bern, 1999).
110 Schmalzried, T.P., Peters, P.C. and Maurer, B.T. Long duration metal on metal total hip arthroplasties with low wear on the articulating surfaces. *J. Arthroplasty*, 1996, **11**, 322.
111 McKellop H., Park S-H. and Chisea R. In vivo wear of 3 types of metal on metal hip endoprostheses during 2 decades of use. *Clinical Orthopaedics and Related Research*, 1996, **329**(Supl 1), s128.
112 Djerf, K. and Wahlström, O. Total hip replacement comparison between the McKee-Farrar and Charnley prostheses in a 5-year follow-up study. *Arch Orthop Trauma Surg.*, 1986, **105**(3), 158-162.
113 Jacobsson, S.A., Djerf, K. and Wahlström, O. A comparative study between McKee-Farrar and Charnley arthroplasty with long-term follow-up periods. *J. Arthroplasty*, 1990, **5**(1), 9-14.
114 Bowsher J. G., Nevelos J., Pickard J. and Shelton J. C. Do heat treatments influence the wear of large diameter metal on metal hip joints? An invitro study under normal and adverse gait conditions. *49th Annual Meeting of the Orthopaedic Research Society*, 2003, Poster 1398.
115 Bowsher J. G., Nevelos J., Williams P. A. and Shelton J. C. 'Severe' wear challenge to 'as-cast' and 'double heat-treated' large-diameter metal-on-metal hip bearings. *Proceedings of the Institution of Mechanical Engineers Part H-Journal of Engineering in Medicine*, 2006, **220**(H2), 135-143.
116 Dowson D., Hardaker C., Flett M. and Isaac G. H. A hip joint simulator study of the performance of metal-on-metal joints - Part I: The role of materials. *Journal of Arthroplasty*, 2004, **19**(8), 118-123.
117 Dowson D., Hardaker C., Flett M. and Isaac G. A hip joint simulator study of the performance of metal-on-metal joints Part I: the role of materials. *J. Arthroplasty*, 2004, **19**(8), 118-123.
118 Zhaund and Langer. Effects of alloy additions on the microstructures and tensile properties of cast CoCrMo alloy used for surgical implants *J. Mater Sci.*, 1989, **24**, 4324-4330.
119 Waitz T. and Karthaler P. The fcc to hcp martensitic phse transformation in CoNi studied by TEM and AFM methods. *Acta. Mater.*, 1996, **45**(2), 837-847.
120 Varano R., Bobyn J.D., Medley J. B. and Yue S. The effect of microstructure on the wear of Cobalt-based alloys used in metal-on-metal hip implants. *Proc. IMechE J. Engineering in Medicine*, 2006, **220**(Part H), 145-159.

121 Saldivar-Garcia and Lopez. Microstructural effects on the wear resistance of wrought and as-cast CoCrMoC implant alloys. *J. Biomed. Mater. Res.*, 2005, **74A**, 269-274.
122 Sieber, H.P., Rieker, C.B. and Kotting, P. Analysis of 118 second-generation metal-on-metal retrieved hip implants. *Journal of Bone and Joint Surgery*, 1999, **81-B**(1), 46-50.
123 McMinn D. and Daniel J. History and modern concepts in surface replacement. *Proceedings of the Institution of Mechanical Engineering - Part H Journal of Engineering in Medicine* 2006, **220**, 239-251.
124 Treacy, R.B., McBryde, C.W. and Pynsent, P.B. Birmingham hip resurfacing arthroplasty. A minimum follow up of five years. *Journal of bone and joint surgery*, 2005, **87-B**, 167-170.
125 Amstutz H. C., Beaule P.E., Dorey F. J., Le Duff M. J., Campbell P. A. and Gruen T. A. Metal-on-metal hybrid surface arthroplasty: Two to six year follow up study. *Journal of Bone and Joint Surgery*, 2004, **86-A**(1), 28-40.
126 Visuri T. and Pukkala E. Does metal-on-metal hip prosthesis have influence on cancer? A long term follow up study. In Reiker C., Soberholzer and Wyss U., eds. *World Tribology forum in Arthroplasty* (Hans Huber, 2001).
127 Case P.C., Ellis L., Turner J. C. and B., F. Development of a routine method for the determintion of trace metals in whole blood by magnetic sector inductively coupled plasma mass spectrometry with particular relevence to patients with total hip and knee arthroplasty. *Clinical Chemistry*, 2001, **47**(2), 275-280.
128 Clarke M. T., Lee P. T. H. and Villar R. N. Levels of metal ions after small and large diameter metal-on-metal hip arthroplasty. *Journal of Bone and Joint Surgery- British*, 2003, **85**(B), 913-917.
129 Jacobs J. J., Skipor A. K., Campbell P. A., Hallab N. J., Urban R. M. and C., A.H. Can metal levels be used to monitor metal-on-metal hip arthroplasties. *J. Arthroplasty*, 2004, **19**(8 Suppl. 3), 59-65.
130 Angadji A., Grossmann H., Royle M., Collins S. N. and Shelton J. C. Affect of cup positioning on the wear performance and wear particles from metal-on-metal hip replacements. *World Biomaterials Congress*Amsterdam, 2008).
131 Goldring S.R., Schiller A.L., Roelke M., Rourke C. M., O Neil D. A. and Harris W.H. The synovial-like membrain at the bone cement interface in loose total hip replacements and it's proposed role in bone lysis. *Journal of Bone and Joint Surgery*, 1983, **65A**, 575-584.
132 Horowitz S.M., Doty S. B., Lane J. M. and Burstein A. H. Studies of the mechanism by which the mechanical failure of polymethylmethacrylate leads to bone resorbtion. *Journal of Bone and Joint Surgery*, 1993, **75A**, 802-813.
133 Jiranek W. A., Machado M., Jasty M., Jevsevar D., Wolfe H. J., S.R., G., Goldberg M. J. and W.H., H. Production of cytoknes around loosened cement acetabular components. Analysis with imunohistochemical techniques and in situ hybridization. *Journal of Bone and Joint Surgery*, 1993, **75A**, 863-879.
134 Goodman S. B., Huie P., Song Y, Schurman D., Maloney W., Woolson S. and Sibley R. Celular profile and cytokine production at prosthetic interfaces. Study of tissues retrieved from revised hip and knee replacements. *Journal of Bone and Joint Surgery- British*, 1998, **80B**, 531-539.
135 Horowitz, S.M., Doty, S.B., Lane, J.M. and Burnstein, A.H. Studies of the mechanism by which the mechanical failure of polymethylmethacrylate leads to bone resorbtion. *Journal of Bone and Joint Surgery*, 1993, **75-A**(3).

136 Schmalzried, T.P., Kwong, L.M., Jasty, M. and Sedlacek, R.C. The mechanism of loosening of cemented acetabular components in total hip arthroplasty. *Clin Orthop Related Res*, 1992, **274**, 172-193.

137 Huo, M.H. and Salvati, E.A. *Hip wear: clinical aspects. In biological material and mechanical considerations of joint replacement.* (Raven Press, New York, 1993).

138 Escalas F., Galante J., Rostoker W. and Coogan P. Bio-compatability of materials for total joint replacement. *J. Biomedical Materials Research*, 1976, **10**(175-195).

139 Goodman S. B., Foransier V. L., Lee J. and Kei J. The effects of bulk versus particulate titanium and cobalt chrome alloy implanted into the rabbit tibia. *J. Biomedical Materials Research*, 1990, **24**, 1539-1549.

140 Laing P.G., Ferguson A. B. and Hodge E.S. Tissue reaction in rabbit muscle exposed to metallic implants. *Journal of Biomedical Materials Research*, 1967, **1**, 135-149.

141 Cohen, J. Assay of Foreign body reaction. *Journal of Bone and Joint Surgery*, 1959, **41-A**, 152-166.

142 Heath, J.C., Freeman, M. and Swanson, S. Carcinogenic properties of wear particlesfrom prostheses made in cobalt chromium alloy. *Lancet*, 1971, **1**, 564-566.

143 Barth E., Sullivan T. and Berg E.W. Particle size versus chemical compositions of biomatrials as determining factors in macrophage activation. *Trans. Orthop. Res. Soc.*, 1991, **16**, 187.

144 Gelb H., Schumacher H. R., Cuckler J. and Baker D. G. In vivo inflammatory response to polymethylmethacrylate particulate debris, effect of size morphology and surface area. *J. Orthopaedic Res.* , 1994, **12**, 83-92.

145 Haynes D. R., Rogers S. D., Hay S. J., Pearcy M. J. and Howie D. W. The differences in toxicity and bone resorbing mediators induced by titanium and cobalt chrome alloy wear particles. *Journal of Bone and Joint Surgery*, 1993, **75-A**, 825-834.

146 Howie D. W. and Vernon Roberts B. Synovial macrophage response to aluminium oxide ceramic and cobalt-chrome alloy wear particles in rats. *J. of Biomaterials*, 1988, **9**, 442-448.

147 Rogers, S.D., Pearcy, M.J., Hay, S.J., Haynes, D.R., Bramley, A. and Howie, D.W. A method for production and characterisation of metal prosthesis wear particles. *Journal of orthopaesic research*, 1993, **11**(6), 856-864.

148 Escalas F., Galante J., Gaechter A., Alroy J. and Andrsson G. B. J. Metal Carcinogenesis A study of the carcinogenic activity of solid metal alloys in rats. *Journal of Bone and Joint Surgery*, 1977, **59A**, 622-624.

149 Goodman S. B., Aspenberg P. and Song Y. Tissue in-growth and differentiation in the bone harvest chamber in the presence of cobalt chromium alloy and high density polyethylene particles. *Journal of Bone and Joint Surgery*, 1995, **77A**, 1025-1035.

150 Goodman S. B., Aspenberg P. and Wang J. S. Cement particles inhibit bone growth into titanium chambers implanted into the rabbit
Acta. Orthop. Scand. , 1993, **64**, 627-633.

151 Howie D. W. and Vernon-Robberts B. The synovial response to inter articular cobalt chrome wear particles. *Clinical Orthopaedics and Related Research*, 1988, **232**, 244-254.

152 Howie D. W. and Vernon-Roberts B. Long term effects of interarticular cobalt chrome alloy wear particles in rats. *Journal of Arthroplasty*, 1988, **3**, 327-336.
153 Howie D. W., Haynes D. R., Rogers S. D., McGee M. A. and Pearcy M. J. The response to particular debris. *Orhtop. Clin. North America*, 1993, **24**(571-581).
154 Haynes D.R., Rogers S.D., Hay S.J., Pearcy M.J. and Howie D.W. The differences in toxicity and release of bone resorbing mediators induced by titanium and cobalt chromium alloy wear particles. *Journal of Bone and Joint Surgery*, 1993, **75A**, 825-834.
155 Chiba J., Doyle J.S. and Noguchi K. Biochemical and morphological analyses of activated human macrophages and fibroblasts by particulate materials. *Trans. 38th Annual Meeting Orthop. Res. Soc.* , p. 3431992).
156 Howie D. W. Biological effects of Cobalt chrome in cell and animal models. *Clinical Orthopaedics and Related Research*, 1996, **329S**, s217-s231.
157 Rae T. The toxicity of metals used in orthopaedic prostheses-an experimental study using cultured human synovial fibroblasts. *Journal of Bone and Joint Surgery-British*, 1981, **63-B**, 435.
158 Evans E.J. Cell damage in vitro following direct contact with fine particles of titanium, titanium alloys and cobalt chrome molybdenum alloy. *Journal of Biomaterials* 1994, **15**, 713-717.
159 Evans E.J. and Benjamin M. The effect of grinding conditions on the toxicity of cobalt chrome molybdenum particles in vitro. *Journal of Biomaterials*, 1987, **8**(377-384).
160 Goldring, S.R., Kroop, S.F. and Petrison, K.K. Metal particles stimulate prostaglandin E2(PGE2) release and colygen synthesis in cultured cells. *Trans Orthop res soc*, 1990, **15**, 444.
161 Howie D. W. and Vernon-Robberts B. Longterm effects of intra-articular cobalt chrome alloy wear particles in rats. *Journal of Arthroplasty*, 1988, **3**(327-336).
162 Hallab N. J., Anderson S., Caicedo B. S., Skipor A., Campbell P. and Jacobs J. Immune responces collate with serum-metal in metal-on-metal hip arthroplasty. *Journal of Arthroplasty*, 2004, **19**(8), 88-93.
163 Henstey and Petterson, A. *Allergy Vs hypersensitivity*. (Raven Press, New York, 1993).
164 Niedzwiecki S., Klapperich C., Short J., Jani S., Ries M. and Pruitt L. Comparison of three joint simulator wear debris isolation techniques: acid digestion, base digestion, and enzyme cleavage. *J. Biomed. Mater. Res.*, 2001 Aug, **56**(2), 245-249.
165 Revell P. A., Al-Saffar N. and Kobayashi A. Biological reaction to debris in relation to joint prostheses. *Proceedings of the Institute of Mechanical Engineers Part H-Engineering in Medicine*, 1997, **211**(Part H), 187-197.
166 Gonzalez O., Lane smith R. and Goodman S.B. Effect of size, concentration, surface area, and volume of Polymethylmethacrylate particles on human macrophages in vitro. *Journal of Biomedical Materials Research*, 1996, **30**, 436-473.
167 Yoneda M. In vitro immune responce to acrylic cement particles in patients with cemented joint replacements. *Nippon Seikeigeka Oakkai Zasshi*, 1986, **60**, 11-19.
168 Gelb H., Schumacher H. R., Cuckler J. and Baker D. G. In vivo inflamatory responce to polymethylmethacrylate debris: effects of size mophology and surface area. *Journal of Orthopaedic research*, 1994, **12**, 83-92.

169 Matthews, B., Besong, A.A., Green, T., Stone, M.H., Wroblewski, B.M., Fisher, J. and Ingham, E. Evaluation of the responce of primary human prepheral blood mononuclear phagocytes to chalange with in vitro generated clinically relevent UHMWPE particles of known size and dose. *J. Biomed. Mater. Res.*, 2000, **52**, 296-307.

170 Hans-Georing W. and Gottfried H. B. *Particle disease due to wear of ultra high molecular weight polyethylene findings from retrieval studies.* (Raven Press, New York, 1993).

171 Matthews, J.B., Green, T.R., H. Stone, M., Mike Wroblewski, B., Fisher, J. and Ingham, E. Comparison of the response of primary human peripheral blood mononuclear phagocytes from different donors to challenge with model polyethylene particles of known size and dose. *Biomaterials*, 2000, **21**(20), 2033-2044.

172 Germain, M.A., Hatton, A., Williams, S., Mathews, J.B., Stone, M.H., Fisher, J. and Ingham, E. Comparison of the cytotoxicity of clinically relevant cobalt-chromeium and alumina ceramic wear particles in vitro. *Biomaterials*, 2003, **24**, 469-479.

173 Jasty, M., Goldring, S.R. and Harris, W.H. Comparison of bone cement membrane around rigidly fixed versus loose total hip implants. *Trans. Orthopaedic research society*, 1984, **9**, 125.

174 Jasty, M., Maloney, W.J., Bragdon, C.R., Haire, T. and Harris, W.H. Histomorphological studies of the long-term skeletal responces to well fixed cemented femoral components. *Journal of Bone and Joint Surgery*, 1990, **72-A**, 1220-1225.

175 Hicks, D.G., Judkins, A.R. and Sickel, J.Z. Granular histiocytosis of pelvic lymph nodes following total hip arthroplasty. *Journal of Bone and Joint Surgery*, 1996, **78A**, 482-496.

176 Tipper, J.L., Ingham, E., Hailey, J.L., Besong, A.A., Fisher, J., Wroblewski, B.M. and Stone, M.H. Quantitative analysis of polyethylene wear debris, wear rate and head damage in retrieved Charnley hip prostheses. *Journal of Materials Science-Materials in Medicine*, 1999, **11**(2), 117-124.

177 Firkins P. J., Tipper J. L., Ingham E., Stone M., Farrar R. and Fisher J. Quantitive analysis of wear debris from metal on metal hip prostheses tested in a physiological hip joint simulator. *45th Annual Meeting, Orthopaedic research society*, 1999.

178 Bowsher J. G., Hussain A., Nevelos J. and Shelton J. C. The importance of head diameter in minimising metal-on-metal hip wear. *50th Annual Meeting of tye Orthopaedic Research Society*2004).

179 Wang A., Stark C. and Dumbleton H. J. Mechanistic and morphological origins of ultra-high molecular weight polyethylene wear debris in total joint replacement prostheses. *Proceedings of the Institute of Mechanical Engineers Part H-Engineering in Medicine*, 1996, **210**, 141-155.

180 Smith S. L., Burgess I. C. and Unsworth A. Evaluation of a hip joint simulator. *Proceedings of the Institute of Mechanical Engineers Part H-Engineering in Medicine*, 1999, **213**(part H6), 469-473.

181 Smith S. L. Design, development and applications of hip joint simulators. *School Of Engineering* (Durham, Durham, 1999).

182 Roberts B. J. and Unsworth, A. Modes of lubrication in human hip joints. *Annals of the Rheumatic Diseases*, 1982, **41**, 217-224.

183 Blamey J. Improved tribology and materials for a new generation of hip prosthesis. *Engineering* (Durham, Durham, 1993).

184 Standard, B. BS ISO 14242-2. 1999).
185 Bowsher J. G., J., N., J., P. and Shelton J. C. Do Heat Treatments Influence The Wear of Larger Diameter Metal-on-metal hip joints? An in vitro study under normal and adverse gait conditions. *49th Annual Meeting of the Orthopedic Research Society*, 2003, **Poster #1398**.
186 Liu, F., Jin, Z.M., Hirt, F., Rieker, C., Roberts, P. and Grigoris, P. Effect of wear of bearing surfaces on elastohydrodynamic lubrication of metal-on-metal hip implants. *Proceedings of the Institution of Mechanical Engineers Part H-Journal of Engineering in Medicine*, 2005, **219**(H5), 319-328.
187 Rieker C. B., Schon R., Konrad R., Liebentritt G., Gnepf P., Shen M., Roberts P. and Grigoris P. Influence of the Clearance on In-Vitro Tribology of Large Diameter Metal-on-Metal Articulations Pertaining to Resurfacing Hip Implants. *Orhtopedic Clinics*, 2005, **36**, 135-142.
188 Elfick A. P. D., Green S. M., McCaskie A. W. and Birch M. A. Optimisation of polyethylene wear particles regulates macrophage and osteoblast responses in vitro. *Journal of Biomedical Materials Research Part B-Applied Biomaterials*, 2004, **71B**(2), 244-251.
189 P. Harvie, S. Glyn-Jonrs, H. Pandit, N. Athanasou, D. Murray and C. Gibbons. Pseudo-tumour following resurfacing arthroplasty:A case series. *British Hip Society*, p. 18 (British Hip Society, Leeds Royal Armouries, 2007).
190 Lewis, C.G. and Sunderman Jr, F.W. Metal carcinogenesis in total joint arthroplasty. Animal models. *Clin Orthop Relat Res*, 1996, **329**, S264-268.
191 Scholes, S.C. and Unsworth, A. The wear properties of CFR-peek optima articulating against ceramic assessed on a multidirectional pin-on-plate machine. *I mech E Part H Journal of engineering in medicine*, 2006, **221**, 281-289.
192 Howling, G.I., Sakoda, H., Antonarulrajah, A., Marrs, H., Stewart, T.D., Appleyard, S., Rand, B., Fisher, J. and Ingham, E. Biological response to wear debris generated in carbon based composites as potential bearing surfaces for artificial hip joints. *Journal of Biomedical Materials Research Part B-Applied Biomaterials*, 2003, **67B**(2), 758-764.

Appendix I

Surface Topography equations [1]

P.V is peak to valley height, this is the height from the highest peak to the lowest valley and gives the range of deviation over the surface.

S_a is average roughness $S_a = \frac{1}{l_x l_y} \int_0^{l_x} \int_0^{l_y} |\eta| \, dxdy$

S_{rms} is the root mean squared roughness $S_{rms} = \sqrt{\frac{1}{l_x l_y} \int_0^{l_x} \int_0^{l_y} \eta^2(x,y) dxdy}$

S_{sq} is the Skewness, it is a statistical description of the peaks and valleys of the surface $S_{sk} = \frac{1}{S_{rms}^3} \int_{-\infty}^{\infty} \int_{-\infty}^{\infty} \eta^3(x,y) p(\eta) dxdy$

[1] Elfick, A., Hall, R., Pinder, I., and Unsworth, A. *'The influence of femoral head surface roughness on the wear of UHMWPE sockets in cementless total hip replacements'*, J. Biomed. Mater. Res.: Appl. Biomechanics, 1999 48(5) pp.712-718

Appendix II Cleaning Protocol

Cleaning protocol BHR

- Rinse in tap water then distilled water
- Wipe with lint free wipe (all surfaces)
- Place in Ultrasonic bath in distilled water for 10 minutes
- Rinse in distilled
- Place in ultrasonic bath in weak neutracon solution for 10 minutes
- Rinse in distilled water
- Place in ultrasonic bath in distilled water for 10 minutes
- Rinse in distilled water
- Place in ultrasonic bath in distilled water for 3 minutes
- Rinse in distilled water
- Rinse in isopropanol and wipe with a lint free wipe (all surfaces)
- Dry with a jet of filtered inert gas
- Place in the vacuum oven at room temperature for 30 minutes to dry
- Weigh to achieve 3 consecutive readings which agree to within 0.1mg.

Appendix III Publications

Conference proceedings

Royal Academy of Engineering UK Biomedical Futures Durham University 13th-15th September 2006 - The wear of high carbon cobalt chromium molybdenum with differing microstructures due to heat treatment on a pin-on-plate machine, A. Kinbrum and A. Unsworth.

The 19th Annual symposium of the international society for technology in arthroplasty New York 6-9th October 2006 – Pin-on-plate studies to asses the effects of heat treatment on the wear of high carbon cobalt chrome molybdenum alloy, A. Kinbrum, A. Unsworth.

British Hip society, annual scientific meeting, Leeds Royal Armoires, 1st and 2nd March 2007 –Hip wear simulator testing of new Birmingham THR modular heads against worn BHR cups, S.M. Lee, A. Kinbrum, K. Vassiliou, A. Kamali and A. Unsworth.

Institute of mechanical Engineers, Engineers and Surgeons: Joined at the Hip, London, 19-21st April 2007 – The wear of different high carbon metal-on-metal bearings after different heat treatments A. Kinbrum, A. Unsworth,

45th Annual Meeting of the Orthopedic Research Society, San Francisco March 2-5 2008- The wear of High Carbon Metal-on-metal bearings after different heat treatments, A. Kinbrum, A. Unsworth, A. Kamali,

Journal Papers

A. Knbrum and A. Unsworth, *'The wear of high-carbon metal-on-metal bearings after different heat treatment'*, Proceedings of the institute of Mechanical Engineers Part H: Engineering in Medicine, Volume 222, 2008 (pre press)

P24

PIN-ON-PLATE STUDIES TO ASSESS THE EFFECTS OF HEAT TREATMENT ON THE WEAR OF HIGH CARBON COBALT CHROME MOLYBDENUM ALLOY

A Kinbrum and A Unsworth
Centre for Biomedical Engineering, School of Engineering
Durham University, South Road, DURHAM, DH1 3LE, UK.
Tel: +44 (0)191 334 2507, Fax +44 (0)191 334 2512, amy.kinbrum@durham.ac.uk

INTRODUCTION: Cast Cobalt Chrome Molybdenum alloy (CoCrMo) may be heat treated to improve mechanical properties such as ductility and microporosity. These heat treatments alter the internal microstructure to reduce block carbide formation and increase homogeneity. The wear of as-cast high carbon CoCrMo alloy has been compared with a heat treated form of the same material containing fewer block carbides. Previous wear tests have reported little difference in wear rate between as-cast CoCrMo and heat treated CoCrMo (1, 2).

MATERIALS AND METHODS: Specimens of high carbon (0.266 wt%) CoCrMo alloy either in the as-cast condition or heat treated were tested in a 4 station pin-on-plate machine with reciprocating and rotational motion. A soak control was used in each test to correct for weight fluctuations not caused by wear. All pins and plates tested were manufactured by *SMITH AND NEPHEW ORTHOPAEDICS LTD*. Each test was carried out under the same conditions with a stroke length of 18mm and a force of 40N on each pin during testing. The samples were submerged in 25% bovine calf serum at 37°C which was replaced every 250,000 cycles. The wear was assessed gravimetrically throughout the test and the surface of the pins and plates was investigated using a non-contacting profilometer at the beginning and end of each test. The as-cast test was taken to 2.5 million cycles and the heat treated test to 3 million.

RESULTS: The as-cast CoCrMo gave an average wear factor of 1.670×10^{-6} mm^3/Nm and the heat treated CoCrMo gave a wear factor of 2.406×10^{-6} mm^3/Nm. A statistical test (ANOVA) was carried out on the values and it was found that these two tests are significantly different ($p < 0.05$). These results show that the as-cast alloy performed better than the heat treated alloy.

DISCUSSION: The thermally treated CoCrMo wore 1.44 times more than the as-cast CoCrMo. Carbides could be seen protruding from the as-cast plates surface when analysed at the conclusion of the test whereas the thermally treated plates showed no carbides when analysed. Both tests showed no signs of running in and both sets of results showed linear wear.

CONCLUSION: The well established as-cast CoCrMo has performed better than the thermally treated modified morphology CoCrMo by giving a lower wear factor. Both materials showed a linear wear pattern and therefore no running in. It would appear that the structural differences between the materials cause the different wear factors.

The authors would like to thank SMITH & NEPHEW ORTHOPAEDICS LTD for funding this research.

REFERENCES:

1. D. Dowson *et al.*, *Journal of Arthroplasty* **19**, 118 (Dec, 2004).
2. J. Bowsher, G. *et al.*, *49th Annual Meeting of the Orthopedic Research Society* **Poster #1398** (2003).

RESULTS OF BIRMINGHAM HIP RESURFACING IN INFLAMMATORY ARTHRITIS.

J Daniel, C Pradhan, H Ziaee, DJW McMinn
The McMinn Centre, Birmingham

Introduction: Hip Resurfacing has always been an attractive concept for the treatment of hip arthritis in young patients. Excellent early and medium-term results have been reported with the Birmingham Hip Resurfacing (BHR) device in single and multi-surgeon all-diagnoses and OA series. In the present report we present the results of BHR in inflammatory arthritis.
Methods: This is a single-surgeon consecutive series. There were 15 consecutive hips (12 patients) including 2 women (2 hips) with ankylosing spondylitis (AS) operated at a mean age of 41.7 years (range 29.5 to 54.3 years). Fortytwo hips (31 patients) with seronegative or rheumatoid (RA) arthritis treated with a BHR at a mean age of 40 (13 to 64) years and a follow-up of 2 to 9 (mean 5.9) years were also studied. One patient died 5 years later. Revision for any reason was the end-point and unrevised patients were assessed with Oxford hip scores and reviewed clinico-radiologically with AP and lateral radiographs.
Results: In the RA group there was one failure from femoral neck fracture two months after operation giving a failure rate of 2.4%. There were no failures in this cohort at a follow-up of 1.8 to 8.8 (mean 4.9) years. As a combined group the failure rate of BHRs in inflammatory arthritis is 1.75% and the cumulative survivorship at 9 years is 98.2% (figure).
Discussion: The good results of Birmingham Hip Resurfacing in inflammatory arthritis in this relatively young cohort of patients make this a viable treatment option for these patients. Selection of patients with a reasonable bone quality and adherence to precise operative technique are vital to the success of this procedure.

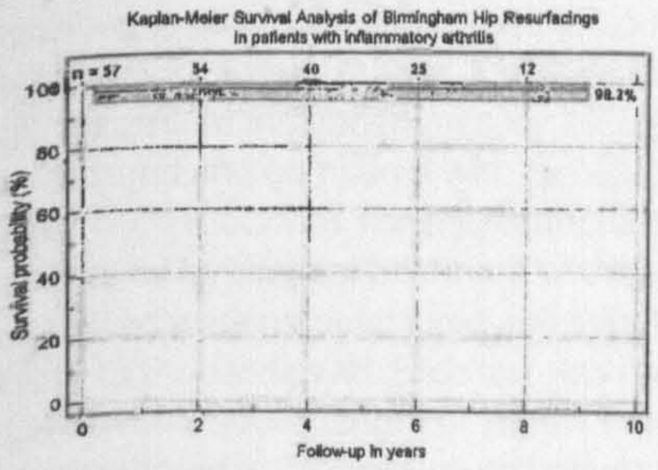

PLACENTAL CONTROL ON THE RATES OF TRANSFER OF COBALT AND CHROMIUM

H Ziaee, J Daniel, PB Pynsent, DJW McMinn
The McMinn Centre, Birmingham

Introduction: The potential adverse effects of metal ion elevation in patients with metal-metal bearings continue to be assessed. We reported earlier that metal ions cross the placenta. The present report is a comparison of the rate of transfer in 14 study patients (with MM devices) and 24 control subjects (with no metal devices).
Methods: Whole blood from concurrent specimens of maternal and umbilical cord blood obtained at the time of delivery were analysed with high resolution inductively coupled plasma mass spectrometry.
Results: Cobalt and chromium were detectable in all specimens in the control subjects and study patients. The mean difference between maternal and cord blood cobalt concentrations was 0.56 µg/l ($p < 0.001$) in the study group and 0.03 µg/l ($p > 0.5$) in the control group respectively (figure). The mean difference between maternal and cord blood chromium concentrations was 0.96 chromium ($p < 0.0005$) in the study group and 0.002 chromium ($p > 0.5$) in the control group respectively. The mean cord cobalt in the study patients was significantly higher than that in the control subjects (difference 0.38µg/l, $p < 0.01$) but the difference in the cord levels of chromium between study and controls (difference 0.13µg/l, $p>0.05$) was not significant.
Discussion: There was almost no difference between the maternal and cord blood levels in the control group implying that the placenta offers almost no resistance to their passage in subjects without a metal device. In the study patients the mean cord cobalt level was 59% of the maternal level and the mean cord chromium level was 26% of the maternal level suggesting that the placenta exerts a modulatory effect on the rate of metal transfer when the maternal levels are higher.

REDUCED DISABILITY AFTER INTRA-ARTICULAR INJECTIONS OF HYLAN G-F 20 IN SYMPTOMATIC HIP OSTEOARTHRITIS

M Venkatesan, A Ahmed, H Mammowalla, B Ilango
Fairfield General Hospital, Bury

Background: Patients suffering from hip osteoarthritis (OA) are frequently symptomatic, and the disease can result in significant limitation of patients' activity and high social costs.
Viscosupplementation, which aims to restore physiological and rheological features of the synovial fluid, is a well-accepted therapeutic option in knee OA patients, but limited data exist in the literature about its potential benefit for the treatment of hip OA.
Aim: To evaluate the efficacy and safety of viscosupplementation (VS) with hyaluronic acid (Hylan GF 20) under fluoroscopic guidance in patients with symptomatic hip OA
Methods: Forty six patients (26 men, 20 women, mean age 56.4 years) with symptomatic hip OA were treated with one injection of 2 ml of hylan G-F 20(Synvisc) under fluoroscopic guidance which could be repeated after at least 3 months. Treatment efficacy was assessed by functional index oxford hip score, pain evaluation on a visual analogue scale and NSAID consumption. All such parameters were recorded at baseline as well as 2, 6 and 12 months after the beginning of the treatment.
Results: We observed a statistically significant reduction of all considered parameters at the timepoints 2 and 6 months, when compared to baseline. At 12 months the changes were still statistically significant for all parameters for about 50% of the patients.
Three patients reported self-limited mild, local pain post-injection otherwise no systemic adverse events were observed.
Conclusion: Viscosupplementation with hylan G-F20 is feasible, easy to perform as well as safely relieves osteoarthritis hip pain, facilitates an improved activity level, decreases the need for pain medication, physiotherapy, and assistive devices.

THE EFFECT OF CUP DEFLECTION ON FRICTION IN METAL-ON-METAL BEARINGS

**A Kamali; *JT Daniel; **SF Javid; **M Youseffi; *T Band; *R Ashton; *A Hussain; *CX Li; ***J Daniel; ***McMinn DJW*
**Smith and Nephew Orthopedics Ltd. Warwick, United Kingdom*
***School of Eng, Design and Technology – Medical Eng, University of Bradford, Bradford, United Kingdom*
****The McMinn Centre, Birmingham, United Kingdom.*

Introduction: Cementless cup designs in metal-on-metal (MoM) hip resurfacing devices generally depend on a good primary press-fit fixation which stabilises the components in the early post-operative period. Press-fitting the cup into the acetabulum generates non-uniform compressive stresses on the cup and consequently causes non-uniform cup deformation. That in turn may result in equatorial contact, high frictional torque and femoral head seizure. It has been reported that high frictional torque has the potential to generate micromotion between the implant and its surrounding bone and as a result adversely affect the longevity of the implant. The aim of this study was to investigate the effects of cup deformation on friction between the articulating surfaces in MoM bearings with various clearances.
Materials and methods: Six Birmingham Hip Resurfacing (BHR) devices with various clearances (80 to 306 µm) were tested in a hip friction simulator to determine the friction between the bearing surfaces. The components were tested in clotted blood which is the primary lubricant during the early post-operative period. The joints were friction tested initially in their pristine conditions and subsequently the cups were deflected by 25-35 µm using two points pinching action before further friction tests were carried out.
Results and Discussions: It has been reported that reduced clearance results in reduced friction. However, none of the previous studies have taken cup deflection into consideration nor have they used physiologically relevant lubricant. The results presented in this study show that for the reduced clearance components, friction was significantly increased when the cups were deflected by only 30 µm. However, for the components with higher clearance the friction did not change before and after deflection. It is postulated that the larger clearances can accommodate for the amount of distortion introduced to the cups in this study.

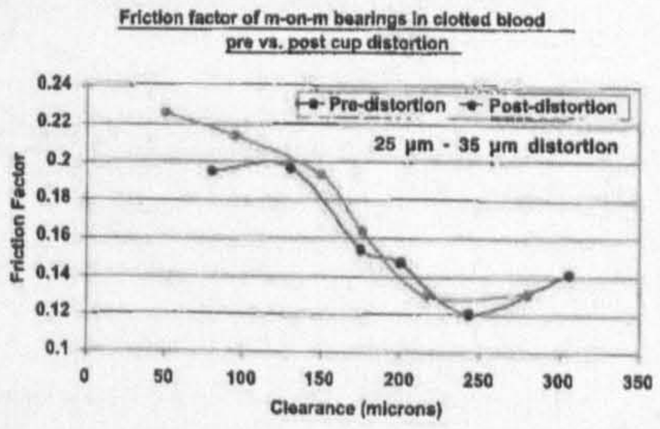

Figure 1. Friction vs. clearance in pre and post distorted cups for MoM joints

IMPORTANCE OF SOFT TISSUE DISSECTION IN PLACEMENT OF REFERENCE MARKER PINS IN COMPUTER AIDED HIP ARTHROPLASTY.

T.N. Board[2], D. Kendoff[1], C. Krettek[1], T. Hüfner[1]
[1] Trauma Department, Hannover University, Germany.
[2] The Hip Centre, Wrightington Hospital, Wigan, UK.

Introduction: Movement of the limb during computer aided arthroplasty may cause soft tissue impingement on the reference marker(RM) and consequently alter the spatial relationship between RM and bone with resulting inaccuracies in navigation. The purpose of this study was to investigate the effect of different degrees of soft tissue dissection on the stability of reference markers during limb movement.
Methods: The stability of both one- and two-pin RM systems inserted using three different levels of soft-tissue dissection was analysed in relation to a super-stable RM in fresh cadaver lower limbs. The spatial relationship of the two RMs was analysed using the VectorVision® system (BrainLAB, Germany) during multiple repetitions of four predefined limb movements. All tests were done with RMs inserted in both the distal-anterior femur and distal-lateral femur.
Results: Analysis of movements of the test RM in relation to the super-stable RM showed that rotations of less than 0.15° and translations of less than 0.4mm occurred in most test combinations. The combination that showed the greatest instability was when a stab incision was used to insert a pin in the distal/lateral femur (translation 0.73mm+/-0.05, rotation 0.25°+/-0.05)($p<0.001$). This instability occurred in both single and double pin RMs($p=0.21$).
Conclusions: RM pins can be placed in the anterior distal femur through simple stab incisions without resulting in significant soft tissue impingement during limb movement. If pins are placed in the lateral distal femur through stab incisions, impingement may occur from the fascia lata. Release of the fascia lata 1cm either side of the pin prevents significant impingement. Wide skin incision is unnecessary in any location.

HIP WEAR SIMULATOR TESTING OF NEW BIRMINGHAM THR MODULAR HEADS AGAINST WORN BHR CUPS

**SM Lee, *A Kinbrum, *K Vassiliou, **A Kamali and *A Unsworth*
**Centre for Biomedical Engineering, School of Engineering, Durham University,*
South road, DH1 3LE
**Smith and Nephew Orthopedics Ltd. Warwick, United Kingdom*

Introduction: The Birmingham Hip Resurfacing (BHR) system comprises both a BHR femoral head and a large modular femoral head for use should a total hip replacement be required. The modular femoral head has identical material chemistry, microstructure, spherical form, and surface roughness of the bearing surfaces of resurfacing femoral head and both BHR and THR devices share the same acetabular components. Hence, if the femoral component of a BHR needs revision surgery, the Birmingham hip system provides the potential of converting it to a THR without the need to also revise the well fixed cup. Although it stands to reason that the wear behaviour of the BHR and Birmingham THR will be similar, it is important to investigate the wear behaviour of new THR modular heads against worn BHR cups, representing revision of BHR to Birmingham THR without cup revision. The aim of this study is to assess the viability of the femoral component revision for BHR devices whilst leaving the acetabular components in situ in the pelvis.
Materials and Methods: The wear and friction tests were conducted with pristine modular heads paired with BHR cups which had already undergone 5 million cycles (Mc) of wear in a hip simulator against BHR heads.
Results and Discussions: The average wear rate of the new Birmingham THR modular heads against worn cups was 0.42 mm^3/Mc whilst the new BHR heads against new cups generated wear rate of 0.67 mm^3/Mc. Supported by the friction test results, it indicated that the new femoral heads paired with worn cup did not negatively affect the substantial amount of fluid-film lubrication that had developed over the course of the original test. Therefore, it is acceptable to use new femoral heads against worn cups, if the cups are not damaged, well fixed and correctly orientated.

IMPERIAL APPROACH, A MODIFICATION OF LETOURNEL'S APPROACH TO ACETABULAR FRACTURES

A I Nakhla, A D Lewis, J P Cobb
Imperial College London

Introduction: The development of the ilioinguinal approach by the pioneering work of Letournel in 1965 has transformed the treatment of acetabular fractures. To date, this approach has been well established and few modifications have been described of the original approach. However, this approach is difficult, takes long time for exposure and closure of abdominal layers. The aim of this article is to report a modification of the approach which the authors have found particularly useful.
Material and Method: Cadaveric dissection showed that it was easier to detach the inguinal ligament from the anterior superior iliac spine and reflect the anterior abdominal wall as one layer, than by the classical approach through layers of the anterior abdominal wall. Closure was also simpler, in the cadaver, with the entire anterior abdominal wall reattaching satisfactorily by a single transosseous suture. The rest of the approach, including division of iliopectineal fascia and developing the three windows remains the same as in the original approach.
Results: To date, three acetabular fractures have been reduced and fixed using this modification. Besides substantially speeding up the exposure and closure, this approach allows superior distal visualization of the anterior column and wall, and the impression of rather less bleeding. No complications developed with the three cases treated through this modified

THE WEAR OF HIGH CARBON COBALT CHROMIUM MOLYBDENUM WITH DIFFERING MICROSTRUCTURES DUE TO HEAT TREATMENT ON A PIN-ON-PLATE MACHINE

Kinbrum A. and Unsworth A.

Durham University, Durham, DH1 3LE

Introduction: Tests on some heat treated CoCrMo hip joints have shown little difference in wear over as-cast CoCrMo (1). In this test as-cast material is compared with a heat treated form of the same material with fewer carbides.

Materials and Methods: A four station pin-on-plate test machine with reciprocating and rotating motion was used to test the two different microstructures of the same alloy against themselves. A soak control was used to correct for weight deviations not caused by wear. A high carbon but low carbide cobalt chromium molybdenum alloy (HCLC CoCrMo) was manufactured and compared with as-cast cobalt chromium molybdenum (CoCrMo). The microstructure of the HCLC alloy was achieved by thermal treatment of the alloy. All pins and plates tested were manufactured and supplied by Smith and Nephew Orthopaedics ltd. Each test was carried out on the same machine with a stroke length of 18mm. The contacting surfaces were submerged in 25% bovine calf serum at 37°C and a 40N force was exerted on the pin during testing. The wear was assessed gravimetrically and the surface of the plates was assessed using a non-contacting profilometer before and after the 2.5million cycle and 3 million cycle tests respectively.

Results: The two different materials CoCrMo and HCLC CoCrMo gave average wear factors of 1.670×10^{-6} and 2.40604×10^{-6} mm^3/Nm respectively. The wear factors show that the as cast CoCrMo performed better than the HCLC CoCrMo.

Discussion: The wear factor is lower on the pins and the plates for the as-cast CoCrMo compared to the HCLC CoCrMo the wear rate of the HCLC is 1.44 times that of the as-cast specimen. The wear factors found for the as-cast CoCrMo are comparable with other work within this laboratory (*2*). In the as-cast tests the pin wear was roughly 100 times higher than the plate wear. Both materials showed no signs of running in. Both graphs show linear wear. The distribution of wear rates among samples was lower in the as-cast test showing a higher reliability. With larger numbers of specimens on actual hips, an outlier is usually observed (*3, 4*), although this is not yet understood. This phenomenon was not seen in these tests.

Conclusion: The well established as-cast CoCrMo with a block carbide morphology has performed better than the thermally treated, modified microstructure HCLC CoCrMo. Not only has it given a lower wear factor it has also shown itself to be a more reliable material. Linear wear was seen showing no tendency for running in for either material. As the percentage carbon is the same in the materials it appears to be the structural differences that cause the difference in wear factor between the two test specimens.

References:

1. Dowson D. *et al., J. Arthroplasty* **19**, 118 (2004).
2. Scholes S. C. *et al., J. Mater. Sci. Mater. Med.* **12**, 299 (2001).
3. Vassiliou K. *et al., Proc. Inst. Mech. Engrs.* **220**, 269 (2006).
4. Essner A. *et al., Wear* **259**, 992 (2005).

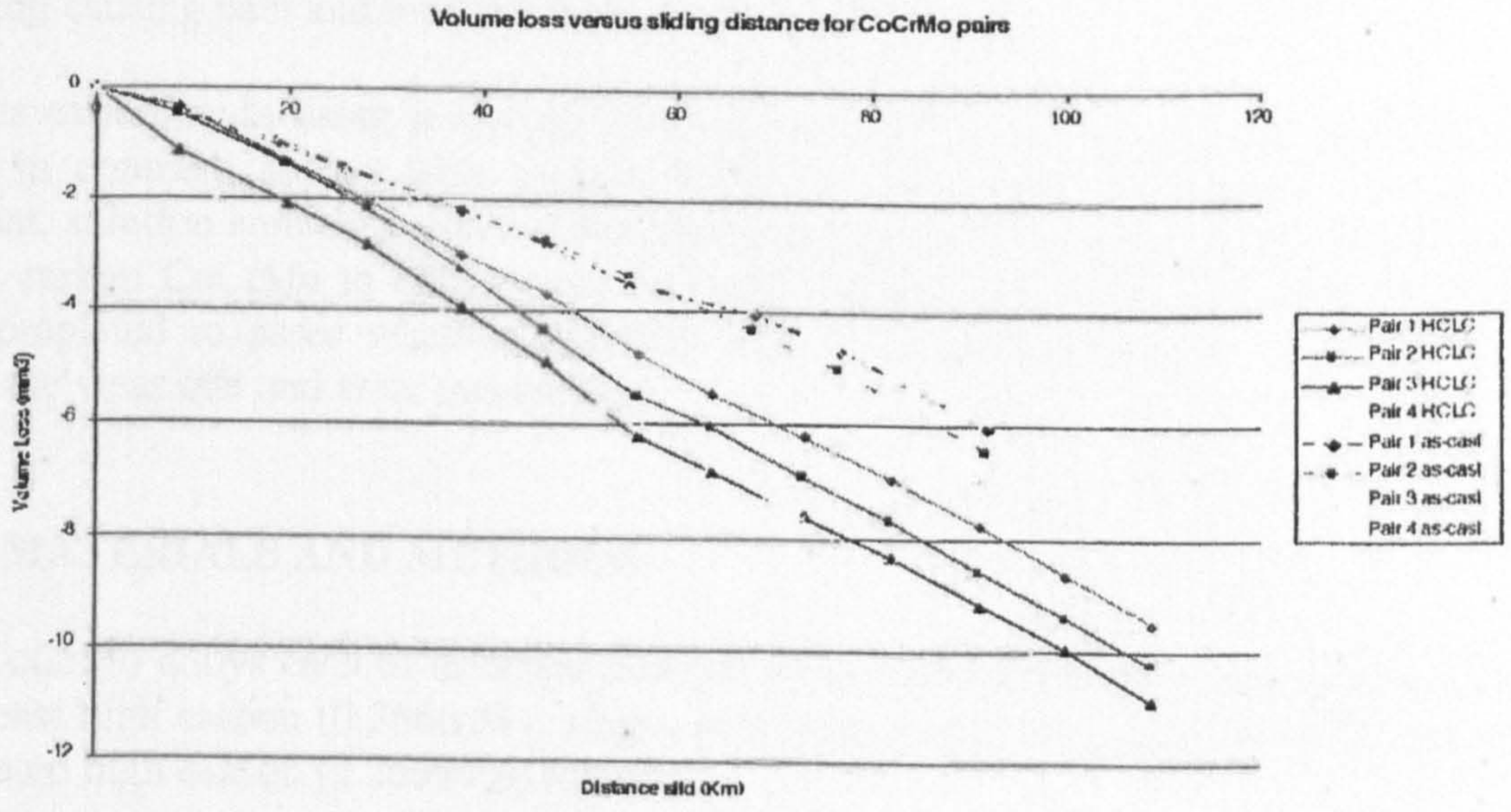

Figure 1 As-cast and HCLC CoCrMo volume lost vs distance slid.

The Wear of High Carbon Metal-on-Metal Bearings After Different Heat Treatments

A.Kinbrum, A. Unsworth
Centre for Biomedical Engineering, Durham University, Durham, England

SYNOPSIS

Three paired samples of CoCrMo alloy were tested in a pin-on-plate wear machine. One pair was in the "as-cast" condition, a second pair was heat treated once to allow some of the carbides to go into solution and a third pair was double heat treated to ensure all the carbides went into solution. The as-cast specimens showed the lowest wear rate, the reduced carbide samples had the next lowest wear rate whilst the specimens without carbides wore most.

1. INTRODUCTION

In recent years there has been revived interest in metal-on-metal implants due to the association of osteolysis with polyethylene wear debris (1). Osteolysis can lead to aseptic loosening causing pain and revision of the total hip arthroplasty.

Previous experiments using a low carbon content CoCrMo alloy produced high wear rates (2),but in contrast, as-cast high carbon proved to be a good bearing material (3). Heat treatment, solution annealing and hot isostatic pressing (HIP) allow the hard blocky carbides in high carbon CoCrMo to diffuse into the softer matrix material. Pin-on-plate studies have been completed to asses whether different amounts of heat treatment of CoCrMo alloys change the wear rate and wear mechanism.

2. MATERIALS AND METHODS

Three CoCrMo alloys each of different microstructure have been tested on a pin-on-plate test rig; as-cast high carbon (0.266wt%), single heat treated high carbon (0.266wt%) and double heat treated high carbon (0.266wt%) material.

For each microstructure condition of CoCr alloy five pin and plate pairs were tested on the Durham pin on plate machine to 3 million cycles. Four of the pins and plates underwent rotation and reciprocation at a frequency of 1 Hz and the final pair was used as a control. The stroke length was 18mm and the load on the pins was 40N. Surface topography was measured at the start and end of the test using a Zygo NewView 100 non-contacting 3D profilometer. Ten roughness measurements of Ra, Rrms, PV and skewness were taken from each of the plates and one from the pins. Only one reading of the pins was taken initially as the hemispherical head could only be analysed at the pole. The method described and equipment used is identical for each of the 3 tests performed.

The pins and plates used were manufactured from the same material as the as-cast CoCrMo material used for Birmingham hip resurfacing (BHR) devices. The pins were 6mm diameter and cylindrical in shape. The bearing end was hemispherical and a flat was added to the upper side to secure them with a grub screw in the pin holder. The plates were 25mm diameter with a segment ground off on one edge to hold them with a grub screw in the lubricant bath. These were made from the same materials as the pins. All the samples were chemically identical to each other, although the test parts underwent various heat treatments to alter the internal morphology.

Specimens were cleaned and weighed initially (ISO 14242-2) and after each period of approximately 250 000 cycles of wear. A Mettler AE200 balance was used to weigh the samples. This balance measured up to 205g with a sensitivity of 0.1mg. The changes in weight were recorded and the volume loss was calculated using the density of the material ($0.0082 g/mm^3$).

The test was carried out in bovine serum lubricant (batch number 5030401, Harlan Sera-lab, total protein content 56g/l) diluted to 25% with distilled water. Added to this was 0.2% sodium azide and 20mM EDTA (ethylenediaminetetraacetic acid) to help resist biodegradation of the lubricant and calcium deposit formation respectively. The test was carried out at 37°C and the lubricant temperature was monitored using a K-type thermocouple which was attached over the edge of the bath. The unused serum was kept frozen at -20°C and made up as needed, after which it was kept refrigerated at 4°C.

3. RESULTS

Figure 1 shows the wear rate of the pins, the plates and the total wear rate over 3 million cycles for the 3 different materials. The error bars indicate one standard deviation. Average wear rates for the as-cast, partially heat treated and fully heat treated are 1.69×10^{-6} mm^3/Nm, 2.1×10^{-6} mm^3/Nm and 2.41×10^{-6} mm^3/Nm respectively.

Figure 2a shows a scanning electron micrograph (SEM) of the worn surface of the as-cast material. All the images were taken at 80° to the vertical. The hard carbides can be seen on the wear track. Figure 2b shows the worn surface of the single heat treated plate. Small pits and scratches can be seen in this image and the carbides are less obvious. Figure 2c shows an SEM image of the wear track of the double heat treated material. The large pits shown are where pieces have been pulled out of the surface. No carbides can be seen.

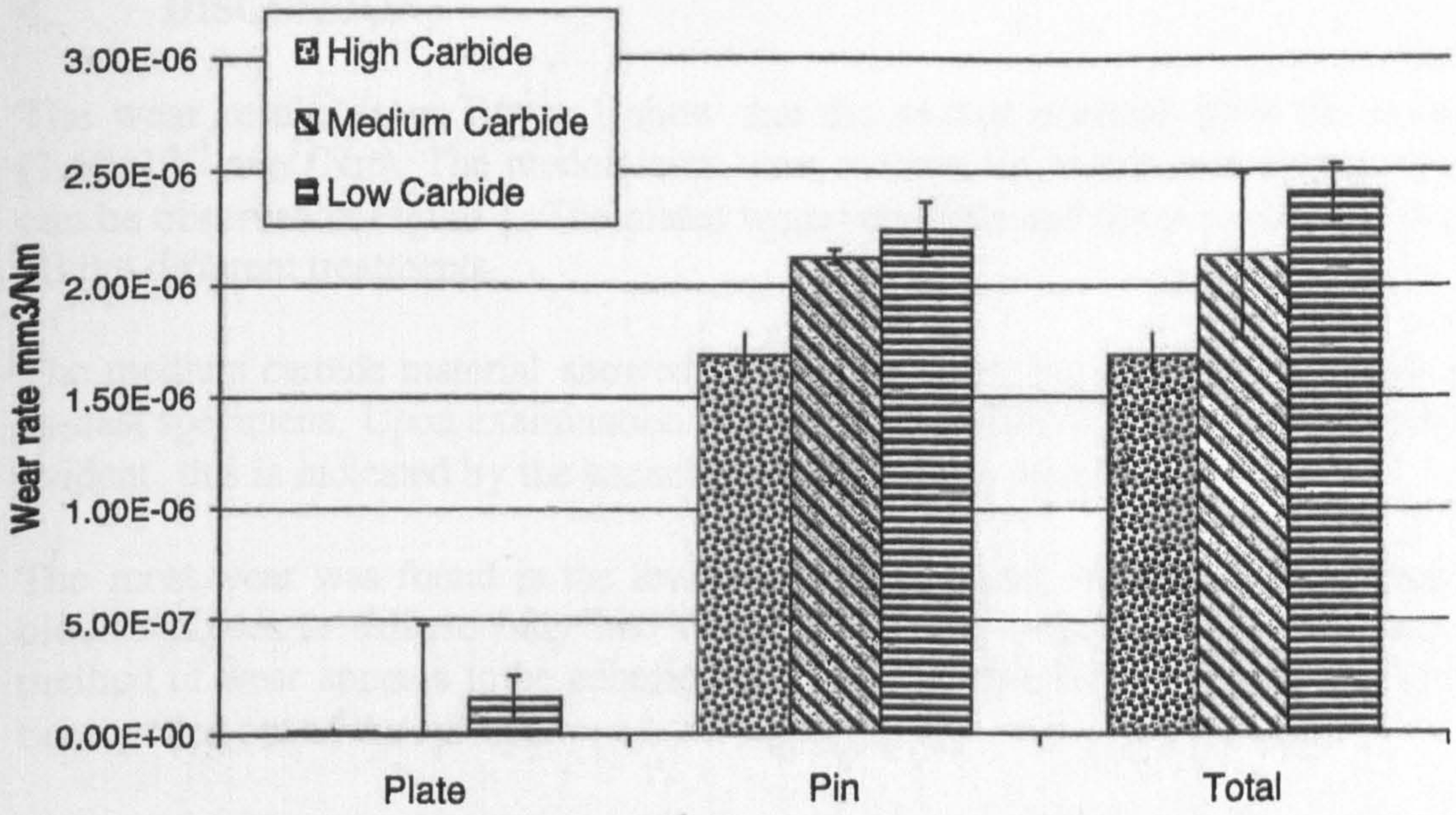

Figure 1: Comparison of the wear factors of varying carbide CoCrMo

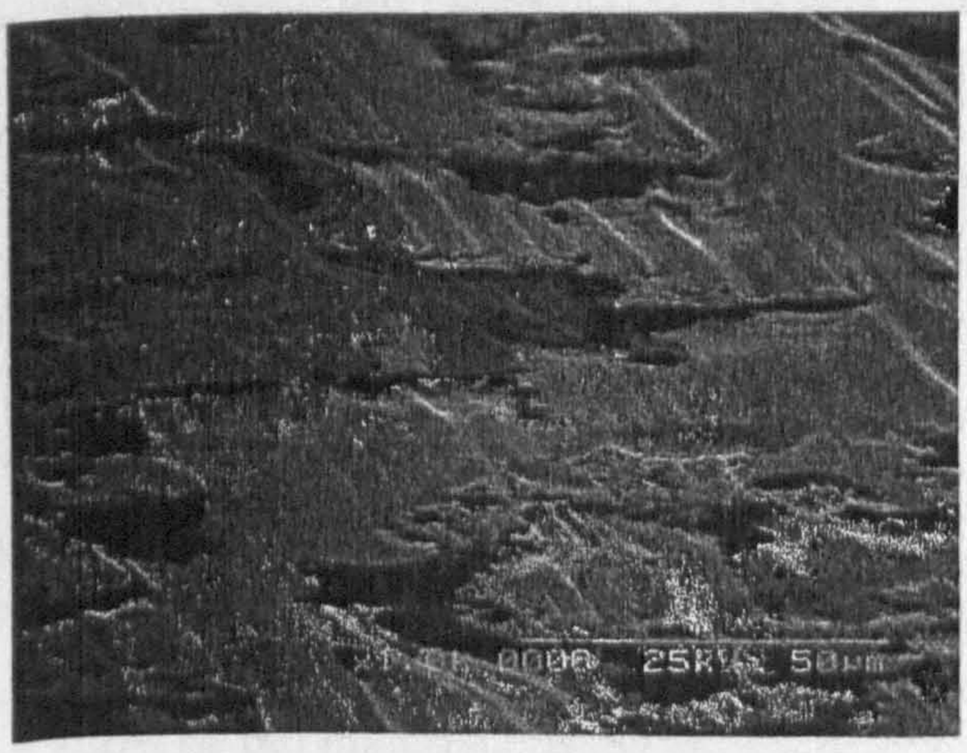

Figure 2a: As-cast at 1k mag.

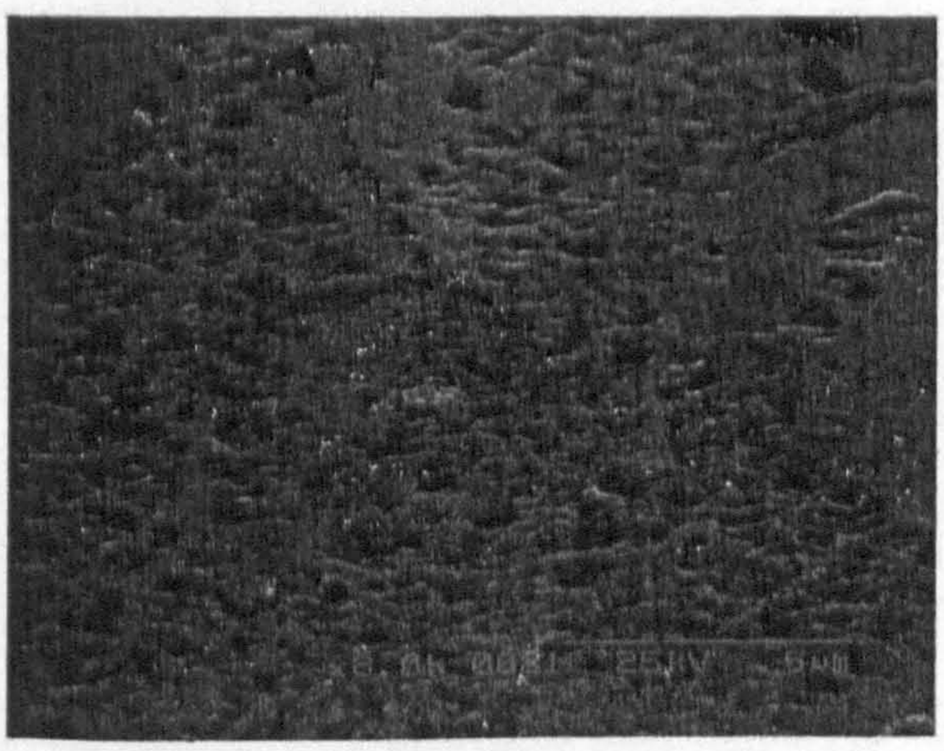

Figure 2b: Partially heat treated at 8k mag.

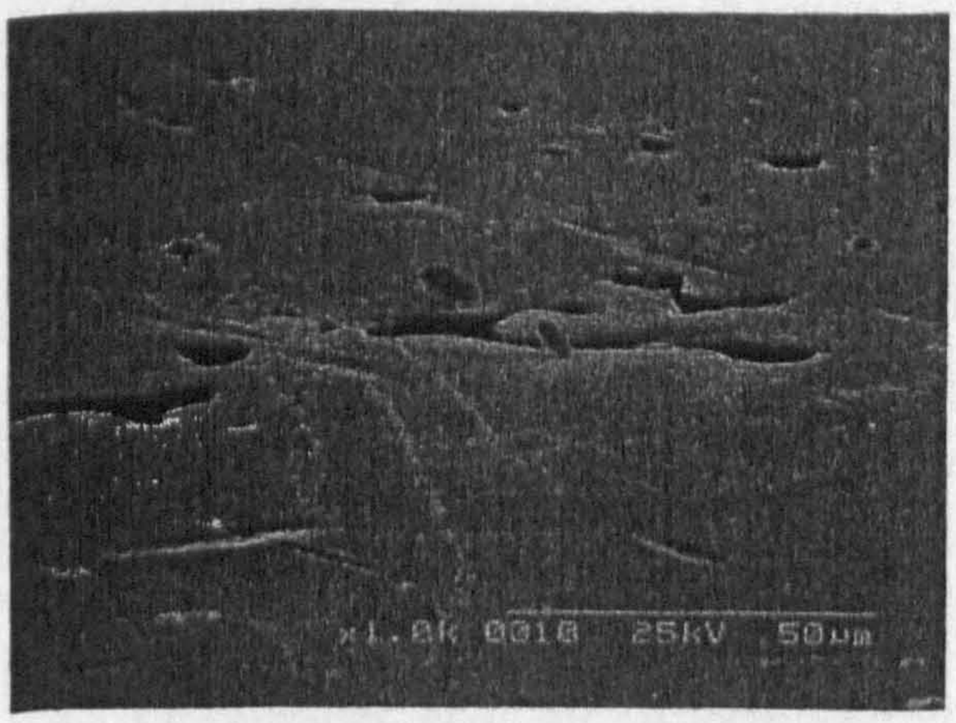

Figure 2c: Fully heat treated at 1k mag.

Figures 2 a, b, c: SEM of the plate surfaces after 3million cycles wear.

4. DISCUSSION

The wear results from Figure 1 show that the as-cast material gave the lowest total wear ($1.69x10^{-6}$ mm^3/Nm). The predominant wear mechanism in this case was abrasive wear, as it can be observed in Figure 1. The plates wore very little and the pins showed the least wear of all the different treatments.

The medium carbide material showed similar plate wear but slightly higher pin wear than the as-cast specimens. Upon examination of the surface, abrasive and adhesive wear seemed to be evident, this is indicated by the scratches and small pits visible in Figure 2b.

The most wear was found in the lowest carbide material, where heat treatment had allowed block carbides to diffuse fully into the matrix. Upon inspection of the surface the primary method of wear appears to be adhesion. Figure 2c shows large pits where material may have been pulled out of the surface.

Due to the nature of pin on plate testing the lubrication regime is likely to differ from that of a prosthetic joint. Previous authors (4) show no statistical difference in wear rates between as-cast and solution annealed or HIPped materials when testing large diameter hip prostheses in joint simulators. This is likely to be because in the full simulator, using real joint components, fluid film lubrication can be generated (5) whereas in pin-on-plate machines the contact will eliminate any fluid film lubricant so that the effects of material properties can be tested

5. CONCLUSION

Wear results show the as-cast material to give the lowest wearing of the three microstructures that were tested. Surface assessment of the as-cast CoCrMo indicates that the wear regime is mainly abrasive wear. The medium carbide material proved to be the next lowest wearing and surface analysis indicated both abrasive and adhesive wear. The low carbide material wore the most of the materials tested and surface analysis indicated mainly adhesive wear.

ACKNOLEGEMENTS

The authors would like to thank Smith and Nephew Orthopaedics for funding this work and supplying the materials.

REFERENCES

1 D. W. Howie, *et al,* J. Bone Joint Surg. Vol 70-A No2 pp257-263 (1988).
2 D. Dowson, *et al,* J. Arthroplasty vol 19 supl. 3 pp118-123 (2004).
3 M. Schmidt, *et al*, Clinical Orthopaedics and related research vol 329S pps35-s47 (1996).
4 J. G. Bowsher, *et al,* 49th Annual Meeting of orthopaedic research society Poster 1398.
5 K.Vassiliou *et al*, Proc. Inst. IMechE Vol. 220 Part H J. Engineering in Medicine pp269-279 (2006)

The Wear of High Carbon Metal-on-Metal Bearings After Different Heat Treatments

Amy Kinbrum[1], Anthony Unsworth[1], Amir Kamali[2]
[1]Centre for Biomedical Engineering, Durham University, Durham, United Kingdom; [2]Implant Development Centre, Smith & Nephew Orthopaedics Ltd., Leamington Spa, United Kingdom
tony.unsworth@durham.ac.uk

Introduction: In recent years there has been revived interest in metal-on-metal implants due to the association of osteolysis with polyethylene wear debris (1). Osteolysis can lead to aseptic loosening causing pain and revision of the total hip arthroplasty.

Previous experiments using an as-cast low carbon content CoCrMo alloy produced high wear rates (2), but in contrast, as-cast high carbon CoCrMo alloy proved to be a good bearing material (3). Heat treatment, solution annealing and hot isostatic pressing (HIP) cause the hard blocky carbides in high carbon CoCrMo to diffuse into the softer matrix material. Pin-on-plate studies have been completed to asses whether different amounts of heat treatment of CoCrMo alloys change the wear rate and wear mechanism.

Materials and Methods: High carbon (0.266wt%C) CoCrMo specimens have been tested on a pin-on-plate test rig in one of 3 different conditions; as-cast, single heat treated and double heat treated material.

For each specimen five pin and plate pairs were tested on the Durham pin on plate machine to 3 million cycles. Four of the pins and plates underwent rotation and reciprocation at a frequency of 1 Hz and the final pair was used as a control. The stroke length was 18mm and the load on the pins was 40N. Surface topography was measured at the start and end of the test. The method described and equipment used was identical for each of the 3 tests performed.

The pins and plates used were manufactured from the same material as the as-cast CoCrMo material used for Birmingham hip resurfacing (BHR) devices. The pins were 6mm diameter, cylindrical in shape and the bearing end was hemispherical. The plates were 25mm diameter with a segment ground off on one edge to hold them with a grub screw in the lubricant bath. These were made from the same materials as the pins. All three materials were chemically identical to each other, although the materials underwent various heat treatments to alter the metalurgical structure.

Specimens were cleaned and weighed initially (ISO 14242-2) and after each period of approximately 250 000 cycles of wear. The volume loss was calculated using the density of the material (0.0082g/mm3) and the serum was collected at each of these intervals and analysed.

The test was carried out at 37OC in bovine serum lubricant (batch number 5030401, Harlan Sera-lab, total protein content 56g/l) diluted to 25% with distilled water. Added to this was 0.2% sodium azide and 20mM EDTA (ethylenediaminetetraacetic acid) to help resist biodegradation of the lubricant and calcium deposit formation respectively. The unused serum was kept frozen at -20OC and made up as needed, after which it was kept refrigerated at 4OC.

Analysis of the particles in the serum involved digesting the protein using Papain and Protease K. Deionised water, sodium dodecyl sulphate, acetone and buffers were used to wash the particles before and after the protein digestion. Subsequently the particles were separated from the solution in an ultracentrifuge. This pellet was resuspended in 1.5 ml of water and analysed using a Nanosight LM10. The LM10 estimates the size of the particles by tracking their movement as they scatter a laser beam. The particles move due to Brownian motion and if the temperature is known the Stokes-Einstein equation can be used to compute the size of the particles from their paths.

Results: Figure 1 shows the wear rate of the pins, the plates and the total wear rate over 3 million cycles for the 3 different CoCr microstructures

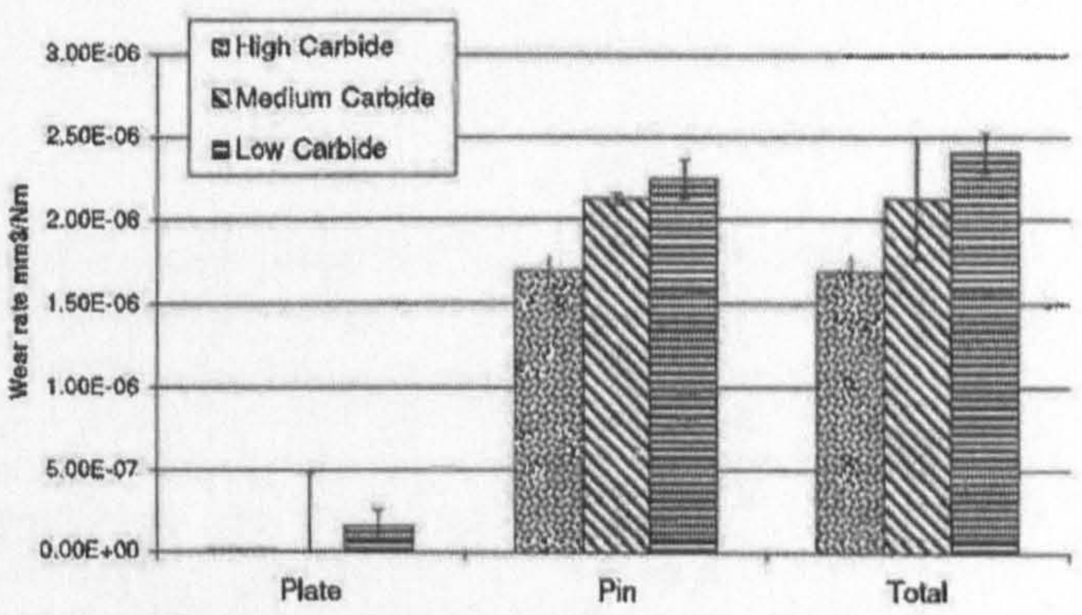

Figure 1. Comparison of the CoCr wear with various carbide volume fractions

. The error bars indicate one standard deviation. Average wear rates for the as-cast(high carbide), single heat treated (medium carbide) and double heat treated (low carbide) are 1.69×10^{-6} mm^3/Nm, 2.1×10^{-6} mm^3/Nm and 2.41×10^{-6} mm^3/Nm respectively.

Discussion: The wear results show that the as-cast material gave the lowest total wear (1.69×10^{-6} mm^3/Nm). The plates wore very little in this study.

The as-cast material was the lowest wearing of the three materials tested. Surface assessment of the as-cast CoCrMo indicated that the wear regime was mainly abrasive wear. The medium carbide material was the next lowest wearing and surface analysis indicated both abrasive and adhesive wear. The low carbide material had the greatest wear and surface analysis indicated mainly adhesive wear.

High carbide (as-cast) material produced wear particles of a similar size over the 3 million cycles typically less than 400nm. There was very little variation in size distribution and concentration. Low carbide (double heat treated) material produced an initially low concentration of particles whose sizes were distributed over a large range. As the test progressed the concentration increased and the average size reduced.

References: 1 D. W. Howie, et al, J. Bone Joint Surg. Vol 70-A No2 pp257-263 (1988).

2 D. Dowson, et al, J. Arthroplasty vol 19 supl. 3 pp118-123 (2004).

3 M. Schmidt, et al, Clinical Orthopaedics and related research vol 329S pps35-s47 (1996).

Acknowledgements: The authors would like to thank Smith and Nephew Orthopaedics for funding this work and supplying the materials.

The wear of high-carbon metal-on-metal bearings after different heat treatments

A Kinbrum* and **A Unsworth**
Centre for Biomechanical Engineering, School of Engineering, Durham University, Durham, UK

The manuscript was received on 17 December 2007 and was accepted after revision for publication on 4 March 2008.

DOI: 10.1243/09544119JEIM387

ABSTRACT: To study the tribological performance of metal-on-metal hip joint resurfacings the wear performance of three pairs of Co–Cr–Mo alloy samples (pins and plates) were tested in a multidirectional pin-on-plate wear machine. An 'as-cast', a single-heat-treated, and a double-heat-treated set of specimens were tested to 3×10^6 cycles. The two heat treatments resulted in partial and full solution of the carbides into the matrix. An increasing trend in wear rate was found from 'as-cast' to the double-heat-treated specimens. The as-cast specimens showed the lowest wear rate ($1.69\times10^{-6}\,mm^3/N\,m$), the reduced carbide samples had the next lowest wear rate ($2.1\times10^{-6}\,mm^3/N\,m$), whilst the specimens without carbides wore the most ($2.41\times10^{-6}\,mm^3/N\,m$).

Keywords: metal-on-metal bearings, wear, Co–Cr–Mo alloy

1 INTRODUCTION

One of the most commonly used hip replacements has been the Charnley metal-on ultra-high-molecular-weight polyethylen (UHMWPE) low-friction arthroplasty [1], however, concern is growing over their use. The volume of wear particles produced by a metal-on-UHMWPE total hip arthroplasty is much larger than the alternative bearing materials such as metal-on-metal or ceramic-on-ceramic prostheses [2–8].

As the average age of people demanding hip arthroplasty decreases, alternative prostheses have to be devised.

The Archard [9] wear equation shows that the total volume of wear is inversely proportional to the hardness of the softer material comprising the bearing surfaces. Thus theoretically metal-on-metal prostheses should give lower wear than metal-on-polymer joints. One such metal-on-metal joint (the Mckee–Farrar prosthesis) was used in the midtwentieth century, but many of these arthroplasties failed. The main causes of failure were seizure and loosening. However, some of these joints went on to give excellent service lifetimes in excess of 30 years; therefore, in recent times the idea of metal-on-metal joints has been revived. Studies of successful hip joints have shown that the clearance should not be too small and that surface finish is an important factor [10, 11]. A higher relative velocity, due to the larger head rotating over the same angle, is more likely to bring about full fluid film lubrication than that due to a smaller-diameter head. Additionally the larger area of a larger head increases the supporting area for the load, decreasing the lubricant pressure; this may help to create fluid-film lubrication.

A further refinement is the head size. The trend of total hip replacements has been to have small-diameter heads (22–32 mm) because of the Archard equation which shows that lower wear is attained under dry rubbing conditions by smaller-diameter joints [9]. However, if the joints are designed to run under fluid-film-lubricated conditions, the two surfaces may be separated by a fluid film for much of the time and wear will consequently be reduced. Vassiliou *et al.* [12] have shown experimentally that larger diameter metal-on-metal joints encourage fluid-film lubrication owing to the higher entraining velocity.

**Corresponding author: Centre for Biomechanical Engineering, School of Engineering, Durham University, South Road, Durham, DH1 3LE, UK. email: amy.kinbrum@durham.ac.uk*

jeim387 23-4-08 09:50:52 Rev 7.51n/W (Jan 20 2003)
The Charlesworth Group, Wakefield 01924 204830

Another important aspect of large-diameter heads is their stability and range of motion. Larger-diameter heads resist joint dislocation and yield a greater range of motions, thereby allowing younger, more active patients to benefit when a large-diameter metal-on-metal joint is used. Once the concept of a large diameter head has been accepted, then this lends itself to a resurfacing procedure rather than total hip replacement (depending on the bone density). Advantages such as bone preservation for young patients allow a better opportunity for a subsequent total hip replacement, should any problems arise with the resurfacing.

Numerous joint manufacturers offer metal-on-metal prostheses as part of their product range and these tend to be high-carbon Co–Cr–Mo alloy. However, they are not all heat treated in the same way. 'As-cast', solution-annealed once or several times, and hot isostatically pressed components are available. These processes change the internal structure of Co–Cr–Mo and this may well be important to the wear performance of the joints.

Experiments using low-carbon-content Co–Cr–Mo alloys have been shown to produce high wear rates [13] compared with as-cast high-carbon (0.266 wt %) material [5]. All manufacturers have now moved away from low-carbon products as bearing materials within the body.

Heat treatment in the form of solution annealing and hot isostatic pressing allow the hard blocky carbides formed in high-carbon Co–Cr–Mo to diffuse into the softer matrix material. This gives a homogeneous material structure and changes the nature of the surface topography achieved through polishing. Single-treatment annealing leads to smaller carbides in the material whereas double-treatment annealing leads to almost no visible carbides (using scanning electron microscpy (SEM)).

The aim of the current work is to determine and compare the wear properties of as-cast (high-carbide), single-annealed (medium-carbide) and double-annealed (low-carbide) Co–Cr–Mo alloys under identical tribological conditions.

2 MATERIALS AND METHODS

Identical high-carbon-content (0.266 wt %) components were manufactured with three different treatments. These were 'as- cast', single heat treated, which was held at 1200 °C for 4 h, and double heat treated, which was held at 1200 °C for 4 h on two separate occasions. These heat treatments replicate current standard heat treatment methods in the orthopaedic industry.

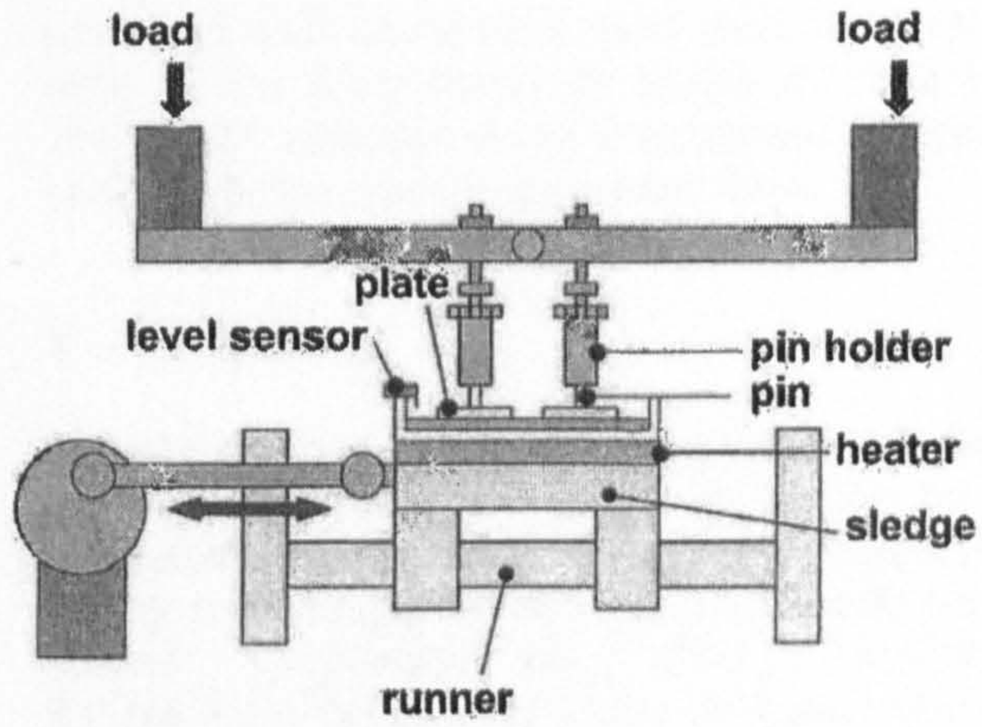

Fig.1 Schematic diagram of a pin-on-plate machine

Five pin-and-plate pairs for each treatment were tested, using the Durham pin-on-plate machine, to 3×10^6 cycles (Fig. 1). Four of the pins and plates underwent rotation and reciprocation at a frequency of 1 Hz with the final pair used as a control. The specimen were immersed within a bath of lubricant (25 per cent bovine serum with added ethylene diamine tetraacetic acid (EDTA) and sodium azide), held at 37 °C. The plates were secured into the bath using a plastic insert and the pins were located into holders attached to the individual motors which produced rotation. The load on the plate through the pin was 40 N. The pins and plates were removed, cleaned, dried, and weighed every 250 000 cycles. A stroke length of 18 mm was used which is comparable with the length of the wear scar using 30° flexion and 15° extension on a prosthesis of 50 mm diameter. The control samples were immersed in 25 per cent serum within a jar and kept in a heated water bath at 37 °C for the duration of this experiment. The control sample was removed, cleaned, dried, weighed, and analysed together with the test specimens.

Figure 1 shows the specimen located within a bath into which lubricant was poured. The lubricant was maintained at the desired level and at 37 °C. The motor on the left drove a crank which produced reciprocating motion by driving the sledge along the bars. The four smaller motors drove the pins in a rotational motion. A magnetic counter recorded the number of cycles thus enabling the distance slid to be calculated.

The Co–Cr–Mo specimens used for the pins and plates were manufactured from the same material as that used for the Birmingham hip resurfacing

jeim387 23-4-08 09:50:53 Rev 7.51n/W (Jan 20 2003)
The Charlesworth Group, Wakefield 01924 204830

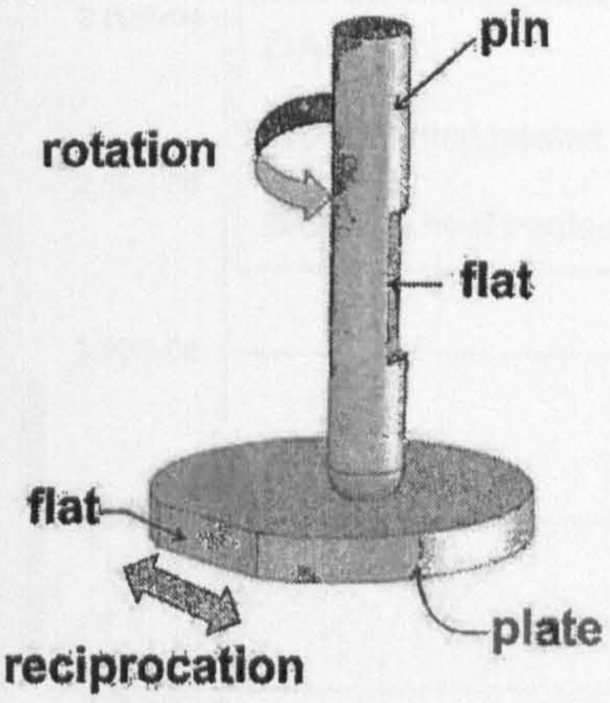

Fig. 2 Diagram of a pin and plate

devices. The cylindrical pins had a 6 mm diameter. The bearing end was hemispherical and a flat was added to the upper side of the pin (Fig. 2) to secure it with a grub screw in the pin holder. The plates had a diameter of 25 mm with a segment ground off along one edge (Fig. 2) to hold them in the lubricant bath whilst maintaining the same orientation throughout the test.

Specimens were initially cleaned and weighed using the protocol described in ISO 14242-2 at intervals of approximately 250 000 cycles. A Mettler AE205 balance, which had a maximum load of 205 gf and a sensitivity of 0.01 mgf was used to weigh the samples. The changes in weight were recorded and the volume loss was calculated using a density of 0.0082 g/mm^3.

The test was carried out in bovine serum lubricant (batch number 5030401, Harlan Sera-lab; total protein content, 56 g/l) diluted to 25 per cent with distilled water. In addition, 0.2 per cent sodium azide was used to help to resist degradation of the lubricant and 20 mM EDTA to reduce calcium phosphate deposition. The unused serum was frozen at −20 °C and diluted as needed, after which it was refrigerated at 4 °C.

Surface topography was measured initially and at the end of the test using a Zygo NewView 100 non-contacting three-dimensional profilometer; this instrument had a 0.1nm vertical resolution and the scan had a 40 μm vertical measurement range. Ten roughness measurements of the average roughness R_a), the r.m.s. roughness R_q, the peak-to-valley height, and the skewness were taken from each of the plates [14]. Only one set of roughness measurements was taken from the pins initially as the bearing surface was hemispherical. In the final measurements a flattened end allowed additional repeated measurements to be taken. The method described and equipment used were identical for each of the three materials tested. All data were statistically analysed using a univariate analysis of variance in the statistical package SPSS.

3 RESULTS

Figure 3 shows the wear rates of the pins, the plates, and the total wear rate over 3×10^6 cycles for the three material treatments. Average ($n=4$) wear rates for the as-cast, single-heat-treated and double-heat-treated specimens are 1.69×10^{-6} mm^3/N m, 2.1×10^{-6} mm^3/N m, and 2.41×10^{-6} mm^3/N m respectively. The regression of the linear wear of all three sets of samples is shown (from 0.5×10^6 to 3 $(2.5)\times10^6$ cycles). A univariate analysis of variance was conducted on all of the 12 wear rates using the SPSS statistical package.

Figure 4 shows the linear wear demonstrated by all three specimens. The high- and low-carbide results showed statistically different wear rates from each other ($p \leqslant 0.001$ using a univariate analysis of variance in the statistical package SPSS) and the medium carbide results were in between these two sets of results. The graph shows the average points with ± one standard deviation indicated by the error bars. The test was run to 3×10^6 cycles; however, the high-carbide test ran dry after 2.5×10^6 cycles and was terminated at that point.

The control graph for the as-cast specimen showed little change, a maximum weight variation of 0.000 18 gf for the plate. The pin initially lost 0.0008 gf (perhaps something stuck to the surface) and had very little variation after that, 0.0001 gf. The single-heat-treated specimens showed very little change; the maximum variation for the plate was 0.0001 gf and for the pin 0.0004 gf. The double-heat-treated specimens consistently lost weight over the course of the test. By the end of the test, both the pin and the plate had lost 0.0018 gf. All changes in the control specimens were compensated for in the test samples.

Figure 5(a) shows a scanning electron micrograph of the worn plate surface of the as-cast metal: the image was taken at 30° to the horizontal surface and the hard carbides can be seen to protrude from the worn surface with grooves running along the length of the wear track. Figure 5(b) shows the worn plate surface of the single-heat-treated plate. Small pits and scratches can be identified in this image; however, the carbides are less obvious. Figure 5(c) shows an SEM image of the wear track on the plate of the double-heat-treated material. The large pits

jeim387 23-4-08 09:50:56 Rev 7.51n/W (Jan 20 2003)
The Charlesworth Group, Wakefield 01924 204830

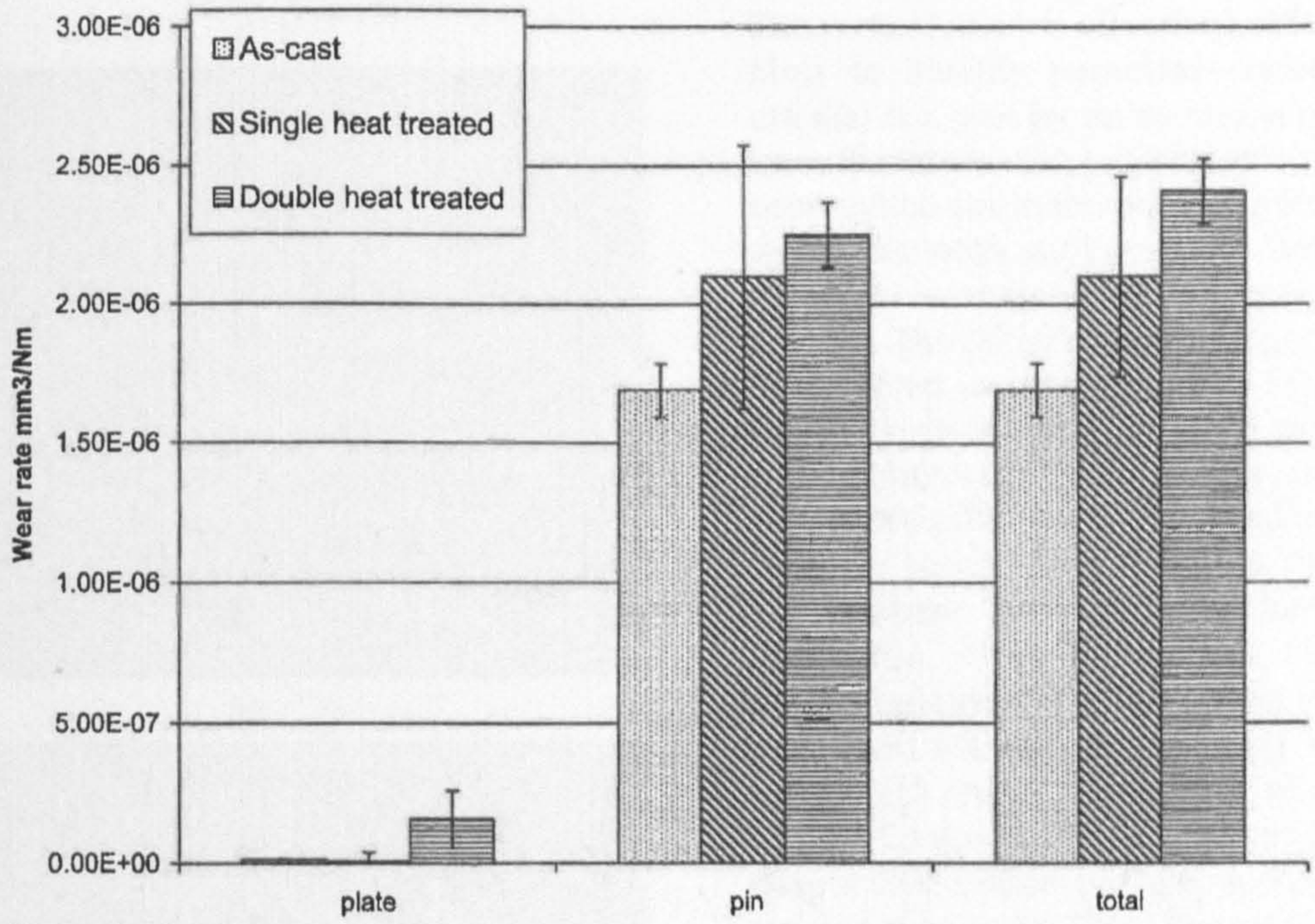

Fig. 3 Comparison of the wear rates of Co–Cr–Mo alloy containing various amounts of carbide Data represents the mean values ($n = 4$) of the wear rates over the test; error bars represent the standard deviation

shown which indicates matrix material being plucked from the surface. No carbides can be seen.

Table 1 shows the topographical measurements taken with the non-contacting interferometer; the average values for the peak-to-valley height, R_a, R_q, and skewness are given for all three differently treated materials ($n = 40$). A univariate analysis of variance was carried out on the unaveraged data set and the resulting statistics are quoted where appropriate.

Figure 6, 7 and 8 show the surfaces of all three specimens both initially and at the end of the test.

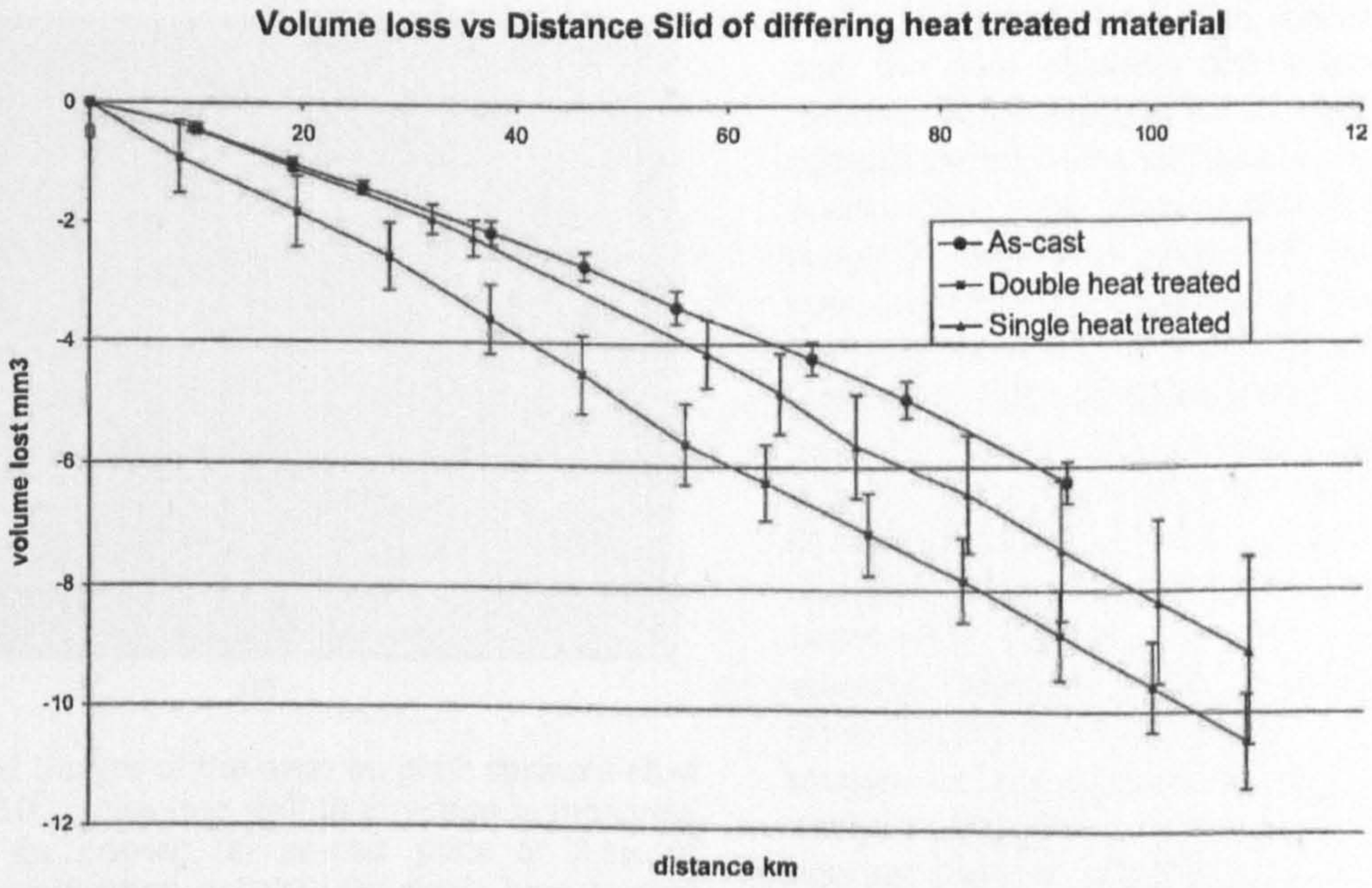

Fig. 4 Linear wear of all three components: volume 1 ms versus distance slid of materials with different heat treatment Data represents of mean values ($n = 4$) of the wear volumes, error bars represent the standard deviation

jeim387 23-4-08 09:50:58 Rev 7.51n/W (Jan 20 2003)
The Charlesworth Group, Wakefield 01924 204830

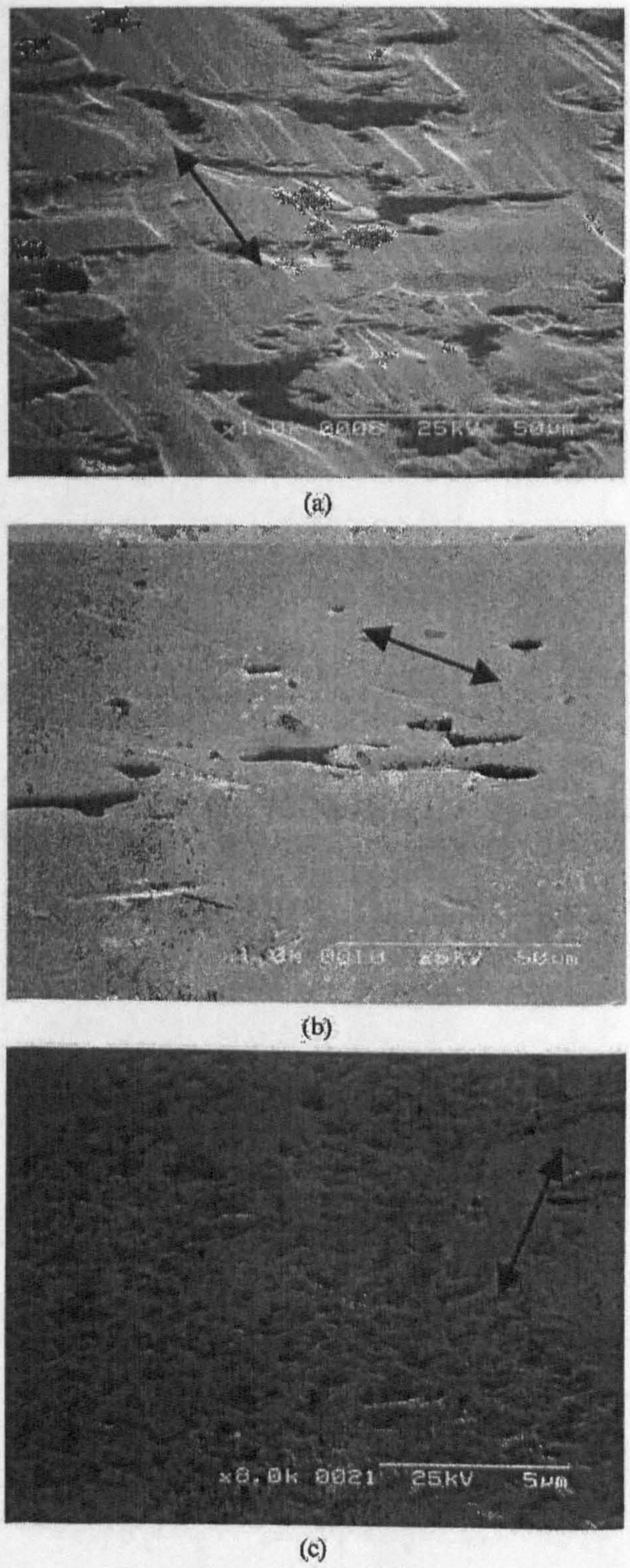

Fig. 5 SEM images of the wear on plate surfaces after 3×10^6 cycles (the sliding direction is indicated by an arrow): (a) as-cast plate at 2.5×10^6 (magnification, ×1000); (b) single-heat-treated plate at 3×10^6 cycles (magnification, ×8000); (c) double-heat-treated plate at 3×10^6 cycles (magnification, ×1000)

The vertical scale (z direction) differ for some of the plots to identify particular surface features. Figure 6(a) is a plot for an as-cast specimen showing a smooth surface with large holes where carbides have been pulled out in the polishing process. Figure 6(b) shows the worn surface of the final as-cast sample along the wear track where protruding carbides are obvious. The initial surface topography of the single-heat-treated sample shown in Fig. 7(a) indicates a smooth surface with numerous carbides protruding a little way out of the surface and copious holes where the carbides have been pulled out. Figure 7(b) shows a rough surface with a few medium-sized holes where carbides have been plucked out. Figure 8(a) shows the surface topography of the double-heat-treated Co–Cr–Mo specimen at the start of the test where there are many tiny holes visible. Figure 8(b) shows the surface of the double-heat-treated Co–Cr–Mo after 3×10^6 cycles. There are no deep holes visible but the surface is rougher on average than in Fig. 8(a). Figure 8(b) does not show the large deep holes visible in Fig. 5(a) as the large step change in the surface profile caused a loss in the surface detail; this plot was chosen to show how the roughness of the surface had changed.

4 DISCUSSION

The wear results (Fig. 3) show that the as-cast material gave the lowest total wear ($1.69\times10^{-6}\,\mathrm{mm^3/N\,m}$). The plates wore very little and the pins showed the least wear of all the different treatments. The as-cast pins and plates contain hard blocky carbides in a softer Co–Cr–Mo matrix. The long grooves shown in the final SEM image of the as-cast plate (Fig. 5a) indicate that the hard carbides of the pin cut grooves into the softer matrix material on the opposing bearing surface. The large protruding carbides of the pins and plates are also evident in the surface topography images (Fig. 6). These show that the softer matrix material surrounding the carbides was smeared in the direction of motion. This provides evidence of the contrasting hardness of the carbide and matrix material. Because of the differing imaging techniques, the grooves that can be seen in the final SEM images are not apparent in the surface topography analysis (Fig. 6(b)). The results indicat that the bearing surfaces wear through abrasion. The small variation in wear (Fig. 4) between the four as-cast specimens indicated good reproducibility of the experimental results.

jeim387 23-4-08 09:50:59 Rev 7.51n/W (Jan 20 2003)
The Charlesworth Group, Wakefield 01924 204830

Table 1 Data from non-contacting microscopy showing the surface roughnesses

Parameter	Double heat treated		Single heat treated		As cast	
	Initial value	Final value	Initial value	Final value	Initial value	Final value
Peak-to-valley height	1.206	1.171	2.206	0.377	0.837	2.579
Skewness	−8.458	−3.794	−12.474	0.202	−2.363	0.862
R	0.0238	0,0945	0.023	0.028	0.027	0.206
R_a	0.0123	0.0723	0.038	0.047	0.019	0.118

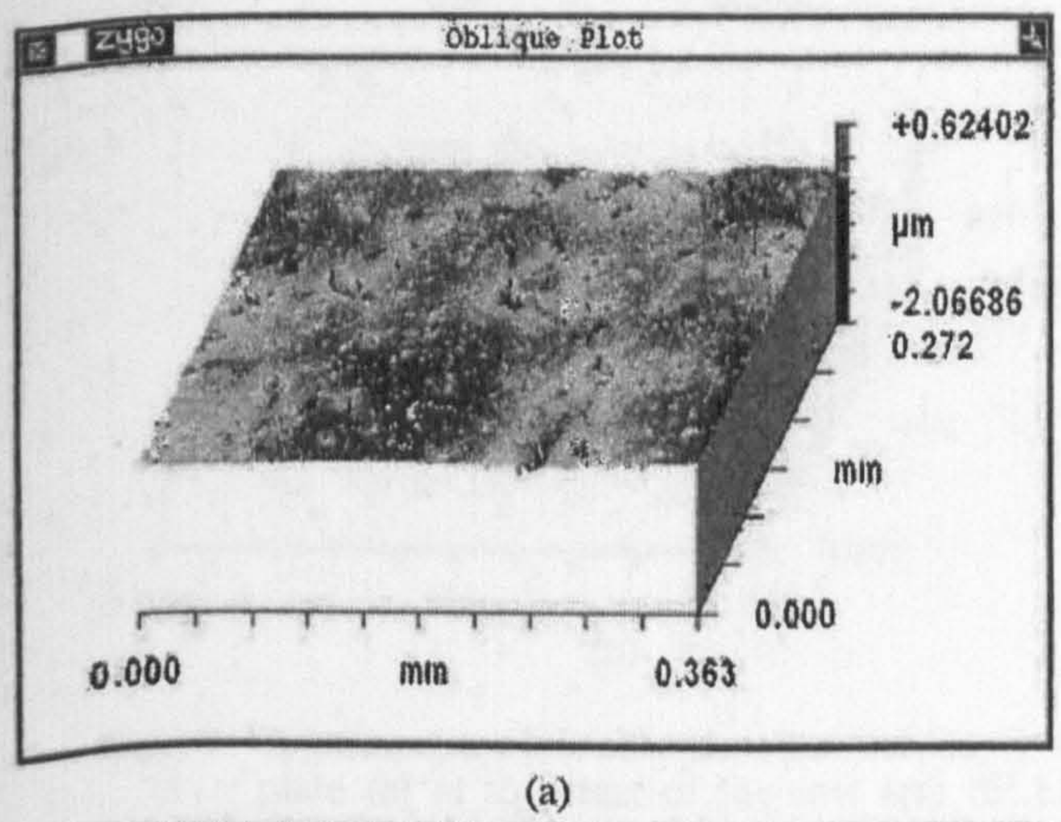

(a)

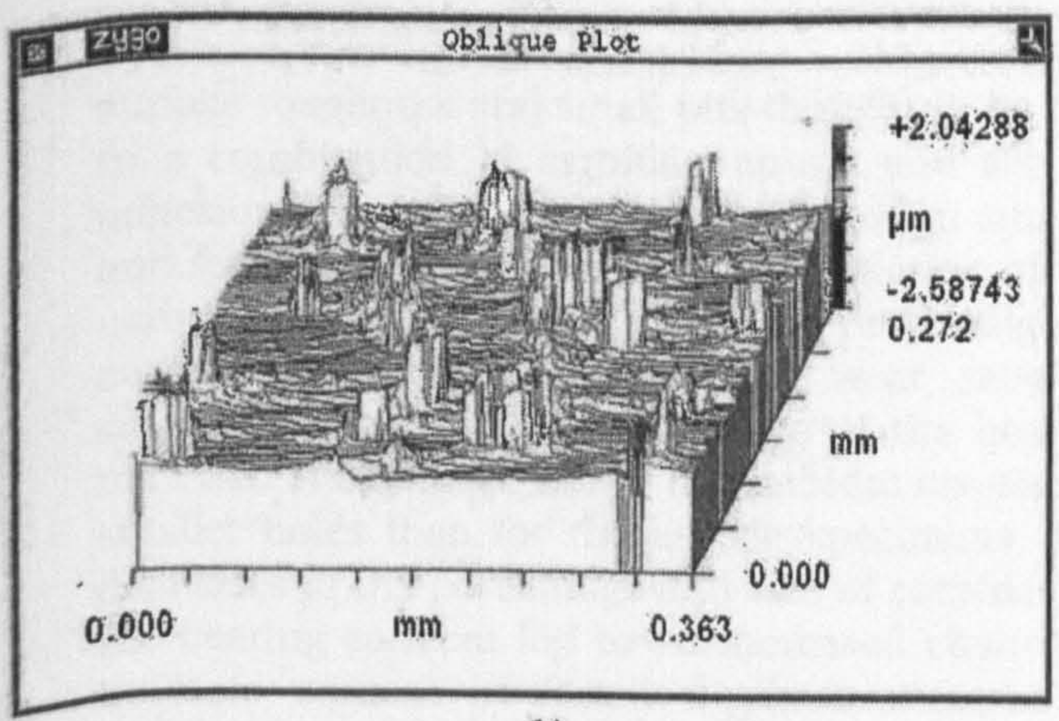

(b)

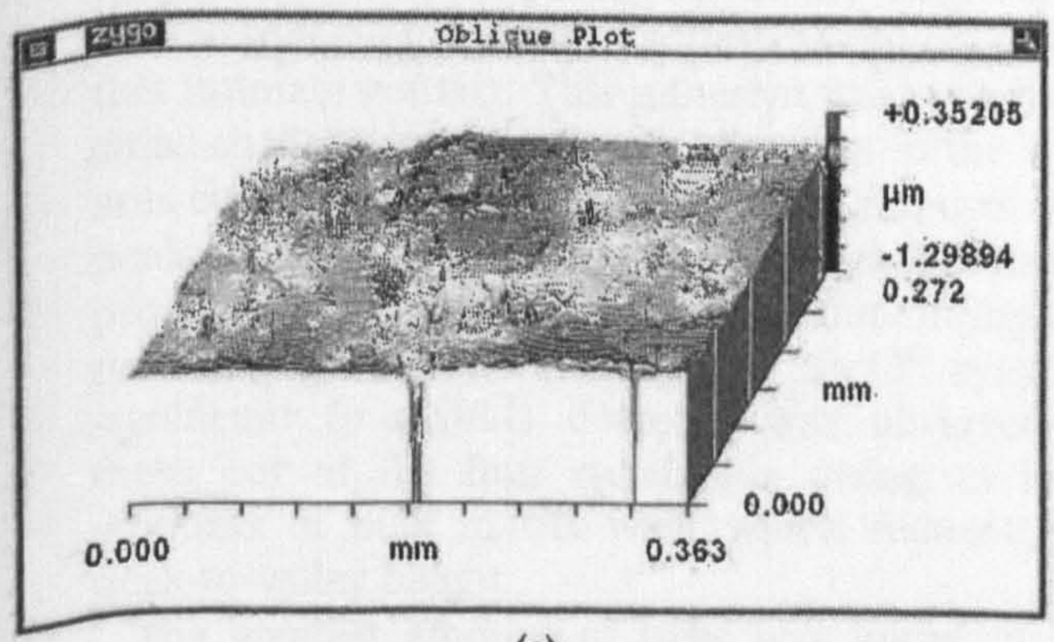

(c)

Fig. 6 Zygo images of as-cast Co–Cr–Mo plate (a) at the start of the test and (b) after 2.5×10^6 cycles

The as-cast specimen showed protruding carbides; these are not seen in the hip wear simulator tests, and running-in and steady state periods were not defined. This may be due to the self-polishing of the as-cast material and, once smooth, the surfaces are more likely to undergo full fluid lubrication more often, causing low wear. The set-up of the pin-on-plate machine does not allow full fluid lubrication to occur.

The single-heat-treated material showed similar plate wear to but slightly higher pin wear than the as-cast specimens. The surface topography after 3×10^6 cycles (Fig. 7(b)) showed an increase in

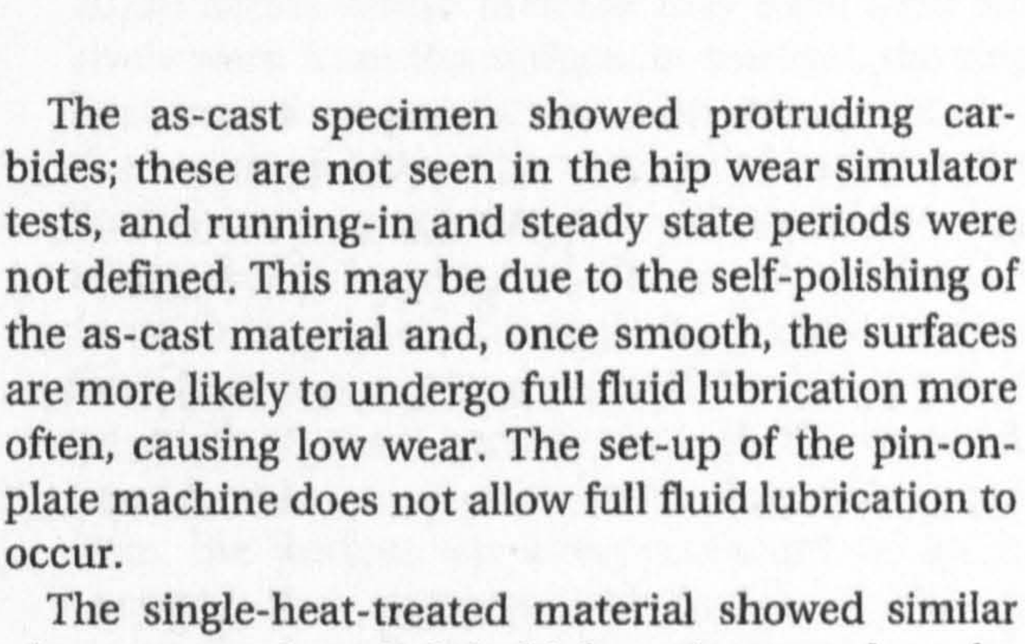

(a)

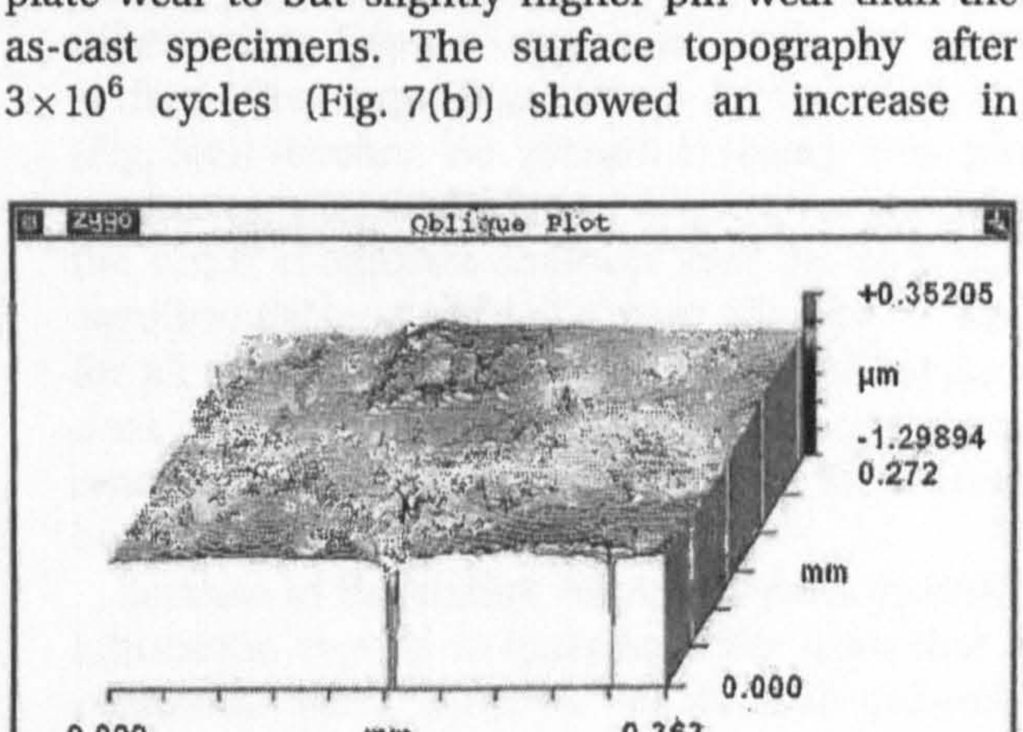

(b)

Fig. 7 Zygo images of double-heat-treated Co–Cr–Mo plate (a) at the start of the test and (b) after 3×10^6 cycles

jeim387 23-4-08 09:51:11 Rev 7.51n/W (Jan 20 2003)
The Charlesworth Group, Wakefield 01924 204830

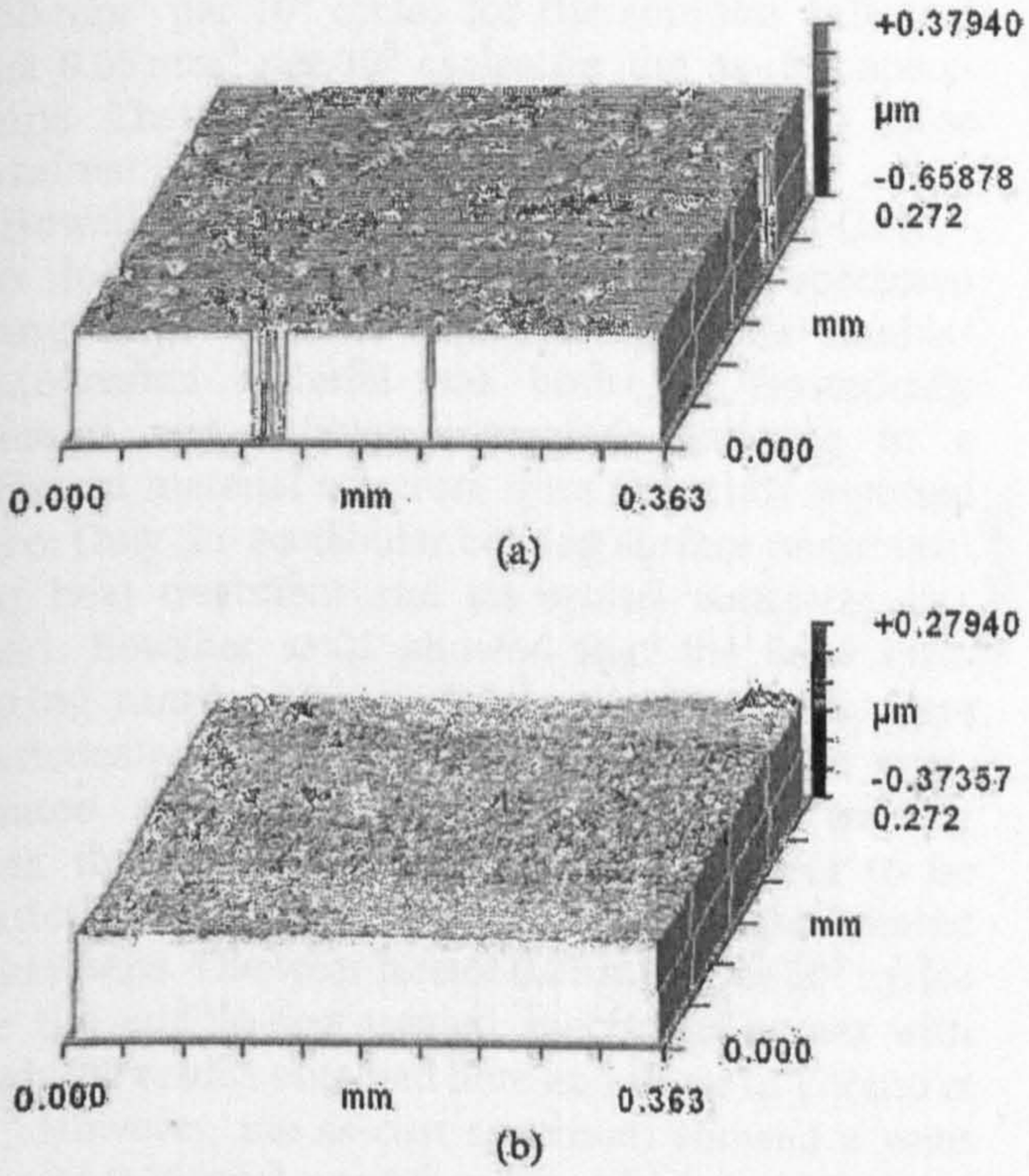

Fig. 8 Zygo images of double-heat-treated Co–Cr–Mo plate (a) at the start of the test and (b) after 3×10^6 cycles

surface roughness and small pits thought to be due to a combination of carbide pull-out and surface adhesion. Single heat treatment resulted in smaller and fewer carbides owing to partial solution of the carbon into the matrix lattice. The remaining tall carbide asperities cause abrasive wear seen as scratching on the apposing surface of the bearing material. The reduced size of the carbides resulted in smaller holes than for the as-cast specimens. The decreases in the percentage and size of carbides on the bearing surfaces led to an increased chance of intimate contact of identical phase material. A proportion of the holes shown in the single-heat-treated specimen are due to adhesive wear caused by this intimate contact. This adhesive wear results in small shallow areas of material removal in the wear area compared with large deep carbide removal. The peak-to-valley height was initially large because a proportion of carbides were pulled out during the polishing process. However, after 3×10^6 cycles a significant ($p \leqslant 0.001$) decrease was observed in three out of the four specimens owing to large amounts of bulk matrix wear which reduced the peak-to-valley height.

The greatest amount of wear was found in the double-heat-treated material. The block carbides initially formed during casting were completely diffused into the matrix owing to the double heat treatment. Upon inspection of the unworn surface, a very small surface roughness was found, and no carbides were visible. This structure caused adhesion to be the primary method of wear, owing to intimate contact of identical matrix material. The final SEM image of the double-heat-treated specimen (Fig. 5(c)) showed large pits approximately 20 μm across where material may have been adhesively worn from the surface. In contrast, the single-heat-treated material showed an average pit size in the region of 5 μm. The absence of carbides in the double-heat-treated structure allows large volumes of material to be removed. The presence of carbides (as seen in as-cast and single-heat-treated material) interrupts the matrix structure, hindering the propagation of crack growth through the material. A smaller volume of material is therefore removed from the surface on every occasion of intimate contact. The topographical image of the final double-heat-treated sample (Fig. 8(b)) shows an increased roughness compared with the unworn surface. The large pits shown in the SEM image (Fig. 5(c)) cannot be identified using this profilometer technique. Both the average roughness and the r.m.s. roughness indicate that the surface was significantly ($p \leqslant 0.001$) rougher after 3×10^6 cycles, for all four specimens. Self-polishing of the surface does not occur because the continuous material removal caused a high proportion of the surface to be pitted at all times.

Because of the nature of pin-on-plate testing, the lubrication regime is likely to differ from that of a prosthetic joint. Bowsher *et al.* [**15**] showed no statistical difference between the wear rates of as-cast and solution-annealed or hot isostatically pressed materials when testing large-diameter hip prostheses in joint simulators. This is probably because the geometry of *in-vitro* hip joint simulation allows fluid-film lubrication to be generated [**12**]. In contrast, the contact of pin-on-plate machines due to the specimen geometry and testing conditions will eliminate any fluid-film lubrication; therefore the effects of material properties and any possible boundary lubrication can be tested.

Varano *et al.* [**16**] examined the effect of microstructure on the wear of cobalt-based alloys. High-carbon as-cast and solution-annealed specimens were among those tested. The unworn surfaces showed similar results to those shown in this study with larger carbides visible at the surface of the as-cast specimen and smaller sparser carbides visible after a single annealing treatment. Using reciprocating pin-on-plate apparatus, wear results showed

jeim387 23-4-08 09:51:26 Rev 7.51n/W (Jan 20 2003)
The Charlesworth Group, Wakefield 01924 204830

$0.25\,mm^3$ per 10^6 cycles for the solution annealed and $0.05\,mm^3$ per 10^6 cycles for the as-cast specimens. These results show similar trends to those obtained in this study.

Bowsher *et al.* [15] also compared as-cast Co–Cr–Mo joints with a double-heat-treated specimen using large-diameter hip bearings. The double-heat-treated material was both hot isostatically pressed and solution annealed, resulting in a different material structure from the study reported here. Only the acetabular bearing surface underwent the heat treatment and an orbital simulator was used. Bowsher *et al.* showed that the wear rates during running in, steady state, and jogging were statistically similar for the as-cast and the heat-treated specimens. However, additional walking after the jogging cycles found as-cast wear to be statistically higher than wear for the heat-treated specimens. The wear rate of $0.25\,mm^3$ per 10^6 cycles for the double-heat-treated specimens agrees with both the results obtained here and those of Varano *et al.*. However, the as-cast specimen showed a wear rate of $0.76\,mm^3$ per 10^6 cycles which is 15.2 times greater than the results obtained by Varano *et al.*

5 CONCLUSION

The as-cast material gave the lowest wear rates of the three specimens tested. Surface assessment of the as-cast Co–Cr–Mo specimens indicated that the wear regime was mainly abrasive wear. The peak-to-valley height significantly increased ($p \leqslant 0.005$) as did the roughnesses R_a and R_q roughness whilst the skewness significantly decreased ($p \leqslant 0.005$).

The single-heat-treated material was the next lowest wearing, and surface analysis indicated that both abrasive and adhesive wear were present. The peak-to-valley height increased significantly ($p < 0.001$), and the topographical results showed that holes of significant depth were created on the surface; however, the average roughness R_a showed no significant difference ($p > 0.4$).

The double-heat-treated material had the greatest wear of the materials tested, and surface analysis indicated mainly adhesive wear. Surface roughness significantly increased ($p < 0.001$); however, the peak-to-valley height showed no significant change ($p > 0.1$).

These results indicate that heat treatment by solution annealing of a Co–Cr–Mo material significantly increased ($p < 0.005$) the wear rates. That is, in the absence of fluid-film lubrication, which would usually be found within a prosthetic hip joint with a large diameter of 50 mm the wear of the material would be greater for heat-treated Co–Cr–Mo alloy.

ACKNOWLEDGEMENTS

The authors would like to thank Smith and Nephew Orthopaedics for funding this work and supplying the materials.

REFERENCES

1 **Berry, D. J., Scott Harmsen, W., Cabanela, M. E.,** and **Morrey, B. F.** Twenty-five-year survivorship of two thousand consecutive primary charnley total hip replacements. *J. Bone Jt Surg. AM.*, 2002, **84**(2), 171–177.

2 **Semlitsch, M.** CoCrMo metal/metal articulations as a solution to the problem of wear of hip joint replacements. In Proceedings of the SERC/IMechEAnnual Expert Meeting on *Failure of Joint Prostheses*, 28–30 November 1993, pp. 40–45.

3 **Chan, F., Bobyn, J. D., Medley, J. B., Krygier, J. J., Yue, S.,** and **Tanzer, M.** Engineering issues and wear performance of metal on metal hip implants. *Clin. Orthop. Related Res.*, 1996, **333**, 96–107.

4 **Schmalzried, T. P., Peters, P. C., Maurer, B. T., Bragdon, C. R.,** and **Harris, W. H.** Long duration metal-on-metal total hip arthroplasties with low wear of the articulating surfaces. *J. Arthroplasty*, 1996, **11**(3), 322–331.

5 **Schmidt, M., Weber, H.,** and **Schom, R.** Cobalt chromium molybdenum metal combination for modular hip prostheses. *Clin. Orthop. Related Res.*, 1996, **329**(Suppl.), s35–s47.

6 **McKellop, H., Park, S., Chiesa, R., Doorn, P., Lu, B., Normand, P., Grigoris, P.,** and **Amstutz, H. C.** *In vivo* wear of 3 types of metal on metal hip prostheses during 2 decades of use. *Clin. Orthop. Related Res.*, 1996, **329**(Suppl.), S128–S140.

7 **Kothari, M., Bartel, D. L.,** and **Booker, J. F.** Surface geometry of retrieved Mckee–Farrar total hip replacements. *Clin. Orthop. Related Res.*, 1996, **329**(Suppl.), S141–S147.

8 **Scholes, S. C., Green, S. M.,** and **Unsworth, A.** The wear of metal-on-metal total hip prostheses measured in a hip simulator. *Proc. Instn Mech. Engrs, Part H: J. Engineering in Medicine*, 2001, **215**, 523–530.

9 **Archard, J. F.** Contact and rubbing of flat surfaces. *J. Appl. Physics*, 1953, **24**(3), 981–988.

10 **Jin, Z. M.** Analysis of fluid film lubrication in artificial hip joint replacements with surfaces of high elastic modulus. *Proc. Instn Mech. Engrs, Part H: J. Engineering in Medicine*, 1997, **211**(3), 247–256.

11 **Scholes, S. C.** and **Unsworth, A.** The tribology of metal-on-metal total hip replacements. *Proc.*

jeim387 23-4-08 09:51:31 Rev 7.51n/W (Jan 20 2003)
The Charlesworth Group, Wakefield 01924 204830

Imech F, Part I J. Engineering in Medicine, 2005, **220**(2), 183–194.

12 **Vassiliou, K., Elfick, A. P. D., Scholes, S. C.,** and **Unsworth, A.** The effect of 'running-in' on the tribology and surface morphology of metal-on-metal Birmingham hip resurfacing device in simulator studies. *Proc. IMechE, Part H: J. Engineering in Medicine*, 2006, **220**, 269–277.

13 **Dowson, D., Hardaker, C., Flett, M.,** and **Isaac, G. H.** A hip joint simulator study of the performance of metal-on-metal joints – Part I: The role of materials. *J. Arthroplasty*, 2004, **19**(8), 118–123.

14 **Elfick, A., Hall, R. M., Pinder, I. M.,** and **Unsworth, A.** The influence of femoral head surface roughness on the wear of UHMWPE sockets in cementless total hip replacements. *J. Biomed. Mater. Res.: Appl. Biomechanics*, 1999, **48**(5), 712–718.

15 **Bowsher, J. G., Nevelos, J., Pickard, J.,** and **Shelton, J. C.** Do heat treatments influence the wear of large diameter metal on metal hip joints? An *in vitro* study under normal and adverse gait conditions. In Proceedings of the 49th Annual Meeting of the Orthopaedic Research Society, 2003, poster 1398 (Orthopaedic Research Society, Rosemont, Illinois).

16 **Varano, R., Bobyn, J. D., Medley, J. B.,** and **Yue, S.** The effect of microstructure on the wear of cobalt-based alloys used in metal-on-metal hip implants. *Proc ImechE, Part H: J. Engineering in Medicine*, 2006, **220**, 145–159.

jeim387 23-4-08 09:51:31 Rev 7.51n/W (Jan 20 2003)
The Charlesworth Group, Wakefield 01924 204830